CARDIFF UNIVERSITY

Kinase D-interacting substrate of 220kDa (Kidins220) in pancreatic cancer, molecular and cellular mechanism for its association with disease progression

By

Shuo Cai

Cardiff China Medical Research Collaborative

School of Medicine, Cardiff University

Cardiff

May 2018

Thesis submitted to Cardiff University for the degree of Doctor of Medicine

DECLARATION

This work has not been submitted in substance for any other degree or award at this or any other university or place of learning, nor is being submitted concurrently in candidature for any degree or other award.

Signed …… (candidate) Date ……

STATEMENT 1

This thesis is being submitted in partial fulfilment of the requirements for the degree of MD.

Signed …… (candidate) Date ……

STATEMENT 2

This thesis is the result of my own independent work/investigation, except where otherwise stated. Other sources are acknowledged by explicit references. The views expressed are my own.

Signed …… (candidate) Date ……

STATEMENT 3

I hereby give consent for my thesis, if accepted, to be available for photocopying and for inter-library loan, and for the title and summary to be made available to outside organisations.

Signed …… (candidate) Date ……

STATEMENT 4: PREVIOUSLY APPROVED BAR ON ACCESS

I hereby give consent for my thesis, if accepted, to be available for photocopying and for inter-library loans after expiry of a bar on accesspreviously approved by the Academic Standards & Quality Committee.

Signed …… (candidate) Date ……

Acknowledgements

Firstly, I would like to thank my supervisor Dr Lin Ye for his great support and guidance throughout my two-year MD study. I would especially like to express my great thanks to Professor Wen G. Jiang for his kindness and help over the years. I would also like to thank to my co-supervisors Dr Jun Cai, Dr Stephen Hiscox and Mr Jared Torkington who have always been patient and supportive throughout the whole period of my MD study. I am also grateful to Dr Andrew Sanders, Dr Tracey Martin, Dr Catherine Zabkiewicz，Dr Faris Soliman，Dr Sioned Owen and Mrs Fiona Ruge, for their support to my MD study over the years. Meanwhile, I would like to thank all the PhD, MD, post-doctoral, senior and administrative staff members in CCMRC who have been really friendly and helpful all the time.

Finally, I would like to dedicate this work to my parents and my husband whose support and encouragement gave me the motivation and determination to overcome all the difficulties and frustrations in order to complete my study. I would not be where I am today without them.

Abstracts and conference presentations

Shuo Cai, Ping-Hui Sun, Xiangyu Gao, Ke Ji, Xiuyun Tian, Jiafu Ji, Chunyi Hao, Bilal Al-Sarireh, Paul Griffiths, Steven Hiscox, Jared Tonkington, Jun Cai, Wen G. Jiang and Lin Ye. Kinase D-interacting substrate of 220kDa (Kidins220) is reduced in pancreatic cancer and the potential link with distant metastases. May 2016. China-United Kingdom Cancer (CUKC) Conference, Beijing China.

Shuo Cai, Xiangyu Gao, Ping-Hui Sun, Catherine Zabkiewicz, Yi Feng, Jun Li, Ying Liu, Sioned Owen, Ke Ji, Lee Campbell, Jared Torkington, Steve Hiscox, Jun Cai, Jiafu Ji, Wen G. Jiang and Lin Ye. Overexpression of Kinase D-interacting substrate of 220kDa (Kidins220) is associated with disease progression and poor prognosis in gastric cancer. April 2017. The 12th International Gastric Cancer Congress (IGCC), Beijing China.

Shuo Cai, Xiangyu Gao, Ke Ji, Yi Feng, Ping-Hui Sun, Lee Campbell, Chunyi Hao, Jiafu Ji, Jun Cai, Steve Hiscox, Wen G. Jiang and Lin Ye. Reduced expression of Kinase D-interacting substrate of 220kDa (Kidins220) in pancreatic cancer is associated with disease progression and aggressive traits of pancreatic cancer cells. September 2017. 2017 RSM President's Day.

Shuo Cai, Xiangyu Gao, Ke Ji, Yi Feng, Ping-Hui Sun, Lee Campbell, Chunyi Hao, Jiafu Ji, Jun Cai, Steve Hiscox, Wen G. Jiang and Lin Ye. Reduced expression of Kinase D-interacting substrate of 220kDa (Kidins220) in pancreatic cancer is associated with disease progression and aggressive traits of pancreatic cancer cells. April 2018. AACR Annual Meeting.

Publications

CAI, S., SUN, P. H., RESAUL, J., SHI, L., JIANG, A., SATHERLEY, L. K., DAVIES, E. L., RUGE, F., DOUGLAS-JONES, A., JIANG, W. G. & YE, L. 2017. Expression of phospholipase C isozymes in human breast cancer and their clinical significance. Oncol Rep, 37, 1707-1715.

CAI, S., CAI, J., JIANG, W. G. & YE, L. 2017. Kidins220 and tumour development: Insights into a complexity of cross-talk among signalling pathways (Review). Int J Mol Med, 40, 965-971.

Summary

Kidins220 (Kinase D-Interacting Substrate, 220kDa) is a transmembrane scaffold protein and has been implicated in several malignancies. However, its role in pancreatic cancer remains unknown. The present study aims to investigate the role of Kidins220 in pancreatic cancer. A QPCR analysis showed that Kidins220 mRNA expression was reduced in pancreatic tumour tissues compared with adjacent normal pancreatic tissues. Reduced expression was also observed in the advanced tumours compared with tumours of an early stage. Furthermore, immunohistochemistry (IHC) staining presented reduced protein expression of Kidins220 in pancreatic tumour tissues compared with adjacent normal tissues and normal pancreatic tissues. Its reduced expression was also seen in invasive cancer originating in intraductal papillary mucinous neoplasm (IPMN) compared with normal pancreatic tissue. Moreover, primary tumours with distance metastasis exhibited a decreased level of Kidins220 protein expression compared to those without metastasis. Knockdown of Kidins220 promoted proliferation, migration and invasion of pancreatic cancer cells. Panc-1 cells with Kidins220 knockdown also exhibited an enhanced metastatic capability *in vivo* in peritoneal metastatic mouse model. An enhanced epithelial–mesenchymal transition (EMT) was observed in the pancreatic cancer cell lines with the knockdown of Kidins220 following an elevated expression and activation of EGFR and consequent activation of its downstream signalling pathways including extracellular signal-regulated kinase (ERK) and Protein kinase B (AKT) pathways. Taken together, a reduced expression of Kidins220 is observed in pancreatic cancer which is associated with disease progression, distant metastases and poor prognosis. The loss of Kidins220 in pancreatic cancer may contribute to the disease progression through an upregulation of EGFR signalling. It suggests that Kidins220 is a putative negative regulator for development and progression of pancreatic cancer. Further study will shed light on the interaction between Kidins220 and EGFR, and potential of this molecule in targeted therapy, for example EGFR or other HER family members for pancreatic cancer.

Contents

Chapter2 Methodology

Chapter3 Expression of Kidins220 in pancreatic cancer and the clinical relevance

Chapter4 Influence of Kidins220 knockdown on cellular functions of pancreatic cancer cell lines

List of figures

Chapter1

Chapter2

Chapter3

Chapter4

Chapter5

List of tables

Chapter1

Chapter2

Chapter3

Chapter4

Chapter5

Abbreviations

5-FU: 5-Fluorouracil

ACC: adrenocortical carcinoma

AD: Alzheimer's disease

ADPC : androgen-dependent prostate cancer

AMPARs: α-amino-3-hydroxy-5-methyl-4-isoxazolepropionic acid receptors

ARMS: Ankyrin repeat-rich membrane spanning

BCR: B cell antigen receptor

BDNF: brain-derived neurotrophic factor

BLCA: bladder urothelial carcinoma

BRCA: breast invasive carcinoma

BSA: bovine serum albumin

CA 19-9: carbohydrate antigen 19-9

CA: celiac axis

CAPS: Cancer of the Pancreas Screening

CDK4: cyclin-dependent kinase 4

CDKN2A: cyclin-dependent kinase inhibitor 2A

cDNA: complementary DNA

CESC: cervical squamous cell carcinoma and endocervical adenocarcinoma (CHOL), cholangiocarcinoma

CNS: central nervous system

COAD: colon adenocarcinoma

COADREAD: colorectal adenocarcinoma

CRC: colorectal cancer

CRPC: castration resistance prostate cancer

CT: computerized tomography

DEPC: diethylpyrocarbonate

DLBC: lymphoid neoplasm diffuse large B-cell lymphoma

DMEM: Dulbecco's Modified Eagles' Medium

DMSO: dimethyl sulfoxide

dNTPs: Deoxynucleotide triphosphates

ECM: extracellular matrix

EGF: epidermal growth factor

EGFR: epidermal growth factor receptor

EMT: epithelial-mesenchymal transition

EMT-TFs: EMT-inducing transcription factor

EPIC: European Prospective Investigation into Cancer and Nutrition

ERBB-1: v-erb-b2 erythroblastic leukaemia viral oncogene homolog 1

ERK: extracellular signal-regulated kinase

ESCA: oesophageal carcinoma

ETS: environmental tobacco smoke

EUS: endoscopic ultrasonography

EUS-FNA: EUS-guided fine needle aspiration

FAP: familial adenomatous polyposis

FBS: foetal bovine serum

FDA: Food and Drug Administration

FGF: fibroblast growth factor

FPC: familial pancreatic cancer

GBM: glioblastoma multiforme,

GBMLGG: glioma

HA: hepatic artery

HAND: HIV-associated neuro-cognitive disorders

HER-1: human epidermal growth factor 1

HIV: Human Immunodeficiency Virus Type-1

HNPCC: hereditary non-polyposis colorectal cancer

HNSC: head and neck squamous cell carcinoma

HRP: horseradish peroxidise

IHC: Immunohistochemical staining

IKK: IκB kinase

IPMA: intraductal papillary mucinous adenoma

IPMC: intraductal papillary mucinous carcinoma

IPMN: intraductal papillary mucinous neoplasm

JAK: mammalian target of rapamycin, and Janus kinase

KICH: kidney chromophobe

Kidins220: Kinase D-interacting substrate of 220kDa

KIM: kinase light chain (KLC)-interacting motif

KIRC: kidney renal clear cell carcinoma

KIRP: kidney renal papillary cell carcinoma

KLC1: Kinesin light chain 1

KPS: karnofsky performance status

K-ras: kirsten rat sarcoma oncogene homolog

LAML: acute myeloid leukaemia

LGG: brain lower grade glioma

LIHC: liver hepatocellular carcinoma

LUAD: lung adenocarcinoma

mAbs: monoclonal antibodies

MAPK: Mitogen-Activated Protein Kinase

MAPs: Microtubule-associated proteins

MESO: mesothelioma

MET: mesenchymal to epithelial transition

miRNAs: microRNAs

mOS: median overall survival

MPACT: Metastatic Pancreatic Adenocarcinoma Clinical Trial

MRI: magnetic resonance imaging

NF-κB: nuclear factor-kappa B

NGF: never growth factor

NSCLC: Non-small-cell lung cancer

N-type: Neuroblastic cells.

OV: ovarian serous cystadenocarcinoma

PanIN: pancreatic intraepithelial neoplasia

PCa: prostate cancer

PCPG: pheochromocytoma and paraganglioma

PCR: polymerase chain reaction

PDAC: Invasive pancreatic ductal adenocarcinoma

PDZ: PSD-95, Dlg, ZO-1

PET: positron emission tomography

PFS: progression-free survival

PI3K: Phosphoinositide 3-Kinase

PKD: Protein kinase D

PPPD: pylorus preserving pancreaticoduodenectomy

PRAD: prostate adenocarcinoma

PV: portal vein

QPCR: real time quantitative PCR

RalGEF: Ral Guanidine exchange factor

READ: rectum adenocarcinoma

RNAi: RNA interference

RT: reverse transcription

RTKs: tyrosine kinase receptors

SAM: Sterile alpha motif

SARC: sarcoma

SCCHN: Squamous Cell Carcinoma of the Head and Neck

SH2: Src homology 2

SKCM: skin cutaneous melanoma

SMA: superior mesenteric artery

SMV: superior mesenteric vein

STAD: stomach adenocarcinoma

STAT: signal transducer and activator of transcription

STES: stomach and oesophageal carcinoma

S-type: Schwannian stromal cells

TCR: T cell receptor

TFs: transcription factors

TGCT: testicular germ cell tumour

TGF-α: transforming growth factor alpha

TGF-β: transforming growth factor beta

THCA: thyroid carcinoma

THYM: thymoma

TKIs: small-molecule tyrosine kinase inhibitors

TMA: pancreatic adenocarcinoma tissue microarray

Trk: tropomyosin-related kinase

Tween 20: Polyoxyethylene (20) sorbitan monolaurate

UCEC: uterine corpus endometrial carcinoma

US: trans-abdominal ultrasound

UVB: ultraviolet radiation B

UVM: uveal melanoma

VEGFRs: vascular endothelial growth factor receptors.

Chapter 1

General Introduction

1.1 Pancreatic cancer

Pancreatic cancer is the fifth leading cause of cancer death in the UK with around 8,800 pancreatic cancer patients died from this disease in 2014 (Cancer Research UK). The five-year survival rate for all stages of pancreatic ductal adenocarcinoma (PDAC), the most common pancreatic malignancy, is just 8%. This falls to 3% in advanced pancreatic cancer patients (American Cancer Society) (Chiaravalli et al., 2017). Early diagnosis for pancreatic cancer is challenging, as patients often present no obvious symptoms until the cancer is advanced. Accordingly, most patients have inoperable tumours, metastases and consequently a high mortality rate. The majority of patients die within one year after diagnosis. The predicted increased incidence of pancreatic cancer in the United States, coupled with a low survival rate, projects pancreatic cancer as the second leading cause of cancer deaths by 2030 (Rahib et al., 2014).

To date, the combination of cytotoxic therapy including FOLFIRINOX or gemcitabine plus nab-paclitaxel (Nanoparticle albumin-bound paclitaxel) has been used as the standard of care for those advanced pancreatic cancer patients with good performance status (Borazanci and Von Hoff, 2014). However, the remaining challenge is to find more efficient methods for early diagnosis and novel treatments (Pereira, 2012).

1.1.1 The biology of the pancreas

1.1.1.1 Pancreatic anatomy

The pancreas is an important organ of the digestive system. It is a retroperitoneal organ located in the upper abdomen directly behind the stomach. In most adults, it is about 15cm long and 5cm wide. In general, the pancreas is divided into four regions; head, neck, body, and tail. The head is surrounded by the duodenum. The neck is about 2.5 cm wide and lies between the head and the body and is anterior to the superior mesenteric artery and vein. The body is the largest part of the pancreas that is located behind the stomach. The tail abuts the spleen.

The pancreas has two secretory functions including endocrine hormones (endocrine) and digestion (exocrine). The exocrine anatomy consists of secretory acinar cells in lobules, linked by tubules and larger ducts coalescing into a main duct. Dispersed throughout the pancreatic tissue are the islets of Langerhans, which perform the endocrine function of the gland and comprise 1-2% of the pancreas.

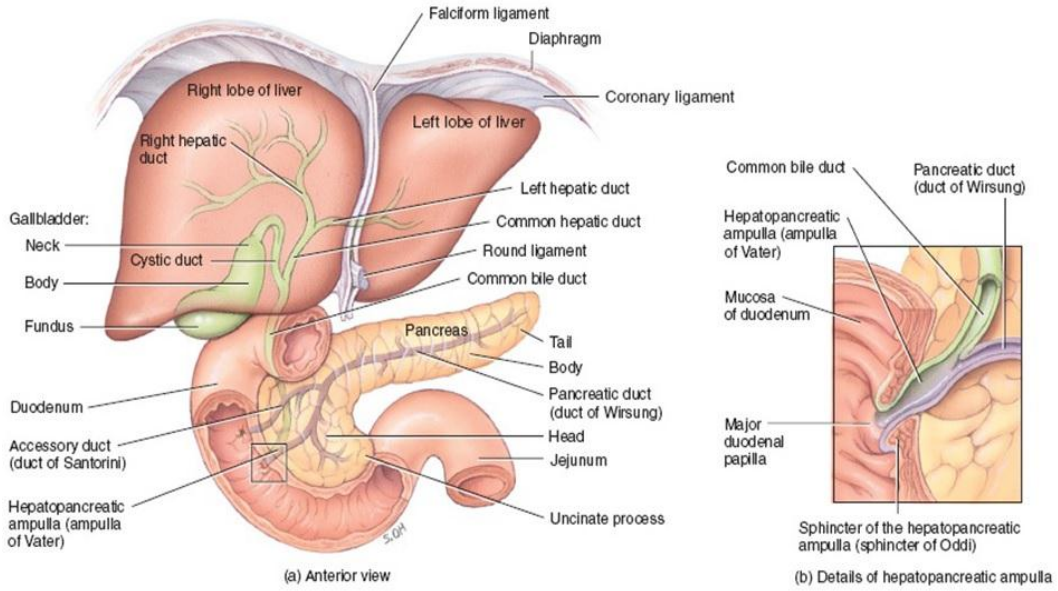

Figure1.1: The anatomy of pancreas. Source Pancreatic Duct Anatomy. Available at http://www.flspinalcord.us/pancreatic-duct-anatomy/#s.

1.1.1.2 Pancreatic Functions

The islets of Langerhans endocrine function is to make and secrete insulin, glucagon, somatostatin and pancreatic polypeptide into the bloodstream, with the function of regulating blood glucose, energy metabolism and storage. The exocrine function produces enzymes that help to digest food. Pancreatic amylase breaks down carbohydrates or starches into glucose. Proteases break down protein into amino acid, and lipase breaks down fats. These exocrine digestive enzymes are confined in the secretory structure while in the pancreas, and remain as inactive precursors, such as trypsinogen until reaching the gastrointestinal tract. To reach the gastrointestinal tract, the digestive enzymes travel through the pancreatic ducts and eventually reach the duodenum at the major papilla, also

known as the Ampulla of Vater (Figure 1.1). Bile from the gallbladder also enters the duodenum at the major papilla. Bile emulsifies fat droplets to aid digestion action of lipase. Proteases such as trypsinogen are activated by enterokinase produced in the intestinal mucosa, with subsequent activated trypsin performing autocatalytic function in a cascade of activation. When the pancreas is healthy, it contributes to a healthy digestive system, however, when pancreatic function is impaired, digestion, metabolism, and blood sugar control can become unbalanced. The consequent symptoms may include steatorrhea, weight loss, malnutrition, poor blood sugar control, and diabetes. Alcohol consumption, high-fat diet, obesity, and smoking can contribute to pancreatic dysfunction.

1.1.2 Incidence and genetics of pancreatic cancer

1.1.2.1 Incidence and mortality

According to incidence estimated in the GLOBOCAN 2012, pancreatic cancer is the eleventh most common malignancy worldwide, with 338,000 new cases in 2012 (available from: http://globocan.iarc.fr.). Globally, its causes more than 331,000 deaths per year, making it the seventh leading cause of cancer-related death (Ferlay et al., 2015) (Ilic and Ilic, 2016). The incidence and mortality for both genders has increased in the past few years, however, it is more common in men (Ilic and Ilic, 2016). In 2012, the worldwide incidence of pancreatic cancer was 4.9

per 100,000 in men and 3.6 per 100,000 in women (available from: http://globocan.iarc.fr.). Men also have a higher age standardised mortality rate for pancreatic cancer.

Gender differences are also apparent with geographic variation with the highest incidence of pancreatic cancer in Armenia and the Czech Republic in men, and Hungary and Denmark in women. In contrast, the lowest incidence of pancreatic cancer was Pakistan and Guinea in men, and Guinea and Tanzania in women (Figure 1.2).

In terms of mortality, Latvia and Hungary have the highest age standardised mortality rates for pancreatic cancer in men, whereas the highest mortality for women was in Hungary and Malta. The lowest rate was recorded in Bahrain and Belize for men, and Georgia and Belize for women (Figure 1.3).

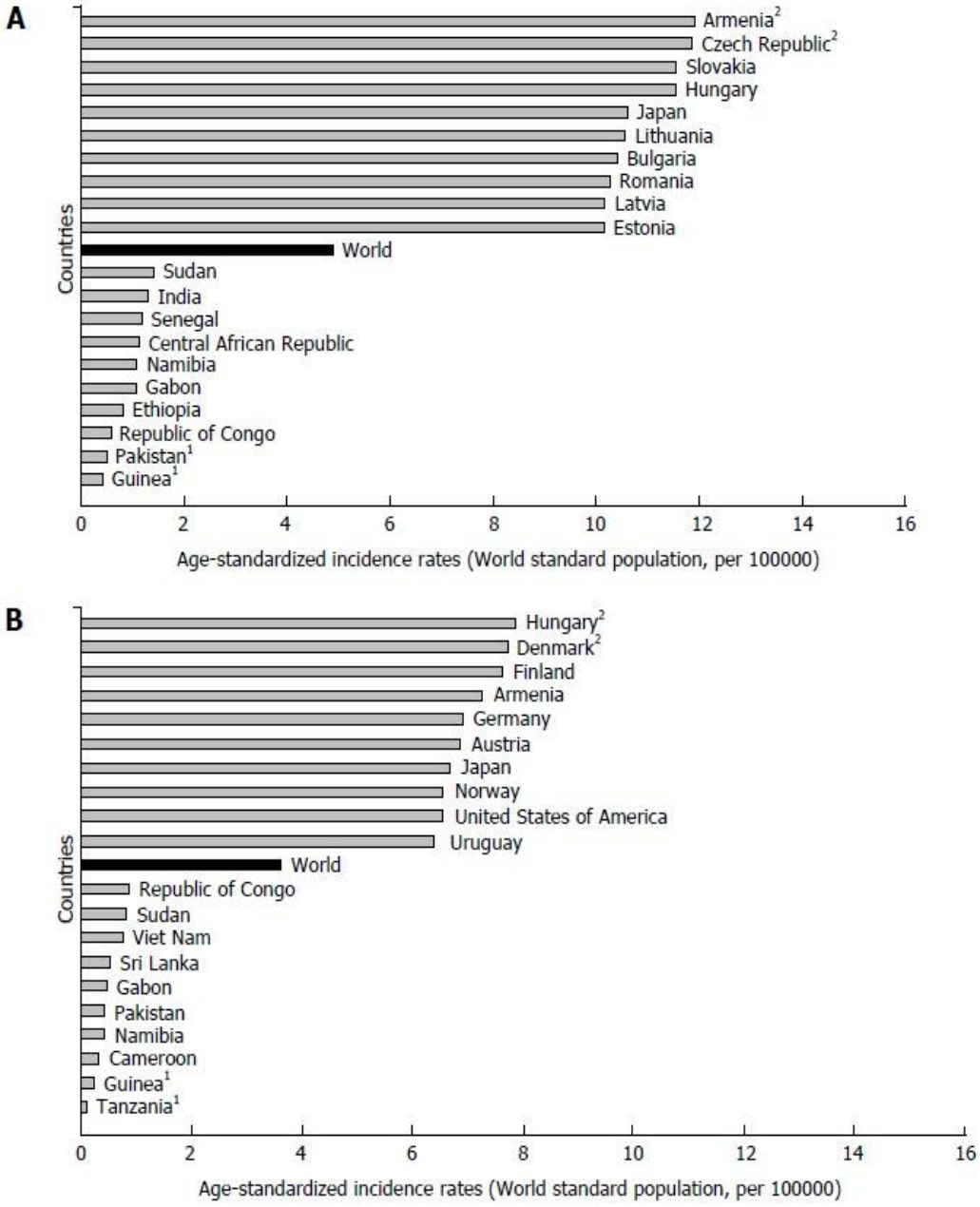

Figure 1.2: Pancreatic cancer incidence in men (A) and women (B), GLOBOCAN 2012 estimates. [1]Country with the lowest incidence rates; [2]Country with the highest incidence rates. GLOBOCAN 2012 estimates. Source: Epidemiology of pancreatic cancer (Ilic and Ilic, 2016).

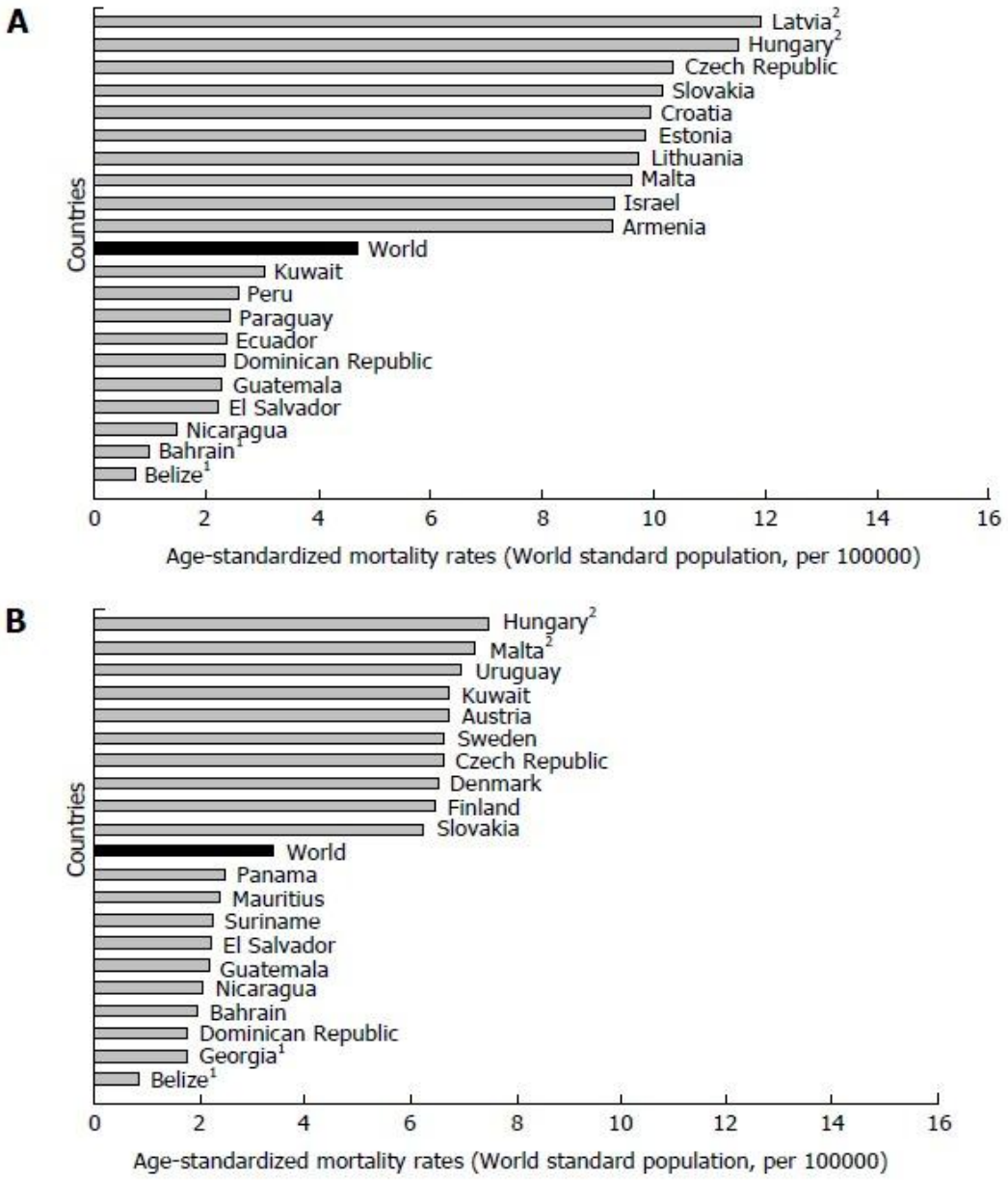

Figure 1.3: Pancreatic cancer mortality in men (A) and women (B), GLOBOCAN 2012 estimates. [1]Country with the lowest mortality rates; [2]Country with the highest mortality rates. GLOBOCAN 2012 estimates. Source: Epidemiology of pancreatic cancer (Ilic and Ilic, 2016).

1.1.2.2 Geographic virafication

In addition to gender, the incidence of pancreatic cancer is varied in different countries and populations. More than half of new cases (55.5%) were registered in more developed countries and less than half (41.0%) of all new cases of pancreatic cancer were recorded in Asia in 2012. Moreover, the highest rates were seen in Northern America and Western Europe, around 7.4 per 100,000 people and 7.3 per 100,000 people, respectively, and the lowest incidence rate was seen in Middle Africa and South-Central Asia, being 1.0 per 100,000 people (Figure 1.4).

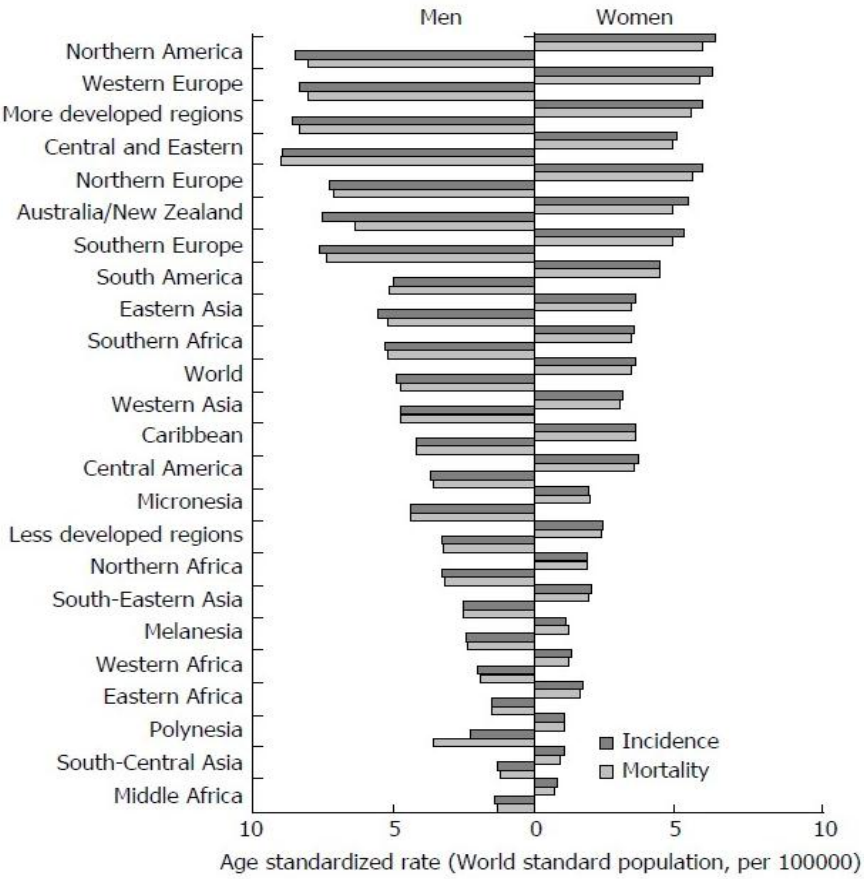

Figure1.4: The incidence and mortality of pancreatic cancer in both sexes. GLOBOCAN 2012 estimates. Source: Epidemiology of pancreatic cancer (Ilic and Ilic, 2016).

1.1.2.3 The genetics of pancreatic cancer

Approximately 5-10% of pancreatic cancers are inherited (McWilliams et al., 2005). People with a family history of pancreatic cancer in more than one first degree relative will have nearly double the risk of developing pancreatic cancer compared to those without a family history (Schenk et al., 2001).

Several inherited syndromes contribute to an increased risk of pancreatic cancer, such as Peutz-Jeghers syndrome and Lynch syndrome. Similarly, the risk is also increased in patients with hereditary pancreatic disorders, *e.*g. hereditary pancreatitis (Lowenfels et al., 2001).

Peutz-Jeghers syndrome is an autosomal dominant disorder, and the clinical syndrome includes hamartomatous polyps in the gastrointestinal tract and pigmented macules of the lips, buccal mucosa, and digits. It has been reported that patients with this syndrome would have an 11-32% lifetime risk for developing pancreatic cancer (Giardiello et al., 2000, Korsse et al., 2013). The mutation of the STK11 gene exists in more than 80% of Peutz-Jeghers cases. Considering this higher risk for Peutz-Jeghers patients, screening tests for the detection of early pancreatic neoplasia has been proposed (Canto et al., 2006, Sato et al., 2001, Wolfgang et al., 2013).

Lynch Syndrome, also known as hereditary non-polyposis colorectal cancer (HNPCC), is an autosomal dominant disease caused by germline mutations in genes responsible for DNA mismatch repair. Patients with Lynch Syndrome have

shown an increased risk of pancreatic cancer (Rustgi, 2007). An 8.6-fold increased risk of pancreatic cancer was seen in a study of 147 families with this syndrome compared with the general population (Kastrinos et al., 2009). In these families, patients with pancreatic cancer always demonstrated microsatellite instability (MSI^+) and a distinct poorly differentiated medullary histopathology, together with MSI+ colorectal cancers (Alexander et al., 2001, Wilentz et al., 2000).

Hereditary pancreatitis is a rare autosomal dominant genetic disorder caused by mutations in the cationic trypsinogen gene (*PRSS1).* The risk of having pancreatic cancer is almost 58-fold higher compared with the risk in the general population. The lifetime risk (by age 70) of pancreatic cancer is 30–40% in patients with hereditary pancreatitis (Lowenfels et al., 1997, Lowenfels et al., 2001). This risk can be even higher in patients with smoking history (Lowenfels et al., 2001).

1.1.3 Other risk factors

Increasing age is an important factor associated with the incidence of pancreatic cancer in both genders (Bosetti et al., 2012). Most patients diagnosed with pancreatic cancer are aged between 60-80 years. It is rare before the age of 40, and more than half of patients diagnosed with pancreatic adenocarcinoma are over 70 years old (Ilic and Ilic, 2016).

The causal relationship between pancreatic cancer and tobacco smoking has been confirmed by The International Agency for Research on Cancer (Ezzati et al., 2005).Tobacco smoking doubles the risk of pancreatic cancer, and the risk is accumulated with the years of smoking and the number of cigarettes smoked per day. Parkin *et al.* estimated that around 26.2% of pancreatic cancers in men and 31.0% in women were associated with tobacco smoking in the United Kingdom in 2011 (Parkin et al., 2011). Lodice *et al.,* (2008) performed a meta-analysis based on 82 studies that included the epidemiologic information about smoking and pancreatic cancer. The result showed that people who smoke cigarettes would have a 75% increased risk for pancreatic cancer in comparison with non-smokers, with the risk persisting for at least 10 years after smoking cessation (Iodice et al., 2008). The results from the European Prospective Investigation into Cancer and Nutrition (EPIC) also showed that the increased risk of pancreatic cancer can be detected in both active cigarette smokers and people exposed to environmental tobacco smoke (ETS), and that risk is decreased in people who quit smoking for 5 or more years (Vrieling et al., 2010)

The positive correlation between obesity and the risk of pancreatic cancer has been highlighted as a landmark in 2003 (Calle et al., 2003). The American Cancer Society also report that increased mortality from pancreatic cancer is associated with obesity. Those with a BMI ≥ 30 have a higher risk for pancreatic cancer compared with people with normal body mass index (Calle et al., 2003). Recent

meta-analysis presented the association between general and abdominal obesity and the elevated risk of pancreatic cancer (Berrington de Gonzalez et al., 2003). In the UK, it was estimated that around 12.8% of pancreatic cancers in men and 11.5% in women are related to obesity (Parkin et al., 2011).

Both type I and type II diabetes have been associated with increased risk of pancreatic cancer (Maisonneuve and Lowenfels, 2015). The United States National Cancer Institute estimates that patients with diabetes have around a 1-1.8 fold increased risk of pancreatic cancer, and this trend is more obvious in Hispanic men and Asians compared with Caucasian and black populations (Li et al., 2011). In Italy, it was estimated that 9.7% of pancreatic cancers might be caused by diabetes (Rosato et al., 2015). Moreover, the risk of pancreatic cancer attributed to diabetes can be reduced by the uptake of anti-hyperglycaemics or insulin (Li et al., 2011, Bosetti et al., 2014).

1.1.4 The diagnosis of pancreatic cancer

Since pancreatic cancer is mainly asymptomatic at an early stage and symptoms that do occur are often nonspecific, diagnosis is usually at an advanced stage. (Boulaiz et al., 2017). Yachida *et al.* report that around 21 years elapse from the onset of the tumour until metastasis (Yachida et al., 2010). Thus, there is a

potentially long latent phase in which early diagnosis could be made, and early diagnosis may improve the survival rate for pancreatic cancer patients.

The most common symptoms of pancreatic cancer include abdominal pain, jaundice, and weight loss. Pain is a symptom in about 70% of pancreatic cancer cases. It may be caused by tumour invasion of the celiac or mesenteric plexus. Pain in the upper back (not the lower lumbar region) can occur if the cancer spreads to the nerves around the pancreas. Jaundice occurs in about 50% of pancreatic cancer cases. It may occur when pancreatic cancer is of an early stage if the tumour is within the head of the pancreas adjacent to the common bile duct and can press on the duct leading to obstructive jaundice while the tumour is still fairly small. However, cancers located in the body or tail of the pancreas have little impact on the duct until they are larger or have spread through the pancreas, and thus are more likely to have metastasised by the time jaundice is apparent. Jaundice can also occur when pancreatic cancer spreads to the liver.

Diabetes can develop if a tumour interferes with the endocrine function of the pancreas. People with diabetes often feel thirsty, pass more urine than normal, lose weight and feel weak and lacking in energy. Diabetes is particularly associated with pancreatic cancer in older people.

Pancreatic premalignant lesions have been identified, such as pancreatic intraepithelial neoplasia (PanIN) and intraductal papillary mucinous neoplasm

(IPMN), which may be of use in screening populations with high risk of pancreatic cancer (Poruk et al., 2013, Brosens et al., 2015).

Populations with the relevant hereditary and non-hereditary diseases can be chosen for conducting screening. Age >55 years, smoking, obesity, diabetes, dietary factors, and chronic pancreatitis are the common non-hereditary risk factors. Familial pancreatic cancer (FPC), Peutz-Jeghers syndrome, and familial adenomatous polyposis (FAP) are included in hereditary factors (Urayama, 2015, Del Chiaro et al., 2014, Midha et al., 2016). The International Cancer of the Pancreas Screening (CAPS) consortium agreed that those with familial and hereditary conditions at high risk of pancreatic cancer would be suitable for endoscopic ultrasonography (EUS) or magnetic resonance imaging (MRI) based screening (Canto et al., 2012). This is in keeping with the findings of other screening studies from the U.S (Kimmey et al., 2002), Germany (Langer et al., 2009), and Holland (Poley et al., 2009).

As well as genetic mutation testing, adjunct laboratory blood tests for pancreatic cancer biomarkers would add to the efficacy of a screening program. Carbohydrate antigen 19-9 (CA 19-9), is the most widely used biomarker for pancreatic cancer; included in clinical practice for monitoring after a diagnosis of pancreatic cancer. However, due to its relatively low sensitivity and specificity (Goonetilleke and Siriwardena, 2007) it is not an ideal biomarker for the screening

and early detection of pancreatic cancer, but it is useful for determining the progression and monitoring the response to therapy (Poruk et al., 2013).

Many imaging techniques play a significant role in identifying neoplasms in patients who are highly suspected having pancreatic cancer, which include trans-abdominal ultrasound (US), computerized tomography (CT), magnetic resonance imaging (MRI), endoscopic ultrasound (EUS) and positron emission tomography (PET) (Poley et al., 2009, Boulaiz et al., 2017). US is a suitable screening test on the grounds of low price, wide availability and innocuity (Collins and Bloomston, 2009). EUS is however more accurate than US and in 2011, the EUS technique was improved by conducting a computer-aided method for distinguishing the EUS image of pancreatic cancer and extracting and classifying its textural features (Boulaiz et al., 2017). A further advantage is that EUS allows a hollow needle to be passed down the endoscope for biopsy. EUS-guided fine needle aspiration (EUS-FNA) has been developed to improve the characterization of the lesions detected by EUS, and it is particularly useful for the diagnosis of pancreatic tumours and helping to test therapeutic regimens. It has a sensitivity of 54-96%, a specificity of 96-98%, and accuracy of 83-95% for the diagnosis of pancreatic cancer (Kamata et al., 2016).

CT scanning can clearly present the pancreas and is also used to guide a biopsy needle to sample a suspect pancreatic tumour. It is also suitable for identifying small tumours and helps to decide whether the tumour can be surgically removed.

CT scans can be used to assess tumour invasion and invasive spread to other organs, and to what extent blood vessels are involved. When CT scanning is indeterminate, or for patients with contraindication, MRI may be useful for the diagnosis of pancreatic cancer especially when pancreatic and bile ducts are blocked, narrowed, or dilated (Duell et al., 2012).

Imaging and biopsy are used to determine the stage of the pancreatic cancer. This is based on the size of tumour and whether the disease has spread to the nearby structures, mainly blood vessels and organs. Stages I & II include localised tumours with or without local lymph node involvement. At stage III, the tumour may be invading tissues locally including other organs and important arteries or veins. This means they cannot be removed surgically. This stage is also called 'locally advanced'. Stage IV indicates that cancer cells have spread to other organs, most commonly the liver or the peritoneum of the abdominal cavity. Other common sites include lung and bone. Staging helps to guide which treatment and approach to take and also been related to outcomes. Survival rates are higher for the stage I&II diseases. Staging and TNM classification of pancreatic cancer is listed in Table 1.1 (Edge and Compton, 2010).

Table 1.1: TNM staging of pancreatic cancer. Source: AJCC Cancer Staging Manual, Eight Edition (Amin et al., 2017).

T category	T Criteria
TX	Primary tumour cannot be assessed
T0	No evidence of primary tumour
Tis	Carcinoma in situ. This includes high-grade pancreatic intraepithelial neoplasia (PanIn-3), intraductal papillary mucinous neoplasm with high-grade dysplasia, intraductal tubulopapillary neoplasm with high-grade dysplasia, and mucinous cystic neoplasm with high-grade dysplasia.
T1	Tumour ≤2 cm in greatest dimension
T1a	Tumour ≤0.5 cm in greatest dimension
T1b	Tumour > 0.5 cm and < 1cm in greatest dimension
T1c	Tumour 1=2 cm in greatest dimension
T2	Tumour > 2 cm and≤ 4cm in greatest dimension
T3	Tumour > 4 cm in greatest dimension
T4	Tumour involves celiac axis, superior mesenteric artery, and/or common hepatic artery, regardless of size

N Category	N Criteria
NX	Regional lymph nodes cannot be assessed
N0	No regional lymph node metastases
N1	Metastasis in one to three regional lymph nodes
N2	Metastasis in four or more regional lymph nodes

M Category	M criteria
cM0	No distant metastasis
cM1	Distant metastasis
pM1	Distant metastasis, microscopically confirmed

0	Tis	N0	M0
IA	T1	N0	M0
IIB	T1	N1	M0
III	T1	N2	M0
IB	T2	N0	M0
IIB	T2	N1	M0
III	T2	N2	M0
IIA	T3	N0	M0
IIB	T3	N1	M0
III	T3	N2	M0
III	T4	Any N	M0
IV	Any T	Any N	M1

1.1.5 The treatment of pancreatic cancer

1.1.5.1 Surgery

At diagnosis, surgery with an intention to cure is only possible for around 10-20% of patients. The evaluation before surgery of pancreatic cancer includes the assessment of the relationship between the tumour and the adjacent major vessels such as the portal vein (PV), superior mesenteric vein (SMV), superior mesenteric artery (SMA), celiac axis (CA) and hepatic artery (HA), together with the presence of metastases (Ansari et al., 2016). The surgical procedure is a pancreaticoduodenectomy, also named Whipple's procedure (Figure 1.5), which was established by Allen Oldfather Whipple. The operation is conducted by removal of the distal half of the stomach, gallbladder, distal portion of the common bile duct, head of the pancreas, duodenum, proximal jejunum and lymph nodes. Pancreaticojejunostomy, choledochojejunostomy, and gastrojejunostomy are then required for reconstruction of the digestive tract. A portion of the pancreas remains, as a total pancreatectomy often leads to brittle diabetes. An important modification of the Whipple's procedure is the pylorus preserving pancreaticoduodenectomy (PPPD) which preserves the whole stomach and is suitable for localised pancreatic cancer in pancreatic head part. However, no significance was found in age, sex distribution, tumour localization, and staging when comparing PPPD with standard Whipple’s operation in a prospective randomized multicentre study (Michalski et al., 2007, Tran et al., 2004).

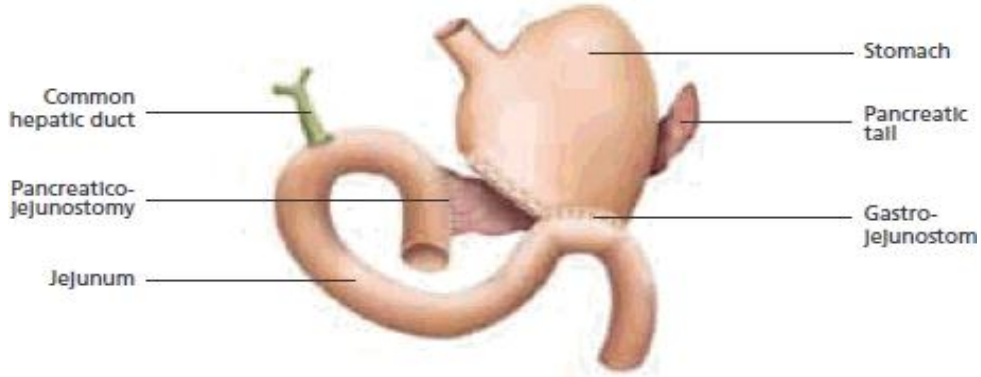

Figure 1.5: Anatomy and anastomoses after a Whipple's procedure. Source: The role of surgery for pancreatic cancer: a 12-year review of patient outcome (Badger et al., 2010)**.**

1.1.5.2 Chemotherapy

Over the years, chemotherapy for the treatment of pancreatic cancer has only provided modest progress in improving patient survival. The single agent gemcitabine had been a standard-of-care first-line treatment for advanced pancreatic cancer for more than 2 decades, as it was indicated to be superior to 5-Fluorouracil (5-FU) in patients with a Karnofsky performance status (KPS) ≥ 50. Gemcitabine made an improvement of 5-weeks' survival duration and improved quality of life for advanced pancreatic cancer patients compared to 5-FU. Burris *et al.,* (1997) conducted a randomized controlled trial of 126 patients with advanced pancreatic cancer using either gemcitabine (1,000mg/m^2weekly for 7 weeks followed by 1 week off, then on days 1, 8, and 15 of a 28-day cycle), or 5-FU 600mg/m^2 weekly. The result showed that patients who took gemcitabine presented not only a clinical benefit, but also a better median overall survival and

overall one-year survival rate (Burris et al., 1997). Thus, gemcitabine was approved by the Food and Drug Administration (FDA) as the first-line treatment for advanced pancreatic cancer.

Several studies have been conducted by adding other drugs to gemcitabine, but the results are unsatisfactory. The combination of gemcitabine, cisplatin, epirubicin and 5-FU (PEFG regimen) was considered promising due to an extra progression-free survival (PFS) of 4 months in 60% of the combination group compared with a control group. However, this result is difficult to be generalised because of the small sample of patients (Reni et al., 2005).

Overexpression of epidermal growth factor receptor (EGFR), a transmembrane tyrosine kinase receptor, is present in up to 90% of pancreatic cancer samples (Fjallskog et al., 2003, Tobita et al., 2003), and indicates that small molecule inhibitors targeting the EGFR tyrosine kinase domain, could prove to be promising therapeutic agents. In a phase III trial involving 569 patients with locally advanced or metastatic pancreatic adenocarcinoma, the combination therapy of gemcitabine with erlotinib (an inhibitor of EGFR tyrosine kinase) presented a statistically significant improvement in survival compared to gemcitabine treatment alone (Moore et al., 2007). It has been approved by the FDA for the treatment of advanced pancreatic adenocarcinoma.

Currently, two phase III studies of combination therapies have shown a significant benefit for overall survival of patients and the proposed regimens were approved by FDA as standard treatment regimens for patients with advanced pancreatic cancer. The FOLFIRINOX (the 5-FU, leucovorin, irinotecan, combination) chemotherapy regimen is able to improve the survival of patients with advanced pancreatic cancer compared with gemcitabine alone (Conroy et al., 2011). Conroy *et al.,* (2011) performed a randomized phase II/III trial including 342 patients with previously untreated metastatic pancreatic cancer using FOLFIRINOX or gemcitabine. The result showed that patients treated with FOLFIRINOX had a significantly improved median overall survival of 11.1 months compared with 6.8 months taking gemcitabine (Conroy et al., 2011). In 2015, Ferrone *et al.* found that patients with borderline resectable pancreatic cancer presented a significant decrease in tumour size, lymph node positivity, operative morbidity, and peri-neural invasion by treated with neoadjuvant FOLFIRINOX (Ferrone et al., 2015). Currently, FOLFIRINOX has been considered as one of the first-line regimens for patients with metastatic pancreatic cancer who have a good performance status. The second trial examined a combination of gemcitabine and nab-paclitaxel. When comparing gemcitabine and gemcitabine-nab-paclitaxel in the Metastatic Pancreatic Adenocarcinoma Clinical Trial (MPACT), the median overall survival (mOS) was 8.5 months in the combination group versus 6.7 months in the control arm (HR, 0.72; 95% CI, 0.62–0.83; $P < 0.001$). However, combination therapy does

appear to have significant side effects, such as neutropaenia (38%), fatigue (54%), peripheral neuropathy and alopecia (50%)(Vishnu and Roy, 2011).

1.2 Molecular and cellular mechanisms in pancreatic cancer

Molecular alterations lead to the development and progression of pancreatic cancer. The occurrence and development of pancreatic cancer is affected by numerous factors and events including genetic and epigenetic alterations, as well as deregulated signalling pathways (Khan et al., 2017). A better understanding of the molecular mechanisms involved in pancreatic tumorigenesis may help to identify novel biomarkers for the early diagnosis of pancreatic cancer, and therapeutic targets. In recent years, some critical molecules have been implicated in the progression of pancreatic cancer (Bhardwaj et al., 2016, Zubair et al., 2016, Whatcott et al., 2015). The formation and metastasis of pancreatic cancer undergoes a multistep process from pancreatic intraepithelial neoplasia (PanIN) lesions to invasive carcinomas (Figure 1.6) (Hidalgo, 2010, Makohon-Moore and Iacobuzio-Donahue, 2016). According to the cellular and nuclear atypia, PanIN is further classified into low grade lesions (PanIN-1A/B) to high grade lesions (PanIN-3) (Hruban et al., 2000). During this process from PanIN1 to PanIN3, several genetic changes such as gain or loss of tumour promoting/suppressor genes and microRNAs (miRNAs) are accumulated and finally lead to an invasive phenotype

(Weissmueller et al., 2014, Makohon-Moore and Iacobuzio-Donahue, 2016, Yonemori et al., 2017, Khan et al., 2013).

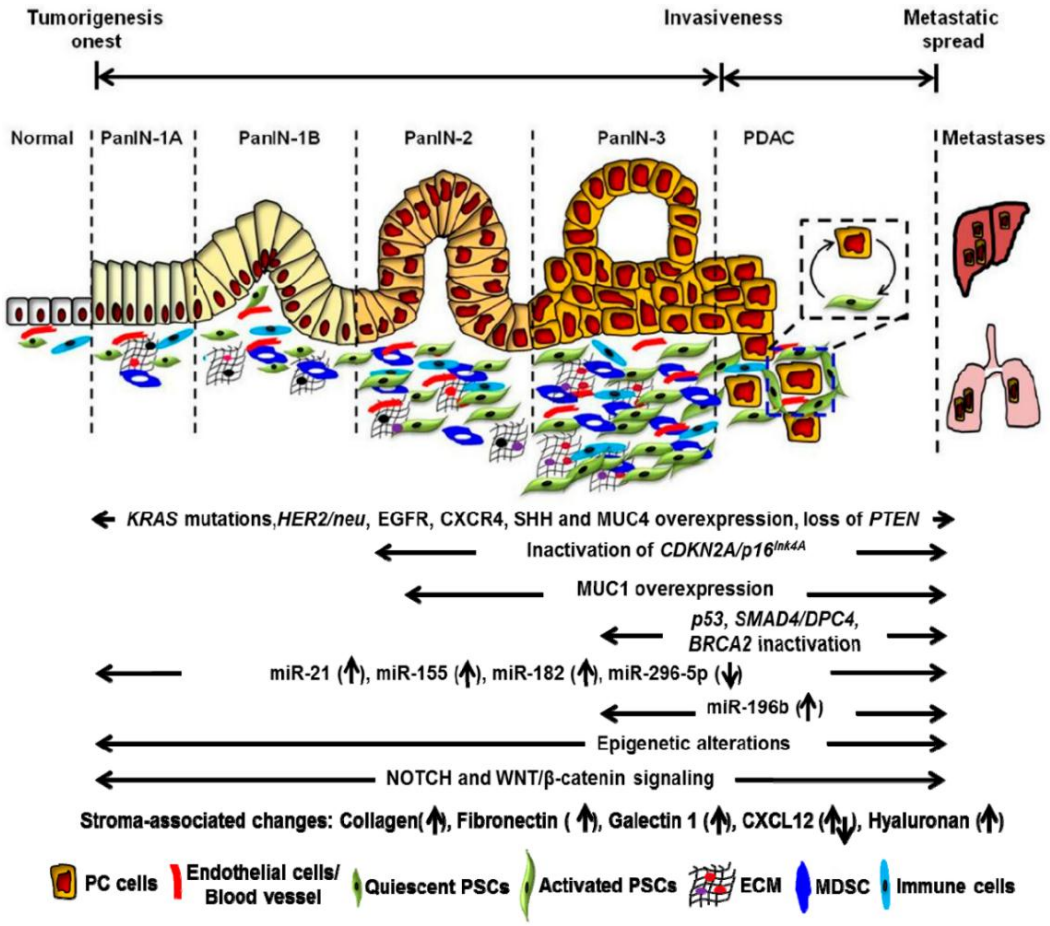

Figure 1.6: Histopathological and molecular changes in the progression of pancreatic adenocarcinoma. The development of pancreatic cancer includes normal epithelium, low-grade pancreatic intraepithelial neoplasia (PanINs), high-grade PanIN, and invasive carcinoma. During this process, numerous genetic alterations such as KRAS, CDKN2, TP53, SMAD4/DPC4 and BRCA2 are involved. Resource: Molecular drivers of pancreatic cancer pathogenesis: Looking inward to move forward by Khan MA Int J Mol Sci (Khan et al., 2017).

1.2.1 K-ras mutation

The mutation of Kirsten rat sarcoma oncogene homolog (K-ras) has been found in 30% of early panIN1 lesions, however, K-ras mutation is present in 95% of advanced pancreatic cancers (Pylayeva-Gupta et al., 2011, Eser et al., 2014). This evidence is also supported by mouse models whereby the activation of a mutant K-ras allele resulted in the mice developing PanIN lesions, and when in combination with the deletion of a tumour suppressor allele resulted in progression to invasive PDAC (Aguirre et al., 2003).

Point mutation of K-ras mainly occurs in codon 12 with the substitution of glycine with asparate, valine or arginine, and its mutation results in GTP-bound protein accumulation leading to an active conformation (Jonckheere et al., 2017). The mutation of K-ras leads to a constitutive activation of its downstream oncogenic signalling, which is required for initiation, progression and maintenance of pancreatic cancer (Pylayeva-Gupta et al., 2011, di Magliano and Logsdon, 2013). The most direct regulators attribute to the activation of Mitogen-Activated Protein Kinase (MAPK), Phosphoinositide 3-Kinase (PI3K) and Ral Guanidine exchange factor (RalGEF) signalling pathways (Jonckheere et al., 2017). The activation of MAPK pathway is associated with a poor prognosis in pancreatic cancer (Handra-Luca et al., 2012). K-ras induced Extracellular signal-Regulated Kinase (ERK) signalling pathway promotes migration and invasion of pancreatic cancer cells

leading to a poorer survival (Neuzillet et al., 2013, Endo et al., 2009, Zhao et al., 2010).

1.2.2 P16

P16, also known as Cyclin-dependent kinase inhibitor 2A (CDKN2A) is a critical regulator involved in cell cycle, targeting CDK4 and CDK6 and abolishing their interaction with cyclinD1 (Asghar et al., 2015). Deregulated progression of cell cycle caused by loss of function of p16 includes mis-sense mutation, promoter methylation, and small deletion or loss of heterozygosity (Scaini et al., 2009). P16 alterations are also related to the aggressiveness of pancreatic cancer. Ohtsubo *et al.,* (2003) found that pancreatic cancer patients with larger tumours present a decreased expression level of p16 (Ohtsubo et al., 2003). Furthermore, pancreatic cancer patients who have a p16 mutation or hypermethylation show larger tumours and shorter survival period compared with pancreatic carcinoma with an unaffected p16 gene (Ohtsubo et al., 2003). There is also a significant correlation in histological grade of pancreatic malignancy with loss of p16, and metastasis is more likely in cases without p16 expression (Hu et al., 1997).

1.2.3 P53

The p53 tumour suppressor gene, located on chromosomal arm 17p, is inactivated in 50% to 75% of pancreatic carcinomas. It has been reported that the inactivation is due to intra-genic mutation, accompanied with a loss of the second allele of p53, which impairs the cell cycle and cell apoptosis (Redston et al., 1994, Morton et al., 2010). The altered p53 gene coupling with other genetic abnormalities, has been shown in some studies. Xiang *et al.,* (2016) found that p53 together with cavin-1, is correlated with poorer survival for patients with resectable pancreatic ductal adenocarcinoma. Moreover, the mutation of p53 increased the invasion and metastasis of pancreatic cancer cells *in vitro* and *in vivo* through up regulation of cavin-1 and enhanced cavin-1/caveolin-1 signalling (Xiang et al., 2016). The altered p53 gene is also related to progression of pancreatic cancer when present in PanIN lesions. Weissmueller *et al.,* (2014) showed that the invasive phenotype of pancreatic cancer cells requires the sustained expression of mutant p53 (Weissmueller et al., 2014).

1.2.4 SMAD4/DPC4

SMAD4, locating on chromosomal arm 18q, is an important transcriptional regulator involved in transforming growth factor-beta (TGFβ) signalling by transducing extracellular signals of TGFβ to the nucleus and regulating cell

functions (Hruban et al., 2001). The major role of SMAD4 is to inhibit cell proliferation by inducing an arrest of cell cycle at the G1 phase. It has been indicated that inactivation of SMAD4 due to allelic deletion or intra-genic mutation mainly occurs in the late stages of PDAC development (Chen et al., 2014). Furthermore, reduced expression of SMAD4 is considered an independent prognostic factor regarding tumour progression, Epithelial-Mesenchymal Transition (EMT) and therapy failure (Lopez-Gomez et al., 2015).

1.2.5 BRCA1 and BRCA2

BRCA1 and BRCA2 have a wide range of biological functions, such as transcription regulation and DNA repair. It has been reported that individuals who have BRCA1 and BRCA2 mutations gain 2.2 and 3.5 fold higher risk respectively for the development of pancreatic cancer (Greer and Whitcomb, 2007, Iqbal et al., 2012, Thompson et al., 2002). Goggins and co-workers found that biallelic inactivation of the BRCA2 gene occurs only at a late stage in the development of pancreatic cancer. This finding was supported by another observation that the loss of wild-type allele of BRCA2 only existed in high-grade PanIN (PanIN-3) lesions rather than in the low-grade PanIN (PanIN-1) lesions (Goggins et al., 1996). A binding partner of BRCA2 named PALB2 was also found be abnormal in familial pancreatic cancer (Jones et al., 2009). PALB2 mutation, together with germline mutations of BRCA2,

is associated with eventual onset of pancreatic cancer due to increased accumulation of damaged DNA by changing the DNA repair pathway (Rustgi, 2014).

1.2.6 Epidermal growth factor receptor (EGFR)

The epithelial growth factor receptor, also known as Human Epidermal Growth Factor 1 (HER-1), or v-erb-b2 erythroblastic leukaemia viral oncogene homolog 1 (ERBB-1), is a tyrosine kinase receptor. Amplification and mutation of this gene has been identified in several cancer types, such as non-small-cell lung cancer (NSCLC), metastatic colorectal cancer, glioblastoma, head and neck cancer, and breast cancer (Normanno et al., 2006). The up regulation of EGFR promotes proliferation, differentiation and metastasis of pancreatic cancer through downstream pro-oncogenic signalling pathways, including the RAS-RAF-MEK-ERK MAPK and AKT-PI3K-mTOR pathways (Oliveira-Cunha et al., 2011).

1.2.6.1 EGFR Structure and expression

EGFR is located at chromosome 7 short arm q22, spanning 110 kb of DNA containing 28 exons (Davies et al., 1980, Kondo and Shimizu, 1983). Generally normal cells express 4×10^4 to 1×10^5 EGF receptors, however, tumour cells can express more than 2×10^6 receptors per cell (Herbst and Shin, 2002). The EGFR protein is synthesized as a 1210 residue precursor that is cleaved at the N-terminal

to result in the mature 1186 residue transmembrane EGFR (Ullrich et al., 1984). From N-terminal to C-terminal, the EGFR consists of an extracellular domain, a hydrophobic transmembrane region, and a tyrosine kinase-containing cytoplasmic region (Roskoski, 2014). EGFR belongs to the ERBB family, which also include HER-2/ERBB2, HER-3/ERBB3, and HER4/ERBB4. All the ERBB family members share the same structures and can form 28 different combinations coupling with each other through homo- and heterodimers (Lemmon and Schlessinger, 2010).

1.2.6.2 EGFR signalling

EGFR activation is generated through the binding of ligands to the extracellular domains of monomeric EGFR. Various ligands are involved in the activation of EGFR and the common ones include Epidermal Growth Factor (EGF) and Transforming Growth Factor alpha (TGF-α). Both EGF and TGF-α are expressed as integral membrane proteins and are able to release soluble mature ligand through a cleavage by metalloproteinases.

The ligand binding to receptor results in dynamic conformational changes, homodimer and heterodimer formation, as well as tyrosine kinase activation (Yarden and Sliwkowski, 2001, Oliveira-Cunha et al., 2011). In the C-terminal tail and the kinase domain, EGFR dimerisation leads to an auto-phosphorylation of the tyrosine residues. These residues act as binding sites for subsequent recruitment

and docking of various signalling modules containing the Src homology 2 (SH2) domain, involving kinases, adaptor proteins, ubiquitin ligases, and transcriptional factors (Yarden and Pines, 2012). Activation of these signalling molecules by binding to EGFR results in activation of downstream signalling pathways, including the RAS/RAF/ MEK/ ERK, PI3K/ AKT/ mammalian target of rapamycin, and Janus kinase (JAK)/ signal transducer and activator of transcription (STAT) pathways. Finally, these signalling pathways induce a variety of cell responses such as the activation of cell proliferation, promotion of angiogenesis, cell survival and apoptosis inhibition (Figure 1.7) (Yamaoka et al., 2017).

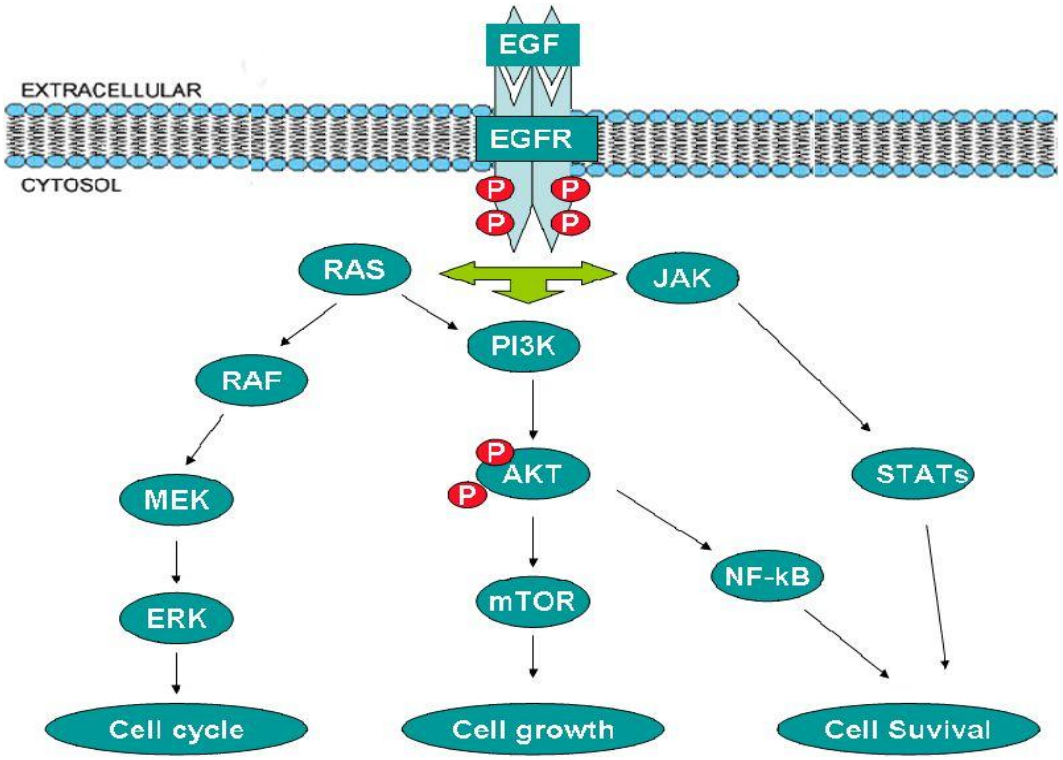

Figure 1.7: Signal transduction pathways controlled by the activation of epidermal growth factor receptor. EGFR is activated by its growth factor ligands, and the dimerisation of EGFR activates its intrinsic intracellular protein-tyrosine kinase activity. The occurrence of EGFR auto-phosphorylation through several tyrosine residues triggers the activation of downstream signalling cascades including the RAS/extracellular signal regulated kinase (ERK) pathway, the phosphatidylinositol 3-kinase/AKT (PI3K/AKT) pathway and the Janus kinase/Signal transducer and activator of transcription (JAK/ STAT) pathway. The activation of these signalling pathways are involved in the regulation of cell growth, cell cycle, and cell survival. Source: The Role of Cyclooxygenase-2, Epidermal Growth Factor Receptor and Aromatase in Malignant Mesothelioma.

1.2.6.3 Mutations and amplification of EGFR in cancer

EGFR mutations have been detected in the extracellular region, the kinase domain, and the C-terminal tail (Pines et al., 2010). These mutations of different sites have been shown in different types of cancer. Ectodomain mutation is present in most glioblastomas, whereas NSCLCs exhibit a preference of harbouring kinase domain mutation (Pines et al., 2010, Lee et al., 2006). Rare EGFR gene mutation has also been identified in colorectal cancers (Moroni et al., 2005). The EGFR variant EGFR VIII generated from the loss of amino acids 6-273 (encoded by exons 2-7) occurs in approximately 20% of glioblastoma (Lee et al., 2006, Gan et al., 2013). Additionally, mutations in the EGFR kinase domain clustered around the ATP-binding pocket of the enzyme have been observed in NSCLC (Sharma et al., 2007).

EGFR gene amplification has been found in various human tumours, including lung, head and neck, oesophageal, and colorectal cancers (Yarden and Pines, 2012). In NSCLC, 40%-80% patients harboured EGFR overexpression due to changes in gene copy number and epigenetic transcriptional activation (Merrick et al., 2006). Amplification of the EGFR gene has also been detected in colorectal cancer (CRC). Several studies using fluorescence *in situ* hybridization have demonstrated that approximately 40% of CRC tumours harbour increased EGFR gene copy number (Barber et al., 2004, Jiang et al., 2013). Increased expression of EGFR and its ligand have been detected in up to 90% of human pancreatic cancers (Lemoine et al.,

1992), but the correlation of EGFR expression and pancreatic tumour grade, size, or lymph node status is unknown (Bloomston et al., 2006).

1.2.6.4 Targeting EGFR therapy

Considering the role of the EGFR signalling pathways in cancer development, several therapeutic agents such as monoclonal antibodies (mAbs) and small-molecule tyrosine kinase inhibitors (TKIs), have been used to target EGFR for the treatment of human cancers (Table 1.2). mAbs compete with endogenous ligands by binding to the extracellular domain of EGFR and block the subsequent EGFR tyrosine kinase activation (Burgess et al., 2003). Currently, Cetuximab and Panitumumab are the two most progressive mAbs applied in clinical treatment which target the extracellular domain of the EGFR. Cetuximab (Erbitux), an IgG1 human mouse chimeric monoclonal antibody, has been used for the treatment of metastatic CRC and Squamous Cell Carcinoma of the Head and Neck (SCCHN) (Yamaoka et al., 2017). Panitumumab (Vectibix) is a human mAb specific to EGFR, approved by the FDA for the treatment of metastatic CRC (Yamaoka et al., 2017).

TKIs are ATP mimetics that bind to the receptor's kinase pocket, which excludes ATP and prevents signal transduction (Ciardiello and Tortora, 2008). To date, both Gefitinib (Iressa) and erlotinib have been approved by the FDA for the treatment of advanced or metastatic NSCLC. A combination of erlotinib with

gemcitabine has been approved for the treatment of locally advanced or metastatic pancreatic cancer (Modjtahedi and Essapen, 2009).

Table 1.2: Epidermal growth factor receptor (EGFR) tyrosine kinase inhibitors and anti-EGFR monoclonal antibodies approved for cancer treatment.

EGFR TKIs	Approved Indication	Target
Gefitinib (*Iressa*)	Metastatic non-small cell lung cancer (NSCLC) with *EGFR* exon 19 deletions or exon 21 mutation (L858R)	EGFR
Erlotinib (*Tarceva*)	Metastatic or locally advanced NSCNC, with EGFR exon 19 deletions or exon 21 mutation (L858R) Metastatic or advanced pancreatic cancer in combination with gemcitabine	EGFR, PDGFR, c-Kit
Afatinib (*Gilotrif*)	Metastatic NSCLC with *EGFR* exon 19 deletions or exon 21 mutation (L858R)	EGFR, HER2, HER4
Osimertinib (*Tagrisso*)	Metastatic *EGFR* T790M mutation-positive NSCLC, with progressive disease following first-line EGFR TKI therapy	EGFR T790M
Olmutinib (*Olita*)	Second-line treatment of NSCLC with the T790M mutation in *EGFR* (in Korea)	EGFR T790M
Lapatinib (*Tykerb*)	HER2-overexpressing breast cancer	EGFR, HER1, HER2
Vandetanib (*Caprelsa*)	Medullary thyroid carcinoma	EGFR, VEGFR, Ret

EGFR-Targeted mAbs	Approved Indication	Target
Cetuximab (*Erbitux*)	Metastatic KRAS-negative CRC/SCCHN	EGFR
Panitumumab (*Vectibix*)	Metastatic KRAS-negative CRC	EGFR

Source: Molecular-Targeted Therapies for Epidermal Growth Factor Receptor and Its Resistance Mechanisms by Yamaoka T. Int J Mol Sci (Yamaoka et al., 2017).

1.2.7 Epithelial-mesenchymal transition (EMT)

EMTs is a cell biological program initially identified as playing a vital role in embryonic development (Kalluri, 2009). EMT is indispensable when a non-motile epithelial cell acquires invasive capacities during the process of losing polarized cellular organization, cell-cell junction breakdown, cell matrix adhesion

remodelling, and changes towards a mesenchymal state (Mitra et al., 2015, Martin and Jiang, 2009).

The association between tumorigenesis and EMT is established through enhanced invasiveness and metastasis and the acquisition of therapy resistance (Singh and Settleman, 2010, Radisky and LaBarge, 2008). The activation of the EMT program triggers cancer cells to disseminate from the primary tumour, invade adjacent tissues, migrate through the bloodstream or lymphatic system and ultimately generate secondary cancer sites. (Ocana et al., 2012, Tsai et al., 2012) (Figure 1.8). However, some metastatic tumours from prostatic cancer, breast carcinoma, colorectal cancer, ovarian cancer may represent some epithelial phenotype and certain histological features of the tissues from where they are derived. Thus, a mesenchymal-epithelial transition (MET) in the metastatic sites was postulated to be happening when the disseminated tumour cells undergo this reverse transition at the site of metastases and is involved in the formation of the secondary tumour (Yao et al., 2011).

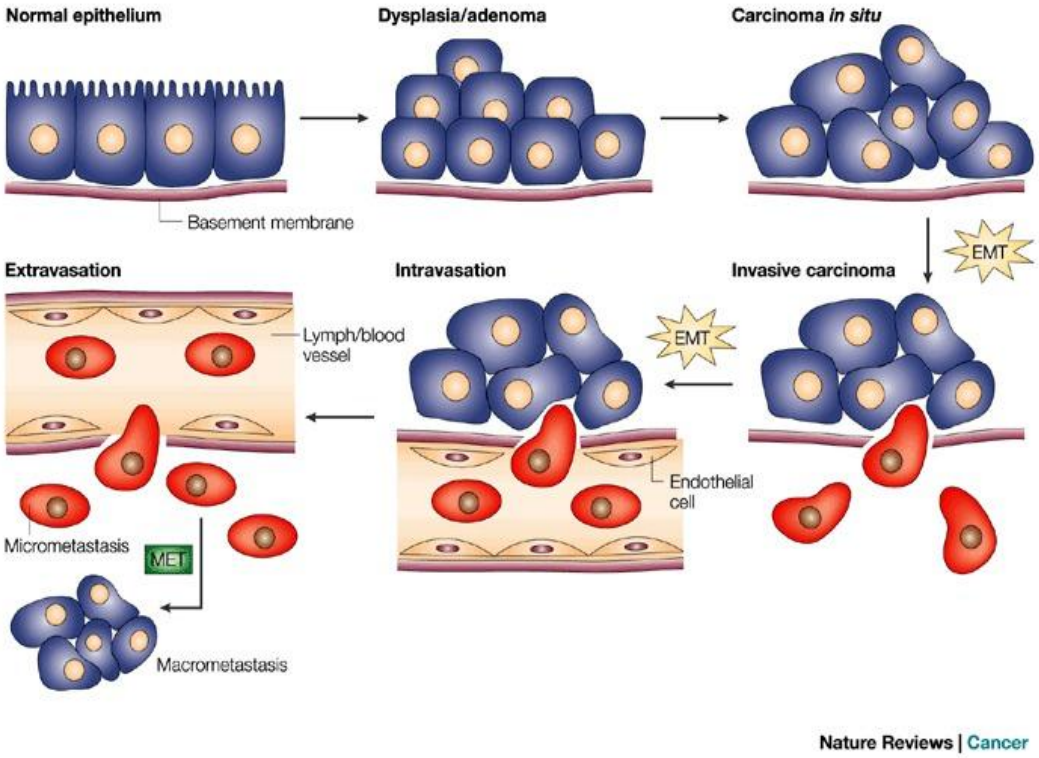

Figure1.8: The progression of carcinoma undergoes EMT and MET. The formation of adenoma can be caused by the local proliferation of normal epithelia lined by a basement membrane, and its further transformation caused by epigenetic changes and genetic alterations give rise to a carcinoma *in situ*. Further alterations can lead to EMT and the carcinoma cells disseminating. The cells extravasate into lymph or blood vessels and are transported to distant organs, where they form a new carcinoma through a MET at secondary sites. Source: Epithelial-mesenchymal transitions in tumour progression by Thiery, J.P. Nat. Rev. Cancer 2, 442-454 (Thiery, 2002).

1.2.7.1 EMT and tumour progression

The transition from an epithelial cell into a mesenchymal cell requires the alteration of cell morphology and cell-matrix adhesion. Also, the acquisition of migration abilities is pivotal in this process. The earliest occurrence of EMT might start from loss of cell polarity, and subsequently a dissolution of tight junctions (McCaffrey et al., 2012, Martin-Belmonte et al., 2007, Li et al., 2014, Huang et al., 2012). Thus, loss of E-cadherin (epithelial marker) and acquisition of vimentin (mesenchymal marker) are considered an important event during the EMT process (Prieto-Garcia et al., 2017). The biological function of E-cadherin is to keep the mobility of tumour cells during dissemination and maintain cell-cell interaction and cytoskeleton stabilisation. Thus, the breakdown of adherens junctions caused by the down-regulation of E-cadherin expression, leads to loss of cell polarity and acquisition of a mesenchymal phenotype with migratory abilities (Wijnhoven et al., 2000, Ghahhari and Babashah, 2015). It has been reported that several factors, such as TGF-β or Fibroblast Growth Factor (FGF) are involved in this complex process. Also, several tyrosine kinase receptor (RTKs), WNT/β-catenin, NOTCH and HEDGE-HOG signalling pathways, transcription factors (TFs), miRNAs, and epigenetic and post-translational modifications are implicated in the activation of EMT (Prieto-Garcia et al., 2017).

1.2.7.2 EMT regulation in cancer

Apart from the role of EMT in normal embryonic development, evidence has also accumulated identifying its role in tissue fibrosis and cancer metastasis (Kalluri and Neilson, 2003). In March 2008, during an EMT meeting at Cold Spring Harbor Laboratory, researchers suggested that EMT was to be classified into three general subtypes according to different functional consequences. Type 1 EMT can give rise to mesenchymal cells that have the potential to generate secondary epithelial cells via mesenchymal-epithelial transition (MET). This process is related to embryonic gastrulation and neuroepithelium generating motile neural crest cells. Type 2 EMT involves secondary epithelial or endothelial cells transitioning to resident tissue fibroblasts, which are induced in response to persistent inflammation in mature tissues. Type 3 EMT occurs when epithelial carcinoma cells undergo genetic and epigenetic changes, and transit to metastatic tumour cells. Carcinoma cells that undergo type 3 EMT may acquire the ability to migrate through the blood stream and generate secondary nodules, thus lead to the formation of distant metastatic lesions (Kalluri and Weinberg, 2009). In pancreatic cancer, EMT associated with cancer development underlying invasion, dissemination, and metastasis, has been widely investigated (Hugo et al., 2007). During EMT, several biomarkers have been used to demonstrate the transition from epithelial cells to mesenchymal cells (Table 1.3). The most commonly used epithelial markers are E-cadherin, integrins, and cytokeratin, whereas the mesenchymal markers are N-cadherin, vimentin or

fibronectin (Thiery et al., 2009). However, not all cells acquire mesenchymal traits in EMT. Cells in early EMT may only include loss of E-cadherin without gaining N-cadherin. This observation reflects different biological results of the intermediate stages and might result in different molecules during migration and invasion compared with those that gain N-cadherin (Chu et al., 2006, Halbleib and Nelson, 2006). According to this phenomenon, it has been suggested that not only these epithelial or mesenchymal markers and traits are altered during EMT, but also other molecules being essential for the biological processes associated with EMT such as invasion, survival and proliferation should be considered as altered too (Zhou et al., 2017).

Table 1.3: EMT markers.

	Acquired markers	Attenuated markers
Cell –surface proteins	N-cadherin	E-cadherin
Cytoskeletal markers	Vimentin β-Catenin	Cytokeratin
Transcriptional factors	Snail slug zeb1 twist	
ECM proteins	α1 (I) collagen α1 (III) collagen	α1 (IV) collagen Laminin1
miRNAs	miR 10b miR-21	Mir-200 family

Source: Biomarkers for epithelial-mesenchymal transitions (Zeisberg and Neilson, 2009).

Downregulation or inactivation of the E-cadherin gene (CDH1) has been described during tumour cell progression, and this may be caused by up regulation of CDH1 transcriptional repressors, known as EMT transcriptional factors (TFs). The EMT-inducing transcription factor (EMT-TFs) not only plays a role in regulation of cell progression, invasion, and migration, but is also involved in protecting cells from senescence and apoptosis. Also, a role for EMT-TFs in resistance to chemotherapy and radiotherapy has been identified (Nieto, 2011, Ansieau et al., 2008, Mejlvang et al., 2007). As TFs, snail, slug, zeb, and twist have been identified in promoting EMT (De Craene and Berx, 2013). Snail, slug and zeb are reported as

direct repressors of E-cadherin since they bind to conserved E-box sequences in the promoter of E-cadherin and repress its transcription (Prieto-Garcia et al., 2017). Furthermore, loss of E-cadherin can also trigger certain epithelial cells switching to a mesenchymal state (Onder et al., 2008). The reexpression of E-cadherin and downregulation of zeb, snail, slug, or twist, are usually referred as important hallmarks of MET (Yao et al., 2011).

It has been indicated that TGF-β, a secreted factor from stroma, is implicated in inducing EMT through activation of SMAD2 signalling or other non-canonical signalling pathways such as PI3K/AKT or MAPK/ERK pathways (Massague, 2012). TGF-β can also interact with other growth factors such as the epidermal growth factor (EGF) to affect the malignant transformation of cancer stem cells as well as the activation of cancer-associated stromal fibrosis (Zhou et al., 2017).

In addition to the regulation of this transcriptional program, a number of small non- coding RNAs or miRNAs have been reported as playing a vital role in the EMT process (De Craene and Berx, 2013). Depending on the different cell contexts, miRNAs can either promote or repress EMT. The most intensively studied miRNAs include the miR-200 family which consists of miR-200a, miR-200b, miR-429 on human chromosome 1, miR-200c and miR-141 on human chromosome 12 (Korpal et al., 2008). miRNAs can target different EMT-related signalling pathways and contribute to cancer development. Parikh *et al.*, (2014) identified that in ovarian cancer, miR-181a can induce TGF-β-mediated EMT through the suppression of

Smad 7 (Parikh et al., 2014). In breast cancer, promotion of EMT and metastasis can be caused by ectopic overexpression of miR-374a through targeting several negative regulators of the Wnt/beta-catenin signalling cascade both *in vivo* and *in vitro* (Cai et al., 2013). Taken together, miRNAs are supposed to modulate EMT networking by coordinating TFs or reinforcing the EMT signalling network.

1.3 Kidins220/ARMS

Scaffold proteins have evolved mechanisms for efficiently interacting with certain signalling pathways and maintaining cellular structure. This is achieved through the regulation of the cytoskeleton, cell adhesion, and migration, allowing cells to survive and grow in a variable environment. Dysregulation of certain scaffold proteins has been implicated in malignancies, including cancer development and metastasis. In mammals, an example of such multi-functional transmembrane scaffold proteins is Kinase D-interacting substrate of 220kDa/ Ankyrin repeat-rich membrane spanning (Kidins220/ARMS). Kidins220 is a highly convserved integral membrane protein, which was initially identified as a substrate for protein kinase D (PKD), a serine/threonine kinase responsible for regulation of several cell processes (Iglesias et al., 2000). Despite recent studies demonstrating the role of Kidins220/ARMS in neurotrophin response, it is increasing apparent that Kidins220 is involved in the regulation of many cellular functions. Kidins220 dysregulation occurs in several human diseases including neurodegeneration and

cancer, and thus there is increasing effort to pharmacologically target this protein. Here, we review our current understanding of Kidins220 and discuss further discuss possible links of Kidins220/ARMS to malignancies.

1.3.1 Kidins220/ARMS

Initially discovered in the nervous system, Kidins220, responding to variable environment cues, coordinates neuronal survival, differentiation, and plasticity (Lipsky and Marini, 2007, Gomez-Palacio-Schjetnan and Escobar, 2013, Benoit et al., 2001). In the nervous system, Kidins220 is one of the downstream substrates for tropomyosin-related kinase (Trk) signalling (Scholz-Starke and Cesca, 2016). In mammal neural tissues, Kidins220 has a high binding affinity for neurotrophins and localizes to the tips of neurites abundant and enriched with expression of ephrin receptors and neurotrophins (Aravind et al., 2004). In the nervous system, Kidins220 acts as a platform for protein-protein interactions, where its multiple domains recruit downstream receptor substrates, resulting in the activation of signalling pathways which lead to neuronal differentiation, survival, cytoskeleton remodelling, synaptic plasticity and dendrite and synapse development (Neubrand et al., 2012). The development of the vascular system involves Kidins220 interacting with vascular endothelial growth factor receptors (VEGFR). Knockout of Kidins220 resulted in the impairment of the VEGF signalling pathway, whilst an

in vivo study revealed that mice lacking Kidins220 developed cardiovascular abnormalities (Cesca et al., 2011).

1.3.2 Kidins220 structure, expression, and localization

The Kidins220 gene encodes a protein of 1715 amino acids. Kidins220 protein comprises 11 ankyrin-repeats within the N-terminal region, a proline-rich stretch, a Sterile alpha motif (SAM) domain (Kong et al.), kinase light chain (KLC)-interacting motif (KIM), and a PSD-95, Dlg, ZO-1 (PDZ)-binding motif at its C-terminal. It contains four transmembrane segments in the central part of the molecule and N- and C-terminal tails both exposed to the cytoplasm. Kidins220 is the target of a molecule called protein kinase D, which first gained attention due to its broad regulation of neuronal properties. Biochemical processes led to the purification and identification of multiple Kidins220 domains which act as regulators in a variety of cell signalling pathways.

Originating from monocytes, immature dendritic cells in peripheral blood have been shown to express high levels of Kidins220. Therefore, currently the cytoskeleton remodelling driven via Kidins220, is best characterised in immature dendritic cells (Riol-Blanco et al., 2004). Upon migration onto extracellular matrices highly polarised immature dendritic cells change stage, from monopolar to symmetrical bipolar. During this process, Kidins220 is highly expressed at the

dendritic cells polarised membrane edges, where F-actin localises (Riol-Blanco et al., 2004). Further immunocytochemistry analysis has revealed that Kidins220 expression was concentrated around proteins which are associated with the raft compartment (Riol-Blanco et al., 2004). Lipid rafts are microdomains of the cell plasma membrane and contain distinctive protein and lipid constituents, which are involved in the regulation of signalling transduction. Chemically induced disruption of lipid rafts resulted in the loss of Kidins220 from the enriched polarised edges, indicating a regulatory role of Kidins220 in cell morphology changes and motility (Riol-Blanco et al., 2004, Cabrera-Poch et al., 2004).

Kidins220 is expressed in developing muscle and has also been observed at the neuromuscular junction (Luo et al., 2005). In rat embryonic muscle, Kidins220 transcript was gradually reduced in the process of muscle development. A prominent protein band of ~220 kDa was detected in muscle throughout development using an antibody that specifically recognized the COOH-terminal fragment of Kidins220. Luo *et al* (2005) proposed a possible model in which Kidins220 bridges a link between α-syntrophin and Eph4, thus contributing in the regulation of synapse formation and plasticity. Further evidence has shown that this interaction occurs through α-syntrophin induction of Kidins220 clustering at the neuromuscular junction. This Kidins220-mediated localization subsequently results in the activation of Eph4 which in turn stimulates postsynaptic signal cascades (Luo et al., 2005). By interacting with a variety of proteins, Kidins220

regulates neuronal activities. For instance, kinesin light chain 1 (KLC1) is a binding partner for Kidins220. Within PC-12 cells, it was demonstrated that after never growth factor (NGF)-stimulation, intracellular trafficking of Kidins220, from trans-Golgi network to the plasma membrane, relied on KLC1-based transport mechanisms (Bracale et al., 2007).

1.3.3 Interacting partners

Kidins220 binds with a variety of interacting partners and is involved in some neuronal activities (Figure 1.9). Kidins220 acts as a downstream substrate of protein kinase D (PKD), where enhanced PKD activity stimulates phosphorylation of Kidins220 at serine 919 in PC-12 cells (Iglesias et al., 2000). The most significant role identified for Kidins220 is to act as a downstream substrate of Trk receptors. Kidins220 is currently the only known membrane-associated protein which interacts with both Trk and p75 neurotrophin receptors, often forming a ternary complex (Chang et al., 2004). Kong *et al.,* (2001) identified that hippocampal neurons stimulated by neurotrophin, exhibited rapid phosphorylation of Kidins220, implicating Kidins220 as a downstream target of neurotrophin (Kong et al., 2001). Further work by Arévalo *et al.,* (2006), revealed that rapid tyrosine phosphorylation of Kidins220 was induced in primary neurons after treatment with neurotrophin. Upon an activation of neurotrophin signalling, phosphorylation of Kidins220 at Tyr1096 leads to a recruitment of CrKl, an upstream component of

the C3G-Rap1-MAP kinase cascade, which in turn activates mitogen-activated protein kinase (MAP kinase) pathways. This sustained MAP kinase activation was affected in PC-12 cells by a mutation within Tyr1096 (Arevalo et al., 2006). Interestingly it appears that the mutation or interference of Kidins220/ARMS only reduces neurotrophin-elicited signalling in the ERK pathway, suggesting an important role played by Kidins220 in mediating neurotrophin-induced signal transduction via this MAP kinase pathway (Arevalo et al., 2004). Kidins220 was also phosphorylated in NG108-15 cells on exposure to ephrin B, suggesting it has actions downstream of ephrin receptors as well (Kong et al., 2001).

Based on yeast two-hybrid screening, Kidins220 activity within muscle has been linked to the binding of α-syntrophin, via the PDZ domain. Kidins220 displays clustering in response to increased expression levels of α-syntrophin which further augments EphA4 signalling (Luo et al., 2005). In brain-derived neurotrophic factor (BDNF) induced nuclear factor-κB (NF-κB) signalling, neurotrophin presented a preference for targeting tropomyosin receptor kinase B (TrkB) (Sniderhan et al., 2008). Sniderhan *et al.,* (2008) demonstrated that silencing Kidins220 or targeting the Kidins220-TrkB interaction abolished NF-κB signalling elicited by BDNF. Further elucidation of the BDNF induced Kidins220-TrkB interaction, suggested that NF-κB signalling was facilitated by the activation of MAP kinase and IκB kinase (IKK) leading to the phosphorylation of RelA (Sniderhan et al., 2008).

Septin 5, which has been implicated in cytoskeleton reorganisation, has also been identified as an interacting partner of Kidins220 and may serve as a regulatory element for intracellular signalling activities (Park et al., 2010). The results of a yeast two-hybrid screen and co-immunoprecipitation revealed that these two proteins are co-localized in hippocampal neurons. In PC-12 cells, Kidins220 and Septin5 expressed in the tips of growing neurites was induced by NGF. Andreazzoli and colleagues (2012) performed a screening for brain cDNA products from a phage display library and demonstrated an interaction between the PDZ-domain of Kidins220 and Pdzrn3, a protein comprising of PDZ-domain and RING-finger. The co-localization of Kidins220 and Pdzrn3 has been observed in PC12 cells at the growing neurites induced by nerve growth factor (Andreazzoli et al., 2012).

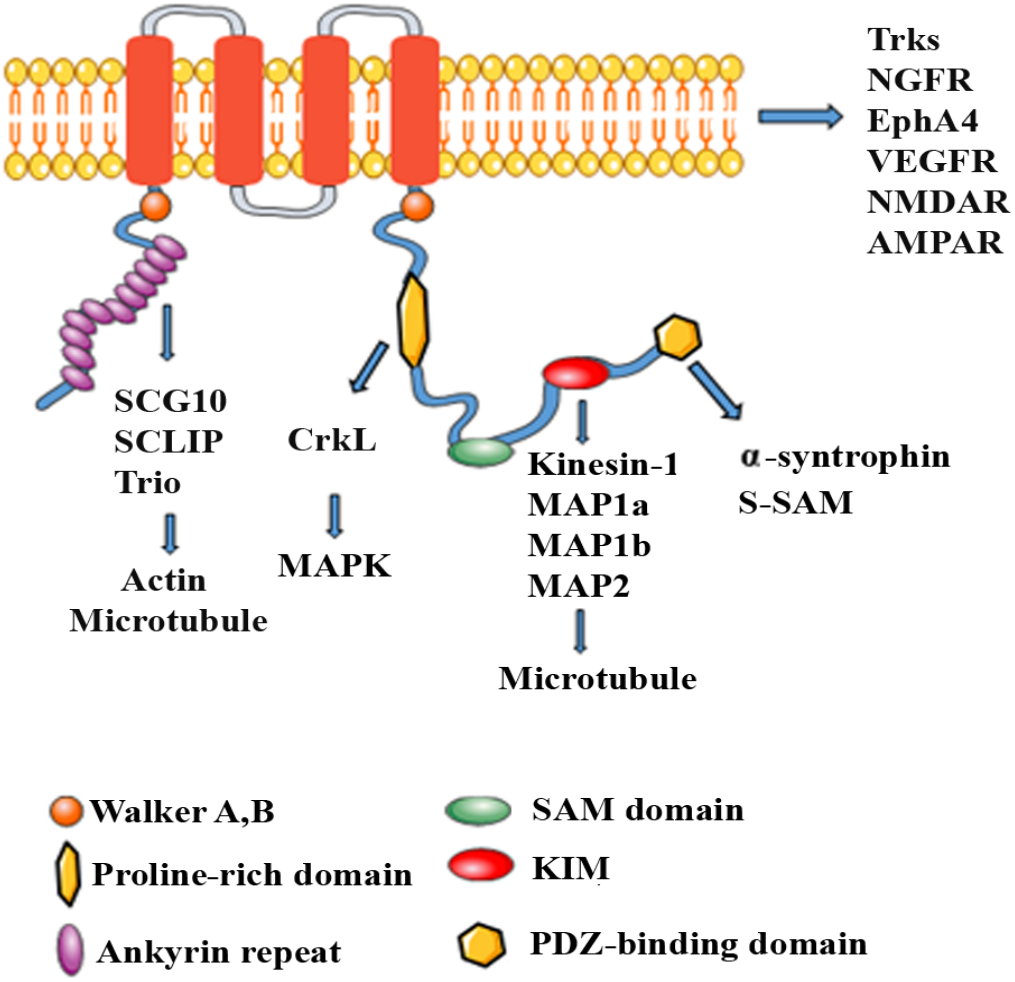

Figure 1.9: The structure of Kidins220 and its binding interaction partners. Schematic structure of Kidins220/ARMS scaffold protein. An archetypal Kidins220/ARMs scaffold protein contains multiple protein binding domains and post-translational modified sites, through which Kidins220/ARMS coordinates signal transduction of various pathways, such as Trk and MAPK. The scaffolding role of Kidins220 appears to be directed based on the different binding partners within the protein. SAM, sterile alpha motif; MAP, microtubule-associated protein; KIM, kinase light chain (KLC)-interacting motif; PDZ, (PSD-95, Dlg, ZO-1)-binding motif); Trks, tropomyosin receptor kinase; NGFR, nerve growth factor receptor; VEGFR vascular endothelial growth factor receptors.

1.3.4 Kidins220, neurite outgrowth, survival, and death

The ankyrin repeats in Kidins220 bind and activate the RhoGEF, Trio. Trio is a RhoGEF for Rac1, RhoG, and RhoA and plays an important role in the regulation of neurite outgrowth. In NGF-differentiated PC-12 cells, Neubrand and colleagues found that Kidins220 and Trio were colocalized in specific sites with F-actin and Rac1 (Neubrand et al., 2010). They identified that overexpression of an ankyrin repeat fragment of Kidins220 in PC-12 cells, inhibited NGF-dependent neurite outgrowth regulated by Trio, and a similar mechanism was also verified in hippocampal neurons (Neubrand et al., 2010). Bracale and colleagues conducted a yeast two-hybrid screen and identified KLC1, the subunit of kinesin1, as an interacting partner of Kidins220. In NGF-induced PC-12 cells, Kidins220 co-localising with kinesin1 was impacted by the overexpression of KIM, a KLC-interacting motif in Kidins220, ultimately interfering with neurite outgrowth (Bracale et al., 2007). Based on the preferential binding of NGF and TrkA neurotrophin receptor, Lopez-Benito *et al.,* (2016) identified a novel signalling pathway, mediated by NGF which includes TrkA, Kidins220, synembryn-B and Rac1, implicated in neuronal secretion in PC-12 cells (Lopez-Benito et al., 2016). Rac1 is the downstream target of Kidins220 and synembryn-B, which themselves directly interact. NGF-mediated secretion is blocked by the overexpression of Kidins220 and synembryn-B, however basal secretion appeared unaffected (Neubrand et al.,

2010). The secretion defects caused by high levels of Kidins220 could be rescued with the expression of dominant-negative Rac1 (Lopez-Benito et al., 2016).

1.3.5 Kidins220 in neuronal polarity, synaptic plasticity, and neurotransmission

The diverse function of neurons depends on the highly polarised morphology regulated by axon and dendrites. Kidins220 interacts with tubulin (SCG10, and SCLIP) and microtubule-associated proteins (MAPs) to regulate neuronal polarity. As members of MAPs, the phosphorylation of MAP1b and stathmins were impaired following the downregulation of Kidins220. Furthermore, downregulation of Kidins220 also led to aberrant dendritic arbors and extensions of the longer axon (Higuero et al., 2010). α-amino-3-hydroxy-5-methyl-4-isoxazolepropionic acid receptors (AMPARs) produce a mature glutamatergic synapse by targeting the cell surface during neuronal development (Hall and Ghosh, 2008). As a subunit of AMPAR, GluA1 can be up-regulated when Kidins220 is down-regulated. Thus, in the process of neuronal mutation and synapse formation, the decreased expression of Kidins220 results in enhanced GLuA1 expression and thus the establishment of a strong synaptic connection (Neubrand et al., 2012). In mature neuronal cultures, there is also evidence of interplay between Kidins220 and NMDA receptors. Upon overstimulation of the NMDA receptors, such as during excitotoxicity, or when neurons are depolarised, Ca^{2+} activity-dependent Ca^{2+} influx, through NMDA receptors, leads to a decrease in

Kidins220 levels through both transcriptional downregulation and protein cleavage by calpain (Lopez-Benito et al., 2016). As Kidins220 knockdown causes a decrease in the amount of phosphorylated MAPK, a reduction in the expression of Kidins220 might contribute to neuronal death through a decrease in MAPK signalling (Neubrand et al., 2012). In hippocampal neurons, the decreased expression of Kidins220 prohibited GABAergic neurotransmission, whereas the overexpression of Kidins220 reverses this effect. Furthermore, the GABAergic neurotransmission regulated by Kidins220 is through a presynaptic mechanism (Sutachan et al., 2010). Within hippocampal neurons with overexpression of Kidins220, increased long-term potentiation was impaired when calpain was prohibited (Wu et al., 2010). Sutachan *et al.,* (2010) found that Kidins220 was implicated in regulating inhibitory neurotransmission (Sutachan et al., 2010).

1.3.6 Kidins220 and vascular development

Cesca *et al.,* (2012) addressed the potential role of Kidins220 in vascular development due to its targeting of and interaction with VEGFRs. Mice with a Kidins220 knockdown phenotype presented with cardiovascular abnormalities. These abnormalities may be caused by impaired VEGF signalling pathways induced by lack of kidins220 (Cesca et al., 2012). Interestingly, Kidins220 interacts with VEGFR2 and VEGFR3 but not Nrp1, although both VEGFR2 and VEGFR3 are co-receptors of Nrp1 in endothelial cells. VEGF signalling is one of the key pathways

in the process of angiogenesis especially mediated by VEGF/VEGFR2, and Kidins220 is demonstrated to interact with VEGFR2 constitutively (Guo et al., 2010). However, mice with more severe vascular abnormalities can be detected in the VEGF knockdown models, VEGRFs, Nrp1 than Kidins220−/− itself (Cesca et al., 2012), suggesting that Kidins220 regulation of angiogenesis may be limited.

1.3.7 Kidins220 and immunomodulation

Apart from the role of Kidins220 in modulating neuronal activities, it also contributes to immunomodulation alongside B cells and T cells. Kidins220 is expressed at the uropod of T lymphocytes and has been shown to be co-immunoprecipitated with ICAM-3 and caveolin-1 (Jean-Mairet et al., 2011). Notably, in primary T lymphocytes, the co-localisation of Kidins220 and ICAM-3 is increased with the induction of morphological polarisation. In contrast, Kidins220 displays different distribution upon change in cell polarity and co-localisation when ICAM-3 becomes disrupted. The identification of Kidins220 in the regulation of T-cell motility was indicated in a Kidins220 knockdown model of human polarised T-cell lines in which basal and stromal cell-derived factor-1α induced migration was increased, following knockdown of Kidins220 (Jean-Mairet et al., 2011). Based on mass spectrometry, Deswal *et al.,* (2013) demonstrated the interaction between Kidins220 and B-Raf in T lymphocytes. In immunoprecipitation and proximity ligation assays, sustained ERK signalling relied

on Kidins220 induced by the T cell receptor (TCR) (Deswal et al., 2013). Furthermore, Fiala *et al.* reported that Kidins220 interacted with stimulated B cell antigen receptor (BCR), in an enhanced Src kinase–independent manner. In B cell-specific Kidins220 knockdown (B-KO) mouse model, Kidins220 couples the BCR to PLCγ2, Ca^{2+}, and ERK signalling and reduces the activation of B cells regulated by BCR *in vitro* and *in vivo*. The role of Kidins220 involved in the PLCγ2 pathway was supported by the six-fold reduction of λ light chain positive B cells (Fiala et al., 2015). Taken together, Kidins220 involves functional performance of both B cell and T cell by coordinating specific signal transduction.

1.3.8 Kidins220 in tumours

Several observations support the importance of Kidins220 in cancer pathogenesis in addition to its function in neuronal activity. A growing body of evidence points to the deregulation of Kidins220 at a cellular level affecting cell proliferation, invasion, migration, and apoptosis, playing an important role in tumour formation and metastasis (Table 1.4). Overexpression of the Kidins220 gene was initially reported in melanoma and associated with shorter overall survival. As a cutaneous malignancy, melanoma originates from the neural crest ontogenetically, and increased expression of Kidins220 was detected in melanoma cell lines (Liao et al., 2007, Liao et al., 2011b). Immunohistochemical staining on different surgical specimens subsequently revealed significantly increased expression of Kidins220

in primary and metastatic melanoma tissues compared with benign tumour tissues (Liao et al., 2007).

Table 1.4: The alteration of Kidins220 in tumorigenesis and related signalling pathways.

Tumour type	Alteration	Effect	Signalling pathways	references
Cutaneous melanoma	Increased expression	Melanoma formation, migration, and invasion	MEK/ERK signalling pathway	(Liao et al., 2007) (Liao et al., 2011a)
Neuroblastoma	Increased expression	Proliferation NGF-regulated signalling Transition from N-type to S-type	P21/Cyclin D1	(Jung et al., 2014) (Rogers and Schor, 2013a)
Castration-resistant prostate cancer (CRPC)	Increased expression	Angiogenesis	VEGF/VEGFR and PI13K/AKT signalling pathways	(Wang et al., 2016)
Ph-like acute lymphoblastic leukaemia (ALL)	Gene fusion with PAX5	Proliferation and survival	ERK signalling pathway	(Sakamoto et al., 2017)
Paediatric high-grade glioma	Intragenic copy number breakpoint	n.d.	n.d.	(Carvalho et al., 2014)

Note: n.d., not determined.

Kidins220 lies upstream of the BRAF gene that encodes proteins as part of the RAS/MAPK signalling pathway, controlling several important cell functions. Overexpression of Kidins220, resulting in sustained activation of MEK/ERK signalling, rather than BRAF mutation, has been identified as leading to acral lentiginous melanoma tumorigenesis. On the other hand, high levels of Kidins220 also enhances ultraviolet radiation B (UVB) (290-320 nm) induced apoptosis in melanoma cells via targeting the activated ERK signalling pathway (Liao et al., 2007). The inhibition of melanoma cell migration and invasion associated with Kidins220 knockdown indicated that Kidins220 can promote tumour migration/invasion through MEK/ERK signalling (Liao et al., 2007, Liao et al., 2011b). Taken together, Kidins220 expression is regarded as a predictor of melanoma patient outcomes, and a target for therapies inhibiting Kidins220/MEK/ERK/MAPK signalling pathways.

The regulatory role of Kidins220 in cancer development can be tumour specific. For example, Kidins220 possesses different regulatory mechanisms of the MAPK signalling pathway in neuroblastoma tumours. Rogers and Schor first reported that neuroblastoma tumours overexpress Kidins220, and that its forced overexpression promotes NGF-stimulated MAPK signalling activity, but not BDNF driven activation of MAPK signalling. Unlike melanoma, Kidins220 knockdown did not affect the survival of neuroblastoma cells under oxidative stress within 24 hours. Furthermore, loss of Kidins220 did not affect migration of neuroblastoma cells (Rogers and Schor, 2013b). During development, neuroblastoma undergoes

a morphology transition between Schwannian stromal (S-type) cells and neuroblastic (N-type) cells. S-type cells are highly adhesive to extracellular matrix (ECM) and non-invasive, whereas N-type are less adhesive and highly invasive. DCX and STMN2 markers for neuronal lineage appear to be reduced in Kidins220-deficient N-type cells, whereas S-type cells containing low levels of Kidins220 (but not Kidins220 depletion) expressed considerable levels of both DCX and STMN2. It suggests an essential role of Kidins220 in regulating morphology alteration in neural crest tumour cells (Rogers and Schor, 2013a). Jung *et al.,* (2014) generated Kidins220-knockdown neuroblastoma cell lines to determine whether Kidins220 is involved in cell proliferation. They found that the wild type cells were 1.8 fold higher in number than the matching knockdown cells on the fourth day of culture. Further analysis revealed that the decreased growth rate of Kidins220-knockdown neuroblastoma cells were due to the arrest of cell cycle at the G1 phase, which was accompanied with decreased expression of both Cyclin D1 and CDK4, and also an up regulation of p21, suggesting that Kidins220 can coordinate cell cycle through a regulation of p21-cyclinD1/CDK4 (Jung et al., 2014).

As previously mentioned, Kidins220 is a direct target of miR-4638-5P. MiR-4638-5P has been related to the growth of castration resistance prostate cancer (CRPC) *in vivo* and *in vitro*. Wang and colleagues discovered a significant downregulation of miR-4638-5P in CRPC. Kidins220 was detected with higher expression levels in both CRPC cell lines and tissues compared with androgen-dependent prostate cancer (ADPC). Western blot analysis showed that only

Kidins220 expression was significantly reduced in PC3 and DU145 cells in the presence of miR-4638-5P. The knockdown of Kidins220 leads to reduced proliferation and growth of CRPC cells *in vitro* and *in vivo*. Furthermore, miR-4638-5P and Kidins220 regulate prostate cancer (PCa) associated angiogenesis. Kidins220 knockdown or overexpression of miR-4638-5P result in similar inhibition of endothelial cell growth and the formation of vasculogenic mimicry. Further molecular analysis indicates that pCDH-miR-4638-5p sponge, a competitive miRNA inhibitor, caused an increase in expression of VEGF, PI3K, and AKT in androgen-independent PCa cells, whereas all three molecules were reduced in Kidins220 knockdown PCa cells, suggesting that both miR-4638-5P and Kidins220 may be involved in androgen-independent PCa-associated angiogenesis. Interestingly, a reduced level of cell growth and angiogenesis was also seen in AKT-knockdown cells which is in accordance with the result from Kidins220-knockdown cells. Taken together, loss of miR-4638-5 may result in the activation of Kidins220 and promote neoangiogenesis and androgen-independent PCa growth through the regulation of VEGF/VEGFR2 and PI3K/AKT signalling pathways (Wang et al., 2016).

As mentioned before, Kidins220 is the substrate of PKD. At the trans-Golgi network, the family members of PKD were found to regulate secretory transport (Yeaman et al., 2004). PKD1 plays an important role in stimulating the secretion of neurotensin, a gut peptide, which modulates gastrointestinal functions such as secretion and growth, as well as being involved in the proliferation of neurotensin receptor-positive cancers (Li et al., 2004, Carraway and Plona, 2006, Evers, 2006).

In human carcinoid BON cells, a novel endocrine cell line that is derived from a human pancreatic carcinoid tumour, Kidins220 and PKD2 regulate the secretion of neurotensin (Evers et al., 1991, Li et al., 2008). Of further interest is the observation that in BON cells, Kidins220, PKD1 and PKD2 present the same localization pattern as neurotensin vesicles. Overexpression of PKD1 nullifies Kidins220 expression and neurotensin secretion in BON cells (Li et al., 2008). Thus, the PKD/Kidins220 signalling pathway provides evidence for their critical role in the regulation of neurotensin hormone secretion. Since neurotensin is involved in secretion and inflammation in both normal and tumour cell growth, the PKD/Kidins220 pathway and neurotensin-containing vesicles are considered as a novel drug target for clinical applications (Li et al., 2008, Castagliuolo et al., 1999).

Apart from its role in solid tumours, a recent study also demonstrated a gene fusion of PAX5 and Kidins220, which leads to leukaemogenesis by inhibiting B lymphocyte differentiation. Kidins220-mediated activation of ERK pathway may contribute to the increased cell proliferation and the survival of leukemic cells (Sakamoto et al., 2016). Controversially, Kidins220 plays a different role in glioma, which was demonstrated in a profiling study of its function as a tumour suppressor in paediatric high-grade glioma (Carvalho et al., 2014).

1.3.9 Summary

Kidins220 is involved in the regulation of diverse cellular activities, especially in neural differentiation and cytoskeleton remodelling (Bracale et al., 2007). Its different domains mediate the function of Kidins220 as well as act as a platform for protein-protein interactions, intracellular signalling and protein transportation. Dysregulation of Kidins220 has been evident in several malignancies. Kidins220 binds to Trio, tubulin, SCG10 and SCLIP to modulate actin and microtubule cytoskeleton, which is critical in coordination with cellular processes, such as cell migration, cell polarity, and cell cycle progression (Fife et al., 2014). Tumour cell migration and invasion requires the remodelling of the cell cytoskeleton. The reorganization of the actin cytoskeleton that enables dynamic cell elongation and directional motility is also found in EMT, a critical process involved in tumour development (Thiery et al., 2009). Further investigation will shed light on the role played by Kidins220 in the dynamic arrangement of cytoskeleton and EMT, and its implication in tumorigenesis and cancer progression.

Kidins220 regulates cell survival and death through MAPK signalling after the binding of neurotrophins and Trk receptors (Neubrand et al., 2012). Since the dysregulation of MAPK signalling is linked to tumorigenesis in several types of cancer, and the inhibition of MAPK signalling pathways is critical for the progress of anticancer agents, it is necessary to gain insight into the corresponding involvement of Kidins220 (Fang and Richardson, 2005, Mirzoeva et al., 2009).

Targeting its specific multiple domains such as the proline-rich domain and transmembrane segments may provide the possibility of more precise targeting.

In addition to its involvement in VEGF/VEGFR regulated angiogenesis, Kidins220 has been shown as a target gene of miR-4638-5p, and its overexpression has been seen in androgen independent PCa and tumour associated angiogenesis (Wang et al., 2016). However, its potential for targeted tumour associated angiogenesis therapy in these malignancies requires further investigation.

1.4 Hypothesis and aims

To date, the role of Kidins220 in pancreatic cancer still remains unknown. According to the profound role played by this molecule in the regulation of cellular functions and signal transduction, and also aberration of its expression observed in other malignancies, we performed an initial assessment of its expression in pancreatic cancer by analysing publically available gene expression array data. A reduced expression was seen in pancreatic adenocarcinomas compared with adjacent non-cancerous pancreatic tissues which is presented in Chapter 3. Therefore, we proposed that Kidins220 is involved in the development and disease progression of pancreatic cancer.

The aims of the present study are:

1) To determine the expression of Kidins220 in pancreatic cancer and its implication in development and disease progression;

2) To examine its impact on the functions of pancreatic cancer cells, which may contribute to its role in the disease;

3)To dissect the underlying molecular mechanism.

Objective 1: Kidins220 expression in pancreatic cancer and its clinical relevance.

The expression of Kidin220 transcripts in a cohort of pancreatic cancer tissue samples will be determined using real time quantitative PCR (QPCR). Kidin220 protein expression and distribution will be evaluated using immunohistochemical staining (IHC) of Kidins220 in a pancreatic tumour tissue microarray. The association with histopathological and clinical characteristics will be evaluated accordingly. Additional analyses will be performed on relevant public gene expression array data to further validate our findings.

Objective 2: Kidins220 and function of pancreatic cancer cells.

The impact of Kidins220 on cellular function in pancreatic cancer cells will be determined using *in vitro* cell line models. A knockdown model using lentiviral shRNAs will be employed. Cellular functions such as proliferation, migration and invasion will be determined using corresponding *in vitro* assays.

Objective 3: Molecular mechanisms.

Underlying molecular mechanism for altered cellular functions and EMT will be investigated by determing expression and activation of candidate molecules, for example EMT markers including snail, slug and twist etc. In a parallell study of Kidins220 in gastric cancer from the host laboratory, involvement of EGFR was observed in Kidins220 knockdown gastric cancer cell lines from an analysis of protein activation using a protein array. Therefore, we may focus on the influence of Kidins220 on EGFR and its signalling in pancreatic cancer and the corresponding implication in the disease progression.

Chapter 2

Methodology

2.1 Materials

2.1.1 Cell lines

The current study used three pancreatic cancer cell lines; Panc-1, Mia paca-2 and ASPC-1. All these cell lines were purchased from the American Type Culture Collection (ATCC, Rockville, MD, USA). All cell lines were verified at the source for identity and were at low passage on acquisition. Full details of these cell lines are listed in Table 2.1.

Table 2.1: Details of pancreatic cancer cells used in this study.

	Panc-1	**Mia paca-2**	**ASPC-1**
Species	Human	Human	Human
Tissue	Pancreas/duct	Pancreas	Pancreas; derived from metastatic site: ascites
Gender	Male	Male	Female
Age	56	65	62
Morphology	Epithelial	Epithelial	-
Growth mode	Adherent	Adherent	Adherent
Disease	Epithelial carcinoma	Carcinoma	Adenocarcinoma
Country	UK	UK	UK

2.1.2 General compounds

Chemicals and reagents used throughout the study, together with their suppliers are outlined in table 2.2.

Table 2.2: Chemicals and reagents.

Material/Reagent	Supplier
10% Foetal calf serum (FCS)	Sigma-Aldrich, Pooled, Dorset, UK
A/G protein agarose beads	Santa-Cruz Biotechnology, UK
Acetic acid	Fisher Scientific, Leicestershire, UK
Acrylamide mix (30%)	Sigma-Aldrich, Poole, Dorset, UK
Agarose	Melford Laboratories Ltd, Suffolk, UK
Ammonium persulphate (APS)	Sigma-Aldrich, Poole, Dorset, UK
Amphotericin B	Sigma-Aldrich, Poole, Dorset, UK
Ampicillin	Sigma-Aldrich, Poole, Dorset, UK
Bio-Rad DC™ Protein Assay	Bio-Rad Laboratories, Hercules, CA, USA
Boric acid	Duchefa Biochemie, Haarlem, Netherlands
Bovine serum albumin (BSA)	Sigma-Aldrich, Poole, Dorset, UK
Bromophenol Blue	Sigma-Aldrich, Poole, Dorset, UK
Calcium chloride ($CaCl_2$)	Sigma-Aldrich, Poole, Dorset, UK
Chloroform	Sigma-Aldrich, Poole, Dorset, UK
Commasine Blue	Sigma-Aldrich, Poole, Dorset, UK
Crystal violet	Sigma-Aldrich, Poole, Dorset, UK
Diethylpyrocarbonate (DEPC)	Sigma-Aldrich, Poole, Dorset, UK
Dimethylsulphoxide (DMSO)	Sigma-Aldrich, Poole, Dorset, UK
Disodium phosphate (Na_2HPO_4)	BDH Chemicals Ltd, Poole, Dorset, UK
Dithiothreitol	Sigma-Aldrich, Poole, Dorset, UK
Dulbecco's Modified Eagles' Medium/Nutrient mixture F12	Sigma-Aldrich, Poole, Dorset, UK
Ethylenediaminetetraacetic acid (EDTA)	Sigma-Aldrich, Pooled, Dorset, UK
Ethanol	Fisher Scientific, Leicestershire, UK
Formalin	Sigma-Aldrich, Poole, Dorset, UK
GoTaq® Green Master Mix	Promega
G418	Sigma-Aldrich, Poole, Dorset, UK
Hydrochloric acid (HCl)	Sigma-Aldrich, Poole, Dorset, UK
Isopropanol	Sigma-Aldrich, Poole, Dorset, UK

Matrigel®	Corning Incorporated, Flintshire, UK
Methanol	Fisher Scientific, Loughborough, UK
Na_2HPO_4	BDH Chemicals Ltd., Poole, Dorset, UK
NaN_3	Sigma-Aldrich, Poole, Dorset, UK
PVDF membrane	EMD Millipore Corporation, Billerica, MA, USA
Penicillin	Sigma-Aldrich, Poole, Dorset, UK
Ponceau S Stain	Sigma-Aldrich, Poole, Dorset, UK
Precision qScript™ RT PCR kit	Primerdesign Ltd, Southampton, UK
Potassium chloride (KCl)	Fisons Scientific Equipment, Loughborough, UK
GoTaq Green master mix	Promega, Madison, USA
RPMI	Sigma-Aldrich, Poole, Dorset, UK
Sodium dodecyl sulphate (SDS)	Melford Laboratories Ltd, Suffolk, UK
Sodium chloride (NaCl)	Sigma-Aldrich, Poole, Dorset, UK
Sodium fluoride	Sigma-Aldrich, Poole, Dorset, UK
Sodium hydroxide (NaOH)	Sigma-Aldrich, Poole, Dorset, UK
Sodium nitrate	Sigma-Aldrich, Poole, Dorset, UK
Sodium orthovanadate (NA_2VO_4)	Sigma-Aldrich, Poole, Dorset, UK
Sodium pyrophosphate	Sigma-Aldrich, Poole, Dorset, UK
Streptomycin	Sigma-Aldrich, Poole, Dorset, UK
Sucrose	Fisons Scientific Equipment, Loughborough, UK
SYBR®Safe DNA gel stain	Invitrogen, Paisley, UK
Tetramethylethylenediamine (TEMED)	Sigma-Aldrich, Poole, Dorset, UK
TRI Reagent	Sigma-Aldrich, Poole, Dorset, UK
Tris-Cl	Melford Laboratories Ltd, Suffolk, UK
Triton X-100	Sigma-Aldrich, Poole, Dorset, UK
Trypsin	Sigma-Aldrich, Poole, Dorset, UK
Tween 20	Melford Laboratories Ltd, Suffolk, UK
Vectastain Universal ABC kit	Vector Laboratories Inc, Burlingame, CA, USA
Zinc chloride (ZnCl)	Sigma-Aldrich, Poole, Dorset, UK

2.1.3 General plastic consumables, hardware and software

General plastic consumables, hardware and software, together with their suppliers are outlined in table 2.3.

Table 2.3: Instruments, culture vessels and software.

Hardware/Software	Supplier
0.4 µm filtration unit	Sigma-Aldrich, Poole, Dorset, UK
25cm^2 and 75cm^2 culture flasks	Cell Star, Germany
Image J	Public Domain
Lecia DM IRB microscope	Lecia GmbH, Bristol, UK
Microsoft Excel	Microsoft In., Redmond, WA, USA
Neubauer haemocytometer counting chamber	Mod-Fuchs Rosenthal, Hawksley, UK
Protein spectrophotometer	BIO-TEK, Wolf Laboratories, York, UK
RNA spectrophotometer	BIO-TEK, Wolf Laboratories, York, UK
UV light chamber	Germix
Class II laminar flow cabinet	Wolflabs,York, UK
EVOS Auto imaging system	Thermo Fisher Scientific, Waltham, MA USA

2.1.4 Primers

All primers used in this study were designed using the Beacon Design Programme (Biosoft International, Palo Alto, California, USA) and were synthesised by either Invitrogen (Paisley, UK) or Sigma (Poole, Dorset, UK). Details of the primers used

for conventional RT-PCR and real time quantitative PCR (QPCR) are provided in Table 2.4.

Table 2.4: Primers for conventional RT-PCR, QPCR and ribozyme synthesis.

Primer name	Primer sequence (5'-3')	Product size (bp)
GAPDHF8	GGCTGCTTTTAACTCTGGTA	
GAPDHR8	GACTGTGGTCATGAGTCCTT	475
Kidins220F2	AGACGTTCCATGCTCAGA	
Kidins220R2	CTCGAGCCACAAGAACTG	539
Kidins220ZR2	*ACTGAACCTGACCGTACA*TGCCTTCTTCGGTAAGTG	136
Kidins220 Rib1F	CTGCAGACCCGGGGCCCCCTTCTAACTGGCTGATGAGT CCGTGAGGA	
Kidins220 Rib1R	ACTAGTGCCTATAGAGAATACATTGCTCAGATGTTTCGT CCTCACGGACT	
EGFRF1	AGAGTCTCAAAGCCATGTTAT	
EGFRZR1	*ACTGAACCTGACCGTACA*CCATCCTAAGCATGACTCC	120
E-cadF22	CAGGAGCCAGACACATTTAT	
E-cadR22	TCTAAGGTGGTCACTTGGTC	515
VimentinF1	GATGCTTCAGAGAGAGGAAG	
VimentinZR1	*ACTGAACCTGACCGTACA*CTCTTCGTGGAGTTTCTTCA	145
SnailF11	CGCTCTTTCCTCGTCAG	
SnailR11	GTTGCAGTATTTGCAGTTGA	474
SlugF11	CTCTCCTCTTTCCGGATACT	
SlugR11	AGCAGTTTTTGCACTGGTAT	521
TwistF11	AGCAACAGCGAGGAAGAG	
TwistR11	GAGGACCTGGTAGAGGAAGT	318
T7F	TAATACGACTCACTATAGGG	

BGHR	TAGAAGGCAGTCGAGG
RbBMR	TTCGTCCTCACGGACTCATCAG
RbTPF	CTGATGAGTCCGTGAGGACGAA

Note: Z Sequence '*ACTGAACCTGACCGTACA*' is highlighted in green and italic font

2.1.5 Antibodies

2.1.5.1 Primary antibodies

Full details of primary antibodies used in the current study are supplied in Table 2.5.

2.1.5.2 Secondary antibodies

The secondary antibodies used for western blotting were horseradish peroxidise (HRP) conjugated anti-goat IgG, goat anti-rabbit IgG, and rabbit anti-mouse IgG antibodies, all these antibodies are purchased from Sigma (Poole, Dorset, UK).

Table 2.5: Primary and secondary antibodies used in this study.

Antibodies	Molecular weight (kDs)	Supplier	Product code
Rabbit anti-Kidins220	220	Santa Cruz Biotechnology	sc-48738
Mouse anti- β-actin	42	Santa Cruz Biotechnology	sc-47778
Mouse anti-tyrosine（PY99）	-	Santa Cruz Biotechnology	sc-7020
Mouse anti-EGFR	170	Santa Cruz Biotechnology	sc-71034
Mouse anti-p-ERK	42	Santa Cruz Biotechnology	sc-7383
Mouse anti-ERK	42	Santa Cruz Biotechnology	sc-514302
Mouse anti-p-AKT1/2/3	62/56/60	Santa Cruz Biotechnology	sc-81433
Mouse anti- AKT	56	Santa Cruz Biotechnology	sc-5298
Goat anti-E-cadherin	135	Santa Cruz Biotechnology	sc-1500
Mouse anti-vimentin	57	Santa Cruz Biotechnology	sc-66002
Mouse anti-snail	29	Abcam	ab167609
Rabbit anti-mouse (whole molecule) IgG peroxidise conjugate	Dependent on primary	Sigma-Aldrich	A5278
Goat anti-rabbit (whole molecule) IgG peroxidise conjugate	Dependent on primary	Sigma-Aldrich	A0545
Rabbit anti-goat (whole molecule) IgG peroxidise conjugate	Dependent on primary	Sigma-Aldrich	A5420

2.2 Preparation of reagents, buffers and standard solutions

2.2.1 Solutions used in cell culture

Preparation of Complete Cell Culture Medium

Panc-1, Mia paca-2 and ASPC-1 pancreatic cancer cells were cultured in Dulbecco's Modified Eagle's medium supplemented with 50ml of heat inactivated foetal calf serum (FCS) (Sigma-Aldrich, Pooled, Dorset, UK) and 5ml of an antibiotic cocktail comprising penicillin, streptomycin and amphotericin B (Sigma-Aldrich, Pooled, Dorset, UK). The prepared medium was stored at 4°C for up to one month.

Preparation of 0.05M EDTA

A stock solution was prepared by dissolving 40g NaCl, 1g KCl, 5.72g Na_2HPO_4 (BDH Chemical Ltd., Poole, England, UK), 1g KH_2PO_4 (BDH Chemical Ltd., Poole, England, UK) and 1.4g EDTA (Sigma-Aldrich, Pooled, Dorset, UK) in 5 litres of dH_2O. The pH was adjusted to 7.4 using Sodium hydroxide (NaOH) and was autoclaved before use.

Trypsin (25mg/ml)

A 25mg/ml stock solution was prepared by dissolving 500mg trypsin in 20ml 0.05M EDTA. The solution was filtered through a 0.2µm mini-start filter (Sigma-Aldrich, Pooled, Dorset, UK) and stored at -20°C. The working solution was prepared by

further dissolving 250µl of the stock trypsin/EDTA solution in 10ml of 0.05M EDTA to detach cells, and was stored at 4°C until use.

Phosphate-buffered saline (PBS)

To prepare 1L of 1 x PBS, (137mM NaCl, 2.7mM KCl, 10mM Na_2HPO_4, 1.8mM KH_2PO_4) was prepared by dissolving 8g NaCl, 0.2g KCl, 1.44g Na_2HPO_4 and 0.24g KH_2PO_4 in 800ml of dH_2O. The pH was adjusted to 7.4 with HCl and dH_2O added to make up the volume to 1 Litre. The solution was then autoclaved and aliquoted before being stored at room temperature.

100X Antibiotics

100X Antibiotic Antimycotic Solution was purchased from Sigma-Aldrich (Poole, Dorset, UK). 5ml of the solution was added into a 500ml DMEM to obtain a final 1X concentration.

2.2.2 Solutions used in molecular biology

Tris-Boric-Acid (TBE) electrophoresis buffer

TBE buffer 10X concentrate (T4415) was purchased from Sigma-Aldrich (Poole, Dorset, UK), and diluted with distilled water into 1X stock and stored at room temperature for further use.

Diethylpyrocarbonate (DEPC) water

A stock solution of DEPC water was prepared by dissolving 500µl of diethyl pyrocarbonate (DEPC) (Sigma-Aldrich, Poole, Dorset, UK) in 9,500µl distilled water and autoclaved before use.

Loading buffer (used for DNA electrophoresis)

Loading buffer was prepared by dissolving 25mg bromophenol blue (Sigma-Aldrich, Poole, Dorset, UK) and 4g sucrose (Fisons Scientific Equipment, Loughborough, UK) were dissolved in 10ml of H_2O. The buffer was stored at 4°C until use.

2.2.3 Solutions for Western blot

Lysis Buffer

Lysis buffer was prepared by dissolving NaCl 150mM (8.76g), Tris 50mM (6.05g), sodium azide 0.02% (200mg), sodium deoxycholate 0.5% (5g), Triton X-100 1.5% (15ml), Aprotinin 1µg/ml (1mg), Na_3VO_4 5mM (919.5mg) and Leupeptin 1µg/ml (1mg) in 1 litre of dH_2O, and was stored at 4°C until use.

Tris Buffered Saline (TBS)

1L of Tris Buffered Saline 10X solution (T5912) (Sigma-Aldrich, Poole, Dorset, UK) was diluted in 9L of distilled water. The pH was adjusted to 7.4 using HCl and stored at room temperature until use.

10% ammonium persulphate (APS)

The solution was prepared by dissolving 1g APS in 10ml dH_2O and then stored at 4°C for future use.

Running buffer

1L of Tris-Glycine-SDS Buffer 10X concentrate (T7777) (Sigma-Aldrich, Poole, Dorset, UK) was diluted in 9L of distilled water and stored at room temperature for further use.

Transfer buffer

1L of Tris-Glycine Buffer 10X concentrate (T4904) (Sigma-Aldrich, Poole, Dorset, UK) was diluted in 9L of distilled water containing 2L methanol (Fisher Scientific, Loughborough, UK) and stored at room temperature for further use.

2.3 Cell culture, maintenance and storage

2.3.1 Preparation of growth medium and cell maintenance

- Panc-1, Mia paca-2, and ASPC-1 pancreatic cancer cell lines were cultured in Dulbecco's Modified Eagle's Medium/Nutrient F-12 Ham (DMEM-F12, Sigma-Aldrich, Poole, Dorset, UK). This medium contains 2mM L-glutamine and 4.5mM $NaHCO_3$ and supplemented with 10% heat inactivated Foetal Bovine Serum (Sigma-Aldrich, Poole, Dorset, England, UK) and antibiotics in PH 7.3.
- All the cell lines were cultured in 25 cm^2 and 75 cm^2 flasks (Greiner Bio-One Ltd, Gloucestershier, UK) depending on the required application with a loose cap in an incubator at 37^oC, 95% humidification and 5% CO_2.
- Cell lines transfected with lentiviral shRNA or scramble control were initially cultured in DMEM with 500µg/ml G418. The selected transfectants were then cultured in medium supplemented with 100µg/ml G418 to maintain the acquired phenotype. The transfected cell lines were verified for subsequent studies.
- Confluency and viability of Cells were visually assessed with an inverted phase contrast microscope. The confluency of cells was estimated based on the percentage of cells covering the surface of the tissue culture flasks. Cells were left to grow until they reached sub-confluency (80-95%) for experiments. All handing of cells was carried out using a Class II laminar

flow cabinet with autoclaved and sterile equipment. Cells were passaged when they reached 80%-90% confluency.

2.3.2 Cell detachment and cell counting

- The tissue culture flask was taken out from the incubator and the waste medium was aspirated using a glass pipette. Following this, the flask was briefly washed with sterile 5ml EDTA BSS buffer to remove remaining serum which would inhibit the action of trypsin.
- Approximately 1-2ml of trypsin/EDTA solution (Trypsin 0.01% (w/v) and EDTA 0.05% (w/v) in BSS buffer) was added to the tissue culture flask. The adherent cells were detached after the flask was returned to the incubator for 5-10 minutes at 37°C. Flasks were inspected visually under the light microscope to make sure the cells were detached completely.
- Once detached, 5ml DMEM containing 10% FCS was added to the flask to neutralise the trypsin and the detached cells were washed from the surface of the flask. The cell mixture was then transferred to a 30ml universal container (Greiner Bio-One Ltd, Gloucestershire, UK) and centrifuged at 1,800rpm for 10 minutes.
- The supernatant was aspirated and the cell pellet was re-suspended in medium for re-culturing or used in experimental work immediately.

- Cell counting was carried out using a Neubauer haemocytometer counting chamber under a light microscope using the x10 objective lens.
- The haemocytometer calculated the number of cells in a predetermined volume of fluid to obtain the quantity of cells per millilitre. The haemocytometer chamber was divided into 9 squares with dimensions of 1mm x 1mm x 0.2mm. For consistency of cell density and error reduction, four corners of 9 squared areas were counted. The number of cells was calculated by using the following equation:
- Cell number/ml= (the sum of the number of cells in four corners/ 8) x ($1x10^4$)

2.3.3 Storage of cells in liquid nitrogen and cell resuscitation

Cells were detached with trypsin from the flask as described in section 2.3.2. After centrifugation, the cells were re-suspended in medium with 10% dimethyl sulfoxide (DMSO) at a density of $1x10^6$ cells/ml.

- One millilitre of this cell suspension was transferred into 1ml pre-labelled CRYO.STM tubes (Greiner Bio-One, Germany) wrapped in protective tissue paper and then frozen down to -80°C. For a longer-term storage, the cells were transferred and stored at -196°C in a liquid nitrogen tank.
- In order to resuscitate the frozen cells, the CRYO.STM tube was taken from the liquid nitrogen and thawed in a 37°C water bath rapidly. The cell

suspension was then transferred into a 30ml universal container containing 5ml of pre-warmed medium and then centrifuged at 1,800rpm for 5 minutes. The medium was removed by aspiration. The cells were then resuspended in 5ml media. The cells were incubated at 37°C, 95% humidification, and 5% CO_2 for further experiment.

2.4 Methods for RNA detection

2.4.1 Total RNA isolation

There are three main types of Ribonucleic acid (RNA) within the cytoplasm of all living eukaryotic cells known as ribosomal RNA (rRNA), transfer RNA (tRNA), and messenger RNA (mRNA). Cellular mRNA was used in this study based on its important role of carrying genetic information and encoding corresponding protein products. At the transcript level, the presence of specific mRNA thus acting as an indication of which proteins are likely being produced by the cell.

RNA isolation was performed using the Tri Reagent kit (Sigma-Aldrich, Poole, Dorset, UK) as outlined below.

- After cells were cultured in a monolayer to a confluence of approximately 90% (5-10x10^5 cells), the medium was removed and replaced with RNA reagent (1ml per 5-10x10^5 cells) to produce cell lysate.
- The homogenous lysate was then transferred into a sterile microfuge tube, and left at room temperature for 5 min.

- 0.2ml (per 1ml of RNA reagent) chloroform (Sigma-Aldrich, Poole, Dorset, UK) was added to the homogenate and the tube capped and shaken vigorously for 15 seconds.
- The resulting homogenate was then centrifuged at 12,000rpm for 15 minutes at 4°C (Boece, Wolf laboratories, York, UK). The centrifugation resulted in the separation of the lysate into three phases in the acidic environment; a red organic phase containing protein, an interphase containing DNA and a colourless upper aqueous phase containing RNA.
- The upper aqueous phase containing RNA was carefully transferred to a fresh microfuge tube. Following this, 500 µl of 2-propanol (per 1ml TRI Reagent®) was added to the sample, shaken and incubated on ice for 10 minutes before centrifugation, for pelleting precipitated RNA, at 12,000 x g for 10 minutes at 4°C. Subsequently, an RNA pellet was seen at the bottom of the microfuge tube.
- The supernatant was discarded and the RNA pellet was washed with 1ml 75% ethanol (made with DEPC water) twice with vortexing and centrifuging at 7,500rpm for 5 minutes at 4°C.
- The RNA pellet was briefly dried at 55°C for 5-10 min in a Techne, Hybridiser HB-1D drying oven (Wolf laboratories, York, UK), in order to remove any remaining ethanol.

- Finally, the RNA pellet was dissolved in 50-100µl (depending on RNA pellet size) of DEPC water by vortexing. DEPC is used as a histidine specific alkylating agent to inhibit the hydrolysis of RNA by RNAases.

2.4.2 RNA Quantification

- Once RNA isolation was completed, the concentration and purity of the resulting single stranded RNA was quantified by measuring its absorbance at a wavelength of 260nm using a UV 1101 Biotech spectrophotometer (WPA, Cambridge, UK). The RNA samples were measured with Starna glass cuvette (Optiglass limited, Essex, UK). A260nm/ A280nm ratio was used to estimate the purity of RNA sample by measuring the different absorbance between the RNA sample and DEPC water (as a blank control).
- The concentration of RNA samples was then standardised using DEPC water for reverse transcription (RT) or stored at -80°C for future use.

2.4.3 Reverse Transcription of RNA for production of cDNA

To determine the transcript expression, an mRNA template was used to generate complementary DNA (cDNA) using reverse transcription (RT). Transcripts of a particular gene were then determined using RT-PCR and QPCR.

- RT was performed by converting 500 ng of RNA into cDNA using the GoScript™ Reverse Transcription System kit (Promega, Corporation, Madison, WI, USA) Based on the instruction provided by the manufacture, each reaction was set up in 200µl PCR tubes as follows:

Component Volume	Each reaction
GoScript™ 5X Reaction Buffer	4µl
$MgCl_2$	1.2µl
PCR Nucleotide Mix	1µl
Recombinant RNasin Ribonuclease Inhibitor	0.5µl
GoScript™ Reverse Transcriptase	1µl
RNA template (0.5µg/µl)	1µl
Nuclease-Free Water	7.3µl

- The reaction was carried out in a 2720 Thermal Cycler (Applied Biosystems, Paisley, UK). The reaction condition is listed as following:

Time	Temperature
5 minutes	25°C
60 minutes	42°C
15 minutes	70°C

- After the reaction completed, the cDNA was diluted by 1:4 with PCR water as a template for PCR or store at -20°C for future use.

2.4.4 Polymerase chain reaction (PCR)

Polymerase chain reaction (PCR) was first devised by Kary Mullis in 1983. It is a simple technique that is used to detect and amplify a single target DNA, and produce thousands or millions of copies of the DNA sequence (Bartlett and Stirling, 2003). In this reaction, two short DNA sequences (oligonucleotides- i.e. forward and reverse primers), which bind to the template DNA by base pairing, are required and are complementary to a defined sequence on each of the two stands of the DNA. These primers are aligned with the 3' ends facing each other.

The components of a PCR reaction include a DNA template containing the target DNA that is to be amplified, a heat resistant DNA polymerase such as Taq polymerase which synthesises DNA from nucleotides, short DNA fragments called primers which contain complementary sequences to the 3' ends of the sense and anti-sense strand of the target DNA and which act as a starting point for DNA formation by the DNA polymerase, deoxynucleotide triphosphates (dNTPs) from which the polymerase can synthesise new DNA strands and a thermal cycler, which provides repeated cycles of heating and cooling to provide the required temperatures for each step of the reaction. The DNA produced by PCR acts as a further template for replication resulting in a chain reaction and the exponential amplification of DNA.

- In the current study, target genes were amplified using the GoTaq Green master mix (Promega, Madison, USA). The reaction in aliquots of 16µl was set up in PCR tubes as follows:

Component	Volume
cDNA template	2µl
Forward primer (working concentration of 1µM)	1µl
Reverse primer (working concentration of 1µM)	1µl
2X GoTaq Green master mix	8µl
PCR H_20	4µl

- A test sample containing PCR water instead of cDNA template was run alongside to detect any contamination of the reaction.
- The PCR samples were briefly mixed and placed in a 2720 Thermo Cycler The condition of reaction was set as follows:

Step	Temperature	Time	Cycles
Initialisation	94°C	5min	1
Denaturation	94°C	20sec	32 cycles
Annealing	55°C	20 sec	
Extension	72°C	30 sec	
Final extension	72°C	10min	1
Final hold	4°C	∞	1

2.4.5 Agarose gel electrophoresis and DNA visualisation

Agarose gel electrophoresis is the most common method to separate and analyse DNA fragments. It works by using electrical current to separate negatively charged DNA to a positive electrode through an agarose gel matrix, with the speed of migration depending on the size of DNA fragments. Agarose gels containing either 0.8% (1-10kb DNA fragments) or 1-2% (smaller fragments less than 1kb) agarose were prepared for running DNA samples.

- The required amount of agarose powder (Melford Chemicals, Suffolk, UK) was added to 100ml (1X) TBE buffer and heated in a microwave oven until the agarose was completely dissolved. After cooling down for 5 minutes, the solution was stained with SYBR®Safe DNA gel stain (Invitrogen, Paisley, UK) and poured into electrophoresis cassettes (Scie-Plas Ltd, Cambridge, UK). Well forming combs were gently inserted and the gel was left to set at room temperature for 30-40 minutes until completely solidified.
- Once the gel had set, the well forming combs were removed after 1xTBE was poured over and exceed 5mm of the gel surface. 8µL DNA ladder (GenScript®, Piscataway, USA) was loaded into the first lane of the gel and then 8-10µL of DNA samples were loaded into additional wells of the gel by placing the gel loading tips just over the well.
- The gel was run with an Electrophoresis power supply (Gibco BRL, Life Technologies Inc.) at 120V, 100mA and 50W for approximately 30-50

minutes. When the visible dye line had moved the desired distance required for the product size, the electrodes were disconnected.

- The gel was then removed, and the DNA fragments visualised using Syngene U: Genius3 fluorescence UV transilluminator (Synoptics Ltd, Cambridge, UK). Images were saved electronically and printed using a thermal printer.

2.4.6 Real time quantitative PCR (QPCR)

Real-time (or quantitative) PCR is a sensitive technique for gene analysis. It measures PCR amplification in real-time as the reaction proceeds instead of at the end of the reaction in comparison with conventional PCR. This method works by detecting a fluorescent reporter probe which is increased during PCR amplification (PCR product is proportional to the level of fluorescence detected). The fluorescence level is continuously recorded by a sensitive camera attached to the system.

In this study, the Ampliflour™ Uniprimer™ Universal system (Intergen company®, New York, USA) was used to quantify transcript copy number. The ampliflour probe consists of a 3' region specific to the Z-sequence (ACTGAACCTGACCGTACA) present on the target specific primers and a 5' hairpin structure labelled with a fluorophore (FAM). When in this hairpin structure, the fluorophore is linked to an acceptor moiety (DABSYL) which acts to quench the

fluorescence emitted by the fluorophore, preventing any signal from being detected.

During PCR, the probe becomes incorporated and acts as a template for DNA polymerisation in which DNA polymerase uses its 5'-3' exonuclease activity to degrade and unfold the hairpin structure, thereby disrupting the energy transfer between flourophore and quencher, allowing sufficient fluorescence to be emitted and hence detected. The fluorescent signal emitted during each PCR cycle can then be directly correlated to the amount of DNA that has been amplified. This process is illustrated in Figure 2.1.

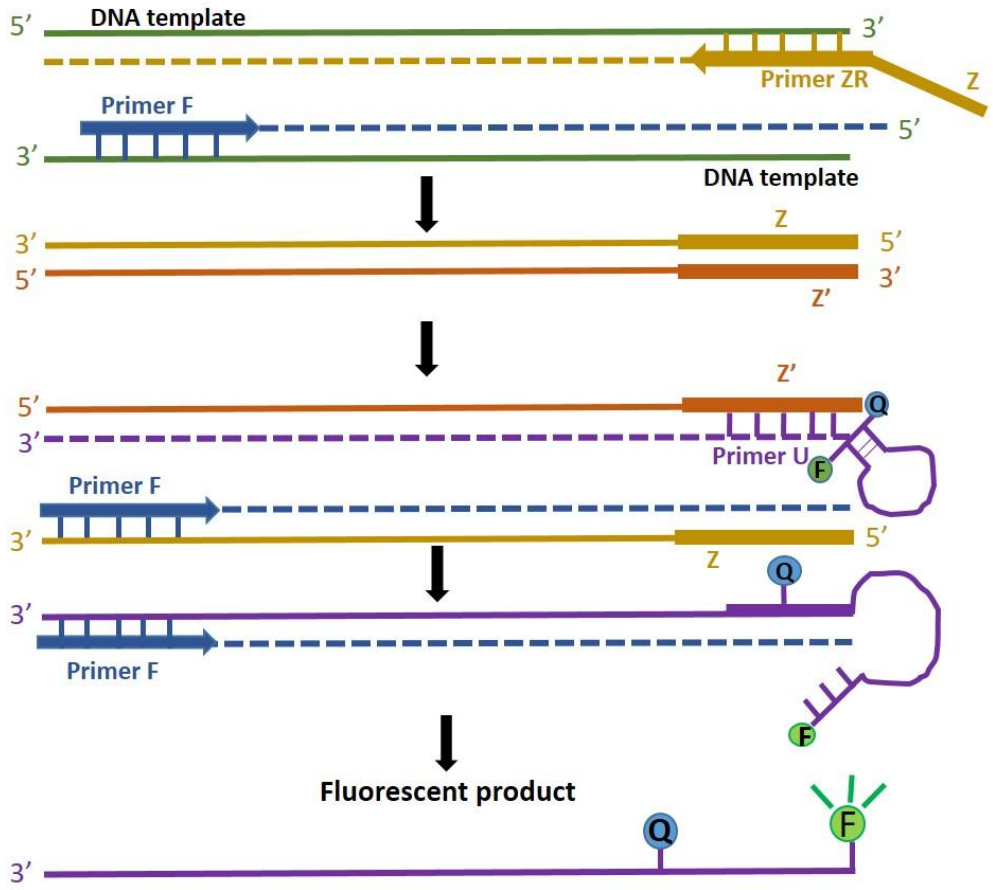

Figure 2.1: Real time quantitative PCR using the fluorescent labelled Uniprimer. Diagram shows function of the u-probe during DNA amplification using QPCR.

- Each reaction to be amplified was set up as follows:

Component	Volume
2x iQ™ Supermix	5µL
Forward primer (10pmol/µL)	0.3µL
Reverse primer (1pmol/µL)	0.3µL
Amplifluor™ probe (10pmol/µL)	0.3µL
cDNA	1µL
PCR H_20	3µL
Total volume per reaction	10µL

- Each sample was loaded into a 96 well plate (Applied Biosystems™, Life Technologies Ltd, Paisley, UK), covered with MicroAmp® Optical Adhesive film (ThermoFisher Scientific, Life Technologies Ltd, Paisley, UK) and run alongside a podoplanin (PDPL) standard of a known transcript number (ranging from 10^8 to 10^1). PDPL is a lymphangiogenesis marker, which is employed as a reference control gene for a standard curve to ensure any differences observed were not due to technical errors and allowed normalization of results. It is also used to calculate relative copy numbers of target genes. The 96 well plate was placed in an iCycler Thermal Cycler which uses a light source to excite the fluorescent molecules in the wells and an image intensifier and a 350,000-pixel charge-coupled device (CCD) detector to image all 96 wells every second and detect fluorescent light at the annealing stage. The conditions used for QPCR are shown as follows:

Step	Temperature (°C)	Time (minutes:seconds)	Number of cycles
Initial denaturation	94	05:00	
Denaturation	94	00:10	80-90 cycles
Annealing	55	00:35	
Extension	72	00:20	

- The fluorescent signal is deteded at the annealing stage by a camera where its geometric increase directly correlates with the exponential increase of product. This is then used to determine a threshold for quantification of genes amplified in each reaction. Copy number of a target transcript is determined using the cycle number of a reaction when its fluorescence signal reaches the threshold.
- The degree of fluorescence emitted by a range of standards with a known copy number of a reference gene (PDPL) are used to compare the amount of fluorescence emitted by each sample, allowing for the transcript copy number of a target gene in each sample to be accurately calculated.
- Furthermore, the transcript copy number of each sample was normalised against the detection of β-actin or GAPDH copy numbers. The procedure was repeated at least three times, and representative data is demonstrated.
- How transcript levels are quantified is shown in Figure 2.2.

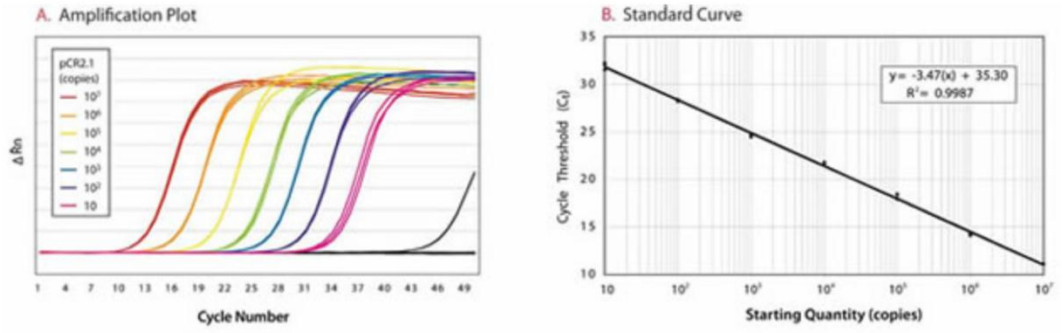

Figure 2.2: (A) Detection of transcript levels from a range of standard samples (10^8 to 10^1 copy number) using the iCyclerIQ thermal cycler. (B) Subsequent generation of a standard curve from these samples.

2.5 Methods for protein detection

2.5.1 Extraction of protein and preparation of cell lysates

- When cells reached sufficient confluence, the medium was removed and the cell monolayer was washed twice with PBS buffer. 5ml PBS was then added to the flask and the cells were scraped with a sterile cell scraper from the flask surface and transferred to a universal tube.
- The cell suspension was centrifuged at 1,800rpm for 10 minutes to obtain a cell pellet. After removal of the supernatant with a vacuum aspirator, 200-300µl (depending on pellet size) of lysis buffer was added to the universal tube and the cell suspension was transferred to a 1.5ml microfuge tube.
- In order to extract protein from cell lysate, the sample was incubated at 4°C for 1 hour with continuous rotation on a Labinoco rotating wheel (Wolf laboratories, York, UK) (25rpm and 4°C)
- After 1 hour, the resulting lysate was centrifuged at 13,000 rpm for 15 minutes. The supernatant containing proteins was then transferred to a fresh tube. The pellet containing insoluble and any unwanted cell debris was discarded.
- The protein sample was then either quantified for western blot or stored at -20°C until further use.

2.5.2 Protein quantification and preparation of protein samples

In order to standardise the concentration of protein samples before they were analysed using sodium dodecyl-polyacrylamide gel electrophoresis (SDS-PAGE) and western blotting, the protein samples were quantified using the Bio-Rad DC Protein Assay kit (Bio-Rad Laboratories, Hemel-Hempstead, UK). The kit utilised a colorimetric assay based on the reaction of protein with an alkaline copper tartrate solution (Reagent A) and Folin reagent (Reagent B), which is used for the determination of protein concentration following detergent solubilisation. The protein reacts with copper in the alkaline medium resulting in the subsequent reduction of the Folin reagent and the production of a characteristic blue colour (with an absorbance between 405-750nm). Bovine serum albumin (BSA) was used as a standard for this protein quantification.

- In a 96 well plate, 50mg/ml BSA standard (Sigma-Aldrich, Poole, Dorset, UK) was diluted in lysis buffer to produce a concentration gradient from 0.78mg/ml to 50 mg/ml. These were used to generate a standard curve for determining concentration of the protein samples.
- 5µl of either protein samples or standards were added into each well on a 96-well plate and 25µl of Reagent A' (prepared by adding 20µl of reagent S to every 1ml of reagent A) was added to each well followed by 200µl of Reagent B.

- After the sample was mixed, the plate was left at room temperature for 30-45 minutes for the colorimetric reaction to occur. The absorbance for each well was then measured at a wave length of 630nm using the ELx800 plate reading spectrophotometer (Bio-Tek, Wolf Laboratories, York, UK).
- The standard curve was set up using the absorbance of the standards. Protein concentration of the test samples was determined according to the standard curve. Appropriate amounts of lysis buffer was used to standardise the protein samples to a final concentration of 1-2mg/ml depending on the lowest concentration of the same collection.
- This sample was finally diluted 1:1 with 2x Lamelli sample buffer concentrate (Sigma-Aldrich, Poole, Dorset, UK) and then denatured by boiling at 100°C for 5-10 minutes. The boiled samples were either used immediately for SDS-PAGE or stored at -20°C until further use.

2.5.3 Protein extraction for Kinexus^{TM} antibody microarrays

- Before protein extraction, each cell type was cultured in two T75 flasks until approximately 80% confluence. Cells were left for serum starvation for 24 hours before collection.
- Upon protein extraction, cells were washed twice with PBS and scraped from the flask using 5ml sterile PBS. The cell suspension from two flasks

was combined and centrifuged at 2,500 rpm for 10 minutes to pellet the cells.

- The cell pellet was then lysed in 600µl lysis buffer and was subsequently placed on a Labinoco rotating wheel (Wolf laboratories, York, UK) (25rpm and 4°C) for 40-60 minutes for sufficient extraction.
- After 15 minutes centrifugation at 13,000rpm, the protein lysate was used for protein quantification.
- 300µl lysis (4mg/ml) was prepared and stored at -20°C before being sent for Kinexus™ antibody microarray analysis (Kinexus Bioinformatics, Vancouver, British Columbia, Canada).

2.5.4 Immunoprecipitation preparation

Immunoprecipitation is an invaluable technique used to analyse intracellular phosphorylation events occurring upon an extracellular stimulation. The process of immunoprecipitation involves cell lysis, followed by an incubation with a specific antibody against target protein or proteins (for example, PY99 is an antibody targeting proteins with phosphorylated tyrosine) presenting within the tested protein samples. The resultant antigen-antibody complexes are then precipitated using agarose beads conjugated with Staphylococcal protein A and protein G followed by SDS-PAGE and immunoprobing. A brief description of the Immunoprecipitation method used in this study is outlined as follows:

- An Antibody targeting a protein of interest was added to the cell lysate samples before being incubated at 4^{o}C for 1 hour with continuous rotation.
- Following the incubation, 20µl of conjugated A/G protein agarose beads (Santa Cruz Biotechnology, UK) were added to each sample. The samples were then incubated at 4^{o}C with continuous rotation overnight which allowed for antibody-protein complexes binding to the beads.
- The samples were then centrifugation at 8,000rpm for 5 minutes, allowing removal of any unbound protein or excess antibodies present in the supernatant. The protein pellet was subsequently washed twice with 300µl of lysis buffer before being resuspended in 40-60µl of 1x Lamelli sample buffer and boiled for 10 minutes. The resulting samples were then run on SDS-PAGE gels as explained below.

2.5.5 Sodium Dodecyl Sulphate Polyacrylamide Gel Electrophoresis (SDS-PAGE)

- Four glass plates were prepared and assembled in two gel cassettes on a casting stand. Once assembled, ethanol was used to fill the space between the glass plates to test for leakages.
- The system used to conduct SDS-PAGE in this study was an OmniPAGE VS10 vertical electrophoresis system (Cleaver Scientific Ltd., Rugby, Warwickshire, UK). The required percentage of resolving gel was

dependant on the protein size. A mixture of 15ml (enough for 2 mini gels) was prepared by adding all the constituents listed in the following:

8% Resolving gel (protein size over 100 kDa)	
Distilled water	*6.9ml*
30% acrylamide mix (Sigma-Aldrich, Poole, Dorset, UK)	*4.0ml*
1.5 M Tris (pH8.8)	*3.8ml*
10% SDS	*0.15ml*
10% Ammonium persulphate	*0.15ml*
TEMED (Sigma-Aldrich, Poole, Dorset, UK)	*0.009ml*

10% Resolving gel (protein size less than 100 kDa)	
Distilled water	5.9ml
30% acrylamide mix (Sigma-Aldrich, Poole, Dorset, UK)	5.0ml
1.5 M Tris (pH8.8)	3.8ml
10% SDS	0.15ml

10% Ammonium persulphate	0.15ml
TEMED (Sigma-Aldrich, Poole, Dorset, UK)	0.006ml

- The resolving mixture was then added into space between the two glass plates carefully until it reaches a level about 1cm below the comb. In order to prevent gel oxidation, 1ml 2-propanol was added to cover the top of resolving gel.
- The gels were then left to polymerise at room temperature for about 30 minutes, or until set completely. The excess 2-propanol was poured off before a sufficient amount of stacking gel was added. The ingredients for staking gel are listed in the following:

Component	**Stacking gel**
Distilled water	3.4ml
30% acrylamide mix (Sigma-Aldrich, Poole, Dorset, UK)	0.83ml
1.0M Tris (PH 6.8)	0.63ml
10% SDS	0.05ml
10% Ammonium persulphate	0.05ml
TEMED (Sigma-Aldrich, Poole, Dorset, UK)	0.005ml

- A well forming Teflon comb was inserted immediately after adding the stacking gel, and the gel was left at room temperature for around 20 minutes for polymerisation to occur.
- After the gel was set, the loading cassette was transferred into an electrophoresis tank and covered with 1X running buffer before the well comb was removed. 10µl of Broad range markers (Santa Cruz Biotechnology, UK) were loaded into the first well of the gel, followed by 10-15µl of the required protein samples.
- The proteins were then separated at 100-120V, 50mA, and 50W for a period up to 3 hours depending on the degree of separation required for target proteins according to their molecular weight.

2.5.6 Transferring proteins from gel to PVDF membrane

- After SDS-PAGE, the gel containing protein samples was electrically transferred onto a PVDF membrane. Following SDS-PAGE separation, the electrophoresis cassettes were disassembled and the gels were taken out. The stacking gel on each gel was cut off and discarded. The resolving gel was then placed on the bottom graphite base electrode in a SD20 SemiDry Maxi System blotting unit (SemiDRY, Wolf Laboratories, York, UK) on top of 3 pieces of 1X transfer buffer pre-soaked filter paper (Whatman International Ltd., Maidstone, UK), and 1 sheet of PVDF membrane.

An additional 3 sheets of pre-soaked filter paper were placed on top of the gel to form a sandwich arrangement in an order as filter papers, gel, membrane, filter papers (from cathode to anode) (Figure 2.3). Electroblotting was then conducted at 15V, 500mA, and 8W for 40-60 minutes according to the protein size. Once the proteins had been transferred sufficiently, the membranes were blocked with 10% milk solution (10% milk skimmed powder and 0.1% polyoxyethylene (20) sorbitan monolaurate (Tween 20) in TBS for at least one hour at room temperature. This step aims to reduce background, i.e. non-specific binding to the membrane and subsequently subject to a probing with antibodies.

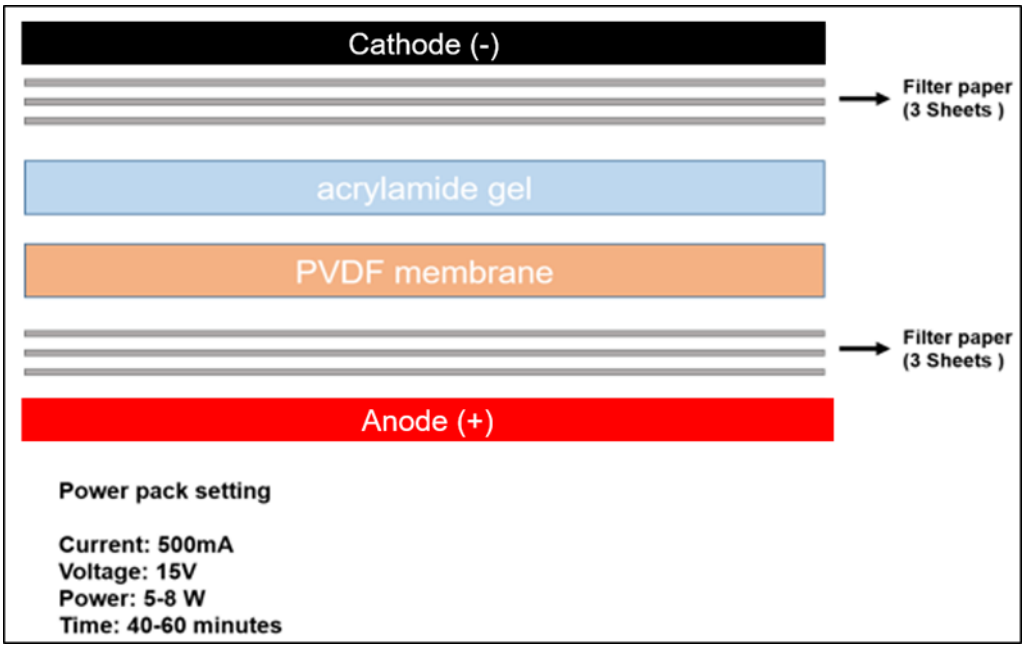

Figure 2.3: Diagram depicting process of western blotting; the transferring of proteins onto a PVDF membrane.

2.5.7 Protein detection using specific immuno-probing

- Once blocking was completed, the membrane was transferred into 50ml falcon tubes (Nunc, Fisher-Scientific, Leicestershire, UK) with the membrane surface facing upwards. Then the membrane was incubated in 10ml 3% milk solution (3% milk powder, 0.1% Tween 20 in TBS) with primary antibody diluted 1:500 overnight at 4^{o}C.

- After probing with primary antibody, the membrane was washed with 5ml TBST (TBS with 0.2% Tween 20) for three times (10 mins each) to remove remaining unbound antibodies.
- The membrane was subsequently incubated with 5ml of 1:1000 horse radish peroxidase (HRP) conjugated secondary antibody diluted in 3% milk for one hour with continuous rotation.
- The membrane was washed for three times (10 mins each) with 5ml TBST before undertaking chemiluminescent detection.

2.5.8 Chemiluminescent protein detection

Chemiluminescent protein detection was carried out using the Luminate Forta Western HRP substrate (Cat. No. WBLUF0500, Merk-Millipore, Hertfordshire, UK). This solution consists of a highly sensitive chemiluminescent substrate and is used to detect the HRP for visualising the probed protein bands. The protocol was undertaken as follows:

- 1ml reagent was added onto the membrane with a 5-minute incubation at room temperature with constant agitation.
- Excessive solution on the membrane was removed before putting the membrane into a plastic tray. The chemiluminescent signal was detected using an UVITech Imager (UVITech Inc., Cambridge, UK) which contains both an illuminator and a camera linked to a computer.
- The exposure time was adjusted as necessary until the protein bands were sufficiently visible and the image was captured and analysed using ImageJ for the protein band quantification.
- In this study, β-actin was used as a loading control and ran alongside when detecting any other proteins for additional normalisation of the sample. β-actin is used because of its high abundancy and conserved nature within eukaryotic cells and is one of the most widely employed and accepted internal controls in determining mRNA and protein expression.

2.5.9 Immunohistochemical staining

- After rehydration of the tissue section, the section was blocked with a blocking solution containing horse serum (Vector Laboratories Inc., Burlingame, USA) for 30 minutes at room temperature. The blocking solution was prepared by adding 1-2 drops of horse serum into 5ml of 1X OptiMax Wash Buffer (BioGenex, San Ramon, USA).

- After blocking, the slide was washed three times with wash buffer before being incubated for an hour at room temperature with primary antibody (the dilution may vary depending on a specific antibody used, but generally 1:100 was used) diluted in blocking solution.
- Any unbound antibody was subsequently washed off with wash buffer, this was repeated three times before incubating the samples for another 30 minutes at room temperature, with the corresponding secondary antibody diluted 1:1000 in blocking solution.
- After three washes with wash buffer, the sections were incubated with 200µl of VECTASTAIN® Universal ABC complex (Vector Laboratories Inc., Burlingame, USA) for 30 minutes. The ABC complex was made up 30 minutes before use by mixing 4 drops of the supplied reagent A, with 4 drops of regent B.
- The ABC solution was subsequently removed by washing three times with wash buffer before a few drops of 3,3'-Diaminobenzidine (DAB) chromogen (Vector Laboratories Inc., Burlingame, USA) were added onto the tissue followed by a 5-minute incubation in the dark to allow colour development. DAB was made up as follows; 2 drops of the provided buffer (pH 7.5), 4 drops of DAB, and 2 drops of hydrogen peroxide diluted in 5ml of distilled water.
- Following DAB addition and development of a brown colouration, indicative of protein presence, the DAB was washed off using distilled

water before the sections were counterstained with Mayer's haemotoxylin for approximately 5 minutes.

- After three washes with distilled water, slides were dehydrated for 5 minutes in each sequential solution; 50% ethanol, 70% ethanol, 90% ethanol, 100% ethanol, 50% ethanol/ 50% xylene, 100% xylene.
- After dehydration, slides were mounted with DPX mountant and left to dry.
- The intensity of IHC staining was quantified using Image J software (https://imagej.nih.gov/ij/).

2.6 Targeting Kidins220 gene expression

2.6.1 Knocking down Kidins220 using Ribozyme Transgenes

Hammerhead ribozyme transgenes were used to knockdown the expression of Kidins220 by specifically targeting and cleaving the Kidins220 transcript. Hammerhead ribozymes targeting Kidins220 were designed using the mfold mRNA folding programme (http://unafold.rna.albany.edu/?q=mfold/RNA-Folding-Form) based on the secondary structure of Kidins220 mRNA (Figure 2.4). The transgenes were synthesised using touchdown PCR and the products were then run on a 2% agarose gel to verify their presence and size before being cloned into the pEF6/His plasmid vector (Figure 2.5). Subsequently, the ribozymes obtained from the above procedure were cloned into the pEF6/V5-His-TOPO vector, and this was followed by transferring the reaction mixture to a vial of

TOP10 chemically competent *E.coli*. After 30 minutes on ice, the bacteria were subject to heat shock at 42^{o}C for 30 seconds, before being placed on ice for 2 minutes. The bacterial mixture was added to SOC media and placed on an orbital shaker for 1 hour, at a speed of 200rpm. The bacterial solution was plated on agar plates containing 100µg/ml amplicillin and allowed to grow overnight. As the pEF plasmid has antibiotic resistance genes to ampicillin and blasticidin, only the cells containing the plasmid were able to grow on the agar. Colonies of transformed *E.coli*, transgenes of Kidins220 cloned into pEF6/V5-His-TOPO plasmids (Invitrogen Inc., Paisley, UK) were analysed using RT-PCR with the T7F primer coupled either with RbBMR and RbTPF primers. After amplifying the correct colonies, the plasmids were extracted using the Sigma GenElute Plasmid MiniPrep Kit (Sigma-Aldrich, Poole, Dorset, UK). Control plasmid and the plasmid containing the ribozyme transgene was used to transfect both Panc-1 and Mia paca-2 cell lines respectively. The transfected cells were cultured in selection media containing 5µg/ml blasticidin for around 1-2 weeks so that only those cells containing the plasmid would survive. Following selection, the cells were transferred into maintenance media containing 0.5µg/ml blasticidin. To verify the knockdown of Kidins220, RT-PCR, QPCR and western blot procedures were carried out as previously described.

Figure 2.4: Secondary structure of Kidins220 mRNA, generated using the mfold (http://unafold.rna.albany.edu/?q=mfold/RNA-Folding-Form).

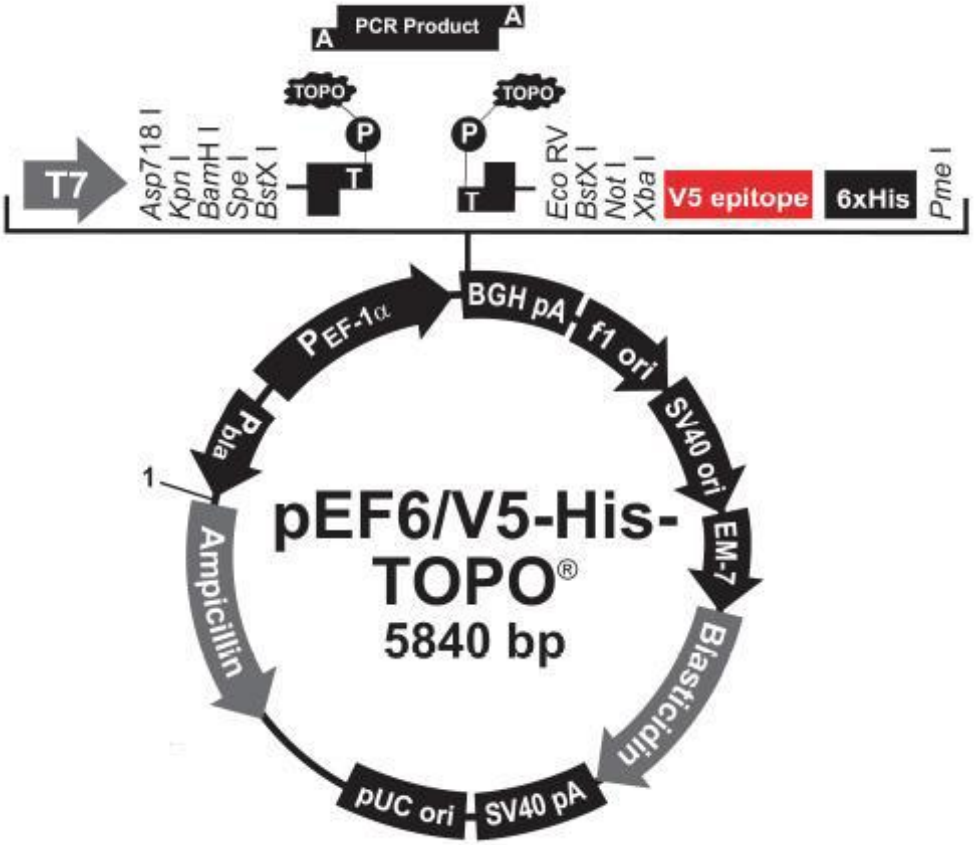

Figure 2.5: Schematic of the pEF6 plasmid (From pEF6/V5-His TOPO TA Expression Kit protocol).

2.6.2 Knocking down gene expression using lentivirus shRNA

RNA interference (RNAi) has been used as a research tool to regulate the expression of specific genes in several experimental organisms. Its role in controlling gene expression also contributes to therapeutic strategies targeting specific genes linked to onset or progression of a particular disorder. RNAi can be achieved through a vector-based shRNA. Lentiviral vectors are capable of delivering genetic material into cells (*in vivo* or *in vitro*) and can stably integrate

shRNAs into the genome of both dividing and non-dividing cells, resulting in long term expression of the transgene.

The current study used the pLV lentivirus vector with a Kidins220 shRNA construct which comprises three selective markers, i.e. a green fluorescent protein and resistance genes to Ampicillin for prokaryotes and Neomycin/G418 for mammals (Figure 2.6).

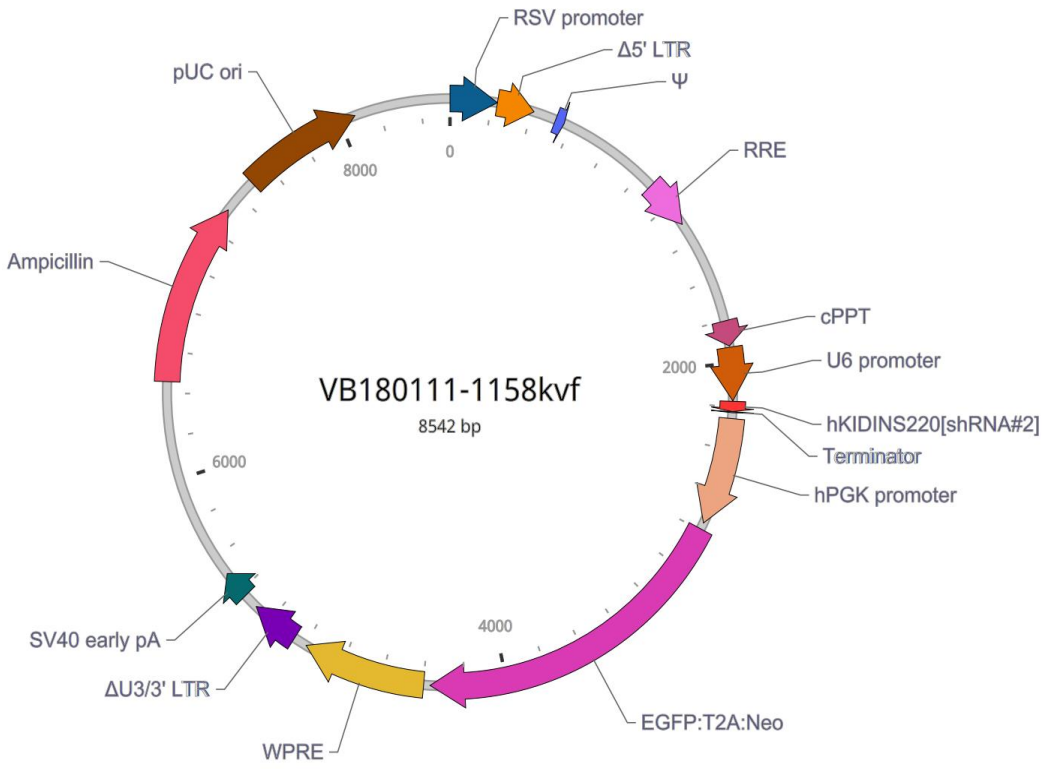

Figure 2.6: Schematic of the pLV lentivirus plasmid. The lentivirus plasmid containing shRNA was generated using the online vector designing tool. (https://www.Vectorbuilder.com).

2.6.3 Plasmid amplification and purification

- shRNA was picked from the tube and inoculated in 10ml of LB broth with 100µg/ml ampicillin and subsequently incubated at 37^{o}C overnight with constant agitation.
- The amplified *E. coli* were then pelleted by centrifugation at 4^{o}C for 15 minutes at 6,000rpm and then used for plasmid extraction. This was carried out using the Sigma GenElute Plasmid MiniPrep kit (Sigma-Aldrich, Poole, Dorset, UK) according to the provided protocol, outlined below.
- The bacterial pellet was resuspended in 200µl of resuspension fluid (containing RNase A) before being mixed thoroughly and transferred into the 2ml collection tubes provided.
- This was followed by the addition of 200µl lysis solution and gentle mixing by inverting the tubes 5-6 times. The resulting mixture was left at room temperature for 5 minutes before adding 350µl of neutralisation solution.
- The tube was inverted several times, and centrifuged at 12,000rpm for 10 minutes. The resulting supernatant was then transferred into a fresh collection tube containing a Mini Spin Column, which binds the plasmid DNA. This was centrifuged at 12,000rpm for 1 minute.
- The flow through was discarded before the column was washed with 700µl of wash solution (containing ethanol) and centrifuged at 12,000rpm for 1 minute. The flow through was discarded once more, before the column was dried by another centrifugation for one minute.

- The column was then transferred into a fresh collection tube for elution. This was carried out by adding 100µl of elution solution and centrifugation at 12,000rpm for 1 minute. The resulting flow through containing the purified plasmid was collected, and approximately 4µl was run on a 0.8% agarose gel in order to confirm the presence and purification of the plasmid.

2.6.4 Production of lentivirus particles

- For each plasmid to be transfected, 7 x 10^5 HEK-293T cells in 5ml of media was added into a 6cm^2 tissue culture plate, and the cells were incubated at 37^oC, 5% CO_2 until 50-80% confluent.

- The transfection reagent (Santa Cruz Biotechnology, UK) was mixed and added in polypropylene microfuge tubes to 20µl serum-free OPTI-MEM as follows:

1µg	pLV shRNA plasmid
750 ng	psPAX2 packing plasmid
250ng	pMD2.G envelope plasmid

- The transfected reagent was added into HEK-293T cells and the cells were incubated at 37^{o}C, 5% CO_2 for 12-15 hours.
- Following incubations, the medium containing transfection reagent was removed and replaced with 5ml fresh medium. The medium was pipetted onto the side of the plate so as not to disturb the transfected cells and the cells were incubated for an additional 24 hours.
- The media was harvested from cells and transferred to a polypropylene tube. The medium containing lentiviral particles was stored at 4^{o}C.
- 5ml fresh medium was added to the cells and incubated at 37^{o}C and 5% CO_2 for another 24 hours.
- The medium was harvested from the cells and pooled together with the previously collected medium.
- The medium was centrifuged at 1,250 rpm for 5 minutes to pellet any HEK-293T cells that were inadvertently collected during harvesting. The lentiviral particles were stored at -80^{o}C for future use.

2.6.5 Infecting target cells

- Target cells were seeded in 6-well plates and grow at 37^{o}C and 5% CO_2 overnight.

- When cells were approximately 70% confluent, fresh medium containing 8µg/ml polybrene, used to increase the transfection efficiency, was added to the plate.

- 0.05-0.1ml Lentiviral particle solution (add 0.5ml for a high multiplicity of infection (MOI), and 0.1ml for a low MOI) was added to the target plate and the cells were incubated at 37^{o}C and 5% CO_2 overnight.

2.6.6 Establishment of stable expression in mammalian cell lines

- Following infection, in order to obtain a stable cell line expressing shRNAs it is necessary to select culture cells.

- The pLV vector contains a resistance sequence against neomycin/G418 and this can be used for selection in mammalian cells. Therefore, the cells were cultured in selection medium containing 500µg/ml G418 for around 1-2 weeks which allowed only infected cells, containing the plasmid to survival.

- After selection, the cells were cultured in maintenance medium containing 100µg/ml G418. Verification of target gene knockdown was performed using RT-PCR and western blotting as outlined previously.

- Once the cells had been verified to stably reduced expression of the desired molecule, they were subject to various *in vitro* assays to detect the

effect on the biological functions of the cells by altering expression of the target gene.

2.7 *In vitro* cell function assay

The hallmarks of cancer characterise the most essential phenotypic features of malignant transformation and progression (Menyhart et al., 2016). The basic aberration that lead to the development of cancer is the continual uncontrolled proliferation of cancer cells. Cancer cells grow and divide in an unregulated manner, invading to surrounding tissues and organs and finally spreading throughout the body (Lopez-Saez et al., 1998). In the current study, we used several *in vitro* function tests, such as cell proliferation assay, adhesion assay, trans-well invasion assay and migration assay to determine the impact of Kidins220 on cellular functions of cancer cells.

2.7.1 *In vitro* cell growth assay (2D model)

- The protocol by Hu *et al.* was followed (Hu et al., 2012). 200µl of media containing 3,000 cells was seeded into 96 well plates.
- These plates were incubated at 37^{o}C, with 5% CO_2, for a period of 24, 48, 72, and 120 hours respectively.

- After incubation, the media was aspirated, and the cells were fixed with 4% formaldehyde for 10-20 minutes before being stained with 0.5% crystal violet for 10 minutes. The plate was then rinsed with tap water and left to air dry.
- The stain was then solubilised using 200µl of 10% acetic acid and the amount of cells was assessed by measuring the absorbance of the resulting solution at 540nm using a spectrophotometer (BIO-TEK, ELx800, UK). The growth rate was calculated as a percentage, using the absorbance from the corresponding plate collected at 24 hours as a baseline.

2.7.2 Tumour spheroid growth assay (3D model)

Three-dimensional (3D) *in vitro* models have been used in cancer research as an intermediate model between *in vitro* 2D models/assays and *in vivo* tumour models. Spherical cancer models represent major 3D *in vitro* models that have been described over the past 4 decades (Weiswald et al., 2015).

- 200µl of media containing 1,000 cells was seeded into 96-well tumour spheroid plates.
- These plates were incubated at 37^{o}C, with 5% CO_2, for a period of 15 days.
- Images of the spheroid were captured using an EVOS automated microscope every 3 days.

- Spheroid size was calculated using ImageJ software.

2.7.3. *In vitro* adhesion assay

- 100µl of serum free media containing 5µg Matrigel® Basement Membrane Matrix (Corning Incorporated, Flintshire,UK) was coated in a 96-well plate. The Matrigel was then left to dry for 2 hours at 55^{o}C.
- 200µl of sterile water was added to each well and left for at least 45 minutes at room temperature to rehydrate the Matrigel.
- The media was aspirated and 20,000 cells, diluted in 200µl media, were seeded into each well and left to adhere at 37^{o}C, with 5% CO_2 for 40 minutes.

- After incubation, the media was discarded and the cells were washed with BSS to remove any non-adherent cells. The remaining adherent cells were then fixed with 4% formalin for 10-20 minutes, and then stained with 0.5% crystal violet for 10 minutes. Following substantial washes, the plates were left to dry before counting adherent cells and capturing images under the microscope. Due to the fluid dynamics within the small size wells of 96 well plate, the unevenly set Matrigel can lead to cell aggregation around the edges of the well. In order to avoid this issue, only the cells that adhered to the central area of the well were counted.

2.7.4 *In vitro* invasion assay

- 8µm pore transwell inserts (FALCON®, pore size 8.0µm, 24 well format, Greiner Bio one, Germany) were placed into wells of a 24 well plate (NUNC™, Greiner Bio one, Germany), using sterile forceps in order to prevent contamination (Figure 2.7).

- Each insert was coated with 100µl of serum free media containing 50µg Matrigel (stock concentration 0.5µg /µl) and left to dry for 2 hours at 55^{o}C.

- The Matrigel was then rehydrated with 200µl sterile water at room temperature for 45 minutes.

- After the water was carefully discarded, 20,000 cells, in 200µl media, were seeded into each insert. 600µl media was then added to the bottom chamber of each well. The cells were incubated for 72 hours, with 5% CO_2 at 37^{o}C.

- After 72 hours incubation, the Matrigel layer and the non-invasive cells were then removed from the insert using a cotton bud. Both the Matrigel layer and the non-invasive cells were thoroughly removed as they can also be stained with crystal violet, impacting quantification of invasive cells that had invaded the Matrigel and porous membrane and established on the underside of the insert.

- The invasive cells were then fixed with 4% formalin for 10-20 minutes and then stained with 0.5% crystal violet for 10 minutes. The crystal violet was then washed off and the plate was left to airdry. The stained cells were subsequently counted and photographed under the microscope.

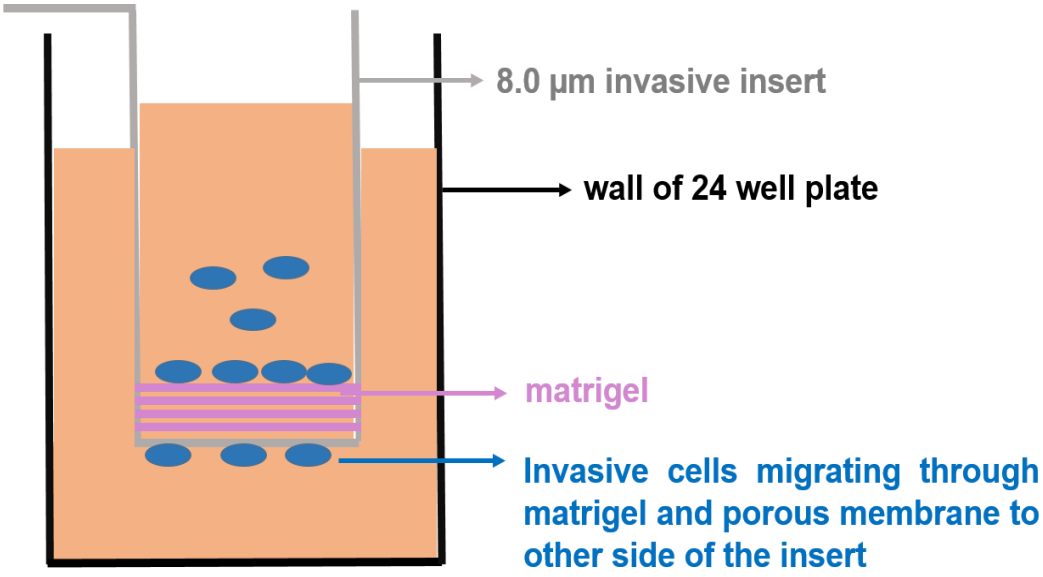

Figure 2.7: Schematic diagram showing *in vitro* invasion assay.

2.7.5 *In vitro* migration assay

- 8µm pore transwell inserts (FALCON®, pore size 8.0µm, 24 well format, Greiner Bio one, Germany) were placed into wells of a 24 well plate (NUNC™, Greiner Bio one, Germany), using sterile forceps in order to prevent contamination (Figure 2.8).

- 20,000 cells, in 200µl media, were seeded into each insert. 600µl media was then added to the bottom chamber of each well. The cells were incubated for 72 hours, with 5% CO_2 at 37°C.

- After 24 hours incubation, non-invasive cells were then removed from the insert using a cotton bud.

- Cells which had migrated through the insert were then fixed with 4% formalin for 10-20 minutes and then stained with 0.5% crystal violet for 10 minutes. The crystal violet was then washed off and the plate was left to airdry. The stained cells were subsequently counted and photographed under the microscope.

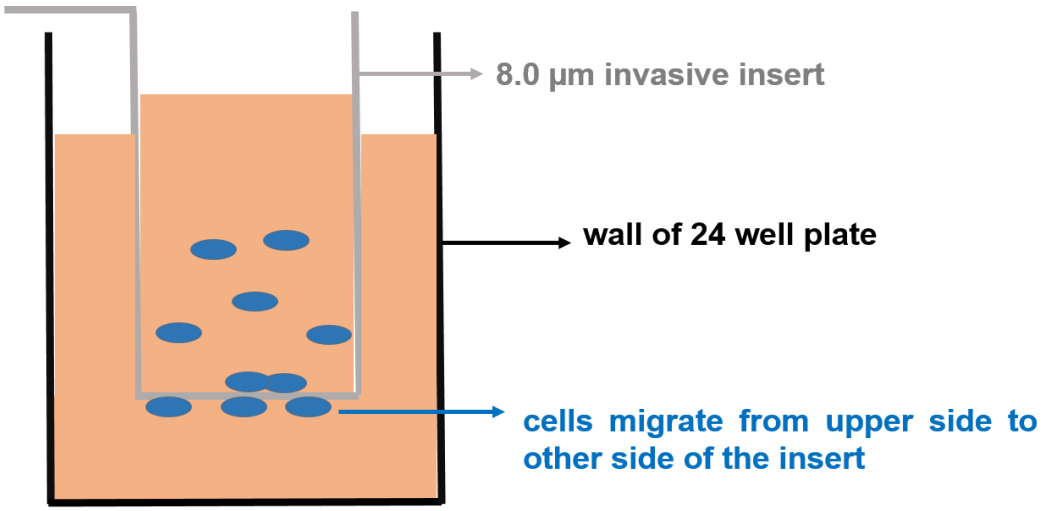

Figure 2.8: Schematic diagram showing *in vitro* migration assay.

2.7.6 *In vivo* peritoneal metastasis model

Athymic nude mice (CD1) were purchased from Charles River Laboratories (Charles River Laboratories International, Inc., Kent, England, UK) and settled down for a week before use. The study was conducted under Home Office Project licence (PPL: PE944FC2). All mice were kept in filter-topped isolation cages and all the procedures were carried out in a class-II cabinet.

Pancreatic cancer cells (scramble and shKidins220) were injected into the peritoneal cavity of athymic nude mice with a volume of 100µl which contained Matrigel at final concentration of 2.5mg/ml in PBS. The mice were then carefully monitored twice a week by measuring body weight. The mice were terminated after 4 weeks and intraperitoneal exploration was conducted to detect metastatic tumours of liver, stomach, pancreas, and duodenum to rectum. Metastatic nodules were photographed using a stero-microscrope (Olympus, Japan) and the volume of metastatic tumours was calculated by using the following formula:

Tumour volume (mm^3) = 0.5× $Width^2$×length

2.8 Collection of clinical cohort

In this study, the clinical cohort included pancreatic tumours (n=149) together with paired adjacent background tissues which were collected immediately after surgery and stored at -80 ºC until use, with written consent from patients at Peking University Cancer Hospital. All protocol and procedures were approved by Peking University Cancer Hospital Research Ethics Committee (Appendix1). The frozen tissues were first sectioned using a Leica CM1900 Cryostat (Leica Microsystems Ltd, Bristol, UK) at 8-10µm thickness. These sections (>50) were divided into three portions:

1. Immediately mounted on glass slides and fixed for routine histology assessment;

2. Mounted on slides and fixed using Superfrost®Plus microscopic slides for subsequent immunohistochemical analysis. These slides were stored at -20^{o}C.

3. The remaining sections were pooled and homogenised to extract RNA for molecular based analysis.

2.9 Statistical analysis

Following a normality check, t-test and One-way ANOVA were employed for normally distributed data whilst non-normally distributed data was analysed using a Mann-Whitney test. Differences were considered to be statistically significant

when $p<0.05$. Graphs were constructed using GraphPad Prism Software (Version6, GraphPad Software). Kaplan-Meier survival analysis was carried out using SPSS software (SPSS Standard version 13.0; SPSS Inc., Chicago, IL, USA).

Chapter 3

Expression of Kidins220 in pancreatic cancer and the clinical relevance

3.1 Introduction

Kidins220/ARMS is a transmembrane protein with predominant expression in nervous and neuroectodermic tissues (Iglesias et al., 2000). Several *in vivo* studies have strongly demonstrated that aberrant expression and function of this molecule is associated with occurrences of certain diseases.

Like the findings in animal models, mutation of Kidins220 has also been evident in human diseases. For instance, heterozygous mutations of Kidins220 has been reported to be a cause of spastic paraplegia, intellectual disability, nystagmus, obesity, and homozygosity (Josifova et al., 2016). Expression of non-functional variants of Kidins220 is associated with enlarged cerebral ventricles and limb contracture in foetuses (Mero et al., 2017, Josifova et al., 2016). In Alzheimer's disease (AD), necropsies for AD patients in different progression stages presented an increased expression level of Kidins220 in the brain which is due to an increased resistance to calpain cleavage upon hyperphosphorylation of Kidins220 (Lopez-Menendez et al., 2013). Furthermore, Kidins220 has a role in the regulation of neurotrophin signalling pathways; mutations of Kidins220 such as A557V, H1085R and A1299G exhibit a potential link with an increasing risk of schizophrenia and psychosis (Kranz et al., 2015).

Involvement of Kidins220 has also been found in HIV-associated neuro-cognitive disorders (HAND) (Singh et al., 2015). HAND is caused by mild to severe neurocognitive impairment due to the long-lasting Human Immunodeficiency

Virus Type-1 (HIV) in the central nervous system (CNS). Kidin220 is expressed in microglia, a kind of resident immune cell that can be infected with HIV directly. Microglia cells subsequently secrete proinflammatory molecules that contribute to HIV-induced neuroinflammation. It was found that knockdown of Kidins220 reduced the HIV Tat-induced proinflammatory response, which was associated with the loss of tumor necrosis factor alpha production and NF-κB activation (Singh et al., 2015). In addition to this, Kidins220 has also been shown to be involved in the immune-inflammation of asthma through the NGF-mediated signalling pathway (Ni et al., 2010). Anti-NGF treatment resulted in a down-regulation of Kidins220/ARMS, IL-1β and IL-4 in a mouse model (Li et al., 2013).

In recent years, emerging evidence has also revealed an altered expression of Kidins220 in different malignancies including melanoma and neuroblastoma (Jung et al., 2014, Liao et al., 2007, Rogers and Schor, 2013b, Liao et al., 2011a). An elevated expression of Kidins220 was also observed in castration-resistant prostate cancer (CRPC) as a direct target of miR-4638-5p (Wang et al., 2016). Kidins220 knockdown or overexpressing miR-4638-5p can reduce proliferation and growth of CRPC cells *in vitro* and *in vivo*.

Taken together, Kidins220 appears to play a positive role in certain malignancies by promoting proliferation and coordinating signal transductions to assist growth and metastasis of tumour cells. To date, little is known about the function of Kidins220 in the digestive system and its involvement in malignancies

of the digestive system. The present study aimed to examine the role of this molecule in pancreatic cancer. The very first objective was set to determine its expression at both mRNA and protein levels in pancreatic cancers using QPCR and IHC, respectively. Implication of Kidins220 expression in the development and disease progression of pancreatic cancer was to be analysed to evaluate the clinical relevance before further investigation of cellular and molecular machinery underlying its implication in pancreatic cancer.

The current section of the study aims to explore the expression and association of this molecule at both transcript and protein level using QPCR and IHC and to associate such expression with the clinical pathological patient information.

3.2 Materials and methods

3.2.1 Pancreatic cancer tissues

Pancreatic tumours (n=149) together with paired adjacent background tissues were collected immediately after surgery and stored at -80°C until use, with written consent from the patients at Peking University Cancer Hospital. All protocols and procedures were approved by Peking University Cancer Hospital Research Ethics Committee. RNA was extracted and converted to complementary DNA for subsequent quantification using real time quantitative PCR (QPCR).

3.2.2 Primers and antibody

Polyclonal rabbit anti-Kidins220 antibody (sc-48738) was obtained from Santa Cruz Biotechnology. All the primers used were synthesised and provided by Invitrogen (Paisley, UK). Primer sequences are shown in Table 2.4.

3.2.3 RNA extraction, reverse transcription, PCR and QPCR

Total RNA was isolated using TRI Reagent (Sigma-Aldrich, Poole, Dorset, UK), first strand cDNA was then synthesis using the GoScript™ Reverse Transcription System kit as described in section 2.4. QPCR was performed using the iCycler IQ5 system (Bio-Rad, Hemmel, Hempstead, UK) to examine the Kidins220 transcripts, whilst GAPDH was also determined as a house-keeping gene.

3.2.4 Immunohistochemistry for pancreatic tissue microarray

Immunohistochemical staining was conducted on a pancreatic adenocarcinoma tissue microarray (TMA) (PA2081a, Biomax, Maryland, US). The primary antibody used was an anti-Kidins220 rabbit monoclonal antibody (SC-48738) at 1:50 concentration (Santa Cruz Biotechnology, UK). The secondary antibody solution consisted of 100µl biotinylated antibody stock at 5ml dilution (Vectastain Universal Elite ABC Kit, PK-6200, Vector Laboratories, Peterborough,UK). Presence of cancerous cells and assessment were performed by two pathologists (Professor Paul Griffiths (PG) and Dr Nadine Burke (NB), Morriston Hospital, ABM University Health Board, Swansea, UK) by determining the intensity and distribution of Kidins220 staining. Intensity of Kidins220 staining was also determined using ImageJ (https://imagej.nih.gov/ij/) by two researchers (Shuo Cai and Ping-Hui Sun) at the host lab. Briefly, the IHC intensity was determined in 10-20 cancerous cells by a subtraction of background of empty area on the slide for each core on the TMA. Average intensity was calculated for each core with duplicates of samples from each tissue, followed by statistical analyses.

3.2.5 Statistical analysis

Kaplan-Meier survival analysis was performed with SPSS software (SPSS Standard version 13.0; SPSS Inc., Chicago, IL, USA). One-way ANOVA, t-test, paired t-test, Mann-Whitney test were employed to analyse Kidins220 transcript levels in tumours regarding different clinic-pathologic characteristics. T-test was used for normally distributed data whilst the Mann-Whitney test was used for non-normally distributed data. Differences were considered to be statistically significant when $p<0.05$.

3.3 Results

3.3.1 Expression of Kidins220 in pancreatic cancer

The expression of Kidins220 in pancreatic cancer was first evaluated by determining the transcript levels of Kidins220 in a clinical cohort comprising pancreatic tumours (n=149) and the paired adjacent normal pancreatic tissues (n=145) using QPCR. Clinical and pathological information together with average Kidins220 transcript levels are shown in the Table 3.1. Kidins220 was significantly reduced in pancreatic tumours in comparison with adjacent normal tissues (p=0.029) (Table 3.1 and Figure 3.2A). Although a relatively lower expression of Kidins220 was observed in tumours from female patients, statistical analyses did not show a significant association. Similarly, variable levels of Kidins220 transcripts were seen in tumours regarding their differentiation but lacked statistical

significance. Variable transcription levels of Kidins220 were also observed in tumours of different histological types, pancreatic adenocarcinoma presented the highest Kidins220 gene expression compared with pancreatic ductal carcinoma and other types of pancreatic carcinoma such as islet cell carcinoma, neuroendocrine carcinoma, and solid pseudopapillary tumour of the pancreas. However, statistical analyses did not shown any significant correlation between Kidins220 transcript levels and the histological types (Table 3.1).

Table3.1: Clinical cohort of Kidins220 in pancreatic cancer.

	N	Mean±SEMean (copies/50ng RNA)	*p*-value
Tumour	149	75150± 576945	0.029
Normal	145	2.13 E+12 ± 9.62 E+11	
Gender			
Male	89	114106±96478	0.32
Female	60	17365±6882	
Node status			
Node negative	56	168646± 1530096	0.28
Node positive	3	986± 9861	
Differentiation			
High	9	1305± 1299	
High-Med	10	17158+118016	
Medium	53	12778± 5732	0.056（Medium&High）
Med-low	59	168403±1454345	
Low	10	1767± 1226	0.8（Low&High）
Histology			
Adeno	61	82114± 65598	
Ductal	6	22796± 22739	0.39
Others	10	26053± 24104	0.42
TNM staging			
1-2	114	20490± 6680	0.0034
3-4	19	519± 226	
Clinical outcomes			
Dead	108	99489±795413	0.28
Alive	33	13124±73627	
Metastasis			
Yes	10	614±338	0.2
No	139	80512±61835	

Note: There are 223 pairs of tumours and adjacent normal pancreatic tissues in the cohort of pancreatic tissues from Beijing Cancer Hospital. The quantitative analysis of Kidins220 transcripts in those tissues is shown above. The number of samples in each category is different subject to availability of both corresponding clinicopathological information and valid Kidins220 quantification. For example, the node status, 89 patients in the collection did not have lymph node involvement, but only 56 patients had valid data. On the other hand, 6 patients had lymph node involvement, but only 3 patients presented valid data. For histology, 192 patients were diagnosed with adenocarcinoma, but only 61 samples had valid data; 8 patients had ductal carcinoma, and 6 samples presented with valid data. For other histological types, 10 of the 21 samples presented valid data.

To examine the protein expression of Kidins220, immunohistochemical staining was performed on a pancreatic adenocarcinoma tissue microarray which has dual cores for each sample including primary tumours, adjacent normal pancreatic tissues, metastases, benign tumours, pancreatic tissues of inflammatory diseases and normal pancreatic tissues. Summative information of this TMA can be seen in the Table 3.2. Presence of cancerous cells was verified by the pathologists (PG and NB) on the TMA slide with a reference of corresponding H&E staining (Appendix 2). The IHC scoring did not show a significant difference of Kidins220 staining in pancreatic tumours compared with adjacent normal tissues and normal pancreatic tissues (Figure 3.1). Nevertheless, further analysis assessing intensity of the staining, using semi-quantification, demonstrated malignant tumours exhibited weaker immunointensity of Kidins220 in comparison with adjacent normal pancreatic tissues (p<0.001) and normal pancreas (p<0.01) (Figure 3.2 B). Representative images of each group can be seen in Figure 3.2 C. Furthermore, in a tumour tissue under a magnification of X400, as a transmembrane protein Kidins220 exhibited an immunoreactivity which was more condensed on joining borders between cells rather than in the intracellular area particularly the nuclei (Figure 3.3).

Table3.2: Summative information of pathology diagnosis of TMA.

Histological characteristic	Number of samples
Normal pancreatic tissue	10
Adjacent normal pancreatic tissue	21
Pancreatic ductal adenocarcinoma	42
Pancreatic adeno squamous carcinoma	3
Pancreatic islet cell carcinoma,	1
Pancreatic metastatic carcinoma	6
Pancreatic islet cell tumour	10
Pancreatic inflammation	11

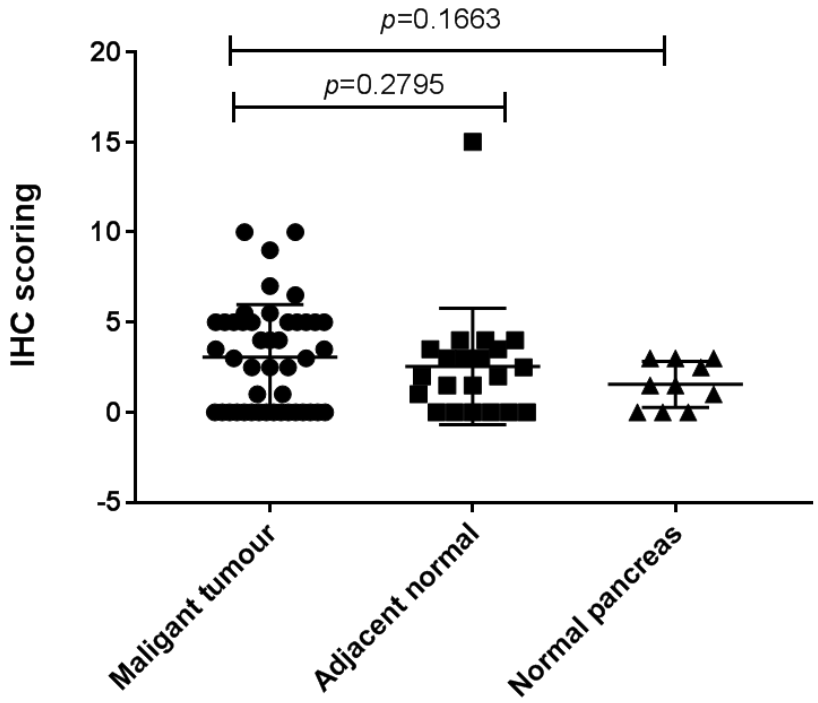

Figure 3.1: Scoring assessment of Kidins220 IHC. Shown is the IHC scoring of Kidins220 in pancreatic tumour tissues, adjacent normal tissues, and normal tissues on the TMA (PA2081a, Biomax, Maryland, US). The IHC scoring was calculated based on the assessment of both distribution and intensity of Kidins220 staining by two pathologists (PG and NB). IHC score = intensity score (0-3) × distribution score (0-5).

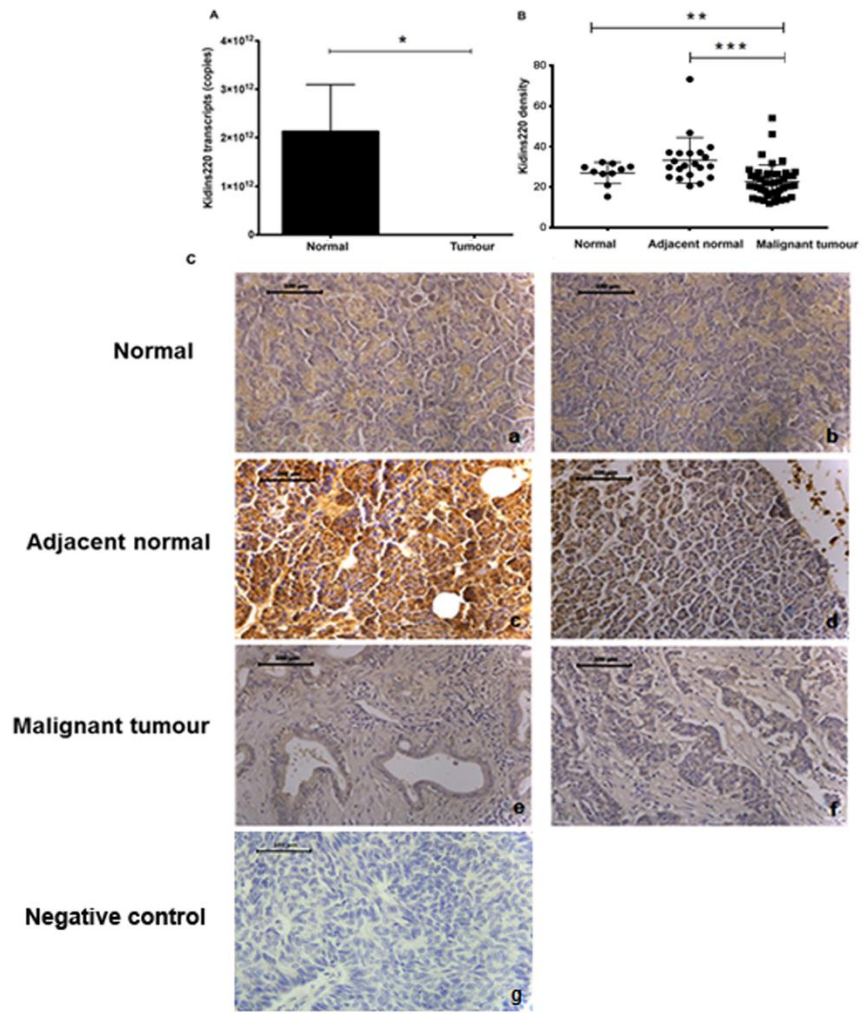

Figure 3.2: Transcript and protein Expression of Kidins220 in pancreatic tumour tissues and normal tissues at mRNA and protein levels. (A) The levels of Kidins220 transcripts were reduced in pancreatic tumours compared with the adjacent normal tissues. Shown are average transcript levels of Kidins220 per 50ng RNA and error bars represent standard error of mean. **(B)** The expression of Kidins220 protein in pancreatic cancer was assessed in a tissue microarray (PA2081a, Biomax) using IHC. Kidins220 protein showed decreased expression level in pancreatic tumour tissues compared with adjacent normal control and normal pancreatic tissues (pancreatic tumour versus adjacent normal control, ***p<0.001; pancreatic tumour versus normal tissue, **p<0.01. **(C)** Representative images of IHC staining in the TMA; a-b are normal pancreatic tissues; c-d are adjacent pancreatic tissues; e-f are malignant tumour tissues; g is the negative control using an endogenous peroxidase H_2O_2. Images were captured at x200 objective magnification.

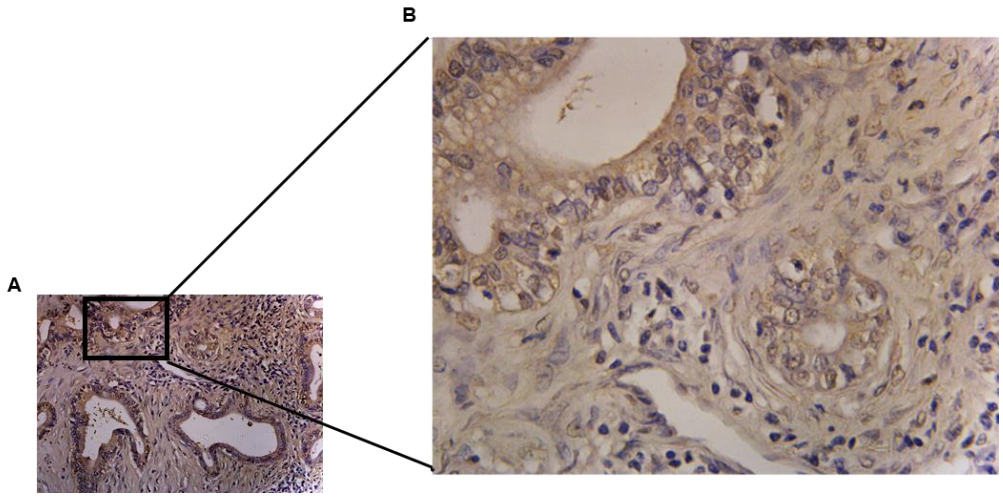

Figure3.3: Representative images of detection of Kidins220 expression in malignant tumour. (A) Expression of Kidins220 in tumour X200 magnification. **(B)** Corresponding magnification at X400, indicating that Kidins220 immunoreactivity is more concentrated on the membranes with a stronger staining at the joint borders between cells.

3.3.2 Kidins220 expression and tumorigenesis of pancreatic cancer

The initial assessment showed a reduced expression of Kidins220 in pancreatic cancer. This led to a question of whether this molecule is involved in the tumorigenesis of pancreatic cancer. To answer this, an analysis of Kidins220 expression in benign lesions proceeding onto cancerous lesions and invasive adenocarcinomas was performed, using gene expression array data (GDS3836) (Hiraoka et al., 2011). It included normal pancreatic tissues (n=7), intraductal papillary-mucinous adenoma (IPMA, n=6), intraductal papillary-mucinous carcinoma (IPMC, n=6) and Invasive cancer originating in intraductal papillary-mucinous neoplasm (IPMN, n=3). As shown in Figure 3.4A, a trend of reduced expression of Kidins220 was observed in lesions which occurred during the tumorigenesis of pancreatic cancer from IPMA, IPMC, and invasive cancer

originating in IPMN compared with normal pancreas. Among which, a decreased Kidins220 expression was seen in invasive cancer originating in IPMN compared with normal pancreatic tissues (p<0.001). There was also a significantly reduced expression of Kidins220 in invasive cancer originating in IPMN compared with IPMC (p<0.01). The lowest expression was seen invasive cancer originating in IPMN samples. Another individual comparison between invasive cancer originating in IPMN and IPMA did not show statistical significance in difference between them. Furthermore, the semi-quantification of Kidins220 IHC staining on the TMA showed that malignant tumours had the lowest expression of Kidins220 compared with normal pancreas, inflammation pancreas, and benign tumour (Figure 3.4B). Lower expression of Kidins220 was also seen in benign tumours compared with inflammation, however, this result was not found to be statistically significant. The representative images are shown in Figure 3.4C. Interestingly, a much stronger staining of Kidins220 was observed in pancreatic tissues with inflammatory disorders compared with normal pancreatic tissue, benign tumours and malignant tumours. Normal pancreas also presented a stronger staining of Kidins220 compared with benign tumours and malignant tumours (Figure 3.4B).

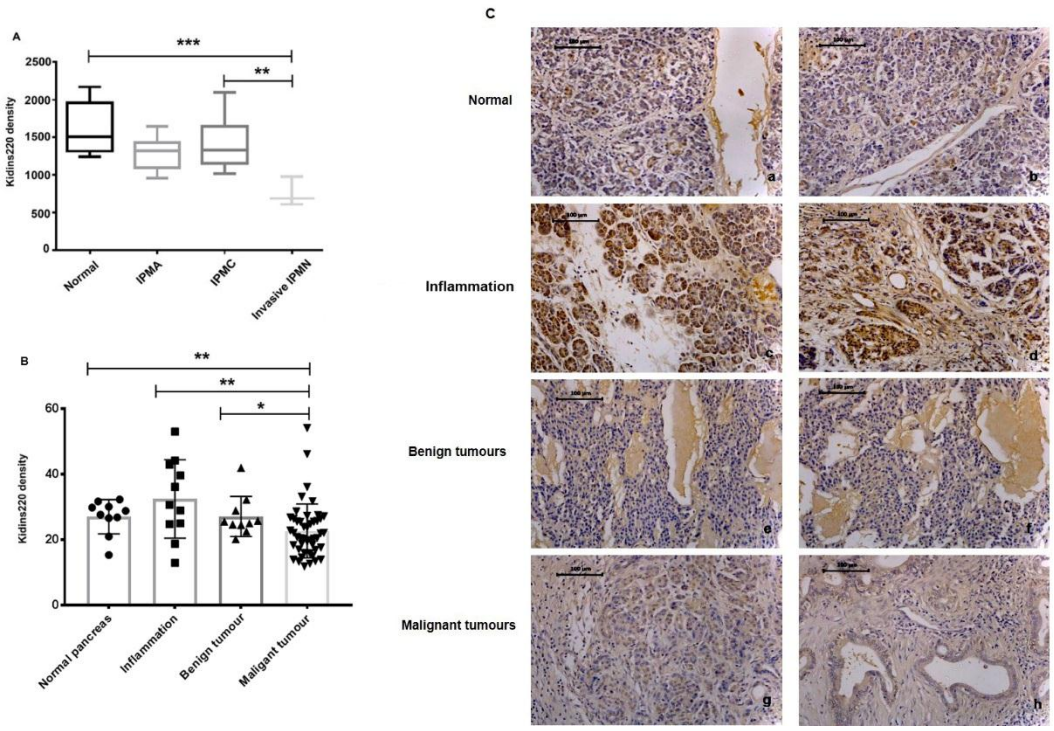

Figure 3.4: Implication of Kidins220 in development of pancreatic cancer. (A) Aberrant expression of Kidins220 can be seen in different lesions during development of pancreatic cancer. The lowest expression of Kidins220 was shown in invasive cancer originating in IPMN (Invasive IPMN) compared with normal pancreas, IPMA, IPMC in a cohort of 145 primary pancreatic ductal adenocarcinomas and 46 pancreas tissues (GDS3836). The classification of different types of neoplasia used in the study was an older system of pathological classification of pancreatic neoplasms. **(B)** IHC of Kidins220 on the pancreatic TMA (PA2081a, Biomax) showed reduced protein expression in pancreatic cancers compared with normal pancreas (**p<0.01), Inflammation (**p<0.01), and benign tumours (*p<0.05). **(C)** Representative images of IHC in TMA from different pathological types. a-b: Normal pancreas; c-d: Inflammation; e-f: benign tumour; g-h: malignant tumour. Images were captured at x200 objective magnification.

3.3.3 Kidins220 and disease progression

Further exploration was carried out on the involvement of Kidins220 in disease progression of pancreatic cancer. In terms of TNM staging, more advanced tumours which developed lymph node and/or distant metastases including TNM3 and TNM4 exhibited lower transcript levels of Kidins220 compared with tumours at earlier stages including TNM stage 1 and 2 (p=0.0034) (Figure 3.5A). It indicated a link between reduced expression of Kidins220 and distant metastasis. After a search of gene expression array data, a dataset comprising primary tumours (n=146) and distant metastases (n=62) was chosen for analysis. The distant metastases showed a decreased expression of Kidins220 compared with the primary tumours (p<0.05) (GSE71729) (Figure 3.5B). The IHC results also presented that primary tumours with distant metastasis exhibited a decreased level of Kidins220 protein expression compared to those without metastasis. Since only two such samples were available on the TMA, statistical comparison did not show a significant link (Figure 3.5C). The same trend was also seen in IHC scoring, which showed a lower score in primary tumours with metastasis compared to tumours without metastasis (Figure 3.6). The representative slides chosen from the TMA presented a stronger staining in primary tumours without metastasis compared with pancreatic tumours with metastasis (Figure 3.5D). Moreover, whether the deregulated expression of Kidins220 in pancreatic cancer played a role in prognosis was then investigated. A Kaplan Meier survival analysis was performed using a gene expression array dataset (GSE71729) which has follow up data. The

analysis showed that the reduced expression of Kidins220 was associated with shorter overall survival (*p*=0.02) (Figure 3.7).

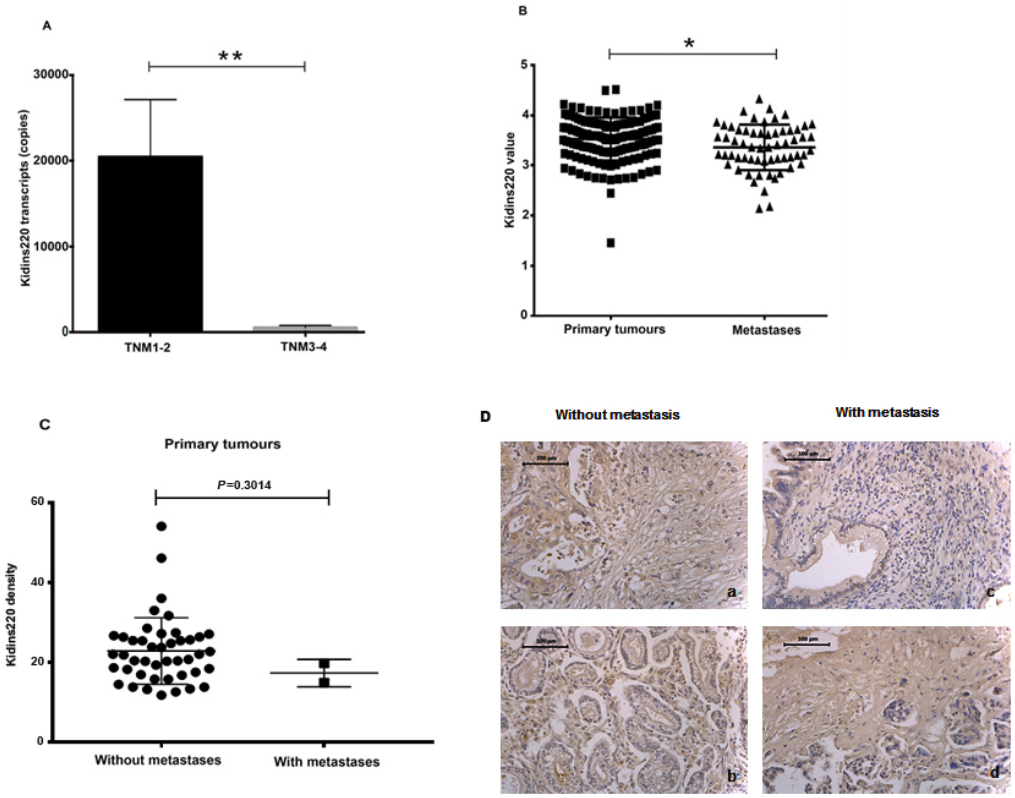

Figure 3.5: Kidins220 and disease progression of pancreatic cancer. (A) The levels of Kidins220 transcripts were determined in a cohort of pancreatic cancer using QPCR. Shown are Kidins220 transcript levels (mean ± standard error of mean) in pancreatic tumours of early stages (TNM1 and TNM2) compared with advanced stages (TNM3 and TNM4) according to TNM staging. ** represent $p<0.01$. **(B)** Kidins220 transcript levels in distant metastases of pancreatic cancer compared with primary tumours were also analysed using a gene expression array data (GSE71729). * represents $p<0.05$. **(C)** Protein expression of Kidins220 in primary tumours at the most advanced stage, i.e. with distant metastases was also analysed in the pancreatic TMA **(**PA2081a, Biomax). Shown are intensity of Kidins220 IHC. **(D)** Representative images of the IHC staining of Kidins220; a and b: primary tumours without metastases; c and d are primary tumours with metastases. Images were captured at x200 objective magnification.

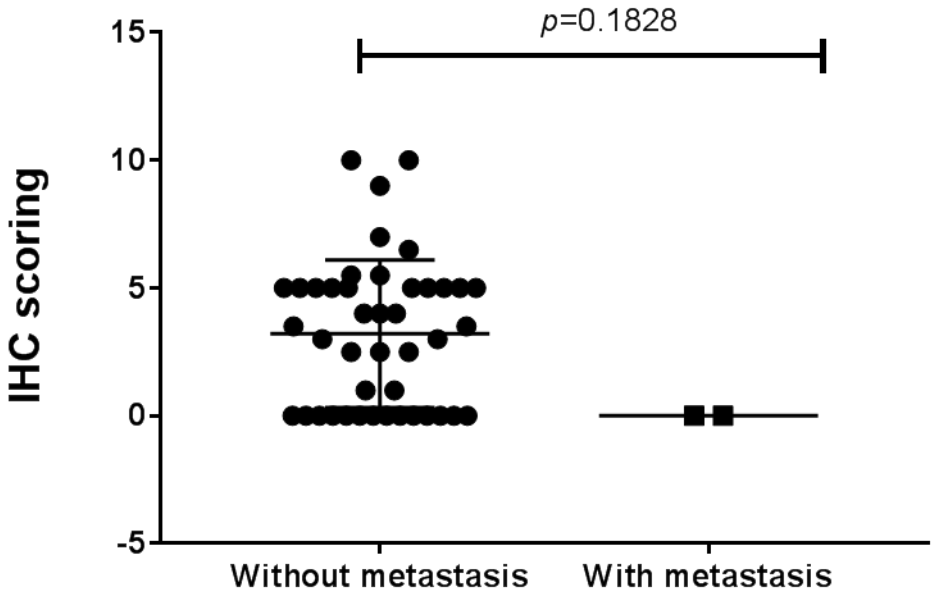

Figure 3.6: IHC scoring of Kidins220 staining in the development of pancreatic cancer. The scores were determined depending the distribution and staining intensity of Kidins220. Primary tumours with metastases had a lower IHC score in comparison with primary tumours without distance metastases (*p*=0.1828). However, the difference was not statistically significant.

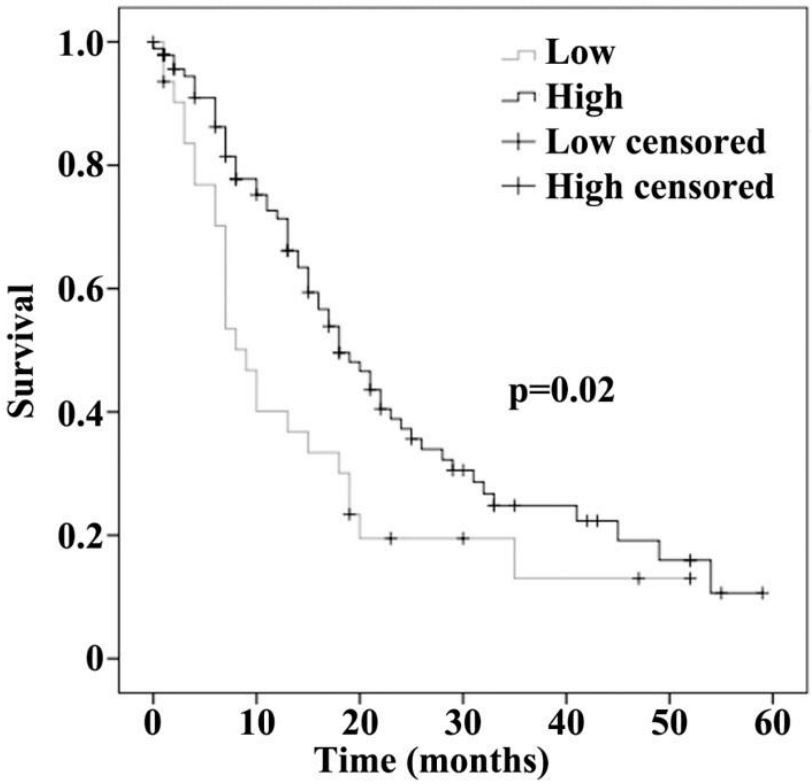

Figure 3.7: Kidins220 expression and overall survival of patients with pancreatic cancer. Correlation between Kidins220 expression (mRNA) and overall survival of patients with pancreatic cancer was analysed in the gene expression array data (GSE71729) using Kaplan-Meier survival analysis (SPSS version 23). Median of Kidins220 expression value was used as a cut-off value.

3.4 Discussion

Despite recent studies demonstrating the role of Kidins220 in neurotrophin response, emerging evidence has suggested the importance of Kidins220 in neural diseases and human cancer which was recently reviewed (Cai et al., 2017). An overexpression of Kidins220 was initially detected in primary malignant melanomas compared with benign tumours (Liao et al., 2007). The expression of Kidins220 in a panel of different malignancies (The Cancer Genome Atlas, https://cancergenome.nih.gov/) was initially analysed using an online analysis tool (Firebrowse Gene Expression Viewer, http://firebrowse.org/). An altered expression level of Kidins220 was present in different cancer types compared with relevant normal controls (Figure 3.8A), and details of aberrant expression in malignancies are listed in Table 3.3. However, no obvious change of Kidins220 expression was noticed in this TCGA cohort which might be due to the small number of normal tissues (n=4) (Figure 3.8B). In our current study, reduced levels of Kidins220 transcripts were observed in pancreatic tumours (n=149) compared with paired adjacent normal pancreatic tissues (n=145) in a pancreatic cancer clinical cohort collected at the Beijing Cancer Hospital. Its protein expression in pancreatic cancer was then examined using immunohistochemical staining of Kidins220 in a pancreatic TMA (PA2081a, Biomax).

The IHC scoring conducted by pathologists did not show any significant change of Kidins220 staining in malignant tumours in comparison with normal pancreas.

Furthermore, we determined the intensity of Kidins220 staining in cancerous cells by a subtraction of background from empty area on the same image, and we found there was a significant decreased expression of Kidins220 in malignant tumours compared with adjacent normal tissue and normal pancreases. Taken together, the results suggested that a contrasting role might be played by Kidins220 in pancreatic cancer compared with the previously identified functions of this molecule in melanomas. However, further investigation should be performed to validate this finding, particularly for its protein expression assessment. An improvement should be made in optimising the Kidins220 antibodies and enhancing the accuracy for IHC assessment. Validation of the altered expression of Kidins220 in pancreatic cancer should also be performed in a larger clinical cohort of pancreatic cancer patients.

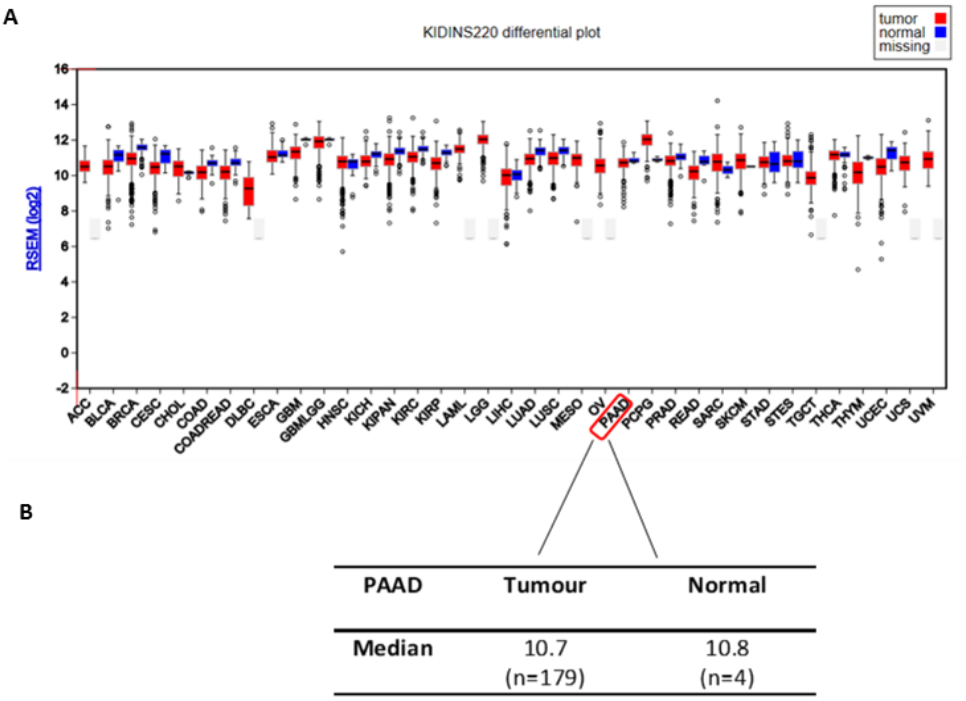

PAAD	Tumour	Normal
Median	10.7 (n=179)	10.8 (n=4)

Figure 3.8: mRNA sequence expression level of Kidins220. (A): overview of Kidins220 expression in different types of cancer compared with normal control. **(B):** The total numbers and median of tumour and normal sample in pancreatic adenocarcinoma. Cancer types are: adrenocortical carcinoma (ACC), bladder urothelial carcinoma (BLCA), breast invasive carcinoma (BRCA), cervical squamous cell carcinoma and endocervical adenocarcinoma (CESC), cholangiocarcinoma (CHOL), colon adenocarcinoma (COAD), colorectal adenocarcinoma (COADREAD), lymphoid neoplasm diffuse large B-cell lymphoma (DLBC), oesophageal carcinoma (ESCA), glioblastoma multiforme (GBM), glioma (GBMLGG), head and neck squamous cell carcinoma (HNSC), kidney chromophobe (KICH), pan kidney cohort (KIPAN, including KICH, KIRC and KIRP), kidney renal clear cell carcinoma (KIRC), kidney renal papillary cell carcinoma (KIRP), acute myeloid leukemia (LAML), brain lower grade glioma (LGG), liver hepatocellular carcinoma (LIHC), lung adenocarcinoma (LUAD), mesothelioma (MESO), ovarian serous cystadenocarcinoma (OV), pancreatic adenocarcinoma (PAAD), pheochromocytoma and paraganglioma (PCPG), prostate adenocarcinoma (PRAD), rectum adenocarcinoma (READ), sarcoma (SARC), skin cutaneous melanoma (SKCM), stomach adenocarcinoma (STAD), stomach and oesophageal carcinoma (STES), testicular germ cell tumour (TGCT), thyroid carcinoma (THCA), thymoma (THYM), uterine corpus endometrial carcinoma (UCEC) and uveal melanoma (UVM).

Table 3.3: Aberrant expression of Kidins220 in malignancies.

	Tumour (median)	Normal (median)	Change (fold vs normal)
ACC	10.5 (n=79)	-	-
BLCA	10.5 (n=408)	11.2 (n=19)	0.637
BRCA	11.0 (n=1100)	11.6(n=112)	0.650
CESC	10.5 (n=306)	11.2 (n=3)	0.595
CHOL	10.5 (n=36)	10.2 (n=9)	1.25
COAD	10.2 (n=459)	10.7 (n=41)	0.7
COADREAD	10.2 (n=626)	10.7 (n=51)	0.706
DLBC	9.27 (n=48)	-	-
ESCA	11 (n=185)	11 (n=11.1)	0.930
GBM	11.3 (n=166)	12 (n=5)	0.627
GBMLGG	11.9 (n=696)	12 (n=5)	0.940
NHSC	10.8 (n=522)	10.8 (n=44)	1.01
KICH	10.8 (n=66)	11.2 (n=25)	0.736
KIPAN	10.9 (n=891)	11.4 (n=129)	0.735
KIRC	11.1 (n=534)	`11.5 (n=72)	0.751
KIPR	10.7 (n=291)	11.3 (n=32)	0.670
LAML	11.5 (n=173)	-	-
LGG	12.0 (n=530)	-	-
LIHC	10.0 (n=373)	10.1 (n=50)	0.963
LUAD	11.0 (n=517)	11.4 (n=59)	0.724
LUSC	11.0 (n=501)	11.4 (n=51)	0.742
MESO	11.0 (n=10.5)	-	-
OV	10.6 (n=307)	-	-
PADD	10.7 (n=179)	10.8 (n=4)	0.942
PCPG	12.0 (n=184)	10.9 (n=3)	2.25
PRAD	10.8 (n=498)	11.1 (n=52)	0.853
READ	10.2 (n=167)	10.8 (n=10)	0.686
SARC	10.8 (n=263)	10.3 (n=2)	1.37
SKCM	10.9 (n=47)		
STAD	10.8 (n=415)	10.7 (n=35)	1.07
STES	10.8 (n=600)	10.8 (n=46)	1.01
TGCT	9.87 (n=156)	-	-
THCA	11.2 (n=509)	11.2 (n=59)	1.00
THYM	10.2 (n=120)	11.0 (n=2)	0.564
UCEC	10.5 (n=546)	11.4 (n=35)	0.529
UCS	10.7 (n=57)	-	-
UVM	10.9 (n=80)	-	-

Note: Summative information is prepared from an analysis of TCGA data using the Firebrowse (http://firebrowse.org/).

In order to determine whether the expression of Kidins220 is related to the tumorigenesis of pancreatic cancer, analysis of its expression in different lesions during tumorigenesis was performed which included the normal pancreas, IPMA, IPMC, and invasive cancer originating in IPMN. IPMN is one of the morphologically distant precursors of pancreatic adenocarcinoma (Patra et al., 2017). Based on the gene array data, the lowest expression of Kidins220 was seen in the invasive cancer originating in IPMN when compared with IPMC and normal pancreas. Kidins220 has been shown to be involved in the differentiation of neuroblastoma through maintaining the morphology of N-type cells, the phenotype with invasive characteristics (Rogers and Schor, 2013a). Several types of cancer have been related to inflammatory origins, such as colorectal cancer, gastric cancer, and bladder cancer (Farrow and Evers, 2002). Patients with hereditary pancreatitis and chronic pancreatitis have 53 times risk and 17 times for developing pancreatic cancer respectively compared with patients without pancreatitis (Lowenfels et al., 1993, Whitcomb et al., 1999). In the current study, the semi-quantification of Kidins220 IHC did not show any change of its protein expression in the pancreatic tissues of inflammatory disorders compared with normal tissues. However, due to the size of the cohort, the observation should be validated in a large cohort of pancreatic tissues collection. K-ras mutations, loss of p53 and SMAD are important factors during tumorigenesis of pancreatic cancer, and mutations of K-ras and SMAD have been found in chronic pancreatitis (Rozenblum et al., 1997) (Popovic Hadzija et al., 2007). The correlation between Kidins220 and these factors

contributes to the tumorigenesis of pancreatic cancer and needs to be further investigated.

Kidins220 expression was upregulated in metastatic melanoma in comparison with benign tumours (Liao et al., 2007). In the current study, we found primary tumours with distant metastasis exhibited a reduced immunointensity of Kidins220 rather than those without metastasis, and a decreased expression level of Kidins220 in the distant metastases of pancreatic cancer compared with primary tumours according to the analysis of the gene array data (GSE71729). Furthermore, by contrast, melanoma tissues with nodal metastasis had a stronger expression of Kidins220 in comparison with those without nodal metastasis, and also the stronger expression of Kidin220 was also present in melanoma when tumour thickness was more than 1.0mm (Liao et al., 2011a). The different expression pattern of Kidins220 in melanoma and pancreatic cancer may be a result of different signalling pathways involved. Since pancreatic cancer patients are always diagnosed at late stage where cancer cells are often locally invasive or spreading to other parts of the body, pancreatic cancer commonly have a poor prognosis and lower survival rate (Ryan et al., 2014). TNM is used for classifying the extent of cancer spread and helps to evaluate the prognosis of cancer patients (Sobin and Fleming, 1997). The association between Kidins220 and disease progression was determined in the Beijing clinical cohort by analysing its expression in pancreatic cancer tumours according to their TNM staging. This showed that more advanced tumours in the late stage (TNM3 and TNM4) had a

decreased Kidins220 expression in comparison with tumours at early stages of the disease (TNM1 and TNM2). Moreover, the reduced Kidins220 expression is also related to a shorter overall survival of patients with pancreatic cancer, indicating an important role played by Kidins220 in the prognosis of pancreatic cancer.

Taken together, the results show that the expression of Kidins220 is reduced in pancreatic cancer. The reduced expression may occur during the tumorigenic process of pancreatic cancer. This is associated with the disease progression and poor prognosis, i.e. a shorter overall survival. Current findings suggest that Kidins220 has prognostic potential for pancreatic cancer. Furthermore, the findings from our initial analyses of Kidins220's expression in pancreatic cancer led to a further investigation for its function in pancreatic cancer cells. This will help to answer the questions; 'why is Kidins220 downregulated in pancreatic cancer?' and 'How does it elicit a protective effect during the development and progression of pancreatic cancer?'.

Chapter 4

Influence of Kidins220 knockdown on cellular functions of pancreatic cancer cell lines

4.1 Introduction

In the initial investigation, reduced expression of both Kidins220 transcript and protein was evident in human pancreatic cancer. The down-regulation of Kidins220 may occur at an early stage during the tumorigenesis as such a trend was observed in IPMA, IPMC and Invasive cancer originating in IPMN. Furthermore, pancreatic cancer patients with lower expression of Kidins220 have a shorter overall survival, suggesting its implication in the prognosis of the disease. However, previous studies of Kidins220 in other malignancies revealed an oncogenic effect, such as in melanoma and neuroblastoma (Jung et al., 2014, Liao et al., 2007, Liao et al., 2011a, Rogers and Schor, 2013b). The different expression pattern of Kidins220 in pancreatic cancer suggest that it may have different functions in the pancreas and pancreatic cancer which is yet to be investigated.

The fundamental abnormality that contributes to cancer development is caused by the continual unregulated proliferation of cancer cells. Normal cells respond to internal and external signals appropriately. The balance between proliferation and senescence/apoptosis ensures the homeostasis of tissues and organs. However, cancer cells exhibit aberrations in these signals, growing and dividing in an uncontrolled manner (Hanahan and Weinberg, 2011).

Cancer cells can also metastasise from the primary site to spread throughout the body and progressively colonise distant organs (Steeg, 2016). The tumour cells broadly undergo three main processes in a metastatic cascade; invasion,

intravasation and extravasation. The process of invasion occurs when tumour cells dissociate from the primary tumour mass and invade the surrounding tissue through an alteration of cell-matrix interaction and degradation of extracellular matrix. The tumours cells may subsequently disseminate through blood or lymph vessels to distant organs (Tracey A. Martin, 2013). Cancer metastasis remains the major cause of cancer-related death (Guan, 2015). Therefore, the cellular and molecular machinery underlying cancer metastasis has been a pivotal part of cancer research. Metastasis is a multiple-step procedure that requires proliferation, adhesion, invasion, and migration of cancer cells, orchestrated through various molecules and pathways. Study of the cellular and molecular aberrations occurring in cancer cells could permit identification of new markers and targets for diagnosis and treatment.

The present study revealed a reduced expression of Kidins220 in pancreatic cancer, indicating that it may act as a tumour suppressor in disease progression of pancreatic cancer. Considering the different expression pattern of Kidins220 in other types of cancer in comparison with our findings in pancreatic cancer, together with its role in the regulation of cellular function in other malignancies, we aimed to examine whether Kidins220 has a very different function in pancreatic cancer cells, thus contributing to the development of pancreatic cancer. A Kidins220 knockdown cell model was employed to examine the corresponding effect on cellular functions of pancreatic cancer cells, including cell proliferation (2D&3D culture), adhesion, invasion, and migration using various *in vitro* assays.

4.2 Materials and methods

4.2.1 Cell lines

Panc-1, Mia paca-2, and ASPC-1 pancreatic cancer cell lines were used in the current study. All these cancer cell lines were cultured in DMEM medium with 10% FBS and antibiotics and described in Chapter2.

4.2.2 Silencing of Kidins220 using ribozyme transgene

Anti-Kidins220 ribozyme transgenes have been constructed and tested in a pilot study. After plasmid amplification and extraction, the ribozyme plasmids were transfected into pancreatic cancer cells using electroporation. The transfected cells were selected with 5μg/ml blasticidin and maintained with 0.5μg/ml blasticidin. Knockdown of Kidins220 in the transfected cells was determined using both RT-PCR and western blot.

4.2.3 Generation of Kidins220 lentivirus shRNA transgenes

Lentivirus shRNA (shRNA2, shRNA3 and shRNA6) targeting Kidins220 was obtained from Cyagen Biosciences (CA, USA). After amplification and purification, plasmids containing lentiviral shRNA or scramble control, together with lentiviral packaging plasmids (psPAX2) and envelope plasmid (pMD2.G) were transfected into HEK-293T cells respectively, to generate lentiviral particles. The lentiviral particles

carrying either Kidins220 shRNA or scramble shRNA were then used to infect target cells, respectively. The scramble shRNA was employed as a control for the following experiments. After a selection using 500ng/ml G418, knockdown of Kidins220 was verified using both RT-PCR and western blot. Full details of the cloning process have been provided in section 2.6. The stable Panc-1 and Mia paca-2 sublines and corresponding scramble control cells were maintained in the same medium and supplemented with 100µg/ml G418.

4.2.4 RNA isolation, cDNA synthesis, RT-PCR, and QPCR

RNA was extracted using a Tri Reagent kit (Sigma-Aldrich, Poole, Dorset, UK), and cDNA was then converted using the the GoScript™ Reverse Transcription System kit as described in section 2.4. RT-PCR was carried out using the following conditions; 94˚C for 5 minutes, followed by 94˚C for 30 seconds (30 to 42 cycles), 56˚C for 30 seconds, and 72˚C for 1 minute and a final extension of 7 minutes at 72˚C. The PCR products were separated on an agarose gel and stained using SYBR®Safe DNA gel stain (Invitrogen, Paisley, UK).

4.2.5 Protein extraction, SDS-PAGE, and western blot analysis

Proteins were extracted using lysis buffer and then quantified using the Bio-Rad DC Protein Assay kit (Bio-Rad Laboratories, Hemel-Hempstead, UK). Proteins were

transferred onto PVDF membranes after separation in the SDS-PAGE gel, and subsequently blocked and probed with anti-Kidins220 primary antibody and a corresponding peroxidise-conjugated secondary antibody. Information on the antibodies used in this study is provided in Table 2.5. The protein bands were eventually visualised using the chemiluminescence detection kit (Luminata, Millipore).

4.2.6 *In vitro* cell growth assay

3,000 cells were seeded into 200µl medium in three 96-well plates, and incubated for 1, 3, and 5 days respectively. Following incubation, the cells were fixed and stained with crystal violet. The absorbance was measured after dissolving the crystal violet with acetic acid (10% v/v) and the absorbance was determined at a wave length of 540nm using a spectrophotometer (BIO-TEK, Elx800, UK).

4.2.7 *In vitro* cell adhesion assay

The cells were seeded into a 96-well plate pre-coated with Matrigel (5µg/well) as described in section 2.7.2. The cells were left to adhere over a period of 40 minutes, before being fixed and stained with crystal violet. The adhered cells were then counted.

4.2.8 *In vitro* cell invasion assay

20,000 cells were seeded into transwell inserts (pore size, 8µm) coated with 50µg Matrigel followed by an incubation of three days. After the incubation, cells that had invaded through the Matrigel and migrated on to the other side of the insert were fixed and stained with crystal violet, and then counted.

4.2.9 *In vitro* transwell migration assay

20,000 cells were seeded into transwell inserts (pore size, 8µm) in a 24-well plate. After 24-hour incubation, the cells that had migrated through and moved onto the other side of the insert were fixed with 4% formaldehyde and stained with crystal violet. Cells which had migrated were then counted.

4.2.10 *In vitro* tumour spheroid assay

1,000 cells were seeded into 200µl DMEM medium into 96-well non-coated U-shape bottom 3D culture plate (Greiner Bio-One, Ltd. Stonehouse, UK). The cells were incubated for a period up to two weeks. Images were taken every three days to monitor tumour growth. Culture media was topped up every two or three days. Size of the spheroids was measured using ImageJ software.

4.2.11 *In vivo* peritoneal metastasis assay

Athymic nude mice (CD1) were purchased from Charles River Laboratories (Charles River Laboratories International, Inc., Kent, UK). All the mice were kept in filter-topped isolation cages and all the procedures were carried out in a class-II cabinet. The study was conducted under the Home Office Project licence (PPL: PE944FC2). After the mice were settled for a week in the designated laboratory, Panc-1 scramble and Kidins220 knockdown cells were injected into the peritoneal cavity of the mice at a volume of 100µl which contained Matrigel at final concentration of 2.5mg/ml in PBS. The mice were then carefully monitored twice a week by measuring body weight. The intraperitoneal exploration was conducted after 4 weeks. Metastatic nodules were photographed using a stero-microscrope (Olympus, Japan) and the volume of metastatic tumours were calculated by using the following formula:

Tumour volume (mm^3)= 0.5× $Width^2$×Length.

4.3 Results

4.3.1 Kidins220 expression and the knockdown of Kidins220 in pancreatic cancer cell lines

The expression of Kidins220 was detected in three pancreatic cancer cell lines originated from human carcinoma including Panc-1, Mia paca-2, and ASPC-1.

Panc-1 was derived from an epithelioid carcinoma of the pancreas while Mia paca-2 was isolated from a pancreatic carcinoma, and ASPC-1 was derived from metastatic ascites of a pancreatic adenocarcinoma. Kidins220 transcripts in the three pancreatic cancer cell lines were determined using RT-PCR. Overall, Kidins220 is generally expressed in all three cancer cell lines, although the expression levels displayed differences between the cell lines. A higher expression of Kidins220 was seen in Panc-1 and ASPC-1 cancer cells compared with Mia paca-2 (Figure 4.1A). All these three cell lines were included in preliminary experiments for knockdown of Kidins220.

Initially, anti-Kidins220 ribozyme transgenes were used to knockdown Kidins220. However, due to the low transfection efficiency and the difficulties in the selection with blasticidin, a satisfactory knockdown of Kidins220 was not achieved in pancreatic cancer cell lines. Ribozyme transfection relies on the electroporation and lipo transfection and the structure of cell membrane can be impacted during these processes. The cells became very sensitive to the selective antibiotics and this resulted in poor rates of survival. Afterwards, knockdown of Kidins220 using lentiviral Kidins220 shRNA (shRNA2, shRNA3 and shRNA6) was conducted in Panc-1, Mia paca-2, and ASPC-1 pancreatic cancer cell lines. Initial tests showed that a knockdown of Kidins220 in Panc-1 and Mia-paca-2 but not in ASPC1. The knockdown of Kidins220 in both Panc-1 and Mia-paca-2 cell lines was then verified using both RT-PCR (Figure 4.1 B) and Western bolt (Figure 4.1 C).

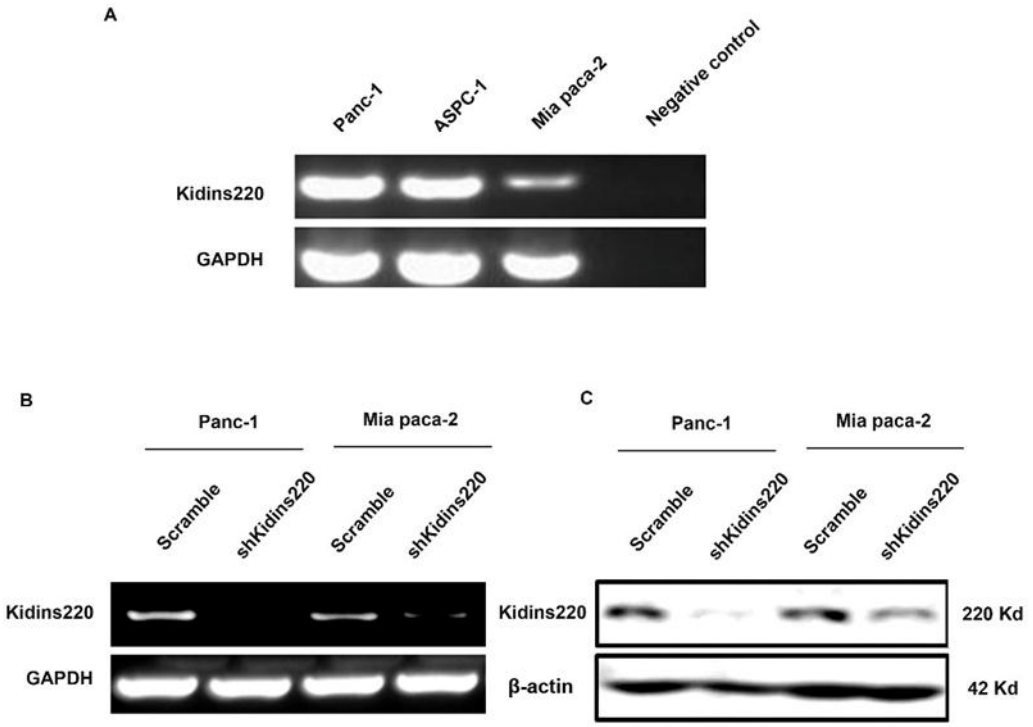

Figure 4.1: Kidins220 expression in pancreatic cancer cell lines and knockdown of Kidins220 in Panc-1 and Mia-paca-2. (A) The mRNA expression of Kidins220 in pancreatic cancer cell lines (Panc-1, ASPC-1, and Mia paca-2) was examined using conventional PCR. PCR water was used as a negative control to exclude any contamination in the PCR reactions, and GAPDH was employed as a house-keeping control. **(B)** Expression of Kidins220 mRNA in Panc-1 and Mia pca-2 pancreatic cancer cells infected with Kidins220 lentiviral shRNA particles were determined using RT-PCR. **(C)** The verification of Kidins220 knockdown at protein level in the Panc-1 and Mia paca-2 pancreatic cancer cells was performed using western bolt. β-actin was employed as a loading control.

4.3.2 Effect of Kidins220 on proliferation of pancreatic cancer cells

Deregulated and un-controlled cellular proliferation is an important trait of cancer cells. The impact of Kidins220 knockdown on proliferation of these two pancreatic cell lines was first evaluated using the *in vitro* growth assay. The knockdown of Kidins220 resulted in an increasing proliferation in both cell lines but to variable levels (Figure 4.2). A marginal increase of proliferation was seen in the Panc-1 cells following the Knockdown of Kidins220 at Day 5 compared with the scramble control with the difference statistically significant ($p<0.05$) (Figure 4.2A). Similarly, in the Mia paca-2 cells, the cells with Kidins220 knockdown exhibited a significant increase of cell proliferation compared to control as seen in Figure 4.2B.

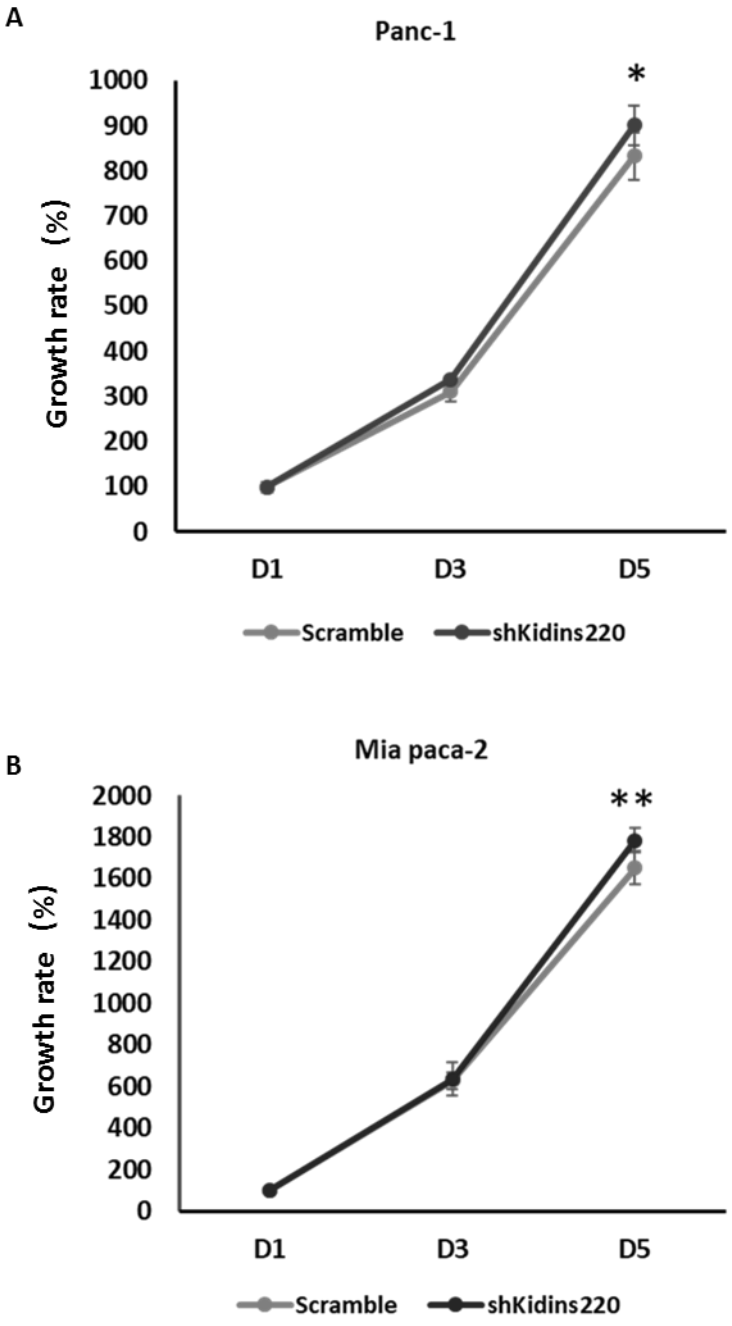

Figure 4.2: Knockdown of Kidins220 has a significant increase in the growth of the Panc-1 and Mia paca-2 cells. Cells were incubated for 1, 3, and 5 days respectively. Six repeats were included for each cell lines on each plate. Growth rate (%) was calculated using the following formula; growth rate (%) = Absorbance (Day X) / Absorbance (Day 1) × 100. Shown are representative results of one experiment out of three performed. Error bars represent standard deviation. * represents $p<0.05$ and ** represent $p<0.01$, respectively.

4.3.3 Effect of Kidins220 on adhesion of pancreatic cancer cells

Adhesion mediated by adhesion molecules, such as integrins is a critical cellular event for cancer cells to interact with the local environment and also for their migration and invasion during the local invasion and distant dissemination. As aforementioned, the association between reduced expression of Kidins220 in pancreatic cancer and disease progression suggests a possible role of this protein in the regulation of adhesion, migration and invasion. Following the *in vitro* proliferation test, the influence on cell-matrix adhesion was assessed using a Matrigel, comprising collagen 4 and laminin being similar to the major components of the basal membrane underlying epithelial cells, adhesion assay. The Kidins220 knockdown cell lines including both Panc-1 and Mia paca-2 exhibited enhanced adhesion to the Matrigel in comparison with their corresponding scramble controls (Figure 4.3). The increase in adhesiveness was approximately 2-4 folds in both cell lines compared with the control.

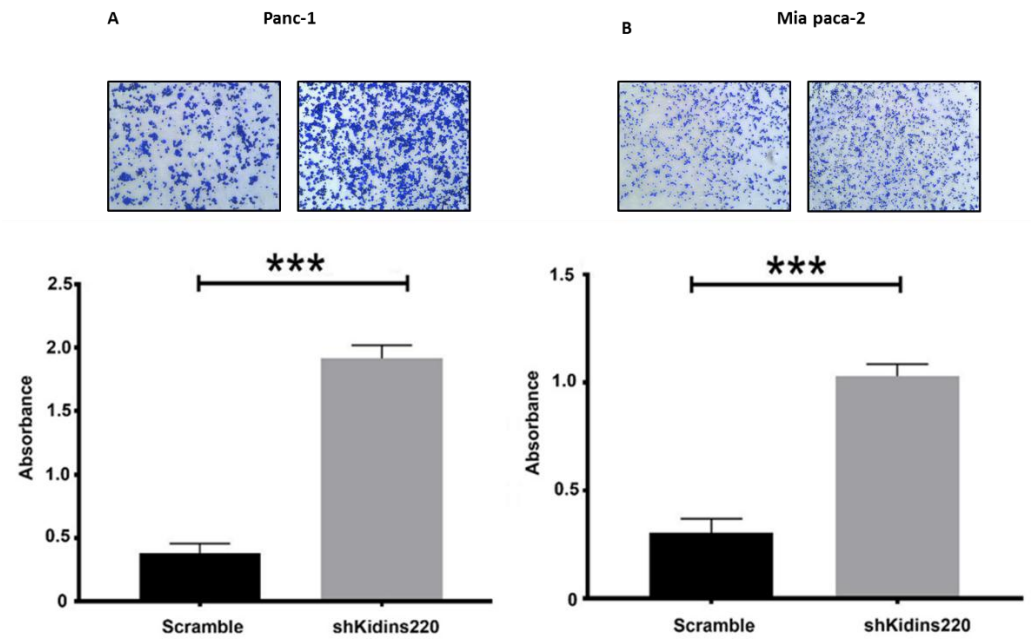

Figure 4.3: Impact on adhesion of Panc-1 and Mia paca-2 pancreatic cancer cells by the knockdown of Kidins220. (A) There was a significant increase in cell adhesion in the Kidins220 knockdown cells compared with scramble control in Panc-1 cells (*** p<0.001). **(B)** Adhesion of Mia paca-2 cancer cells was also enhanced following the knockdown of Kidins220 compared with the scramble control (*** p<0.001). Six repeats were included for each cell line in the experiment. Three experiments were carried out to validate the observations. Error bars are standard deviations. Representative images of each cell line are shown above the bar graph.

4.3.4 Influence of the Kidins220 knockdown on cell invasion of pancreatic cancer cell lines

Cancer cells invading into surrounding tissue and the vasculature is an initial step during cancer metastasis (Yamaguchi et al., 2005). In order to investigate whether Kidins220 is involved in regulation of invasiveness of pancreatic cancer cells, an *in vitro* trans-well invasion assay was performed. The invasive ability of cells was determined by measuring the number of cells that invaded through the Matrigel and also the membrane onto the bottom of the insert. Figure 4.4A shows that Panc-1 cells with knockdown of Kidins220 significantly increased in invasiveness compared with scramble control (**$p<0.01$) (Figure 4.4A). Meanwhile, knockdown of Kidins220 also promoted the invasive capacity of Mia paca-2 cancer cells in comparison with scramble cells (**$p<0.01$) (Figure 4.4 B).

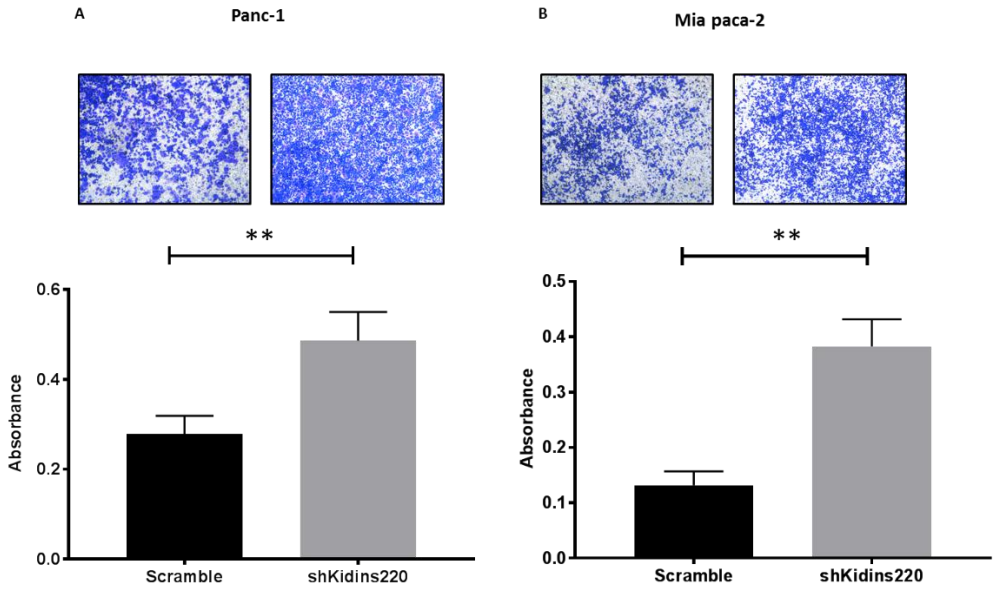

Figure 4.4: Knockdown of Kidins220 increases the invasive capacity of both Panc-1 and Mia paca-2 cell lines. (A) Representative images of Panc-1 cells after staining (upper panel) and the absorbance measured by dissolving the crystal violet stained invaded cells (bar graph). ** represent $p<0.01$. **(B)** Representative images of Mia paca-2 invaded cells (upper panel) and bar graph shows the measurement of absorbance of stained cells. ** represent $p<0.01$. Three experiments were performed. Error bars represent standard deviation.

4.3.5 Effect of Kidins220 on the migration of pancreatic cancer cells

During cancer metastasis, cancer cells migrate and spread to distant organs and form a new mass. In the current study, a trans-well migration assay was used to assess the impact of Kidins220 knockdown on the migration of pancreatic cancer cells. This assay is similar to the transwell invasion but with a lack of Matrigel coating in the insert. The ability of cell migration was determined by measuring the number of cells which had migrated to the bottom of the insert from the upper culture chamber over a period of 24 hours. The result showed that there was significantly enhanced cell migration in Panc-1 and Mia paca-2 pancreatic cancer cells as a result of the Kidins220 knockdown. After 24 hours incubation, Kidins220 knockdown Panc-1 cells exhibited an increased migration in comparison with the scramble control ($p<0.001$) (Figure 4.5 A). This result was also in accordance with a measurement of cell migration using wound (scratch) assay in Panc-1 cells using the IncuCyte Live-Cell Analysis System (Essen Bioscience, UK). The migration of cells was monitored over a period of 2 days following the wounding. It was shown that Panc-1 cells with knockdown of Kidins220 migrated faster compared with the scramble control cells (Figure 4.5B and Figure 4.5 C). Furthermore, an increase in migration was also seen in the Mia paca-2 Kidins220 knockdown cells compared with the scramble control ($p<0.01$) (Figure 4.6).

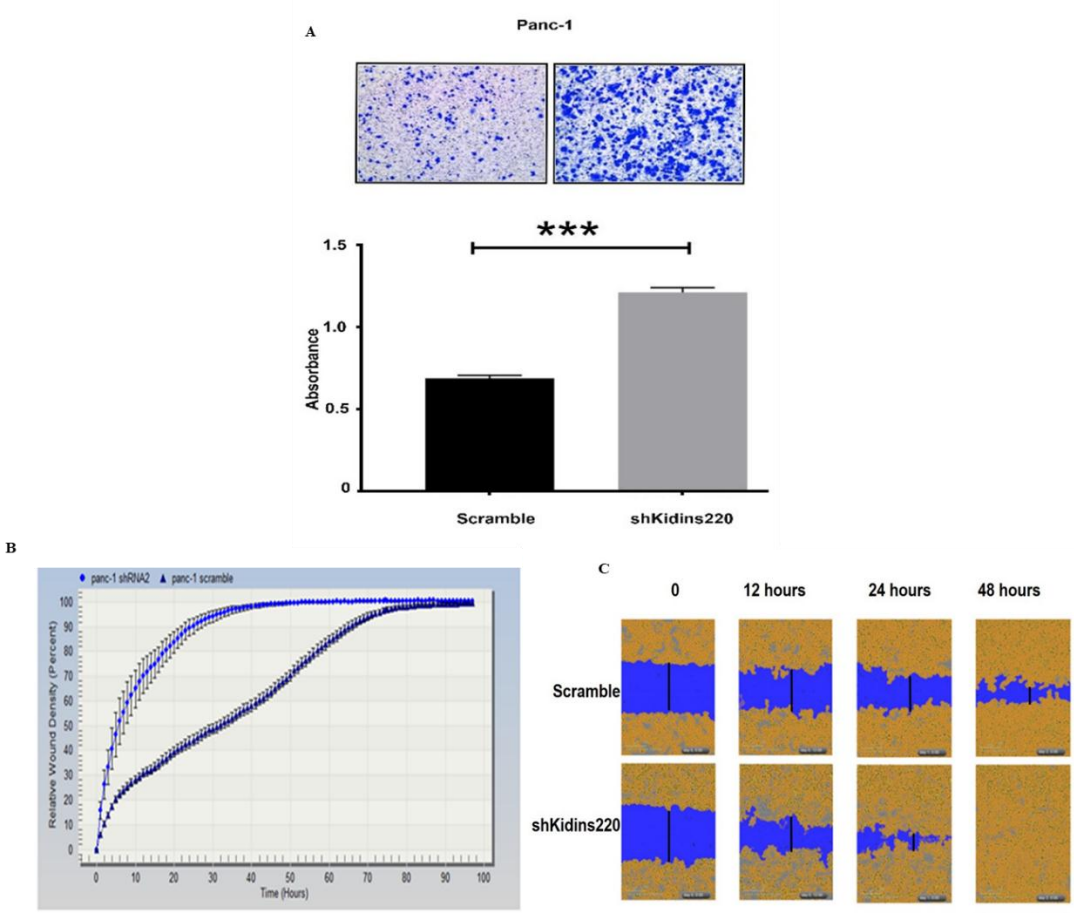

Figure 4.5: Influence of Kidins220 knockdown on the migration of Panc-1 cells. **(A)** Migration of Panc-1 cells was determined using a transwell migration assay, representative images of migrated cells are shown above the bar graph. *** represent $p<0.001$. Error bars are standard deviation. **(B)** A wound assay was also performed using the IncuCyte live cell analysis system. Four repeats were evaluated for each cell line in each experiment. Shown are the average percentage of the closure of the wounds, the migration was measured in wound density. Error bars represent standard deviation. **(C)** The representative images were taken by the IncuCyte live cell analysis system over the first 48 hours following the wounding.

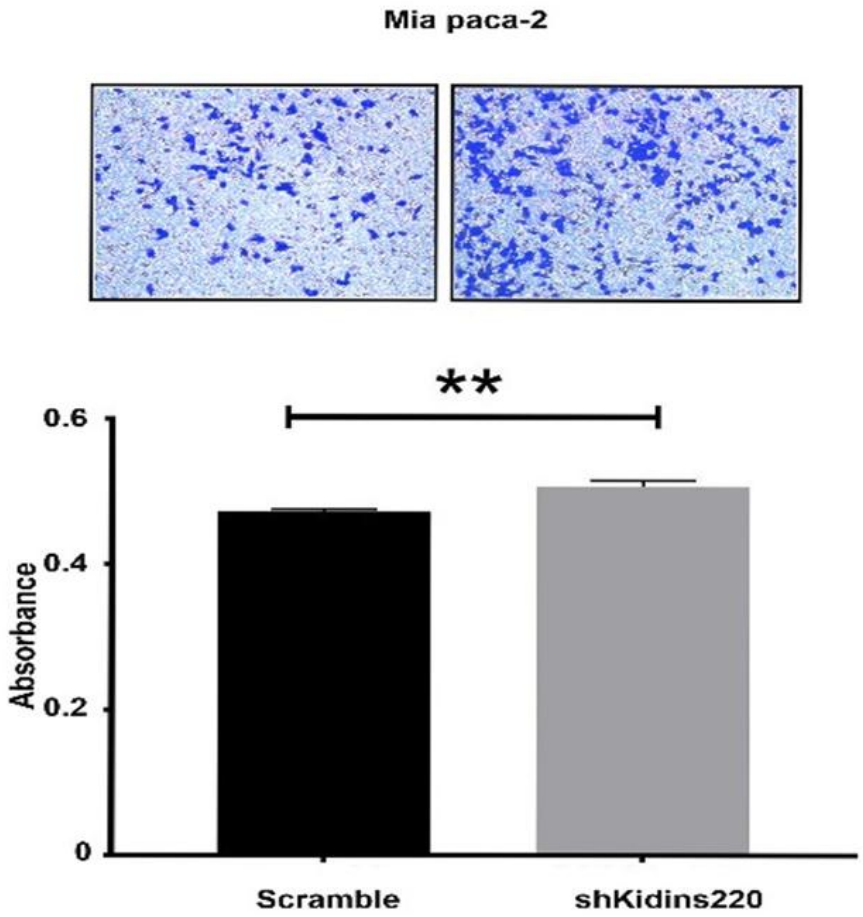

Figure 4.6: Influence of Kidins220 knockdown on migration of Mia paca-2 cells. The migration of Mia paca-2 cells was determined using the transwell migration assay. ** represent $p<0.01$. Error bars are standard deviation.

4.3.6 Effect of Kidins220 on tumour spheroid

Tumour spheroids usually contain a high concentration of stem-like cancer cells (Nath and Devi, 2016). This is the reason that the sphere formation is closely related with cancer recurrence and metastasis. 3D culture mimics a sphere formation procedure, which results in enrichment of the cancer cells expressing stem –like markers. In order to monitor the impact of Kidins220 in the growth of tumour spheroids, the solidity and circularity was determined. Figure 4.7 shows representative optical images of spheroids in Panc-1 cells with knockdown of Kidins220 and scramble control. The images were captured every 3 days. The morphological changes involved several stages during spheroid formation. Initially, single suspending cells assembled themselves to form cell aggregates in each well (day 1). Subsequently, tumour spheroid in Panc-1 cells with knockdown of Kidins220 presented bigger spheroids compared with the scramble control cells at the fourth day. At the final stage, the spheroids formed by Kidins220 knockdown cells became irregular in comparison with the scramble cells (day10-day13). In a similar way, the single and suspended Mia paca-2 cancer cells started to assemble themselves and form cell aggregates (day 1). The difference of spheroid solidity can be observed from Day4. Mia paca-2 cells with knockdown of Kidins220 presented bigger spheroids in comparison with scramble control. From Day 7, the spheroid became circular in the Kidins220 knockdown cells. At the end of the two weeks experiment, the Kidins220 knockdown Mia paca-2 cells grew into much bigger spheroids compared with the scramble control ($p<0.001$) (Figure 4.8).

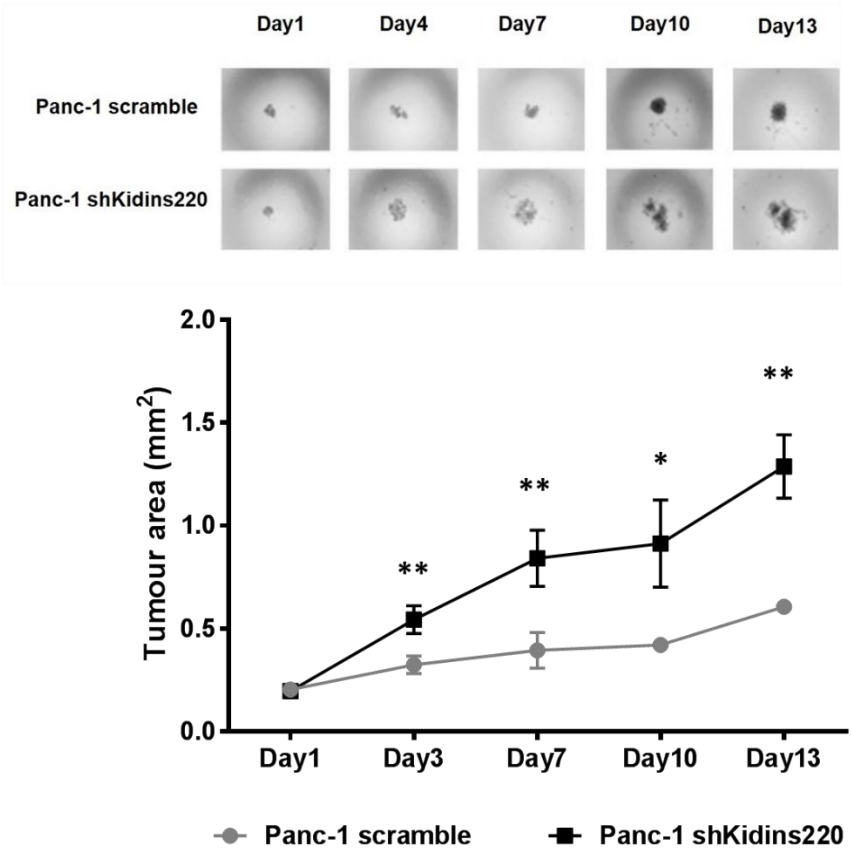

Figure 4.7: Growth of Kidins220 knockdown Panc-1 cells was examined using a 3D spheroid model. 1,000 Panc-1 cells were seeded in the 96-well U-bottom plates. Representative images of Panc-1 spheroids were photographed using the EVOS Auto imaging system (Thermo Fisher Scientific, Waltham, MA USA) at the indicated time over a period of two weeks. Size of the spheroids was measured using Image J software. Each cell line was tested in triplicate. Three experiments were performed. Shown are representative images and results. Error bars are standard deviations. * represents $p<0.05$ and ** represent $p<0.01$.

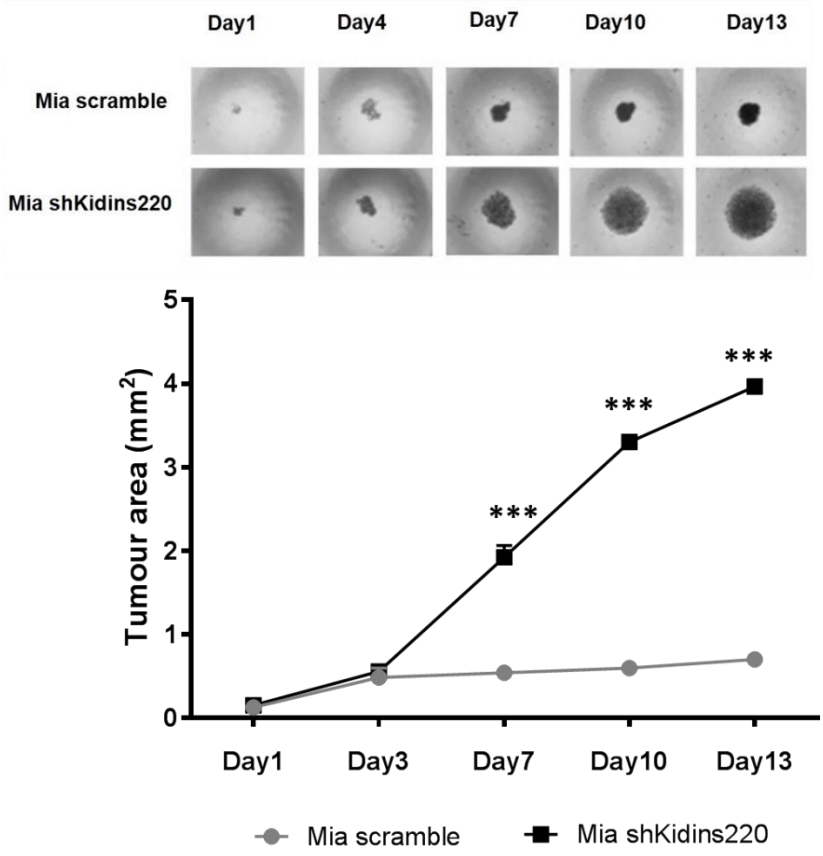

Figure 4.8: Growth of the Kidins220 knockdown Mia paca-2 cells was also examined using the 3D spheroid model. Representative images of Mia-paca-2 spheroids were photographed using the EVOS Auto imaging system (Thermo Fisher Scientific, Waltham, MA USA) at the indicated time over a period of two weeks. Size of the spheroids was measured using Image J software. Each cell line was tested in triplicate. Three experiments were performed. Shown are representative images and results. Error bars are standard deviations. *** represents $p<0.001$.

4.3.7 Knockdown of Kidins220 promoted peritoneal metastasis *in vivo*

Panc-1 pancreatic cancer cells (scramble and shKidins220) were injected into the peritoneal cavity of athymic nude mice (n = 6 mice per group). The mice were terminated after 4 weeks and intraperitoneal exploration was conducted to detect the metastatic tumours in the liver, stomach, pancreas, and duodenum to rectum. In the current study, all the metastatic tumours were found in intestine and the nodule numbers, total and average tumour volume, body weight, and tumour burden of the mice are listed in table 4.1. Knockdown of Kidins220 resulted in an increased number of nodules but this lacked statistical significance. Interestingly, tumour burden of the mice injected with Kidins220 knockdown Panc-1 cells was significantly increased in comparison with scramble control (Figure 4.9). Furthermore, there is a significant increase in total tumour volume and average tumour volume (Figure 4.10) in mice injected with Kidins220 knockdown cells when compared with the control group ($p=0.032$ and $p=0.009$ respectively).

Table 4.1: The analysis of peritoneal metastatic tumours in mice injected with Panc-1 scramble cells and Kidins220 knockdown cells.

	Scramble (mean±SD)	**shKidins220** (mean±SD)	**P value**
Number of nodules	4.17±0.98 (Median: 4)	5.33±2.94 (Median: 5)	*P*=0.394*
Total tumour volume (mm^3/mouse)	7.68±2.00	20.66±10.86	*P*=0.032*
Average tumour volume (mm^3)	1.87±0.43	4.43±1.58	*P*=0.009*
Body weight	22.97±1.07	22.38±0.55	*P*=0.262#
Tumour burden (mm^3/g)	0.33±0.086	0.92±0.48	*P*=0.032*

Note: Different statistical methods were employed; * for which t-test with Welch's correction was used whilst t-test was used for the # labelled data. All data are normally distributed. The t-test with Welch's correction was used for data with unequal variation.

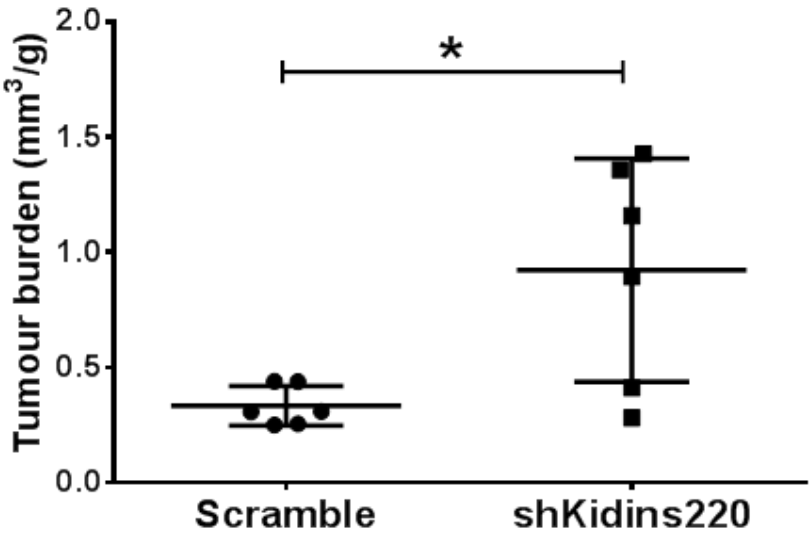

Figure 4.9: The impact of Kidins220 knockdown on peritoneal metastasis of Panc-1 cells in a mouse peritoneal metastatic model. Shown are tumour burden of the peritoneal metastasis nodules developed in each mouse. The tumour burden was determined based on the total tumour volume (mm^3) of each mouse against the corresponding body weight (g). *represent $p<0.05$.

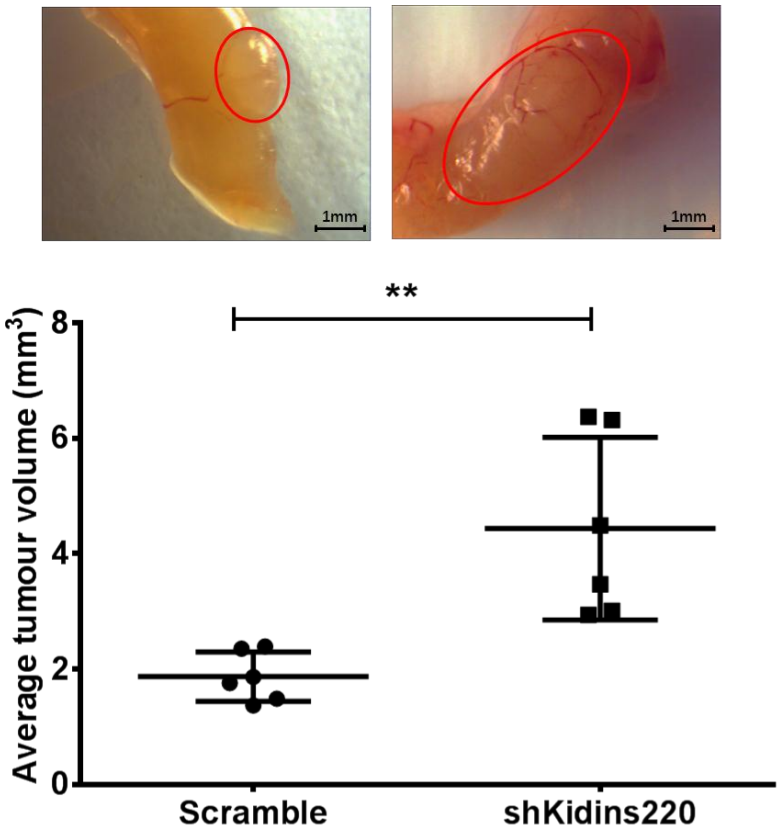

Figure 4.10: The influence of Kidins220 knockdown on the average tumour volume of peritoneal metastatic nodules developed by Panc-1 cells in the nude mouse model. The metastatic tumours volume (mm^3) were determined according to the equation (length × $width^2$)/2. The length and width of the tumour were measured using imageJ. ** represents $p<0.01$.

4.4 Discussion

Initial investigation demonstrated a reduced expression of Kidins220 in human pancreatic cancer tissue samples. The reduced expression is associated with disease progression and poor prognosis. This is very different from the overexpression of Kidins220 seen in melanoma (Liao et al., 2011a). The downregulation of Kidins220 observed in human pancreatic cancer suggests that this molecule acts as a negative regulator for the cellular functions that are acquired by cancer cells during the disease progression. This could be tissue specific or disease specific which is yet to be investigated. Kidins220 has been shown to promote proliferation and survival of melanoma cell lines. As seen in a mouse xenograft model, knockdown of Kidins220 resulted in an increasing population of apoptotic cells compared with control group. Overexpression of Kidins220 was able to protect cells from stress-induced apoptosis, whilst melanoma cells with Kidins220 knockdown resulted in a decrease in anchorage-independent growth in soft agar and an extended cell death following an UVB-induced apoptosis (Liao et al., 2007). Similar to the findings in melanoma, a study of Kidins220 in neuroblastoma also showed a positive role played by this molecule in the regulation of cell proliferation. Knockdown of Kidins220 in neuroblastoma cells induced a decrease of proliferation through an inhibition of cell cycle in which an arrest at G1 phase was observed. The inhibitory effect on cell cycle is accompanied with decreased expression of cyclin D1 and cyclin-dependent kinase 4 (CDK4) and inhibition of hyperphosphorylated pRb to which an upregulation of

p21 may contribute (Jung et al., 2014). In the current study, three pancreatic cancer cell lines were examined for their expression of Kidins220. All three cell lines examined expressed this gene but to variable levels. A knockdown model was successfully established using Kidins220 shRNA in two of the three cell lines, i.e. Panc-1 and Mia paca-2. Due to the lack of an appropriate cDNA library for use in the amplification of the Kidins220 coding sequence, consisting of multiple variants which are generally expressed, combined with the high cost for synthesis of such a long DNA sequence (5316 bps for one of Kidins220 isoforms), the overexpression model was not employed in the current study. An increase was seen in the proliferation of both Panc-1 and Mia paca-2 cell lines following the knockdown of Kidins220. This is in line with the reduced expression of Kidins220 observed in pancreatic cancer tumour tissues, this suggests that Kidins220 is a negative regulator of proliferation of pancreatic cancer cells although the increase was just marginal. Regulation of other cellular functions could be more remarkable and has been shown in the following functional tests.

The unique hallmark of cancer cells is their acquired capability to metastasise. The spread of cancer to distant locations is a major complication and commonly associated with the death of patients with cancer. It also indicates disease progression to a more advanced stage. Metastasis begins when individual cancer cell breaks away from the tumour and invade nearby blood vessels and migrate through bloodstream, lymphatic system, or through body cavity spaces. Once the metastatic cancer cells arrive at a new site, they can begin a process forming a new

tumour by leaving the blood vessel, and begin to colonisation and form a secondary tumour (Klein, 2008).

Cellular and molecular mechanisms of cancer metastasis have been investigated for several decades. Scaffold proteins has been shown to play an important role in cancer development and metastasis due to their critical role in maintaining the cell structure through regulation of the cytoskeleton, adhesion and migration of cells, and also interactions with certain signalling pathways (Bompard et al., 2005, Lin et al., 2005, Yamagishi et al., 2004, Mattila et al., 2003). Also, there is a growing amount of evidence supporting the importance of Kidins220 in cancer development apart from its function in neuronal activity. The aberration of Kidins220 was involved in affecting cell proliferation, invasion, migration, and apoptosis, which play an important role in tumour formation and metastasis (Cai et al., 2017).

In melanoma, Kidins220-knockdown reduced migratory and invasive abilities of melanoma cells *in vitro* and *in vivo* (Liao et al., 2011a). However, the present study detected a contrasting role played by Kidins220 in pancreatic cancer. The effect of Kidins220 on the adhesion of Panc-1 and Mia paca-2 cells showed a significant difference compared with scramble control. With regard to the impact of Kidins220 on the motility of pancreatic cancer cells, trans-well migration assay was performed and the result showed that Kidins220 negatively regulated the motility of both Panc-1 and Mia paca-2 cancer cells. In Panc-1 cells, knockdown of

Kidins220 significantly increased migratory ability compared with scramble control. Similarly, knockdown of Kidins220 also increased migration significantly in Mia paca-2 cancer cells. In line with the findings of the previous clinical study (Chapter3), knockdown of Kidins220 is associated with increased migration and invasiveness of pancreatic cancer cells. It suggests that Kidins220 is a negative regulator of these cellular functions in pancreatic cancer cells.

We also used 3D culture to verify the effect of Kidins220 in regulating cell growth by tumour spheroid assay. It was shown that knockdown of Kidins220 increased the solidity of tumour spheroid in Mia paca-2 cells significantly, and the increase of tumour spheroid was also seen in Panc-1 cells with Kidins220 knockdown compared with scramble control. The 3D spheroid model has been shown as an appropriate *in vitro* model to evaluate tumorigenic and stemness of cancer cells (Nath and Devi, 2016). Indeed, the current finding in the 3D model together with the reduced expression of Kidins220 seen in the early cancerous lesions preceding pancreatic cancer, suggest loss or reduced expression of this gene is implicated in the development and also disease progression of pancreatic cancer. Further investigation will help to shed light on what molecules, such as stem cell markers and epithelial mesenchymal transition markers are affected.

As involvement of Kidins220 in distant metastases of pancreatic cancer was observed in corresponding clinical tissue samples, a peritoneal metastatic model was employed to evaluate the corresponding impact using the Kidins220

knockdown Panc-1 cells. The loss of Kidins220 resulted in an increased tumour burden and increased average tumour volume of metastatic nodules developed by the Panc-1 cells in the peritoneal metastasis model but did not significantly impact the number of nodules formed which remained relatively stable. This result indicated that Kidins220 may not be involve in peritoneal seeding but plays a significant role in growth and invasion of the metastatic tumours following the initial colonisation. A further experiment using more mice per group will increase the statistical power to clarify this finding. Possible targets for corresponding treatment will also be investigated in the following experiments.

In conclusion, the reduced expression of Kidins220 is associated with pancreatic cancer proliferation and hallmarks of disease progression. Knockdown of Kidins220 promoted *in vitro* growth, migration and invasion of pancreatic cancer cells, and peritoneal metastasis *in vivo*. The current study suggests that Kidins220 may act as a tumour suppressor in the development and disease progression of pancreatic cancer thus contributing to the poor prognosis and shorter survival. Further investigation will aim to dissect the signalling pathway and molecules underlying these aberrant cellular functions as a result of loss of Kidins220 in pancreatic cancer cells.

Chapter 5

Molecular machinery underlying the reduced Kidins220 expression in pancreatic cancer

5.1 Introduction

The previous chapter has shown that the knockdown of Kidins220 increased proliferation, adhesion, invasion, and migration of pancreatic cancer cell lines. All these cellular functions are crucial for cancer progression. These findings are in line with the reduced expression of Kidins220 in pancreatic cancer tumour samples and its association with disease progression. This suggests that Kidins220 is a putative tumour suppressor in pancreatic cancer which is opposite to its role evident in some other malignancies, such as melanoma and neuroblastoma (Jung et al., 2014, Liao et al., 2007, Liao et al., 2011a). Molecules and pathways involved in this different role played by Kidins220 in pancreatic cancer are likely to be organ specific but are yet to be investigated.

In a parallel study carried out in the host lab, the implication of Kidins220 in gastric cancer has been examined. Our unpublished data showed that Kidins220 was up-regulated in the gastric cancer compared with normal gastric tissues or adjacent normal gastric tissues. However, *in vitro* experiments showed similar effects on cellular functions of gastric cancer cell lines as seen in the current study of pancreatic cancer. A screening of proteins and protein phosphorylation affected by the Kidins220 knockdown in gastric cancer using a protein microarray (Kinex^{TM} antibody microarray, Kinexus, British Columbia, Canada) identified EGFR to be one of the most affected receptors in a gastric cancer cell line (HGC27). The microarray contains over 850 antibodies that recognise both total protein and phospho-

proteins. An increased level of tyrosine phosphorylation was seen for EGFR including tyr1068, tyr1110, tyr1148, try1197, tyr998 following the knockdown of Kidins220 with ribozyme transgene compared with pEF control (Figure 5.1 A). Meanwhile, the protein level of total EGFR was also increased in the HGC27 Kidins220 knockdown cells compared with the corresponding pEF empty plasmid vector control. Knockdown of Kidins220 enhanced cell invasion in gastric cancer cells, which is in accordance with its role observed in the pancreatic cancer cell lines. We hypothesised that EGFR signalling might be involved in Kidins220-coordinated cellular functions thus contributing to the disease progression of pancreatic cancer. Corresponding alteration of downstream intracellular signalling pathways such as ERK and AKT pathways was also observed in the Kidins220 knockdown cell line. This suggests that EGFR/ERK and AKT pathways are affected or involved in the reduced Kidins220 expression associated cellular events and are implicated in the disease progression.

Epithelial-mesenchymal transition (EMT) occurs when tumour cells lose their epithelial features such as loss of polarity, down regulation of E-cadherin, and spread to distant sites (Thiery et al., 2009). When cells developed a mesenchymal phenotype with elevated expression of mesenchymal markers including N-cadherin and vimentin, they would acquire the ability to disseminate (Acloque et al., 2009). In the past decades, several studies regarding patients with pancreatic cancers have provided evidence for the EMT involvement in the disease progression (Hotz et al., 2007, Rasheed et al., 2010). In human pancreatic tumour

samples, fibronectin and vimentin are increased in high-grade (poorly differentiated) tumours and at foci of poorly differentiated cancer cells in low-grade tumours, with a corresponding decrease in E-cadherin expression. Patients with tumour exhibiting EMT have worse survival than those patients whose tumours demonstrate less evidence of EMT. In a study based on a rapid autopsy program for patients with pancreatic cancer, 75% of the primary tumours with mesenchymal features developed metastatic lesions to liver and lung (Rasheed et al., 2010).

In the previous chapter, it has been shown that Kidins220 knockdown is associated with increased proliferation, adhesion, invasion, and migration in pancreatic cancer cell lines. The following experiments will focus on the EGFR signalling and EMT occurrence in the pancreatic cancer cell lines following the knockdown of Kidins220.

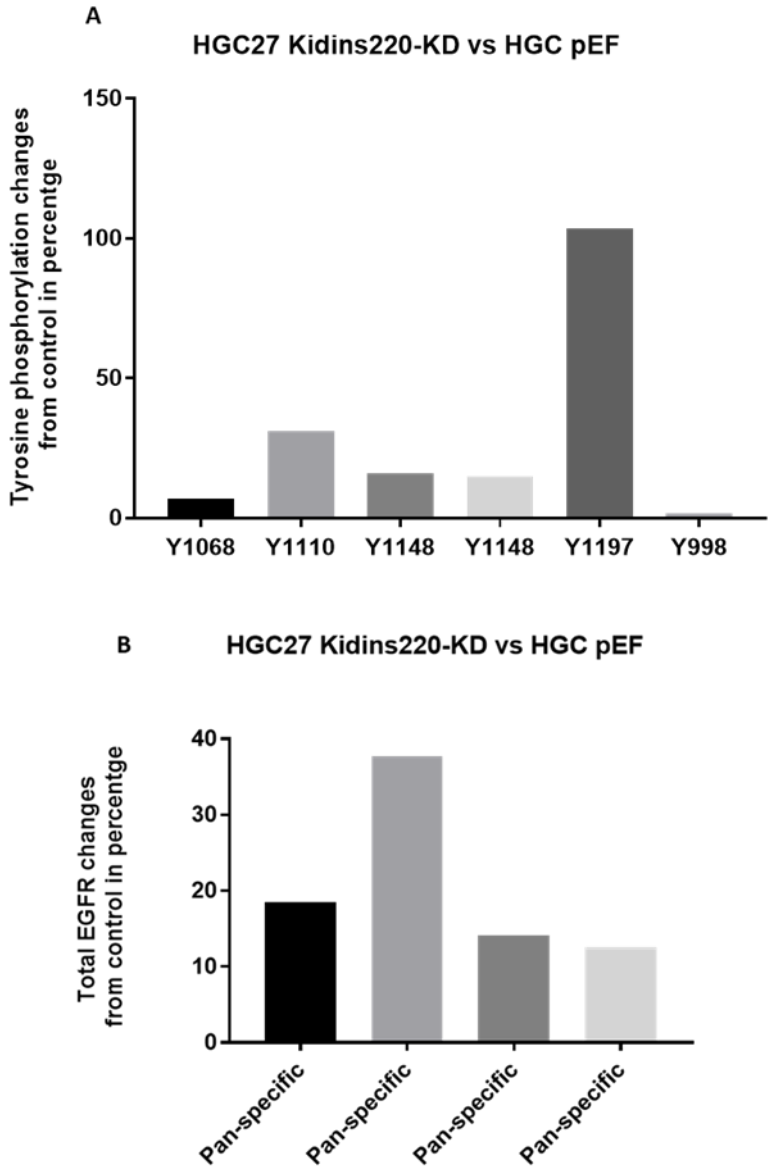

Figure 5.1: Expression and activation of EGFR in Kidins220 Knockdown gastric cancer cell line (HGC27). (A) Tyrosine phosphorylation status of EGFR in HGC27 Kidins220 knockdown cells was determined using the Kinex™ antibody microarray. Y1068: EGFR-pY1068 phosphosite-specific antibody Y1110: EGFR-pY1110 phosphosite-specific antibody Y1148: EGFR-pY1148 phosphosite-specific antibody Y1197: EGFR-pY1197 phosphosite-specific antibody. Y998: EGFR-pY998 phosphosite-specific antibody (B) Expression of total EGFR in the HGC27 Kidins220 knockdown cells was also determined using the same array. Shown are changes as percentage against the HGC27 control cell line which were transfected using the empty plasmid vector. Pan-specific: EGFR-specific antibody.

5.2 Materials and methods

5.2.1 Materials

The primers used in this chapter are shown in Table 2.4, including EGFR, E-cadherin, vimentin, snail, slug, and twist. Details of antibodies for detection of EGFR, ERK, AKT, E-cadherin, vimentin, snail, slug, and phosphor-tyrosine are shown in Table 2.5. Recombinant human EGF was purchased from Santa Cruz Biotechnology, UK (sc-4552).

5.2.2 Protein array in Kidins220 knockdown gastric cancer cells.

Protein samples were collected from HGC27 gastric cancer cells of PEF control and Kidins220 knockdown using anti-Kidins220 ribozyme transgene, respectively. After protein extraction and subsequent quantification, 300µl lysis (4mg/ml) was prepared and being stored at -20°C before sending for an analysis using the Kinexus^{TM} antibody microarray (Kinexus Bioinformatics, Vancouver, British Columbia, Canada).

5.2.3 Determining the expression of EGFR-related signalling molecules and EMT markers using PCR and Western blot.

Both RNA and protein were extracted from stable pancreatic cancer cell lines infected with lentiviral Kidins220 shRNA. The samples were used in either western

blot analysis or PCR to detect the expression level of these molecules involved in cell function. The methods were carried out as per the previous description in section 2.4 and 2.5.

5.2.4 Immunoprecipitation and detection of EGFR with tyrosine phosphorylation

Protein was extracted from Panc-1 and Mia paca-1 cells. Following immunoprecipition with anti-EGFR, immunoprecipitated protein samples were separated on an SDS-PAGE and blotted for detection of EGFR with tyrosine phosphorylation using an antibody (PY-99, Santa Cruz Biotechnology). The details of immunoprecipitation and western blot are provided in section 2.5.4 and 2.5.5.

5.2.5 Statistical analysis

Correlation between Kidins220 and other genes in pancreatic cancer tissue samples was assessed based on gene expression array dataset (GSE71729) and TCGA pancreatic cancer cohort using Spearman correlation test and the statistical analysis software (Sigma Plot version 11). GSE71729 is a validation cohort including 46 normal pancreatic sample, 145 primary pancreatic tumour samples, and 61 metastatic tumour sample. TCGA pancreatic cancer cohort containing 178 primary pancreatic tumour samples.

5.3 Results

5.3.1 Possible link between Kidins220 and EGFR in pancreatic cancer

The possible correlation between Kidins220 and EGFR and other HER family members was evaluated in a gene expression array dataset (GSE71729) using the Spearman correlation test. A positive correlation was seen between Kidins220 transcript and EGFR, whilst an inverse correlation was shown between Kidins220 and HER3 (Table 5.1). To validate this discovery, a similar correlation analysis was performed in the TCGA pancreatic cancer cohort. The positive correlation between Kidins220 and EGFR was also observed in the TCGA pancreatic cancer cohort. A positive correlation was also seen between Kidins220 and HER4 in this TCGA cohort. More interestingly, an inverse correlation was seen between Kidins220 and HER2, but not HER3 (Table 5.2). The inconsistence in the correlation between Kidins220 and Her2 observed in the two cohort of pancreatic cancer gene array data might be due to the variation in the number of the Her2 positive tumour and also the expression of the Her2. The possible link between Kidins220 and Her2 could be explored in the future study.

Table 5.1: Correlation between Kidins220 and HERs in pancreatic cancer (GSE71729).

	EGFR	HER2	HER3	HER4
Kidins220	Cor=0.326 p<0.001 n=145	Cor=-0.001 P=0.989 n=145	Cor=-0.187 p=0.024 n=145	Cor=-0.016 p=0.849 n=145

Note: Cor = correlation coefficient.

Table 5.2: Correlation between Kidins220 and HERs in pancreatic cancer (TCGA_PAAD).

	EGFR	HER2	HER3	HER4
Kidins220	Cor=0.451 p<0.001 n=178	Cor=-0.317 p<0.001 n=178	Cor=-0.096 p=0.203 n=178	Cor=0.317 p<0.001 n=178

Note: Cor = correlation coefficient.

5.3.2 Kidins220 knockdown and EGFR signalling

Positive correlation between Kidins220 and EGFR was observed in both cohorts of pancreatic cancer though there were inconsistences for other HERS. However, the positive correlation was not seen in the gastric cancer cell line following knockdown of Kidins220. Instead, an increased total protein level and tyrosine phosphorylation were evident in the Kidins220 knockdown cells. The inconsistency in findings for the correlation between Kidins220 and EGFR at mRNA and protein levels led to the following investigations.

The expression and tyrosine phosphorylation of EGFR were first determined using western blot. An increased protein level of EGFR was seen in both Panc-1 and Mia paca-2 cancer cell lines following the knockdown of Kidins220. Meanwhile,

levels of phosphorylated EGFR were analysed using immunoprecipitation and western blotting. A marked increase of p-EGFR (Tyr) was seen in the Kidins220 knockdown cells in comparison with the scramble control, suggesting that knockdown of Kidins220 affected EGFR signalling and also the total protein level of EGFR (Figure 5.2A). To detect whether knockdown of Kidins220 affects the expression of EGFR at mRNA level, we examined the expression of EGFR using RT-PCR. The results showed that there was no difference seen at the mRNA level in the expression of EGFR in Kidins220 knockdown cells compared with corresponding scramble control, which indicated that Kidins220 did not affect EGFR expression at the transcript level (Figure 5.2B).

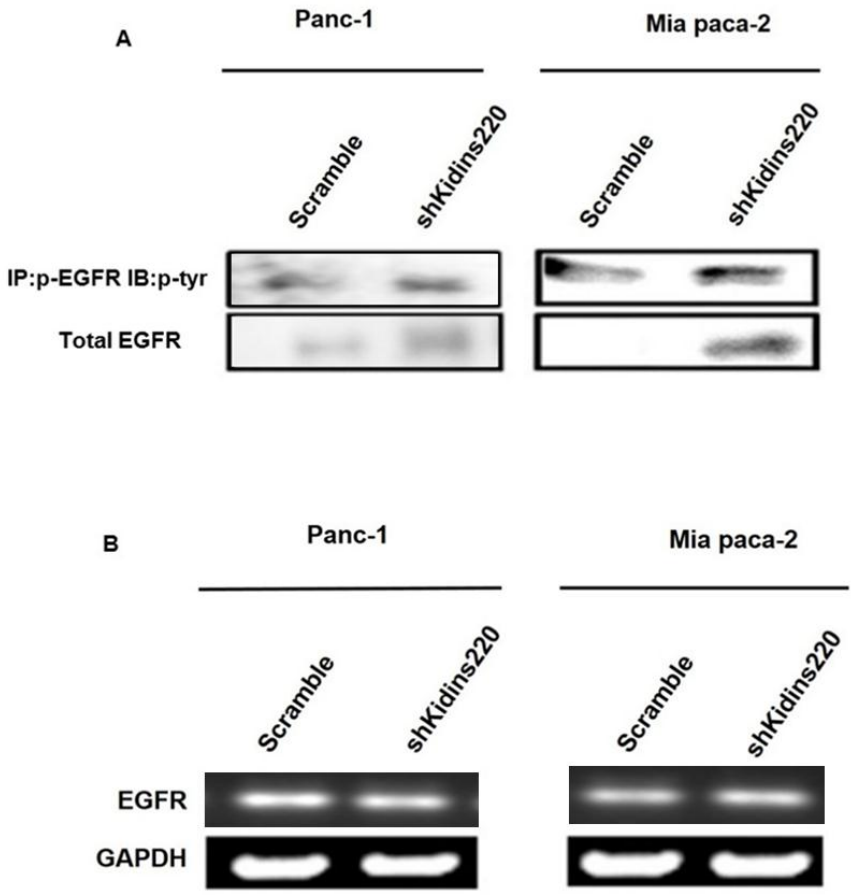

Figure 5.2: The expression and activation of EGFR in the Kidins220 knockdown pancreatic cancer cell lines. (A) The expression of total protein and tyrosine phosphorylation of EGFR were determined using immunoprecipitation and Western blot. p-EGFR: EGFR phosphorylation; p-try: tyrosine phosphorylation. **(B)** EGFR transcripts expressed by both Panc-1 and Mia paca-2 were determined using conventional RT-PCR. Images of the corresponding Western blots and RT-PCR are provided in Appendix 3.

5.3.3 MAPK and AKT pathway

Deregulation of EGFR can induce an activation of pro-oncogenic signalling pathways such as the MAPK and AKT signalling pathways, consequently leading to various biological activities involved in development and progression of certain malignancies (Oliveira-Cunha et al., 2011). The knockdown of Kidins220 in the two pancreatic cancer cell lines resulted in a promotion of cell migration, invasion and proliferation, and consistently upregulation and activation of EGFR in those cells. This provoked an investigation of the intracellular signalling pathways downstream of the EGFR, i.e. ERK and AKT pathways.

The western blots showed a similar total protein level of these proteins in both cell lines which appeared not be affected by the Kidins220 knockdown. Interestingly, but not surprisingly, corresponding activation of both ERK and AKT were seen in both Panc-1 and Mia paca-2 Kidins220 knockdown cell lines. Levels of phosphorylated ERK and AKT were increased in the Kidins220 knockdown sublines of both cell lines compared with their respective scramble control, and there was no difference seen in the expression of total ERK and AKT protein levels in Kidins220 knockdown cells compared with corresponding scramble control (Figure 5.3).

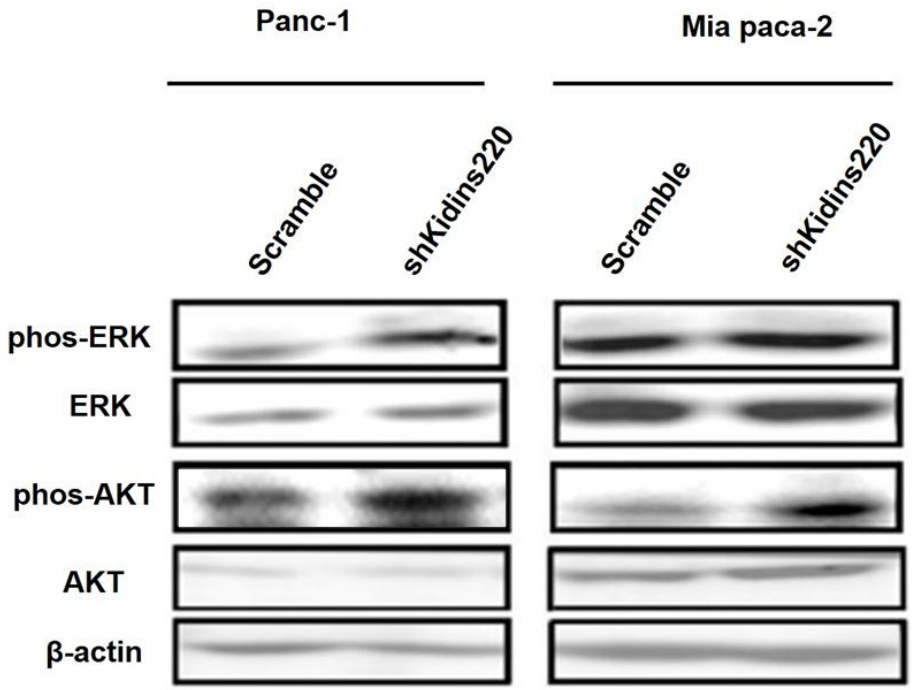

Figure 5.3: Activation of ERK and AKT in Kidins220 knockdown cell lines was determined using western blot analysis. Expression of total protein and protein phosphorylation were determined using corresponding antibodies. Details of the antibodies are provided in the general method. The same experiments were performed three times and shown are representative results of the western blots. Phos-ERK: ERK phosphorylation; ERK: total ERK protein; Phos-AKT: AKT phosphorylation; AKT: total ERK protein.

5.3.4 Kidins220 and EMT

5.3.4.1 EMT markers

Epithelial-mesenchymal transition (EMT) occurs when tumour cells lose their epithelial features such as loss of polarity and spread to distant sites with down regulation of E-cadherin (Thiery et al., 2009). When cells develop a mesenchymal phenotype, they acquire the ability to metastasise expressing mesenchymal markers such as N-cadherin and vimentin (Acloque et al., 2009). To determine whether Kidins220 affects the EMT in pancreatic cancer cells, the expression of EMT markers E-cadherin and vimentin was detected using western bolt. In the Panc-1 cancer cells, knockdown of Kidins220 resulted in a decreased expression of E-cadherin, whilst vimentin was increased. However, E-cadherin did not express in Mia paca-2 cancer cells, and vimentin presented a reduced expression in the cells when Kidins220 was knocked down (Figure 5.4A).

In terms of the mRNA levels of these genes, we examined the expression of E-cadherin and vimentin using RT-PCR for both cell lines. As shown in Figure 5.5B, down-regulation of E-cadherin and up-regulation of vimentin were seen in the Panc-1 cells with Kidins220 knockdown compared scramble control. E-cadherin was undetectable in Mia paca-2 cell lines and reduced expression of vimentin was observed in the Kidins220 knockdown cells compared the scramble control (Figure 5.4B).

5.3.4.2 EMT regulatory transcription factors; snail, slug and twist

The expression and activity of transcription factors (TFs) such as snail, slug, zeb, and twist mediate transcriptional regulation of the aforementioned EMT markers. To determine the involvement of these transcription factors in the Kidins220 knockdown induced EMT, RT-PCR and western blot were employed to examine their expression in the Kidins220 knockdown cell lines.

The results from RT-PCR indicated that there was an increased expression of snail and twist in panc-1 cancer cells with knockdown of Kidins220 in comparison with scramble control, and the expression of slug was undetectable in panc-1 cancer cells. Furthermore, knockdown of Kidins220 enhanced expression of snail and slug in Mia paca-2 cancer cells when compared with the scramble control, however, the expression of twist was not showed at the transcript level (Figure 5.5A).

Expression of these proteins was subsequently determined using western bloting. An elevated expression of snail and slug was seen in Panc-1 Kidins220 knockdown cells. Increased expression of snail was also observed in Mia paca-2 Kidins220 knockdown cells while the slug was undetectable (Figure 5.5B).

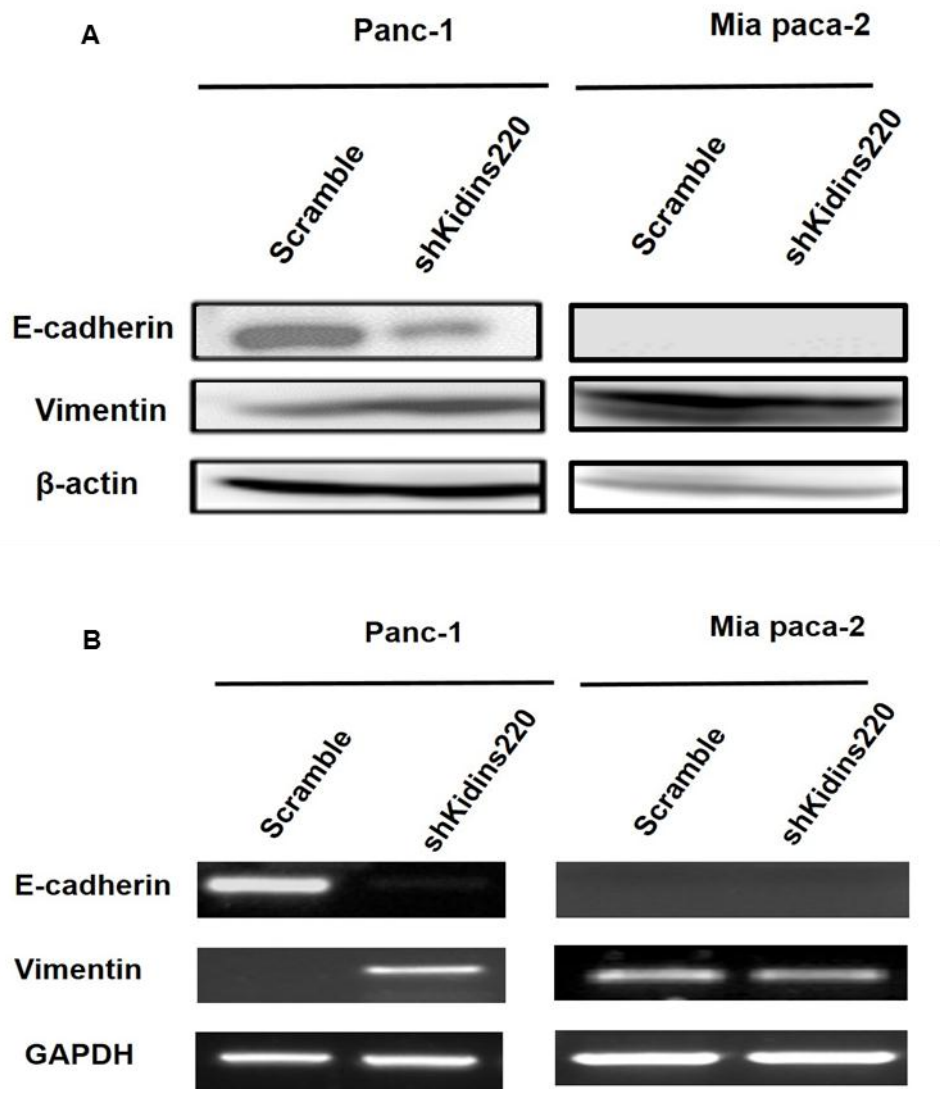

Figure 5.4: Expression of EMT markers in the Kidins220 knockdown cell lines. (A) Protein expression of these EMT markers was determined using western blot. **(B)** Corresponding impact of the EMT markers at mRNA level was examined using RT-PCR.

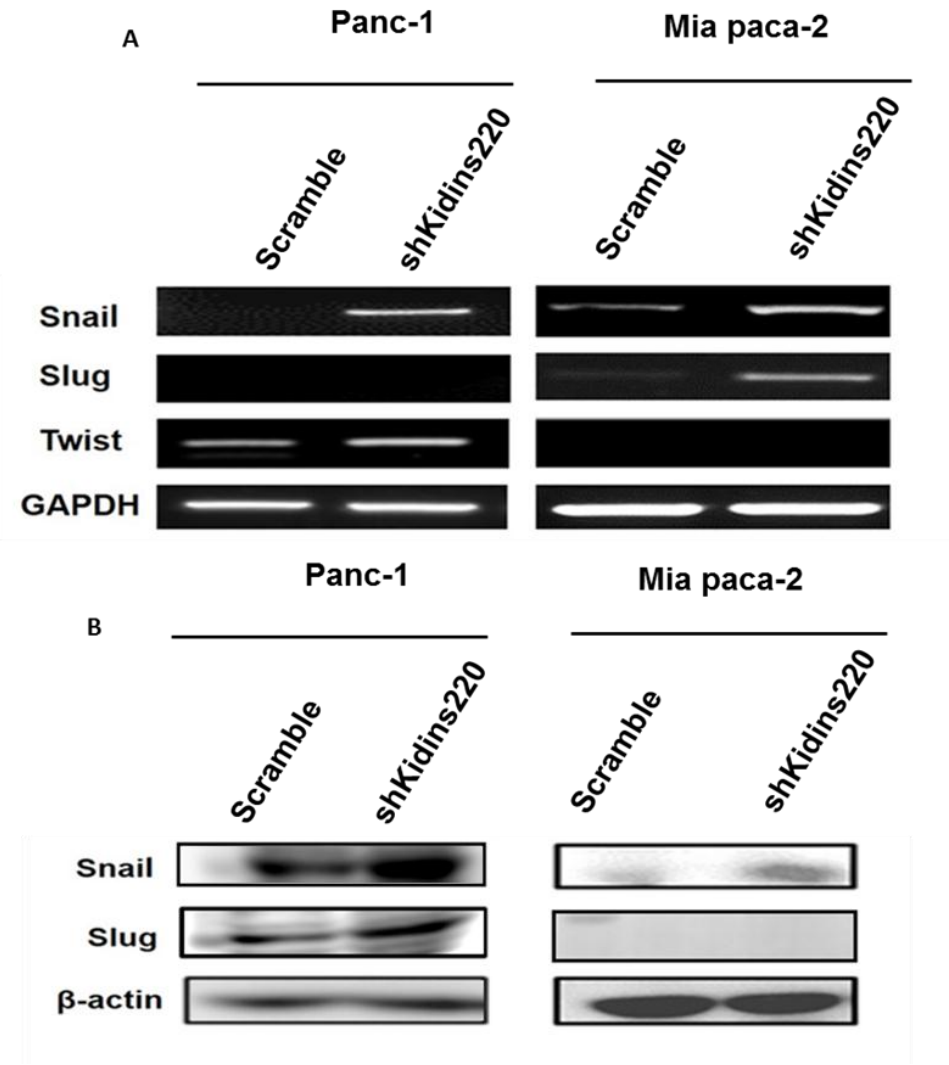

Figure 5.5: EMT related transcriptional factors was determined in the Kidins220 knockdown pancreatic cancer cell lines using RT-PCR and western blot, respectively. (A) The mRNA expression was examined using RT-PCR. **(B)** The impact of Kidins220 Knockdown on the protein expression of these transcriptional factors was then evaluated using Western blot.

5.3.4.3 Kidins220 and EGF/EGFR induced EMT

Following experiments aimed to dissect the role of Kidins220 in EGFR and its downstream signalling, and also the corresponding changes in EMT markers. EGF, a ligand of EGFR, was employed to treat the Panc-1 cancer cells. The increased expression and activation of EGFR protein in Kidins220 knockdown cells were enhanced upon treatment with recombinant human EGF in comparison with the control group. Moreover, both scramble control and Kidins220 knockdown cells showed increased expression of phosphorylated-ERK and total ERK in exposure to EGF. Panc-1 cells with knockdown of Kidins220 showed reduced expression of E-cadherin and increased vimentin expression when they were treated with EGF but to a further level. In terms of the EMT transcriptional factors, the expression of snail was increased in the scramble control cells when treated with EGF, whilst the Kidins220 knockdown cells did not present a greater difference under the treatment of EGF (Figure 5.6).

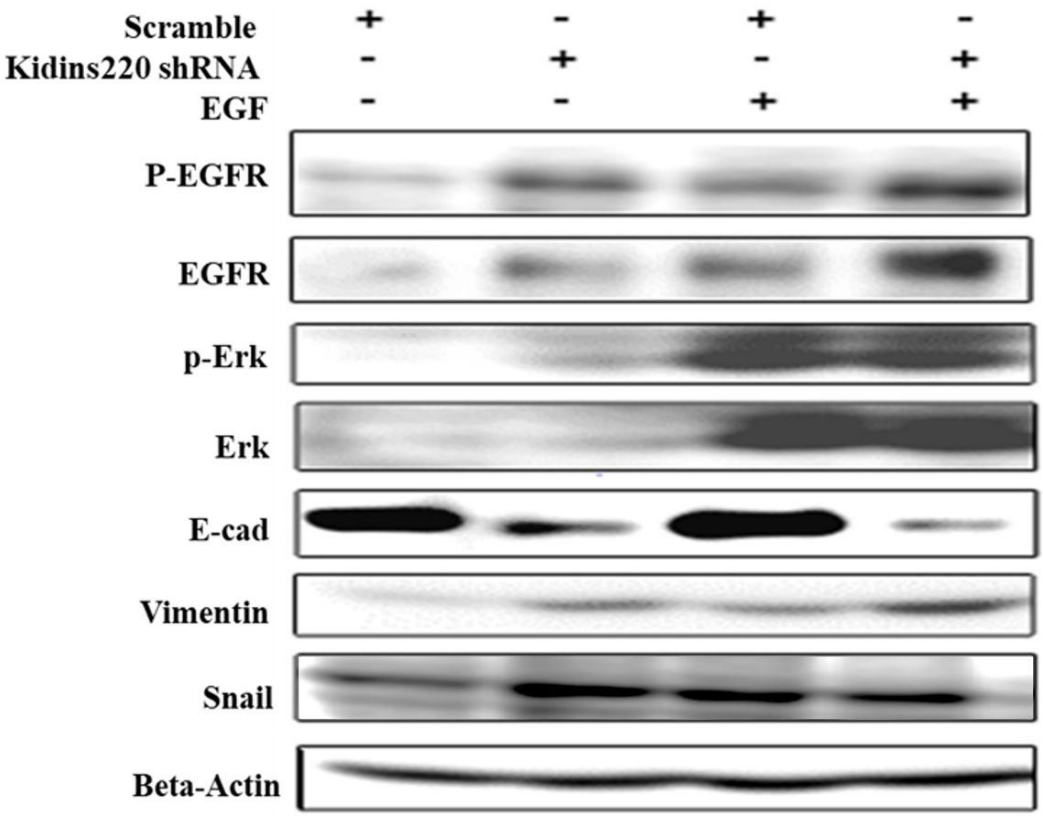

Figure 5.6: The correlation of Kidins220 and EGF-induced EGFR, ERK, and EMT activation in Panc-1 cancer cell lines. Panc-1 scramble and Kidins220 knockdown cells were Serum-starved for 1 h before stimulation with vehicle control (-) and rhEGF (200ng/ml) for 5 min. Protein extracts were analysed using western blot analysis with corresponding antibodies. Actin was included as a loading control. P-EGFR: EGFR phosphorylation.

5.4 Discussion

During cancer metastasis, malignant cells acquire the ability to invade surrounding tissue and spread to a distant site. These malignant traits are orchestrated by several aberrant cellular signalling pathways (Tracey A. Martin, 2013). An important finding from our parallel study of Kidins220 in gastric cancer showed that Kidins220 knockdown increased the protein level of EGFR and also its phosphorylation in gastric cancer cells. Overexpression of EGFR and alterations in its downstream signalling pathways such as MAPK and AKT signalling, are associated with more aggressive behaviours of various human malignancies and poor prognosis (Mendelsohn and Baselga, 2003). The present study was aimed to investigate the role of EGFR and its downstream signalling in the pancreatic cancer cell lines with Kidins220 knockdown. In an initial analysis of mRNA expression in two cohort of pancreatic cancer (GSE71729 and TCGA_PAAD), a positive correlation between Kidins220 transcripts and EGFR transcripts is observed in both cohorts. This suggested that a possible crosstalk may occur between Kidins220 and EGFR which could contribute to disease progression in pancreatic cancer. The experiments in this current study showed an increase of both protein expression of EGFR and phosphorylated EGFR in the Kidins220 knockdown pancreatic cancer cell lines. No change was seen in the mRNA expression of EGFR in the Kidins220 knockdown cell lines compared to their corresponding scramble control. It suggests that Kidins220 is not involved in the transcriptional regulation of EGFR though there is a positive correlation between the transcript levels of these two

genes in the pancreatic cancers. In the Kidins220 knockdown cell lines an upregulation of EGFR was evident for both total protein expression and activation, indicating that reduced expression of Kidins220 in pancreatic cancer may strengthen EGFR signalling and the corresponding implication in the disease progression which is yet to be investigated. For instance, correlation between Kidins220 expression and protein expression/activation of EGFR in human pancreatic cancer should be further examined using immunochemical or other protein analysis techniques. Molecular machinery underlying the Kidins220 regulated protein expression/activation of EGFR is also yet to be explored, for example, the involvement of protein degradation.

Several studies have demonstrated the role of Kidins220 correlated with MAPK signalling in malignancies (Rogers and Schor, 2013b, Liao et al., 2007). Downregulation of Kidins220 resulted in the attenuation of NGF- induced, but not BDNF- induced MAPK signalling in neuroblastoma cells (Rogers and Schor, 2013b). In melanoma cells, Kidins220 -mediated cells migration and invasion is related to kinase (ERK) kinase (MEK)/ERK signalling (Liao et al., 2011a). Kidins220 was also involved in the angiogenesis of castration resistant prostate cancer, which is regulated by miR-4638-5p through the activity of VEGF and PI3K/AKT pathway (Wang et al., 2016). In the present study, the reduction of Kidins220 expression in Panc-1 and Mia paca-2 cells showed a promotion in ERK and AKT signalling pathway. The tyrosine phosphorylation of ERK and AKT were increased in Kidins220 knockdown cells in comparison with the scramble control. Both ERK and

AKT pathways are essential signalling pathways that mediate intracellular signal transduction for EGFR (Oliveira-Cunha et al., 2011). However, whether the enhanced activation of both ERK and AKT is dependent on the Kidins220 regulated EGFR expression and activation is yet to be elucidated.

Furthermore, our study also found that knockdown of Kidins220 was accompanied with a change of EMT in Panc-1 cancer cell lines. To date, the correlation between Kidins220 and EMT in cancers remains largely unknown. Loss of E-cadherin and increase of vimentin are considered as important markers of EMT (Prieto-Garcia et al., 2017). E-cadherin restrains the mobility of tumour cell during tumour dissemination, as it has a role in maintaining cell-cell interaction and cytoskeleton stabilisation. Therefore, the breakdown of adherens junctions caused by the down-regulation of E-cadherin expression, lead to loss of cell polarity and acquisition of a mesenchymal phenotype with migratory abilities (Wijnhoven et al., 2000, Ghahhari and Babashah, 2015). In panc-1 cancer cells, knockdown of Kidins220 decreased the expression of E-cadherin as well as increased vimentin expression. The altered expression pattern of E-cadherin and vimentin was further enhanced by EGF. When cells were treated with EGF, the expression of E-cadherin was reduced in comparison with the untreated group, whereas vimentin caused an increased expression. EMT-inducing transcription factors (EMT-TFs) not only play a role in the regulation of cell progression, invasion, and migration, but are also involved in protecting cells from senescence and apoptosis. Their role in resistance to chemotherapy and radiotherapy has been

identified (Nieto, 2011, Ansieau et al., 2008, Mejlvang et al., 2007). As TFs, snail, slug, are involved in promoting EMT (De Craene and Berx, 2013). Snail, slug and zeb are reported as direct repressors of E-cadherin since they bind to conserved E-box sequences in the promoter of E-cadherin and repress its transcription (Prieto-Garcia et al., 2017). Furthermore, loss of E-cadherin can also trigger certain epithelial cells switching to a mesenchymal state (Onder et al., 2008). In panc-1 cancer cells, knockdown of Kidins220 enhanced the expression of snail and slug. These findings indicate that Kidins220 might play a significant role in EGF/EGFR-induced EMT in pancreatic cancer cells. Further investigation will shed light on the involvement of EGFR, ERK and AKT signalling in the reduced expression of Kidins220 related EMT.

Taken together, the current study showed an increased protein expression and phosphorylation of EGFR in panc-1 Kidins220 knockdown cells which may contribute to the promotion of cell proliferation and migration, although this needs to be further investigated. Among downstream pathways of the receptor tyrosine kinase, ERK1/2 signalling pathway also exhibited increased activation. In addition to these, involvement of EMT markers may also contribute to the metastasis of pancreatic cancer in line with Kidins220. The employment of EGFR and ERK inhibitors will help to clarify the involvement of these signalling in downregulation of Kidins220 related cellular events and corresponding implication in disease progression of pancreatic cancer.

Chapter6

General Discussion

Increased evidence suggests that scaffold proteins are crucial regulators of many key signalling pathways and also engaged in maintaining the cell structure through the regulation of the cytoskeleton, adhesion and migration of the cells (Bompard et al., 2005, Lin et al., 2005, Yamagishi et al., 2004, Mattila et al., 2003). Kidins220 is a scaffold protein and was first identified as a substrate of protein Kinase D (Iglesias et al., 2000). Several studies have indicated its role in mediating neuronal activities such as neuronal differentiation, survival, and cytoskeleton remodelling by interacting with a variety of binding partners (Scholz-Starke and Cesca, 2016). Elevated expression of Kidins220 has been observed in melanoma and neuroblastoma which is associated with disease progression (Jung et al., 2014, Liao et al., 2007, Liao et al., 2011a). In contrast to the increased expression of Kidins220 in melanoma and neuroblastoma, our initial analyses of Kidins220's in pancreatic cancer showed a reduced in pancreatic carcinomas. We hypothesised that aberrant expression of Kidins220 is involved in the development and disease progression of pancreatic cancer being different from its role in the melanoma and neuroblastoma. In the current study, we evaluated the role played by Kidins220 in human pancreatic cancer by analysing its expression of both mRNA and protein in different pancreatic cancer cohorts. Following the analyses of clinical relevance, we determined the influence of Kidins220 on cellular functions of pancreatic cancer cell lines. Finally, molecular machinery was dissected according to the regulation of cellular functions.

6.1 Reduced expression in pancreatic cancer is associated with tumorigenesis and disease progression.

A significantly reduced expression of Kidins220 transcripts was revealed in pancreatic cancers compared with adjacent normal pancreatic tissues. This is supported by the findings from IHC staining of Kidins220 conducted on a pancreatic tumour tissue microarray which presented a reduced expression of kidins220 in pancreatic cancers compared with adjacent normal pancreatic tissues and normal pancreas. The analysis of Kidins220 transcript levels in the cohort of pancreatic cancer tissue samples showed more advanced pancreatic tumours (TNM3 and TNM4) had lower expression of Kidins220 compared with those of early stages (TNM1 and TNM2). Kidins220 expression was also reduced in primary tumours which developed metastases and also distant metastatic tumours of pancreatic cancer. The reduced expression of Kidins220 is also associated with poorer survival of patients with pancreatic cancer. Our following experiments showed that knockdown of Kidins220 in pancreatic cell lines resulted in an increase of cell proliferation, migration and invasion. Furthermore, Knockdown of Kidins220 also promoted peritoneal metastasis of pancreatic cancer cells in a murine peritoneal metastatic model. More interestingly, the Knockdown of Kidins220 resulted in bigger metastatic tumours in the peritoneal metastatic model leading to a remarkedly increased tumour burden but with little effect on number of nodules formed. The effect of Kidins220 Knockdown on proliferation, migration and invasion may contribute to the increased tumour size and tumour

burden in the peritoneal metastatic model, while its influence on attachment of suspending pancreatic cancer cells to the peritoneum was little though it promotes adhesion of pancreatic cancer cells to extracellular matrix. Hyaluronic acid (HA) forms a fluid film which coats on top of mesothelial cells of peritoneum. The specific binding partner to HA such as CD44 and RAHMM may play more in mediating the adhesion and initial seeding of pancreatic cancer during the peritoneal metastasis(Wang et al., 1998, Zhang et al., 1998, Maxwell et al., 2008). The exact cellular and molecular mechanism underlying the enhanced peritoneal metastases following the loss of Kidins220 are yet to elucidated. Collectively, our findings suggest that Kidins220 is an inhibitory factor in the disease progression of pancreatic cancer through a regulation of proliferation, migration and invasion of pancreatic cancer cells.

In contrast to the down-regulation of Kidins220 discovered in pancreatic cancer, an upregulation of Kidins220 was observed in melanoma cancer cells lines and human melanoma tissues. In melanoma, stronger immunointensity of Kidins220 was observed mostly in melanomas with Breslow tumour thickness >1.0mm, or with nodal metastasis, and was correlated with a worse overall survival in melanoma patients (Liao et al., 2011a). Findings of the present study have demonstrated that Kidins220 may act as tumour suppressor in pancreatic cancer in comparison with melanoma and neuroblastoma. Our study showed that the reduced Kidins220 promoted proliferation, migration and invasion of pancreatic cancer cells through an up-regulation of EGFR. This suggests

that Kidins220 plays different roles in different malignancies which can be tissue specific or cancer specific depending on signal pathway involved.

The present study has also indicated that Kidins220 might be involved in the tumorigenesis of pancreatic cancer. Our study was based on the analysis of a gene expression array data (GSE71729). The reduction of Kidins220 expression in invasive cancer originating in IPMN appeared to be significant compared with normal pancreas. Furthermore, according to the IHC staining, there was a significant decrease of Kidins220 expression in malignant tumour compared with normal pancreas, inflammation pancreas, and benign tumour. In line with the findings from the human pancreatic cancers, an enhanced tumorigenic capacity was also observed in the pancreatic cancer cells following the knockdown of Kidins220 in an *in vitro* 3D tumour spheroid experimental model. This suggests that the downregulation of Kidins220 may occur early during the tumorigenesis of pancreatic cancer. Certain molecular and biological changes have been observed in IPMN of pancreas, such as the activation of oncogenic pathways including K-ras and AKT, and downregulation of tumor suppressors such as p16, p53, and SMAD4 (Hayashi et al., 2010). However, the exact molecular and cellular events associated with the reduced expression of Kidins220 in pancreatic cancer are yet to be explored. Furthermore, the reduced expression of Kidins220 in pancreatic cancer was associated with shorter overall survival, which implicated Kidins220 as a potential biomarker for the evaluation of prognosis of pancreatic cancer.

6.2 Knockdown of Kidins220 promoted proliferation, migration and invasion of pancreatic cancer cells

To understand how the reduced expression of Kidins220 in pancreatic cancer is associated with tumorigenesis, disease progression and poor prognosis, the impact on cellular function of pancreatic cancer cells was examined in the current study. To date, 14 splicing variants have identified which encode 11 Kidins220 protein isoforms. The coding sequence for Kidins220 isoform 1 is approximately 5300bps. It is difficult to amplify the coding sequence due to mixture of different variants in the available cDNA libraries. Cost of synthesising such long sequence is unaffordable to the current study. Due to these technical difficulties and the limitations on time required to generate a Kidins220 overexpression cell model, the Kidins220 knockdown cell model was established using lentivirus shRNA. Knockdown of Kidins220 in Panc-1 and Mia paca-2 resulted in an increased proliferation of these two cancer cell lines. In neuroblastoma, knockdown of Kidins220 reduced cell proliferation because of the arrest of cell cycle at G1 phase (Jung et al., 2014). The different signalling pathways regulated by Kidins220 might be involved in the proliferation of pancreatic cancer cells.

Adhesion of cells to the ECM is key to the regulation of cellular morphology, migration, proliferation, survival, and differentiation (Nagano et al., 2012). Following the knockdown, an increase was seen in cell-matrix adhesion of the two

pancreatic cancer cell lines, which adhesion molecules are involved is yet to be determined.

Apart from the impact of Kidins220 on cell growth and adhesion, we also examined the influence of Kidins220 on cell invasion and migration, the two essential cellular functions for cancer metastasis. The results showed that knockdown of Kidins220 increased invasion and migration in pancreatic cancer cells. This is different from the findings in melanoma, in which kidins220 knockdown decreased migratory and invasive abilities of melanoma cells (Liao et al., 2011a). Migration and invasion of melanoma cell regulated by Kidins220 was through the activation of MEK/ERK signalling pathway, but its upstream regulator is still unknown. Our investigations in pancreatic cancer showed that knockdown of Kidins220 increased phosphorylation of ERK and AKT, potentially through the EGFR signalling pathway. FAM120A knockdown abolished liver colonization in a mouse model, which presented its role in liver metastasis of colorectal cancer (Bartolome et al., 2015). In the current study, knockdown of Kidins220 resulted in an increased number of nodules in an *in vivo* mouse model but this lacked statistical significance. However, there was a significant increase in tumour burden, total tumour volume and average tumour volume of the mice injected with Kidins220 knockdown Panc-1 cells compared with scramble control group. These results provide evidence that Kidins220 might be involved in peritoneal metastasis of pancreatic cancer for metastatic cells invasion and proliferation.

6.3 Loss of Kidins220 is accompanied with an enhanced EMT in pancreatic cancer

EMT is a highly conserved process that allows cells to lose epithelial features, such as loss of polarity, and down regulation of E-cadherin. During this process, the cells also gain mesenchymal phenotype, acquiring the capability of motility and invasion, and start expressing mesenchymal markers such as N-cadherin and vimentin (Yeung and Yang, 2017, Thiery et al., 2009). EMT enables cancer cells to disseminate from a primary tumour to a distant site and finally develop a secondary tumour (Thiery, 2002).

In human pancreatic tumour samples, a decreased expression of E-cadherin along with an increased expression of vimentin were detected in high-grade tumours and also poorly differentiated areas of low-grade tumours. Interestingly, the patients with better survival presented less evidence of EMT (Dangi-Garimella et al., 2012). An autopsy program performed on pancreatic cancer patients showed that 75% of the primary tumours with metastases to liver and lung presented mesenchymal features (Rasheed et al., 2010). In pancreatic cancer cells, snail, a key regulator of EMT, exhibited a higher level of expression together with a reduced expression of E-cadherin in poorly differentiated cell lines compared with their expression in moderately differentiated cell lines (Hotz et al., 2007).

Our current study indicated that knockdown of Kidins220 decreased the expression of E-cadherin and increased vimentin expression in Panc-1 cells. Knockdown of Kidins220 also increased the protein expression of snail and slug in

panc-1 cells. Further study will shed light on the Kidins220 coordinated EMT in pancreatic cancer using clinical sample, for example, the correlation between Kidins220 expression and EMT markers in pancreatic cancer particularly in EGFR positive pancreatic tumours.

6.4 Reduced Kidins220 is associated with an enhanced EGFR signalling through an upregulation of its protein expression

Overexpression of EGFR has been indicated in several studies in pancreatic cancer and may be related to disease progression and poor survival of pancreatic cancer patients (Oliveira-Cunha et al., 2011). The two major intracellular pathways activated by EGFR are the PI3K/AKT and MAPK/ERK pathways, which have been implicated in the development of pancreatic cancer and are also being evaluated as target therapies (Roy et al., 2010, Williams et al., 2012).

Knockdown of Kidins220 increased the phosphorylation of EGFR and total EGFR in pancreatic cancer cell lines, without a notable change of Kidins220 transcripts. Corresponding changes of ERK and AKT were also seen in the Kidins220 knockdown cell lines, by which knockdown of Kidins220 increased phosphorylation of ERK and AKT. After treatment with EGF, the Kidins220 knockdown cells showed enhanced activation of EGFR and ERK in comparison with the control group. The altered expression pattern of E-cadherin and vimentin was also further enhanced by the EGF treatment. The expression of E-cadherin was

reduced, whilst vimentin was increased in the EGF treated cells. However, no obvious change was found for snail expression. Involvement of EGFR/ERK and/or AKT in the Kidins220 knockdown resulted in promotion of EMT. Invasion is yet to be elucidated, for example using a small inhibitor, such as Gefitinib. On the other hand, other HER family members, such as HER2, HER3 and HER4 will be investigated for their link with EGFR signalling and involvement in malignancies (Seshacharyulu et al., 2012). Reduced expression of Kidins220 in EGFR overexpressing pancreatic cancer may act as a biomarker for the corresponding target therapy which is yet to be evaluated in human pancreatic tissue samples.

6.5 Conclusion and perspectives

In this present study, a reduced expression of Kidins220 was observed in pancreatic cancer which is associated with disease progression, distant metastases and poor prognosis. *In vitro* cellular function tests have shown that Kidins220 knockdown promotes proliferation, migration and invasion of pancreatic cancer cells. The Kidins220 knockdown Panc-1 cells also exhibited an enhanced metastatic capability in an *in vivo* peritoneal metastatic mouse model. This suggests that Kidins220 is a putative tumour suppressor in pancreatic cancer. Enhanced EMT was also observed in the pancreatic cancer cell lines following the knockdown of Kidins220. Further examination showed that the Kidins220 knockdown resulted in an elevated expression and activation of EGFR and

consequent activations of its downstream signalling pathways including ERK and AKT pathways. As a transmembrane scaffold protein, Kidins220 plays an important role in the regulation of cell signalling by recruiting external and internal stimuli to various cellular outputs. Kidins220 exhibited a regulation of EGFR and EGFR signalling in pancreatic cancer cells. These results provoke further investigation for the remaining question and gaps in knowledge. For instance, it would be interesting to discover the molecular mechanism utilised by the Kidins220 to regulate the protein level of EGFR, in which protein degradation cascades may be affected. Molecules that related to protein degradation might be examined using western blot. In term of the impact on cellular function, the involvement of EGFR and its downstream signalling should be further examined in the Kindins220 knockdown cell lines using specific inhibitor or a Kidins220 overexpression model for a validation. More importantly, the exact implication of the reduced expression of Kidins220 in EGFR positive pancreatic cancer should be elucidated with investigation of other HER family members also be included. As for its clinical relevance, the role of Kidins220 in the evaluation of prognosis of pancreatic cancer patients needs to be future investigated using a larger clinical cohort.

Bibliography

ACLOQUE, H., ADAMS, M. S., FISHWICK, K., BRONNER-FRASER, M. & NIETO, M. A. 2009. Epithelial-mesenchymal transitions: the importance of changing cell state in development and disease. *J Clin Invest,* 119**,** 1438-49.

AGUIRRE, A. J., BARDEESY, N., SINHA, M., LOPEZ, L., TUVESON, D. A., HORNER, J., REDSTON, M. S. & DEPINHO, R. A. 2003. Activated Kras and Ink4a/Arf deficiency cooperate to produce metastatic pancreatic ductal adenocarcinoma. *Genes & Development,* 17**,** 3112-3126.

ALEXANDER, J., WATANABE, T., WU, T. T., RASHID, A., LI, S. & HAMILTON, S. R. 2001. Histopathological identification of colon cancer with microsatellite instability. *Am J Pathol,* 158**,** 527-35.

AMIN, M. B., AMERICAN JOINT COMMITTEE ON CANCER. & AMERICAN CANCER SOCIETY. 2017. *AJCC cancer staging manual,* Chicago IL, American Joint Committee on Cancer, Springer.

ANDREAZZOLI, M., GESTRI, G., LANDI, E., D'ORSI, B., BARILARI, M., IERVOLINO, A., VITIELLO, M., WILSON, S. W. & DENTE, L. 2012. Kidins220/ARMS interacts with Pdzrn3, a protein containing multiple binding domains. *Biochimie,* 94**,** 2054-7.

ANSARI, D., TINGSTEDT, B., ANDERSSON, B., HOLMQUIST, F., STURESSON, C., WILLIAMSSON, C., SASOR, A., BORG, D., BAUDEN, M. & ANDERSSON, R. 2016. Pancreatic cancer: yesterday, today and tomorrow. *Future Oncol,* 12**,** 1929-46.

ANSIEAU, S., BASTID, J., DOREAU, A., MOREL, A. P., BOUCHET, B. P., THOMAS, C., FAUVET, F., PUISIEUX, I., DOGLIONI, C., PICCININ, S., MAESTRO, R., VOELTZEL, T., SELMI, A., VALSESIA-WITTMANN, S., CARON DE FROMENTEL, C. & PUISIEUX, A. 2008. Induction of EMT by twist proteins as a collateral effect of tumor-promoting inactivation of premature senescence. *Cancer Cell,* 14**,** 79-89.

ARAVIND, L., IYER, L. M., LEIPE, D. D. & KOONIN, E. V. 2004. A novel family of P-loop NTPases with an unusual phyletic distribution and transmembrane segments inserted within the NTPase domain. *Genome Biol,* 5**,** R30.

AREVALO, J. C., PEREIRA, D. B., YANO, H., TENG, K. K. & CHAO, M. V. 2006. Identification of a switch in neurotrophin signaling by selective tyrosine phosphorylation. *J Biol Chem,* 281**,** 1001-7.

AREVALO, J. C., YANO, H., TENG, K. K. & CHAO, M. V. 2004. A unique pathway for sustained neurotrophin signaling through an ankyrin-rich membrane-spanning protein. *EMBO J,* 23**,** 2358-68.

ASGHAR, U., WITKIEWICZ, A. K., TURNER, N. C. & KNUDSEN, E. S. 2015. The history and future of targeting cyclin-dependent kinases in cancer therapy. *Nat Rev Drug Discov,* 14**,** 130-46.

BADGER, S. A., BRANT, J. L., JONES, C., MCCLEMENTS, J., LOUGHREY, M. B., TAYLOR, M. A., DIAMOND, T. & MCKIE, L. D. 2010. The role of surgery for

pancreatic cancer: a 12-year review of patient outcome. *Ulster Med J,* 79**,** 70-5.

BARBER, T. D., VOGELSTEIN, B., KINZLER, K. W. & VELCULESCU, V. E. 2004. Somatic mutations of EGFR in colorectal cancers and glioblastomas. *N Engl J Med,* 351**,** 2883.

BARTLETT, J. M. & STIRLING, D. 2003. A short history of the polymerase chain reaction. *Methods Mol Biol,* 226**,** 3-6.

BARTOLOME, R. A., GARCIA-PALMERO, I., TORRES, S., LOPEZ-LUCENDO, M., BALYASNIKOVA, I. V. & CASAL, J. I. 2015. IL13 Receptor alpha2 Signaling Requires a Scaffold Protein, FAM120A, to Activate the FAK and PI3K Pathways in Colon Cancer Metastasis. *Cancer Res,* 75**,** 2434-44.

BENOIT, B. O., SAVARESE, T., JOLY, M., ENGSTROM, C. M., PANG, L., REILLY, J., RECHT, L. D., ROSS, A. H. & QUESENBERRY, P. J. 2001. Neurotrophin channeling of neural progenitor cell differentiation. *J Neurobiol,* 46**,** 265-80.

BERRINGTON DE GONZALEZ, A., SWEETLAND, S. & SPENCER, E. 2003. A meta-analysis of obesity and the risk of pancreatic cancer. *Br J Cancer,* 89**,** 519-23.

BHARDWAJ, A., SRIVASTAVA, S. K., SINGH, S., TYAGI, N., ARORA, S., CARTER, J. E., KHUSHMAN, M. & SINGH, A. P. 2016. MYB Promotes Desmoplasia in Pancreatic Cancer through Direct Transcriptional Up-regulation and Cooperative Action of Sonic Hedgehog and Adrenomedullin. *J Biol Chem,* 291**,** 16263-70.

BLOOMSTON, M., BHARDWAJ, A., ELLISON, E. C. & FRANKEL, W. L. 2006. Epidermal growth factor receptor expression in pancreatic carcinoma using tissue microarray technique. *Dig Surg,* 23**,** 74-9.

BOMPARD, G., SHARP, S. J., FREISS, G. & MACHESKY, L. M. 2005. Involvement of Rac in actin cytoskeleton rearrangements induced by MIM-B. *J Cell Sci,* 118**,** 5393-403.

BORAZANCI, E. & VON HOFF, D. D. 2014. Nab-paclitaxel and gemcitabine for the treatment of patients with metastatic pancreatic cancer. *Expert Rev Gastroenterol Hepatol,* 8**,** 739-47.

BOSETTI, C., BERTUCCIO, P., NEGRI, E., LA VECCHIA, C., ZEEGERS, M. P. & BOFFETTA, P. 2012. Pancreatic cancer: overview of descriptive epidemiology. *Mol Carcinog,* 51**,** 3-13.

BOSETTI, C., ROSATO, V., LI, D., SILVERMAN, D., PETERSEN, G. M., BRACCI, P. M., NEALE, R. E., MUSCAT, J., ANDERSON, K., GALLINGER, S., OLSON, S. H., MILLER, A. B., BAS BUENO-DE-MESQUITA, H., SCELO, G., JANOUT, V., HOLCATOVA, I., LAGIOU, P., SERRAINO, D., LUCENTEFORTE, E., FABIANOVA, E., GHADIRIAN, P., BAGHURST, P. A., ZATONSKI, W., FORETOVA, L., FONTHAM, E., BAMLET, W. R., HOLLY, E. A., NEGRI, E., HASSAN, M., PRIZMENT, A., COTTERCHIO, M., CLEARY, S., KURTZ, R. C., MAISONNEUVE, P., TRICHOPOULOS, D., POLESEL, J., DUELL, E. J., BOFFETTA, P. & LA VECCHIA, C. 2014. Diabetes, antidiabetic medications, and pancreatic cancer risk: an analysis from the International Pancreatic Cancer Case-Control Consortium. *Ann Oncol,* 25**,** 2065-72.

BOULAIZ, H., RAMOS, M. C., GRINAN-LISON, C., GARCIA-RUBINO, M. E., VICENTE, F. & MARCHAL, J. A. 2017. What's new in the diagnosis of pancreatic cancer: a patent review (2011-present). *Expert Opin Ther Pat,* 27**,** 1319-1328.

BRACALE, A., CESCA, F., NEUBRAND, V. E., NEWSOME, T. P., WAY, M. & SCHIAVO, G. 2007. Kidins220/ARMS is transported by a kinesin-1-based mechanism likely to be involved in neuronal differentiation. *Mol Biol Cell,* 18**,** 142-52.

BROSENS, L. A., HACKENG, W. M., OFFERHAUS, G. J., HRUBAN, R. H. & WOOD, L. D. 2015. Pancreatic adenocarcinoma pathology: changing "landscape". *J Gastrointest Oncol,* 6**,** 358-74.

BURGESS, A. W., CHO, H. S., EIGENBROT, C., FERGUSON, K. M., GARRETT, T. P., LEAHY, D. J., LEMMON, M. A., SLIWKOWSKI, M. X., WARD, C. W. & YOKOYAMA, S. 2003. An open-and-shut case? Recent insights into the activation of EGF/ErbB receptors. *Mol Cell,* 12**,** 541-52.

BURRIS, H. A., 3RD, MOORE, M. J., ANDERSEN, J., GREEN, M. R., ROTHENBERG, M. L., MODIANO, M. R., CRIPPS, M. C., PORTENOY, R. K., STORNIOLO, A. M., TARASSOFF, P., NELSON, R., DORR, F. A., STEPHENS, C. D. & VON HOFF, D. D. 1997. Improvements in survival and clinical benefit with gemcitabine as first-line therapy for patients with advanced pancreas cancer: a randomized trial. *J Clin Oncol,* 15**,** 2403-13.

CABRERA-POCH, N., SANCHEZ-RUILOBA, L., RODRIGUEZ-MARTINEZ, M. & IGLESIAS, T. 2004. Lipid raft disruption triggers protein kinase C and Src-dependent protein kinase D activation and Kidins220 phosphorylation in neuronal cells. *J Biol Chem,* 279**,** 28592-602.

CAI, J., GUAN, H., FANG, L., YANG, Y., ZHU, X., YUAN, J., WU, J. & LI, M. 2013. MicroRNA-374a activates Wnt/beta-catenin signaling to promote breast cancer metastasis. *J Clin Invest,* 123**,** 566-79.

CAI, S., CAI, J., JIANG, W. G. & YE, L. 2017. Kidins220 and tumour development: Insights into a complexity of cross-talk among signalling pathways (Review). *Int J Mol Med,* 40**,** 965-971.

CALLE, E. E., RODRIGUEZ, C., WALKER-THURMOND, K. & THUN, M. J. 2003. Overweight, obesity, and mortality from cancer in a prospectively studied cohort of U.S. adults. *N Engl J Med,* 348**,** 1625-38.

CANTO, M. I., GOGGINS, M., HRUBAN, R. H., PETERSEN, G. M., GIARDIELLO, F. M., YEO, C., FISHMAN, E. K., BRUNE, K., AXILBUND, J., GRIFFIN, C., ALI, S., RICHMAN, J., JAGANNATH, S., KANTSEVOY, S. V. & KALLOO, A. N. 2006. Screening for early pancreatic neoplasia in high-risk individuals: a prospective controlled study. *Clin Gastroenterol Hepatol,* 4**,** 766-81; quiz 665.

CANTO, M. I., HRUBAN, R. H., FISHMAN, E. K., KAMEL, I. R., SCHULICK, R., ZHANG, Z., TOPAZIAN, M., TAKAHASHI, N., FLETCHER, J., PETERSEN, G., KLEIN, A. P., AXILBUND, J., GRIFFIN, C., SYNGAL, S., SALTZMAN, J. R., MORTELE, K. J., LEE, J., TAMM, E., VIKRAM, R., BHOSALE, P., MARGOLIS, D., FARRELL, J., GOGGINS, M. & AMERICAN CANCER OF THE PANCREAS SCREENING, C.

2012. Frequent detection of pancreatic lesions in asymptomatic high-risk individuals. *Gastroenterology,* 142**,** 796-804; quiz e14-5.

CARRAWAY, R. E. & PLONA, A. M. 2006. Involvement of neurotensin in cancer growth: evidence, mechanisms and development of diagnostic tools. *Peptides,* 27**,** 2445-60.

CARVALHO, D., MACKAY, A., BJERKE, L., GRUNDY, R. G., LOPES, C., REIS, R. M. & JONES, C. 2014. The prognostic role of intragenic copy number breakpoints and identification of novel fusion genes in paediatric high grade glioma. *Acta Neuropathol Commun,* 2**,** 23.

CASTAGLIUOLO, I., WANG, C. C., VALENICK, L., PASHA, A., NIKULASSON, S., CARRAWAY, R. E. & POTHOULAKIS, C. 1999. Neurotensin is a proinflammatory neuropeptide in colonic inflammation. *Journal of Clinical Investigation,* 103**,** 843-849.

CESCA, F., YABE, A., SPENCER-DENE, B., ARRIGONI, A., AL-QATARI, M., HENDERSON, D., PHILLIPS, H., KOLTZENBURG, M., BENFENATI, F. & SCHIAVO, G. 2011. Kidins220/ARMS is an essential modulator of cardiovascular and nervous system development. *Cell Death Dis,* 2**,** e226.

CESCA, F., YABE, A., SPENCER-DENE, B., SCHOLZ-STARKE, J., MEDRIHAN, L., MADEN, C. H., GERHARDT, H., ORRISS, I. R., BALDELLI, P., AL-QATARI, M., KOLTZENBURG, M., ADAMS, R. H., BENFENATI, F. & SCHIAVO, G. 2012. Kidins220/ARMS mediates the integration of the neurotrophin and VEGF pathways in the vascular and nervous systems. *Cell Death Differ,* 19**,** 194-208.

CHANG, M. S., AREVALO, J. C. & CHAO, M. V. 2004. Ternary complex with Trk, p75, and an ankyrin-rich membrane spanning protein. *J Neurosci Res,* 78**,** 186-92.

CHEN, Y. W., HSIAO, P. J., WENG, C. C., KUO, K. K., KUO, T. L., WU, D. C., HUNG, W. C. & CHENG, K. H. 2014. SMAD4 loss triggers the phenotypic changes of pancreatic ductal adenocarcinoma cells. *BMC Cancer,* 14**,** 181.

CHIARAVALLI, M., RENI, M. & O'REILLY, E. M. 2017. Pancreatic ductal adenocarcinoma: State-of-the-art 2017 and new therapeutic strategies. *Cancer Treat Rev,* 60**,** 32-43.

CHU, Y. S., EDER, O., THOMAS, W. A., SIMCHA, I., PINCET, F., BEN-ZE'EV, A., PEREZ, E., THIERY, J. P. & DUFOUR, S. 2006. Prototypical type I E-cadherin and type II cadherin-7 mediate very distinct adhesiveness through their extracellular domains. *J Biol Chem,* 281**,** 2901-10.

CIARDIELLO, F. & TORTORA, G. 2008. EGFR antagonists in cancer treatment. *N Engl J Med,* 358**,** 1160-74.

COLLINS, A. & BLOOMSTON, M. 2009. Diagnosis and management of pancreatic cancer. *Minerva Gastroenterol Dietol,* 55**,** 445-54.

CONROY, T., DESSEIGNE, F., YCHOU, M., BOUCHE, O., GUIMBAUD, R., BECOUARN, Y., ADENIS, A., RAOUL, J. L., GOURGOU-BOURGADE, S., DE LA FOUCHARDIERE, C., BENNOUNA, J., BACHET, J. B., KHEMISSA-AKOUZ, F., PERE-VERGE, D., DELBALDO, C., ASSENAT, E., CHAUFFERT, B., MICHEL, P.,

MONTOTO-GRILLOT, C., DUCREUX, M., GROUPE TUMEURS DIGESTIVES OF, U. & INTERGROUP, P. 2011. FOLFIRINOX versus gemcitabine for metastatic pancreatic cancer. *N Engl J Med,* 364**,** 1817-25.

DANGI-GARIMELLA, S., KRANTZ, S. B., SHIELDS, M. A., GRIPPO, P. J. & MUNSHI, H. G. 2012. Epithelial-mesenchymal transition and pancreatic cancer progression. *In:* GRIPPO, P. J. & MUNSHI, H. G. (eds.) *Pancreatic Cancer and Tumor Microenvironment*. Trivandrum (India).

DAVIES, R. L., GROSSE, V. A., KUCHERLAPATI, R. & BOTHWELL, M. 1980. Genetic analysis of epidermal growth factor action: assignment of human epidermal growth factor receptor gene to chromosome 7. *Proc Natl Acad Sci U S A,* 77**,** 4188-92.

DE CRAENE, B. & BERX, G. 2013. Regulatory networks defining EMT during cancer initiation and progression. *Nat Rev Cancer,* 13**,** 97-110.

DEL CHIARO, M., SEGERSVARD, R., LOHR, M. & VERBEKE, C. 2014. Early detection and prevention of pancreatic cancer: is it really possible today? *World J Gastroenterol,* 20**,** 12118-31.

DESWAL, S., MEYER, A., FIALA, G. J., EISENHARDT, A. E., SCHMITT, L. C., SALEK, M., BRUMMER, T., ACUTO, O. & SCHAMEL, W. W. 2013. Kidins220/ARMS associates with B-Raf and the TCR, promoting sustained Erk signaling in T cells. *J Immunol,* 190**,** 1927-35.

DI MAGLIANO, M. P. & LOGSDON, C. D. 2013. Roles for KRAS in pancreatic tumor development and progression. *Gastroenterology,* 144**,** 1220-9.

DUELL, E. J., LUCENTEFORTE, E., OLSON, S. H., BRACCI, P. M., LI, D., RISCH, H. A., SILVERMAN, D. T., JI, B. T., GALLINGER, S., HOLLY, E. A., FONTHAM, E. H., MAISONNEUVE, P., BUENO-DE-MESQUITA, H. B., GHADIRIAN, P., KURTZ, R. C., LUDWIG, E., YU, H., LOWENFELS, A. B., SEMINARA, D., PETERSEN, G. M., LA VECCHIA, C. & BOFFETTA, P. 2012. Pancreatitis and pancreatic cancer risk: a pooled analysis in the International Pancreatic Cancer Case-Control Consortium (PanC4). *Ann Oncol,* 23**,** 2964-70.

EDGE, S. B. & COMPTON, C. C. 2010. The American Joint Committee on Cancer: the 7th edition of the AJCC cancer staging manual and the future of TNM. *Ann Surg Oncol,* 17**,** 1471-4.

ENDO, H., WATANABE, T., SUGIOKA, Y., NIIOKA, M., INAGAKI, Y. & OKAZAKI, I. 2009. Activation of two distinct MAPK pathways governs constitutive expression of matrix metalloproteinase-1 in human pancreatic cancer cell lines. *Int J Oncol,* 35**,** 1237-45.

ESER, S., SCHNIEKE, A., SCHNEIDER, G. & SAUR, D. 2014. Oncogenic KRAS signalling in pancreatic cancer. *Br J Cancer,* 111**,** 817-22.

EVERS, B. M. 2006. Neurotensin and growth of normal and neoplastic tissues. *Peptides,* 27**,** 2424-33.

EVERS, B. M., TOWNSEND, C. M., JR., UPP, J. R., ALLEN, E., HURLBUT, S. C., KIM, S. W., RAJARAMAN, S., SINGH, P., REUBI, J. C. & THOMPSON, J. C. 1991. Establishment and characterization of a human carcinoid in nude mice and effect of various agents on tumor growth. *Gastroenterology,* 101**,** 303-11.

EZZATI, M., HENLEY, S. J., LOPEZ, A. D. & THUN, M. J. 2005. Role of smoking in global and regional cancer epidemiology: current patterns and data needs. *Int J Cancer,* 116**,** 963-71.

FANG, J. Y. & RICHARDSON, B. C. 2005. The MAPK signalling pathways and colorectal cancer. *Lancet Oncol,* 6**,** 322-7.

FARROW, B. & EVERS, B. M. 2002. Inflammation and the development of pancreatic cancer. *Surg Oncol,* 10**,** 153-69.

FERLAY, J., SOERJOMATARAM, I., DIKSHIT, R., ESER, S., MATHERS, C., REBELO, M., PARKIN, D. M., FORMAN, D. & BRAY, F. 2015. Cancer incidence and mortality worldwide: sources, methods and major patterns in GLOBOCAN 2012. *Int J Cancer,* 136**,** E359-86.

FERRONE, C. R., MARCHEGIANI, G., HONG, T. S., RYAN, D. P., DESHPANDE, V., MCDONNELL, E. I., SABBATINO, F., SANTOS, D. D., ALLEN, J. N., BLASZKOWSKY, L. S., CLARK, J. W., FARIS, J. E., GOYAL, L., KWAK, E. L., MURPHY, J. E., TING, D. T., WO, J. Y., ZHU, A. X., WARSHAW, A. L., LILLEMOE, K. D. & FERNANDEZ-DEL CASTILLO, C. 2015. Radiological and surgical implications of neoadjuvant treatment with FOLFIRINOX for locally advanced and borderline resectable pancreatic cancer. *Ann Surg,* 261**,** 12-7.

FIALA, G. J., JANOWSKA, I., PRUTEK, F., HOBEIKA, E., SATAPATHY, A., SPRENGER, A., PLUM, T., SEIDL, M., DENGJEL, J., RETH, M., CESCA, F., BRUMMER, T., MINGUET, S. & SCHAMEL, W. W. 2015. Kidins220/ARMS binds to the B cell antigen receptor and regulates B cell development and activation. *J Exp Med,* 212**,** 1693-708.

FIFE, C. M., MCCARROLL, J. A. & KAVALLARIS, M. 2014. Movers and shakers: cell cytoskeleton in cancer metastasis. *Br J Pharmacol,* 171**,** 5507-23.

FJALLSKOG, M. L., LEJONKLOU, M. H., OBERG, K. E., ERIKSSON, B. K. & JANSON, E. T. 2003. Expression of molecular targets for tyrosine kinase receptor antagonists in malignant endocrine pancreatic tumors. *Clin Cancer Res,* 9**,** 1469-73.

GAN, H. K., CVRLJEVIC, A. N. & JOHNS, T. G. 2013. The epidermal growth factor receptor variant III (EGFRvIII): where wild things are altered. *FEBS J,* 280**,** 5350-70.

GHAHHARI, N. M. & BABASHAH, S. 2015. Interplay between microRNAs and WNT/beta-catenin signalling pathway regulates epithelial-mesenchymal transition in cancer. *Eur J Cancer,* 51**,** 1638-49.

GIARDIELLO, F. M., BRENSINGER, J. D., TERSMETTE, A. C., GOODMAN, S. N., PETERSEN, G. M., BOOKER, S. V., CRUZ-CORREA, M. & OFFERHAUS, J. A. 2000. Very high risk of cancer in familial Peutz-Jeghers syndrome. *Gastroenterology,* 119**,** 1447-53.

GOGGINS, M., SCHUTTE, M., LU, J., MOSKALUK, C. A., WEINSTEIN, C. L., PETERSEN, G. M., YEO, C. J., JACKSON, C. E., LYNCH, H. T., HRUBAN, R. H. & KERN, S. E. 1996. Germline BRCA2 gene mutations in patients with apparently sporadic pancreatic carcinomas. *Cancer Res,* 56**,** 5360-4.

GOMEZ-PALACIO-SCHJETNAN, A. & ESCOBAR, M. L. 2013. Neurotrophins and synaptic plasticity. *Curr Top Behav Neurosci,* 15**,** 117-36.

GOONETILLEKE, K. S. & SIRIWARDENA, A. K. 2007. Systematic review of carbohydrate antigen (CA 19-9) as a biochemical marker in the diagnosis of pancreatic cancer. *Eur J Surg Oncol,* 33**,** 266-70.

GREER, J. B. & WHITCOMB, D. C. 2007. Role of BRCA1 and BRCA2 mutations in pancreatic cancer. *Gut,* 56**,** 601-5.

GUAN, X. 2015. Cancer metastases: challenges and opportunities. *Acta Pharm Sin B,* 5**,** 402-18.

GUO, S., COLBERT, L. S., FULLER, M., ZHANG, Y. & GONZALEZ-PEREZ, R. R. 2010. Vascular endothelial growth factor receptor-2 in breast cancer. *Biochim Biophys Acta,* 1806**,** 108-21.

HALBLEIB, J. M. & NELSON, W. J. 2006. Cadherins in development: cell adhesion, sorting, and tissue morphogenesis. *Genes Dev,* 20**,** 3199-214.

HALL, B. J. & GHOSH, A. 2008. Regulation of AMPA receptor recruitment at developing synapses. *Trends Neurosci,* 31**,** 82-9.

HANAHAN, D. & WEINBERG, R. A. 2011. Hallmarks of cancer: the next generation. *Cell,* 144**,** 646-74.

HANDRA-LUCA, A., LESTY, C., HAMMEL, P., SAUVANET, A., REBOURS, V., MARTIN, A., FAGARD, R., FLEJOU, J. F., FAIVRE, S., BEDOSSA, P., RUSZNIEWSKI, P. & COUVELARD, A. 2012. Biological and Prognostic Relevance of Mitogen-Activated Protein Kinases in Pancreatic Adenocarcinoma. *Pancreas,* 41**,** 416-421.

HAYASHI, A., AISHIMA, S., MIYASAKA, Y., NAKATA, K., MORIMATSU, K., ODA, Y., NAGAI, E., ODA, Y., TANAKA, M. & TSUNEYOSHI, M. 2010. Pdcd4 expression in intraductal papillary mucinous neoplasm of the pancreas: its association with tumor progression and proliferation. *Hum Pathol,* 41**,** 1507-15.

HERBST, R. S. & SHIN, D. M. 2002. Monoclonal antibodies to target epidermal growth factor receptor-positive tumors: a new paradigm for cancer therapy. *Cancer,* 94**,** 1593-611.

HIDALGO, M. 2010. Pancreatic cancer. *N Engl J Med,* 362**,** 1605-17.

HIGUERO, A. M., SANCHEZ-RUILOBA, L., DOGLIO, L. E., PORTILLO, F., ABAD-RODRIGUEZ, J., DOTTI, C. G. & IGLESIAS, T. 2010. Kidins220/ARMS modulates the activity of microtubule-regulating proteins and controls neuronal polarity and development. *J Biol Chem,* 285**,** 1343-57.

HIRAOKA, N., YAMAZAKI-ITOH, R., INO, Y., MIZUGUCHI, Y., YAMADA, T., HIROHASHI, S. & KANAI, Y. 2011. CXCL17 and ICAM2 are associated with a potential anti-tumor immune response in early intraepithelial stages of human pancreatic carcinogenesis. *Gastroenterology,* 140**,** 310-21.

HOTZ, B., ARNDT, M., DULLAT, S., BHARGAVA, S., BUHR, H. J. & HOTZ, H. G. 2007. Epithelial to mesenchymal transition: expression of the regulators snail, slug, and twist in pancreatic cancer. *Clin Cancer Res,* 13**,** 4769-76.

HRUBAN, R. H., GOGGINS, M., PARSONS, J. & KERN, S. E. 2000. Progression model for pancreatic cancer. *Clin Cancer Res,* 6**,** 2969-72.

HRUBAN, R. H., IACOBUZIO-DONAHUE, C., WILENTZ, R. E., GOGGINS, M. & KERN, S. E. 2001. Molecular pathology of pancreatic cancer. *Cancer J,* 7**,** 251-8.

HU, M., YE, L., RUGE, F., ZHI, X., ZHANG, L. & JIANG, W. G. 2012. The clinical significance of Psoriasin for non-small cell lung cancer patients and its biological impact on lung cancer cell functions. *BMC Cancer,* 12**,** 588.

HU, Y. X., WATANABE, H., OHTSUBO, K., YAMAGUCHI, Y., HA, A., OKAI, T. & SAWABU, N. 1997. Frequent loss of p16 expression and its correlation with clinicopathological parameters in pancreatic carcinoma. *Clin Cancer Res,* 3**,** 1473-7.

HUANG, R. Y., GUILFORD, P. & THIERY, J. P. 2012. Early events in cell adhesion and polarity during epithelial-mesenchymal transition. *J Cell Sci,* 125**,** 4417-22.

HUGO, H., ACKLAND, M. L., BLICK, T., LAWRENCE, M. G., CLEMENTS, J. A., WILLIAMS, E. D. & THOMPSON, E. W. 2007. Epithelial--mesenchymal and mesenchymal--epithelial transitions in carcinoma progression. *J Cell Physiol,* 213**,** 374-83.

IGLESIAS, T., CABRERA-POCH, N., MITCHELL, M. P., NAVEN, T. J., ROZENGURT, E. & SCHIAVO, G. 2000. Identification and cloning of Kidins220, a novel neuronal substrate of protein kinase D. *J Biol Chem,* 275**,** 40048-56.

ILIC, M. & ILIC, I. 2016. Epidemiology of pancreatic cancer. *World J Gastroenterol,* 22**,** 9694-9705.

IODICE, S., GANDINI, S., MAISONNEUVE, P. & LOWENFELS, A. B. 2008. Tobacco and the risk of pancreatic cancer: a review and meta-analysis. *Langenbecks Arch Surg,* 393**,** 535-45.

IQBAL, J., RAGONE, A., LUBINSKI, J., LYNCH, H. T., MOLLER, P., GHADIRIAN, P., FOULKES, W. D., ARMEL, S., EISEN, A., NEUHAUSEN, S. L., SENTER, L., SINGER, C. F., AINSWORTH, P., KIM-SING, C., TUNG, N., FRIEDMAN, E., LLACUACHAQUI, M., PING, S., NAROD, S. A. & HEREDITARY BREAST CANCER STUDY, G. 2012. The incidence of pancreatic cancer in BRCA1 and BRCA2 mutation carriers. *Br J Cancer,* 107**,** 2005-9.

JEAN-MAIRET, R. M., LOPEZ-MENENDEZ, C., SANCHEZ-RUILOBA, L., SACRISTAN, S., RODRIGUEZ-MARTINEZ, M., RIOL-BLANCO, L., SANCHEZ-MATEOS, P., SANCHEZ-MADRID, F., RODRIGUEZ-FERNANDEZ, J. L., CAMPANERO, M. R. & IGLESIAS, T. 2011. The neuronal protein Kidins220/ARMS associates with ICAM-3 and other uropod components and regulates T-cell motility. *Eur J Immunol,* 41**,** 1035-46.

JIANG, Z., LI, C., LI, F. & WANG, X. 2013. EGFR gene copy number as a prognostic marker in colorectal cancer patients treated with cetuximab or panitumumab: a systematic review and meta analysis. *PLoS One,* 8**,** e56205.

JONCKHEERE, N., VASSEUR, R. & VAN SEUNINGEN, I. 2017. The cornerstone K-RAS mutation in pancreatic adenocarcinoma: From cell signaling network, target genes, biological processes to therapeutic targeting. *Crit Rev Oncol Hematol,* 111**,** 7-19.

JONES, S., HRUBAN, R. H., KAMIYAMA, M., BORGES, M., ZHANG, X., PARSONS, D. W., LIN, J. C., PALMISANO, E., BRUNE, K., JAFFEE, E. M., IACOBUZIO-

DONAHUE, C. A., MAITRA, A., PARMIGIANI, G., KERN, S. E., VELCULESCU, V. E., KINZLER, K. W., VOGELSTEIN, B., ESHLEMAN, J. R., GOGGINS, M. & KLEIN, A. P. 2009. Exomic sequencing identifies PALB2 as a pancreatic cancer susceptibility gene. *Science,* 324**,** 217.

JOSIFOVA, D. J., MONROE, G. R., TESSADORI, F., DE GRAAFF, E., VAN DER ZWAAG, B., MEHTA, S. G., STUDY, D. D. D., HARAKALOVA, M., DURAN, K. J., SAVELBERG, S. M., NIJMAN, I. J., JUNGBLUTH, H., HOOGENRAAD, C. C., BAKKERS, J., KNOERS, N. V., FIRTH, H. V., BEALES, P. L., VAN HAAFTEN, G. & VAN HAELST, M. M. 2016. Heterozygous KIDINS220/ARMS nonsense variants cause spastic paraplegia, intellectual disability, nystagmus, and obesity. *Hum Mol Genet,* 25**,** 2158-2167.

JUNG, H., SHIN, J. H., PARK, Y. S. & CHANG, M. S. 2014. Ankyrin repeat-rich membrane spanning (ARMS)/Kidins220 scaffold protein regulates neuroblastoma cell proliferation through p21. *Mol Cells,* 37**,** 881-7.

KALLURI, R. 2009. EMT: when epithelial cells decide to become mesenchymal-like cells. *J Clin Invest,* 119**,** 1417-9.

KALLURI, R. & NEILSON, E. G. 2003. Epithelial-mesenchymal transition and its implications for fibrosis. *J Clin Invest,* 112**,** 1776-84.

KALLURI, R. & WEINBERG, R. A. 2009. The basics of epithelial-mesenchymal transition. *J Clin Invest,* 119**,** 1420-8.

KAMATA, K., KITANO, M., OMOTO, S., KADOSAKA, K., MIYATA, T., MINAGA, K., YAMAO, K., IMAI, H. & KUDO, M. 2016. New endoscopic ultrasonography techniques for pancreaticobiliary diseases. *Ultrasonography,* 35**,** 169-79.

KASTRINOS, F., MUKHERJEE, B., TAYOB, N., WANG, F., SPARR, J., RAYMOND, V. M., BANDIPALLIAM, P., STOFFEL, E. M., GRUBER, S. B. & SYNGAL, S. 2009. Risk of pancreatic cancer in families with Lynch syndrome. *JAMA,* 302**,** 1790-5.

KHAN, M. A., AZIM, S., ZUBAIR, H., BHARDWAJ, A., PATEL, G. K., KHUSHMAN, M., SINGH, S. & SINGH, A. P. 2017. Molecular Drivers of Pancreatic Cancer Pathogenesis: Looking Inward to Move Forward. *Int J Mol Sci,* 18.

KHAN, S., ANSARULLAH, KUMAR, D., JAGGI, M. & CHAUHAN, S. C. 2013. Targeting microRNAs in pancreatic cancer: microplayers in the big game. *Cancer Res,* 73**,** 6541-7.

KIMMEY, M. B., BRONNER, M. P., BYRD, D. R. & BRENTNALL, T. A. 2002. Screening and surveillance for hereditary pancreatic cancer. *Gastrointest Endosc,* 56**,** S82-6.

KLEIN, C. A. 2008. Cancer. The metastasis cascade. *Science,* 321**,** 1785-7.

KONDO, I. & SHIMIZU, N. 1983. Mapping of the human gene for epidermal growth factor receptor (EGFR) on the p13 leads to q22 region of chromosome 7. *Cytogenet Cell Genet,* 35**,** 9-14.

KONG, H., BOULTER, J., WEBER, J. L., LAI, C. & CHAO, M. V. 2001. An evolutionarily conserved transmembrane protein that is a novel downstream target of neurotrophin and ephrin receptors. *J Neurosci,* 21**,** 176-85.

KORPAL, M., LEE, E. S., HU, G. & KANG, Y. 2008. The miR-200 family inhibits epithelial-mesenchymal transition and cancer cell migration by direct

targeting of E-cadherin transcriptional repressors ZEB1 and ZEB2. *J Biol Chem,* 283**,** 14910-4.

KORSSE, S. E., HARINCK, F., VAN LIER, M. G., BIERMANN, K., OFFERHAUS, G. J., KRAK, N., LOOMAN, C. W., VAN VEELEN, W., KUIPERS, E. J., WAGNER, A., DEKKER, E., MATHUS-VLIEGEN, E. M., FOCKENS, P., VAN LEERDAM, M. E. & BRUNO, M. J. 2013. Pancreatic cancer risk in Peutz-Jeghers syndrome patients: a large cohort study and implications for surveillance. *J Med Genet,* 50**,** 59-64.

KRANZ, T. M., GOETZ, R. R., WALSH-MESSINGER, J., GOETZ, D., ANTONIUS, D., DOLGALEV, I., HEGUY, A., SEANDEL, M., MALASPINA, D. & CHAO, M. V. 2015. Rare variants in the neurotrophin signaling pathway implicated in schizophrenia risk. *Schizophr Res,* 168**,** 421-8.

LANGER, P., KANN, P. H., FENDRICH, V., HABBE, N., SCHNEIDER, M., SINA, M., SLATER, E. P., HEVERHAGEN, J. T., GRESS, T. M., ROTHMUND, M. & BARTSCH, D. K. 2009. Five years of prospective screening of high-risk individuals from families with familial pancreatic cancer. *Gut,* 58**,** 1410-8.

LEE, J. C., VIVANCO, I., BEROUKHIM, R., HUANG, J. H., FENG, W. L., DEBIASI, R. M., YOSHIMOTO, K., KING, J. C., NGHIEMPHU, P., YUZA, Y., XU, Q., GREULICH, H., THOMAS, R. K., PAEZ, J. G., PECK, T. C., LINHART, D. J., GLATT, K. A., GETZ, G., ONOFRIO, R., ZIAUGRA, L., LEVINE, R. L., GABRIEL, S., KAWAGUCHI, T., O'NEILL, K., KHAN, H., LIAU, L. M., NELSON, S. F., RAO, P. N., MISCHEL, P., PIEPER, R. O., CLOUGHESY, T., LEAHY, D. J., SELLERS, W. R., SAWYERS, C. L., MEYERSON, M. & MELLINGHOFF, I. K. 2006. Epidermal growth factor receptor activation in glioblastoma through novel missense mutations in the extracellular domain. *PLoS Med,* 3**,** e485.

LEMMON, M. A. & SCHLESSINGER, J. 2010. Cell signaling by receptor tyrosine kinases. *Cell,* 141**,** 1117-34.

LEMOINE, N. R., HUGHES, C. M., BARTON, C. M., POULSOM, R., JEFFERY, R. E., KLOPPEL, G., HALL, P. A. & GULLICK, W. J. 1992. The epidermal growth factor receptor in human pancreatic cancer. *J Pathol,* 166**,** 7-12.

LI, D., TANG, H., HASSAN, M. M., HOLLY, E. A., BRACCI, P. M. & SILVERMAN, D. T. 2011. Diabetes and risk of pancreatic cancer: a pooled analysis of three large case-control studies. *Cancer Causes Control,* 22**,** 189-97.

LI, J., CHEN, L. A., TOWNSEND, C. M., JR. & EVERS, B. M. 2008. PKD1, PKD2, and their substrate Kidins220 regulate neurotensin secretion in the BON human endocrine cell line. *J Biol Chem,* 283**,** 2614-21.

LI, J., LIU, J., LI, P., MAO, X., LI, W., YANG, J. & LIU, P. 2014. Loss of LKB1 disrupts breast epithelial cell polarity and promotes breast cancer metastasis and invasion. *J Exp Clin Cancer Res,* 33**,** 70.

LI, J., O'CONNOR, K. L., HELLMICH, M. R., GREELEY, G. H., JR., TOWNSEND, C. M., JR. & EVERS, B. M. 2004. The role of protein kinase D in neurotensin secretion mediated by protein kinase C-alpha/-delta and Rho/Rho kinase. *J Biol Chem,* 279**,** 28466-74.

LI, N., DONG, X., YANG, C., LIU, Y. & NI, X. 2013. Expression of neuronal protein Kidins220/ARMS in the spleen and peripheral blood of mice following airway allergen challenge. *Mol Med Rep,* 8**,** 1871-5.

LIAO, Y. H., HSU, S. M. & HUANG, P. H. 2007. ARMS depletion facilitates UV irradiation induced apoptotic cell death in melanoma. *Cancer Res,* 67**,** 11547-56.

LIAO, Y. H., HSU, S. M., YANG, H. L., TSAI, M. S. & HUANG, P. H. 2011a. Upregulated ankyrin repeat-rich membrane spanning protein contributes to tumour progression in cutaneous melanoma. *Br J Cancer,* 104**,** 982-8.

LIAO, Y. H., HSU, S. M., YANG, H. L., TSAI, M. S. & HUANG, P. H. 2011b. Upregulated ankyrin repeat-rich membrane spanning protein contributes to tumour progression in cutaneous melanoma. *British Journal of Cancer,* 104**,** 982-988.

LIN, J., LIU, J., WANG, Y., ZHU, J., ZHOU, K., SMITH, N. & ZHAN, X. 2005. Differential regulation of cortactin and N-WASP-mediated actin polymerization by missing in metastasis (MIM) protein. *Oncogene,* 24**,** 2059-66.

LIPSKY, R. H. & MARINI, A. M. 2007. Brain-derived neurotrophic factor in neuronal survival and behavior-related plasticity. *Ann N Y Acad Sci,* 1122**,** 130-43.

LOPEZ-BENITO, S., LILLO, C., HERNANDEZ-HERNANDEZ, A., CHAO, M. V. & AREVALO, J. C. 2016. ARMS/Kidins220 and synembryn-B levels regulate NGF-mediated secretion. *J Cell Sci,* 129**,** 1866-77.

LOPEZ-GOMEZ, M., MORENO-RUBIO, J., SUAREZ-GARCIA, I., CEJAS, P., MADERO, R., CASADO, E., JIMENEZ, A., SERENO, M., GOMEZ-RAPOSO, C., ZAMBRANA, F., MERINO, M., FERNANDEZ-LUENGAS, D. & FELIU, J. 2015. SMAD4 and TS expression might predict the risk of recurrence after resection of colorectal liver metastases. *Clin Transl Oncol,* 17**,** 133-8.

LOPEZ-MENENDEZ, C., GAMIR-MORRALLA, A., JURADO-ARJONA, J., HIGUERO, A. M., CAMPANERO, M. R., FERRER, I., HERNANDEZ, F., AVILA, J., DIAZ-GUERRA, M. & IGLESIAS, T. 2013. Kidins220 accumulates with tau in human Alzheimer's disease and related models: modulation of its calpain-processing by GSK3beta/PP1 imbalance. *Hum Mol Genet,* 22**,** 466-82.

LOPEZ-SAEZ, J. F., DE LA TORRE, C., PINCHEIRA, J. & GIMENEZ-MARTIN, G. 1998. Cell proliferation and cancer. *Histol Histopathol,* 13**,** 1197-214.

LOWENFELS, A. B., MAISONNEUVE, P., CAVALLINI, G., AMMANN, R. W., LANKISCH, P. G., ANDERSEN, J. R., DIMAGNO, E. P., ANDREN-SANDBERG, A. & DOMELLOF, L. 1993. Pancreatitis and the risk of pancreatic cancer. International Pancreatitis Study Group. *N Engl J Med,* 328**,** 1433-7.

LOWENFELS, A. B., MAISONNEUVE, P., DIMAGNO, E. P., ELITSUR, Y., GATES, L. K., JR., PERRAULT, J. & WHITCOMB, D. C. 1997. Hereditary pancreatitis and the risk of pancreatic cancer. International Hereditary Pancreatitis Study Group. *J Natl Cancer Inst,* 89**,** 442-6.

LOWENFELS, A. B., MAISONNEUVE, P., WHITCOMB, D. C., LERCH, M. M. & DIMAGNO, E. P. 2001. Cigarette smoking as a risk factor for pancreatic cancer in patients with hereditary pancreatitis. *JAMA,* 286**,** 169-70.

LUO, S., CHEN, Y., LAI, K. O., AREVALO, J. C., FROEHNER, S. C., ADAMS, M. E., CHAO, M. V. & IP, N. Y. 2005. {alpha}-Syntrophin regulates ARMS localization at the neuromuscular junction and enhances EphA4 signaling in an ARMS-dependent manner. *J Cell Biol,* 169**,** 813-24.

MAISONNEUVE, P. & LOWENFELS, A. B. 2015. Risk factors for pancreatic cancer: a summary review of meta-analytical studies. *Int J Epidemiol,* 44**,** 186-98.

MAKOHON-MOORE, A. & IACOBUZIO-DONAHUE, C. A. 2016. Pancreatic cancer biology and genetics from an evolutionary perspective. *Nat Rev Cancer,* 16**,** 553-65.

MARTIN-BELMONTE, F., GASSAMA, A., DATTA, A., YU, W., RESCHER, U., GERKE, V. & MOSTOV, K. 2007. PTEN-mediated apical segregation of phosphoinositides controls epithelial morphogenesis through Cdc42. *Cell,* 128**,** 383-97.

MARTIN, T. A. & JIANG, W. G. 2009. Loss of tight junction barrier function and its role in cancer metastasis. *Biochim Biophys Acta,* 1788**,** 872-91.

MASSAGUE, J. 2012. TGFbeta signalling in context. *Nat Rev Mol Cell Biol,* 13**,** 616-30.

MATTILA, P. K., SALMINEN, M., YAMASHIRO, T. & LAPPALAINEN, P. 2003. Mouse MIM, a tissue-specific regulator of cytoskeletal dynamics, interacts with ATP-actin monomers through its C-terminal WH2 domain. *J Biol Chem,* 278**,** 8452-9.

MAXWELL, C. A., MCCARTHY, J. & TURLEY, E. 2008. Cell-surface and mitotic-spindle RHAMM: moonlighting or dual oncogenic functions? *J Cell Sci,* 121**,** 925-32.

MCCAFFREY, L. M., MONTALBANO, J., MIHAI, C. & MACARA, I. G. 2012. Loss of the Par3 polarity protein promotes breast tumorigenesis and metastasis. *Cancer Cell,* 22**,** 601-14.

MCWILLIAMS, R. R., RABE, K. G., OLSWOLD, C., DE ANDRADE, M. & PETERSEN, G. M. 2005. Risk of malignancy in first-degree relatives of patients with pancreatic carcinoma. *Cancer,* 104**,** 388-94.

MEJLVANG, J., KRIAJEVSKA, M., VANDEWALLE, C., CHERNOVA, T., SAYAN, A. E., BERX, G., MELLON, J. K. & TULCHINSKY, E. 2007. Direct repression of cyclin D1 by SIP1 attenuates cell cycle progression in cells undergoing an epithelial mesenchymal transition. *Mol Biol Cell,* 18**,** 4615-24.

MENDELSOHN, J. & BASELGA, J. 2003. Status of epidermal growth factor receptor antagonists in the biology and treatment of cancer. *Journal of Clinical Oncology,* 21**,** 2787-2799.

MENYHART, O., HARAMI-PAPP, H., SUKUMAR, S., SCHAFER, R., MAGNANI, L., DE BARRIOS, O. & GYORFFY, B. 2016. Guidelines for the selection of functional assays to evaluate the hallmarks of cancer. *Biochim Biophys Acta,* 1866**,** 300-319.

MERO, I. L., MORK, H. H., SHENG, Y., BLOMHOFF, A., OPHEIM, G. L., ERICHSEN, A., VIGELAND, M. D. & SELMER, K. K. 2017. Homozygous KIDINS220 loss-of-function variants in fetuses with cerebral ventriculomegaly and limb contractures. *Hum Mol Genet,* 26**,** 3792-3796.

MERRICK, D. T., KITTELSON, J., WINTERHALDER, R., KOTANTOULAS, G., INGEBERG, S., KEITH, R. L., KENNEDY, T. C., MILLER, Y. E., FRANKLIN, W. A. & HIRSCH, F. R. 2006. Analysis of c-ErbB1/epidermal growth factor receptor and c-ErbB2/HER-2 expression in bronchial dysplasia: evaluation of potential targets for chemoprevention of lung cancer. *Clin Cancer Res,* 12**,** 2281-8.

MICHALSKI, C. W., WEITZ, J. & BUCHLER, M. W. 2007. Surgery insight: surgical management of pancreatic cancer. *Nat Clin Pract Oncol,* 4**,** 526-35.

MIDHA, S., CHAWLA, S. & GARG, P. K. 2016. Modifiable and non-modifiable risk factors for pancreatic cancer: A review. *Cancer Lett,* 381**,** 269-77.

MIRZOEVA, O. K., DAS, D., HEISER, L. M., BHATTACHARYA, S., SIWAK, D., GENDELMAN, R., BAYANI, N., WANG, N. J., NEVE, R. M., GUAN, Y., HU, Z., KNIGHT, Z., FEILER, H. S., GASCARD, P., PARVIN, B., SPELLMAN, P. T., SHOKAT, K. M., WYROBEK, A. J., BISSELL, M. J., MCCORMICK, F., KUO, W. L., MILLS, G. B., GRAY, J. W. & KORN, W. M. 2009. Basal subtype and MAPK/ERK kinase (MEK)-phosphoinositide 3-kinase feedback signaling determine susceptibility of breast cancer cells to MEK inhibition. *Cancer Res,* 69**,** 565-72.

MITRA, A., MISHRA, L. & LI, S. 2015. EMT, CTCs and CSCs in tumor relapse and drug-resistance. *Oncotarget,* 6**,** 10697-711.

MODJTAHEDI, H. & ESSAPEN, S. 2009. Epidermal growth factor receptor inhibitors in cancer treatment: advances, challenges and opportunities. *Anticancer Drugs,* 20**,** 851-5.

MOORE, M. J., GOLDSTEIN, D., HAMM, J., FIGER, A., HECHT, J. R., GALLINGER, S., AU, H. J., MURAWA, P., WALDE, D., WOLFF, R. A., CAMPOS, D., LIM, R., DING, K., CLARK, G., VOSKOGLOU-NOMIKOS, T., PTASYNSKI, M., PARULEKAR, W. & NATIONAL CANCER INSTITUTE OF CANADA CLINICAL TRIALS, G. 2007. Erlotinib plus gemcitabine compared with gemcitabine alone in patients with advanced pancreatic cancer: a phase III trial of the National Cancer Institute of Canada Clinical Trials Group. *J Clin Oncol,* 25**,** 1960-6.

MORONI, M., SARTORE-BIANCHI, A., BENVENUTI, S., ARTALE, S., BARDELLI, A. & SIENA, S. 2005. Somatic mutation of EGFR catalytic domain and treatment with gefitinib in colorectal cancer. *Ann Oncol,* 16**,** 1848-9.

MORTON, J. P., TIMPSON, P., KARIM, S. A., RIDGWAY, R. A., ATHINEOS, D., DOYLE, B., JAMIESON, N. B., OIEN, K. A., LOWY, A. M., BRUNTON, V. G., FRAME, M. C., EVANS, T. R. & SANSOM, O. J. 2010. Mutant p53 drives metastasis and overcomes growth arrest/senescence in pancreatic cancer. *Proc Natl Acad Sci U S A,* 107**,** 246-51.

NAGANO, M., HOSHINO, D., KOSHIKAWA, N., AKIZAWA, T. & SEIKI, M. 2012. Turnover of focal adhesions and cancer cell migration. *Int J Cell Biol,* 2012**,** 310616.

NATH, S. & DEVI, G. R. 2016. Three-dimensional culture systems in cancer research: Focus on tumor spheroid model. *Pharmacol Ther,* 163**,** 94-108.

NEUBRAND, V. E., CESCA, F., BENFENATI, F. & SCHIAVO, G. 2012. Kidins220/ARMS as a functional mediator of multiple receptor signalling pathways. *J Cell Sci,* 125**,** 1845-54.

NEUBRAND, V. E., THOMAS, C., SCHMIDT, S., DEBANT, A. & SCHIAVO, G. 2010. Kidins220/ARMS regulates Rac1-dependent neurite outgrowth by direct interaction with the RhoGEF Trio. *J Cell Sci,* 123**,** 2111-23.

NEUZILLET, C., HAMMEL, P., TIJERAS-RABALLAND, A., COUVELARD, A. & RAYMOND, E. 2013. Targeting the Ras-ERK pathway in pancreatic adenocarcinoma. *Cancer Metastasis Rev,* 32**,** 147-62.

NI, X., LI, X., FANG, X., LI, N., CUI, W. & ZHANG, B. 2010. NGF/TrkA-mediated Kidins220/ARMS signaling activated in the allergic airway challenge in mice. *Ann Allergy Asthma Immunol,* 105**,** 299-306.

NIETO, M. A. 2011. The ins and outs of the epithelial to mesenchymal transition in health and disease. *Annu Rev Cell Dev Biol,* 27**,** 347-76.

NORMANNO, N., DE LUCA, A., BIANCO, C., STRIZZI, L., MANCINO, M., MAIELLO, M. R., CAROTENUTO, A., DE FEO, G., CAPONIGRO, F. & SALOMON, D. S. 2006. Epidermal growth factor receptor (EGFR) signaling in cancer. *Gene,* 366**,** 2-16.

OCANA, O. H., CORCOLES, R., FABRA, A., MORENO-BUENO, G., ACLOQUE, H., VEGA, S., BARRALLO-GIMENO, A., CANO, A. & NIETO, M. A. 2012. Metastatic colonization requires the repression of the epithelial-mesenchymal transition inducer Prrx1. *Cancer Cell,* 22**,** 709-24.

OHTSUBO, K., WATANABE, H., YAMAGUCHI, Y., HU, Y. X., MOTOO, Y., OKAI, T. & SAWABU, N. 2003. Abnormalities of tumor suppressor gene p16 in pancreatic carcinoma: immunohistochemical and genetic findings compared with clinicopathological parameters. *J Gastroenterol,* 38**,** 663-71.

OLIVEIRA-CUNHA, M., NEWMAN, W. G. & SIRIWARDENA, A. K. 2011. Epidermal growth factor receptor in pancreatic cancer. *Cancers (Basel),* 3**,** 1513-26.

ONDER, T. T., GUPTA, P. B., MANI, S. A., YANG, J., LANDER, E. S. & WEINBERG, R. A. 2008. Loss of E-cadherin promotes metastasis via multiple downstream transcriptional pathways. *Cancer Res,* 68**,** 3645-54.

PARIKH, A., LEE, C., JOSEPH, P., MARCHINI, S., BACCARINI, A., KOLEV, V., ROMUALDI, C., FRUSCIO, R., SHAH, H., WANG, F., MULLOKANDOV, G., FISHMAN, D., D'INCALCI, M., RAHAMAN, J., KALIR, T., REDLINE, R. W., BROWN, B. D., NARLA, G. & DIFEO, A. 2014. microRNA-181a has a critical role in ovarian cancer progression through the regulation of the epithelial-mesenchymal transition. *Nat Commun,* 5**,** 2977.

PARK, H. J., PARK, H. W., LEE, S. J., AREVALO, J. C., PARK, Y. S., LEE, S. P., PAIK, K. S., CHAO, M. V. & CHANG, M. S. 2010. Ankyrin repeat-rich membrane spanning/Kidins220 protein interacts with mammalian Septin 5. *Mol Cells,* 30**,** 143-8.

PARKIN, D. M., BOYD, L. & WALKER, L. C. 2011. 16. The fraction of cancer attributable to lifestyle and environmental factors in the UK in 2010. *Br J Cancer,* 105 Suppl 2**,** S77-81.

PEREIRA, S. 2012. Photodynamic therapy for pancreatic and biliary tract cancer: the United Kingdom experience. *J Natl Compr Canc Netw,* 10 Suppl 2**,** S48-51.

PINES, G., KOSTLER, W. J. & YARDEN, Y. 2010. Oncogenic mutant forms of EGFR: lessons in signal transduction and targets for cancer therapy. *FEBS Lett,* 584**,** 2699-706.

POLEY, J. W., KLUIJT, I., GOUMA, D. J., HARINCK, F., WAGNER, A., AALFS, C., VAN EIJCK, C. H., CATS, A., KUIPERS, E. J., NIO, Y., FOCKENS, P. & BRUNO, M. J. 2009. The yield of first-time endoscopic ultrasonography in screening individuals at a high risk of developing pancreatic cancer. *Am J Gastroenterol,* 104**,** 2175-81.

POPOVIC HADZIJA, M., KOROLIJA, M., JAKIC RAZUMOVIC, J., PAVKOVIC, P., HADZIJA, M. & KAPITANOVIC, S. 2007. K-ras and Dpc4 mutations in chronic pancreatitis: case series. *Croat Med J,* 48**,** 218-24.

PORUK, K. E., FIRPO, M. A., ADLER, D. G. & MULVIHILL, S. J. 2013. Screening for pancreatic cancer: why, how, and who? *Ann Surg,* 257**,** 17-26.

PRIETO-GARCIA, E., DIAZ-GARCIA, C. V., GARCIA-RUIZ, I. & AGULLO-ORTUNO, M. T. 2017. Epithelial-to-mesenchymal transition in tumor progression. *Med Oncol,* 34**,** 122.

PYLAYEVA-GUPTA, Y., GRABOCKA, E. & BAR-SAGI, D. 2011. RAS oncogenes: weaving a tumorigenic web. *Nat Rev Cancer,* 11**,** 761-74.

RADISKY, D. C. & LABARGE, M. A. 2008. Epithelial-mesenchymal transition and the stem cell phenotype. *Cell Stem Cell,* 2**,** 511-2.

RAHIB, L., SMITH, B. D., AIZENBERG, R., ROSENZWEIG, A. B., FLESHMAN, J. M. & MATRISIAN, L. M. 2014. Projecting cancer incidence and deaths to 2030: the unexpected burden of thyroid, liver, and pancreas cancers in the United States. *Cancer Res,* 74**,** 2913-21.

RASHEED, Z. A., YANG, J., WANG, Q., KOWALSKI, J., FREED, I., MURTER, C., HONG, S. M., KOORSTRA, J. B., RAJESHKUMAR, N. V., HE, X., GOGGINS, M., IACOBUZIO-DONAHUE, C., BERMAN, D. M., LAHERU, D., JIMENO, A., HIDALGO, M., MAITRA, A. & MATSUI, W. 2010. Prognostic significance of tumorigenic cells with mesenchymal features in pancreatic adenocarcinoma. *J Natl Cancer Inst,* 102**,** 340-51.

REDSTON, M. S., CALDAS, C., SEYMOUR, A. B., HRUBAN, R. H., DA COSTA, L., YEO, C. J. & KERN, S. E. 1994. p53 mutations in pancreatic carcinoma and evidence of common involvement of homocopolymer tracts in DNA microdeletions. *Cancer Res,* 54**,** 3025-33.

RENI, M., CORDIO, S., MILANDRI, C., PASSONI, P., BONETTO, E., OLIANI, C., LUPPI, G., NICOLETTI, R., GALLI, L., BORDONARO, R., PASSARDI, A., ZERBI, A., BALZANO, G., ALDRIGHETTI, L., STAUDACHER, C., VILLA, E. & DI CARLO, V. 2005. Gemcitabine versus cisplatin, epirubicin, fluorouracil, and gemcitabine in advanced pancreatic cancer: a randomised controlled multicentre phase III trial. *Lancet Oncol,* 6**,** 369-76.

RIOL-BLANCO, L., IGLESIAS, T., SANCHEZ-SANCHEZ, N., DE LA ROSA, G., SANCHEZ-RUILOBA, L., CABRERA-POCH, N., TORRES, A., LONGO, I.,

GARCIA-BORDAS, J., LONGO, N., TEJEDOR, A., SANCHEZ-MATEOS, P. & RODRIGUEZ-FERNANDEZ, J. L. 2004. The neuronal protein Kidins220 localizes in a raft compartment at the leading edge of motile immature dendritic cells. *Eur J Immunol,* 34**,** 108-18.

ROGERS, D. A. & SCHOR, N. F. 2013a. Kidins220/ARMS depletion is associated with the neural-to Schwann-like transition in a human neuroblastoma cell line model. *Exp Cell Res,* 319**,** 660-9.

ROGERS, D. A. & SCHOR, N. F. 2013b. Kidins220/ARMS is expressed in neuroblastoma tumors and stabilizes neurotrophic signaling in a human neuroblastoma cell line. *Pediatr Res,* 74**,** 517-24.

ROSATO, V., POLESEL, J., BOSETTI, C., SERRAINO, D., NEGRI, E. & LA VECCHIA, C. 2015. Population attributable risk for pancreatic cancer in Northern Italy. *Pancreas,* 44**,** 216-20.

ROSKOSKI, R., JR. 2014. The ErbB/HER family of protein-tyrosine kinases and cancer. *Pharmacol Res,* 79**,** 34-74.

ROY, S. K., SRIVASTAVA, R. K. & SHANKAR, S. 2010. Inhibition of PI3K/AKT and MAPK/ERK pathways causes activation of FOXO transcription factor, leading to cell cycle arrest and apoptosis in pancreatic cancer. *J Mol Signal,* 5**,** 10.

ROZENBLUM, E., SCHUTTE, M., GOGGINS, M., HAHN, S. A., PANZER, S., ZAHURAK, M., GOODMAN, S. N., SOHN, T. A., HRUBAN, R. H., YEO, C. J. & KERN, S. E. 1997. Tumor-suppressive pathways in pancreatic carcinoma. *Cancer Res,* 57**,** 1731-4.

RUSTGI, A. K. 2007. The genetics of hereditary colon cancer. *Genes Dev,* 21**,** 2525-38.

RUSTGI, A. K. 2014. Familial pancreatic cancer: genetic advances. *Genes Dev,* 28**,** 1-7.

RYAN, D. P., HONG, T. S. & BARDEESY, N. 2014. Pancreatic adenocarcinoma. *N Engl J Med,* 371**,** 2140-1.

SAKAMOTO, K., IMAMURA, T., KANAYAMA, T., YANO, M., ASAI, D., DEGUCHI, T., HASHII, Y., TANIZAWA, A., OHSHIMA, Y., KIYOKAWA, N., HORIBE, K. & SATO, A. 2016. Ph-like acute lymphoblastic leukemia with a novel PAX5-KIDINS220 fusion transcript. *Genes Chromosomes Cancer*.

SAKAMOTO, K., IMAMURA, T., KANAYAMA, T., YANO, M., ASAI, D., DEGUCHI, T., HASHII, Y., TANIZAWA, A., OHSHIMA, Y., KIYOKAWA, N., HORIBE, K. & SATO, A. 2017. Ph-like acute lymphoblastic leukemia with a novel PAX5-KIDINS220 fusion transcript. *Genes Chromosomes Cancer,* 56**,** 278-284.

SATO, N., ROSTY, C., JANSEN, M., FUKUSHIMA, N., UEKI, T., YEO, C. J., CAMERON, J. L., IACOBUZIO-DONAHUE, C. A., HRUBAN, R. H. & GOGGINS, M. 2001. STK11/LKB1 Peutz-Jeghers gene inactivation in intraductal papillary-mucinous neoplasms of the pancreas. *Am J Pathol,* 159**,** 2017-22.

SCAINI, M. C., ROSSI, E., DE SIQUEIRA TORRES, P. L., ZULLATO, D., CALLEGARO, M., CASELLA, C., QUAGGIO, M., AGATA, S., MALACRIDA, S., CHIARION-SILENI, V., VECCHIATO, A., ALAIBAC, M., MONTAGNA, M., MANN, G. J., MENIN, C.

& D'ANDREA, E. 2009. Functional impairment of p16(INK4A) due to CDKN2A p.Gly23Asp missense mutation. *Mutat Res,* 671**,** 26-32.

SCHENK, M., SCHWARTZ, A. G., O'NEAL, E., KINNARD, M., GREENSON, J. K., FRYZEK, J. P., YING, G. S. & GARABRANT, D. H. 2001. Familial risk of pancreatic cancer. *J Natl Cancer Inst,* 93**,** 640-4.

SCHOLZ-STARKE, J. & CESCA, F. 2016. Stepping Out of the Shade: Control of Neuronal Activity by the Scaffold Protein Kidins220/ARMS. *Front Cell Neurosci,* 10**,** 68.

SESHACHARYULU, P., PONNUSAMY, M. P., HARIDAS, D., JAIN, M., GANTI, A. K. & BATRA, S. K. 2012. Targeting the EGFR signaling pathway in cancer therapy. *Expert Opin Ther Targets,* 16**,** 15-31.

SHARMA, S. V., BELL, D. W., SETTLEMAN, J. & HABER, D. A. 2007. Epidermal growth factor receptor mutations in lung cancer. *Nat Rev Cancer,* 7**,** 169-81.

SINGH, A. & SETTLEMAN, J. 2010. EMT, cancer stem cells and drug resistance: an emerging axis of evil in the war on cancer. *Oncogene,* 29**,** 4741-51.

SINGH, V. B., WOOTEN, A. K., JACKSON, J. W., MAGGIRWAR, S. B. & KIEBALA, M. 2015. Investigating the role of ankyrin-rich membrane spanning protein in human immunodeficiency virus type-1 Tat-induced microglia activation. *J Neurovirol,* 21**,** 186-98.

SNIDERHAN, L. F., STOUT, A., LU, Y., CHAO, M. V. & MAGGIRWAR, S. B. 2008. Ankyrin-rich membrane spanning protein plays a critical role in nuclear factor-kappa B signaling. *Mol Cell Neurosci,* 38**,** 404-16.

SOBIN, L. H. & FLEMING, I. D. 1997. TNM Classification of Malignant Tumors, fifth edition (1997). Union Internationale Contre le Cancer and the American Joint Committee on Cancer. *Cancer,* 80**,** 1803-4.

STEEG, P. S. 2016. Targeting metastasis. *Nat Rev Cancer,* 16**,** 201-18.

SUTACHAN, J. J., CHAO, M. V. & NINAN, I. 2010. Regulation of inhibitory neurotransmission by the scaffolding protein ankyrin repeat-rich membrane spanning/kinase D-interacting substrate of 220 kDa. *J Neurosci Res,* 88**,** 3447-56.

THIERY, J. P. 2002. Epithelial-mesenchymal transitions in tumour progression. *Nat Rev Cancer,* 2**,** 442-54.

THIERY, J. P., ACLOQUE, H., HUANG, R. Y. & NIETO, M. A. 2009. Epithelial-mesenchymal transitions in development and disease. *Cell,* 139**,** 871-90.

THOMPSON, D., EASTON, D. F. & BREAST CANCER LINKAGE, C. 2002. Cancer Incidence in BRCA1 mutation carriers. *J Natl Cancer Inst,* 94**,** 1358-65.

TOBITA, K., KIJIMA, H., DOWAKI, S., KASHIWAGI, H., OHTANI, Y., OIDA, Y., YAMAZAKI, H., NAKAMURA, M., UEYAMA, Y., TANAKA, M., INOKUCHI, S. & MAKUUCHI, H. 2003. Epidermal growth factor receptor expression in human pancreatic cancer: Significance for liver metastasis. *Int J Mol Med,* 11**,** 305-9.

TRACEY A. MARTIN, L. Y., ANDREW J. SANDERS, JANE LANE, AND WEN G. JIANG 2013. Cancer Invasion and Metastasis: Molecular and Cellular Perspective. *In:* JANDIAL, R. (ed.) *Metastatic Cancer: Clinical and Biological Perspectives.* Landes Bioscience.

TRAN, K. T., SMEENK, H. G., VAN EIJCK, C. H., KAZEMIER, G., HOP, W. C., GREVE, J. W., TERPSTRA, O. T., ZIJLSTRA, J. A., KLINKERT, P. & JEEKEL, H. 2004. Pylorus preserving pancreaticoduodenectomy versus standard Whipple procedure: a prospective, randomized, multicenter analysis of 170 patients with pancreatic and periampullary tumors. *Ann Surg,* 240**,** 738-45.

TSAI, J. H., DONAHER, J. L., MURPHY, D. A., CHAU, S. & YANG, J. 2012. Spatiotemporal regulation of epithelial-mesenchymal transition is essential for squamous cell carcinoma metastasis. *Cancer Cell,* 22**,** 725-36.

ULLRICH, A., COUSSENS, L., HAYFLICK, J. S., DULL, T. J., GRAY, A., TAM, A. W., LEE, J., YARDEN, Y., LIBERMANN, T. A., SCHLESSINGER, J. & ET AL. 1984. Human epidermal growth factor receptor cDNA sequence and aberrant expression of the amplified gene in A431 epidermoid carcinoma cells. *Nature,* 309**,** 418-25.

URAYAMA, S. 2015. Pancreatic cancer early detection: expanding higher-risk group with clinical and metabolomics parameters. *World J Gastroenterol,* 21**,** 1707-17.

VISHNU, P. & ROY, V. 2011. Safety and Efficacy of nab-Paclitaxel in the Treatment of Patients with Breast Cancer. *Breast Cancer (Auckl),* 5**,** 53-65.

VRIELING, A., BUENO-DE-MESQUITA, H. B., BOSHUIZEN, H. C., MICHAUD, D. S., SEVERINSEN, M. T., OVERVAD, K., OLSEN, A., TJONNELAND, A., CLAVEL-CHAPELON, F., BOUTRON-RUAULT, M. C., KAAKS, R., ROHRMANN, S., BOEING, H., NOTHLINGS, U., TRICHOPOULOU, A., MOUTSIOU, E., DILIS, V., PALLI, D., KROGH, V., PANICO, S., TUMINO, R., VINEIS, P., VAN GILS, C. H., PEETERS, P. H., LUND, E., GRAM, I. T., RODRIGUEZ, L., AGUDO, A., LARRANAGA, N., SANCHEZ, M. J., NAVARRO, C., BARRICARTE, A., MANJER, J., LINDKVIST, B., SUND, M., YE, W., BINGHAM, S., KHAW, K. T., RODDAM, A., KEY, T., BOFFETTA, P., DUELL, E. J., JENAB, M., GALLO, V. & RIBOLI, E. 2010. Cigarette smoking, environmental tobacco smoke exposure and pancreatic cancer risk in the European Prospective Investigation into Cancer and Nutrition. *Int J Cancer,* 126**,** 2394-403.

WANG, C., THOR, A. D., MOORE, D. H., 2ND, ZHAO, Y., KERSCHMANN, R., STERN, R., WATSON, P. H. & TURLEY, E. A. 1998. The overexpression of RHAMM, a hyaluronan-binding protein that regulates ras signaling, correlates with overexpression of mitogen-activated protein kinase and is a significant parameter in breast cancer progression. *Clin Cancer Res,* 4**,** 567-76.

WANG, Y., SHAO, N., MAO, X., ZHU, M., FAN, W., SHEN, Z., XIAO, R., WANG, C., BAO, W., XU, X., YANG, C., DONG, J., YU, D., WU, Y., ZHU, C., WEN, L., LU, X., LU, Y. J. & FENG, N. 2016. MiR-4638-5p inhibits castration resistance of prostate cancer through repressing Kidins220 expression and PI3K/AKT pathway activity. *Oncotarget,* 7**,** 47444-47464.

WEISSMUELLER, S., MANCHADO, E., SABOROWSKI, M., MORRIS, J. P. T., WAGENBLAST, E., DAVIS, C. A., MOON, S. H., PFISTER, N. T., TSCHAHARGANEH, D. F., KITZING, T., AUST, D., MARKERT, E. K., WU, J., GRIMMOND, S. M., PILARSKY, C., PRIVES, C., BIANKIN, A. V. & LOWE, S. W.

2014. Mutant p53 drives pancreatic cancer metastasis through cell-autonomous PDGF receptor beta signaling. *Cell,* 157**,** 382-394.

WEISWALD, L. B., BELLET, D. & DANGLES-MARIE, V. 2015. Spherical cancer models in tumor biology. *Neoplasia,* 17**,** 1-15.

WHATCOTT, C. J., DIEP, C. H., JIANG, P., WATANABE, A., LOBELLO, J., SIMA, C., HOSTETTER, G., SHEPARD, H. M., VON HOFF, D. D. & HAN, H. 2015. Desmoplasia in Primary Tumors and Metastatic Lesions of Pancreatic Cancer. *Clin Cancer Res,* 21**,** 3561-8.

WHITCOMB, D. C., APPLEBAUM, S. & MARTIN, S. P. 1999. Hereditary pancreatitis and pancreatic carcinoma. *Ann N Y Acad Sci,* 880**,** 201-9.

WIJNHOVEN, B. P., DINJENS, W. N. & PIGNATELLI, M. 2000. E-cadherin-catenin cell-cell adhesion complex and human cancer. *Br J Surg,* 87**,** 992-1005.

WILENTZ, R. E., GOGGINS, M., REDSTON, M., MARCUS, V. A., ADSAY, N. V., SOHN, T. A., KADKOL, S. S., YEO, C. J., CHOTI, M., ZAHURAK, M., JOHNSON, K., TASCILAR, M., OFFERHAUS, G. J., HRUBAN, R. H. & KERN, S. E. 2000. Genetic, immunohistochemical, and clinical features of medullary carcinoma of the pancreas: A newly described and characterized entity. *Am J Pathol,* 156**,** 1641-51.

WILLIAMS, T. M., FLECHA, A. R., KELLER, P., RAM, A., KARNAK, D., GALBAN, S., GALBAN, C. J., ROSS, B. D., LAWRENCE, T. S., REHEMTULLA, A. & SEBOLT-LEOPOLD, J. 2012. Cotargeting MAPK and PI3K signaling with concurrent radiotherapy as a strategy for the treatment of pancreatic cancer. *Mol Cancer Ther,* 11**,** 1193-202.

WOLFGANG, C. L., HERMAN, J. M., LAHERU, D. A., KLEIN, A. P., ERDEK, M. A., FISHMAN, E. K. & HRUBAN, R. H. 2013. Recent progress in pancreatic cancer. *CA Cancer J Clin,* 63**,** 318-48.

WU, S. H., AREVALO, J. C., NEUBRAND, V. E., ZHANG, H., ARANCIO, O. & CHAO, M. V. 2010. The ankyrin repeat-rich membrane spanning (ARMS)/Kidins220 scaffold protein is regulated by activity-dependent calpain proteolysis and modulates synaptic plasticity. *J Biol Chem,* 285**,** 40472-8.

XIANG, J. F., WANG, W. Q., LIU, L., XU, H. X., WU, C. T., YANG, J. X., QI, Z. H., WANG, Y. Q., XU, J., LIU, C., LONG, J., NI, Q. X., LI, M. & YU, X. J. 2016. Mutant p53 determines pancreatic cancer poor prognosis to pancreatectomy through upregulation of cavin-1 in patients with preoperative serum CA19-9 >/= 1,000 U/mL. *Sci Rep,* 6**,** 19222.

YACHIDA, S., JONES, S., BOZIC, I., ANTAL, T., LEARY, R., FU, B., KAMIYAMA, M., HRUBAN, R. H., ESHLEMAN, J. R., NOWAK, M. A., VELCULESCU, V. E., KINZLER, K. W., VOGELSTEIN, B. & IACOBUZIO-DONAHUE, C. A. 2010. Distant metastasis occurs late during the genetic evolution of pancreatic cancer. *Nature,* 467**,** 1114-7.

YAMAGISHI, A., MASUDA, M., OHKI, T., ONISHI, H. & MOCHIZUKI, N. 2004. A novel actin bundling/filopodium-forming domain conserved in insulin receptor tyrosine kinase substrate p53 and missing in metastasis protein. *J Biol Chem,* 279**,** 14929-36.

YAMAGUCHI, H., WYCKOFF, J. & CONDEELIS, J. 2005. Cell migration in tumors. *Curr Opin Cell Biol,* 17**,** 559-64.

YAMAOKA, T., OHBA, M. & OHMORI, T. 2017. Molecular-Targeted Therapies for Epidermal Growth Factor Receptor and Its Resistance Mechanisms. *Int J Mol Sci,* 18.

YAO, D., DAI, C. & PENG, S. 2011. Mechanism of the mesenchymal-epithelial transition and its relationship with metastatic tumor formation. *Mol Cancer Res,* 9**,** 1608-20.

YARDEN, Y. & PINES, G. 2012. The ERBB network: at last, cancer therapy meets systems biology. *Nat Rev Cancer,* 12**,** 553-63.

YARDEN, Y. & SLIWKOWSKI, M. X. 2001. Untangling the ErbB signalling network. *Nat Rev Mol Cell Biol,* 2**,** 127-37.

YEAMAN, C., AYALA, M. I., WRIGHT, J. R., BARD, F., BOSSARD, C., ANG, A., MAEDA, Y., SEUFFERLEIN, T., MELLMAN, I., NELSON, W. J. & MALHOTRA, V. 2004. Protein kinase D regulates basolateral membrane protein exit from trans-Golgi network. *Nat Cell Biol,* 6**,** 106-12.

YEUNG, K. T. & YANG, J. 2017. Epithelial-mesenchymal transition in tumor metastasis. *Mol Oncol,* 11**,** 28-39.

YONEMORI, K., KURAHARA, H., MAEMURA, K. & NATSUGOE, S. 2017. MicroRNA in pancreatic cancer. *J Hum Genet,* 62**,** 33-40.

ZEISBERG, M. & NEILSON, E. G. 2009. Biomarkers for epithelial-mesenchymal transitions. *J Clin Invest,* 119**,** 1429-37.

ZHANG, S., CHANG, M. C., ZYLKA, D., TURLEY, S., HARRISON, R. & TURLEY, E. A. 1998. The hyaluronan receptor RHAMM regulates extracellular-regulated kinase. *J Biol Chem,* 273**,** 11342-8.

ZHAO, S., WANG, Y., CAO, L., OUELLETTE, M. M. & FREEMAN, J. W. 2010. Expression of oncogenic K-ras and loss of Smad4 cooperate to induce the expression of EGFR and to promote invasion of immortalized human pancreas ductal cells. *Int J Cancer,* 127**,** 2076-87.

ZHOU, P., LI, B., LIU, F., ZHANG, M., WANG, Q., LIU, Y., YAO, Y. & LI, D. 2017. The epithelial to mesenchymal transition (EMT) and cancer stem cells: implication for treatment resistance in pancreatic cancer. *Mol Cancer,* 16**,** 52.

ZUBAIR, H., AZIM, S., SRIVASTAVA, S. K., AHMAD, A., BHARDWAJ, A., KHAN, M. A., PATEL, G. K., ARORA, S., CARTER, J. E., SINGH, S. & SINGH, A. P. 2016. Glucose Metabolism Reprogrammed by Overexpression of IKKepsilon Promotes Pancreatic Tumor Growth. *Cancer Res,* 76**,** 7254-7264.

Appendix

Appendix 1: Peking University Cancer Hospital Patients in Consent Information

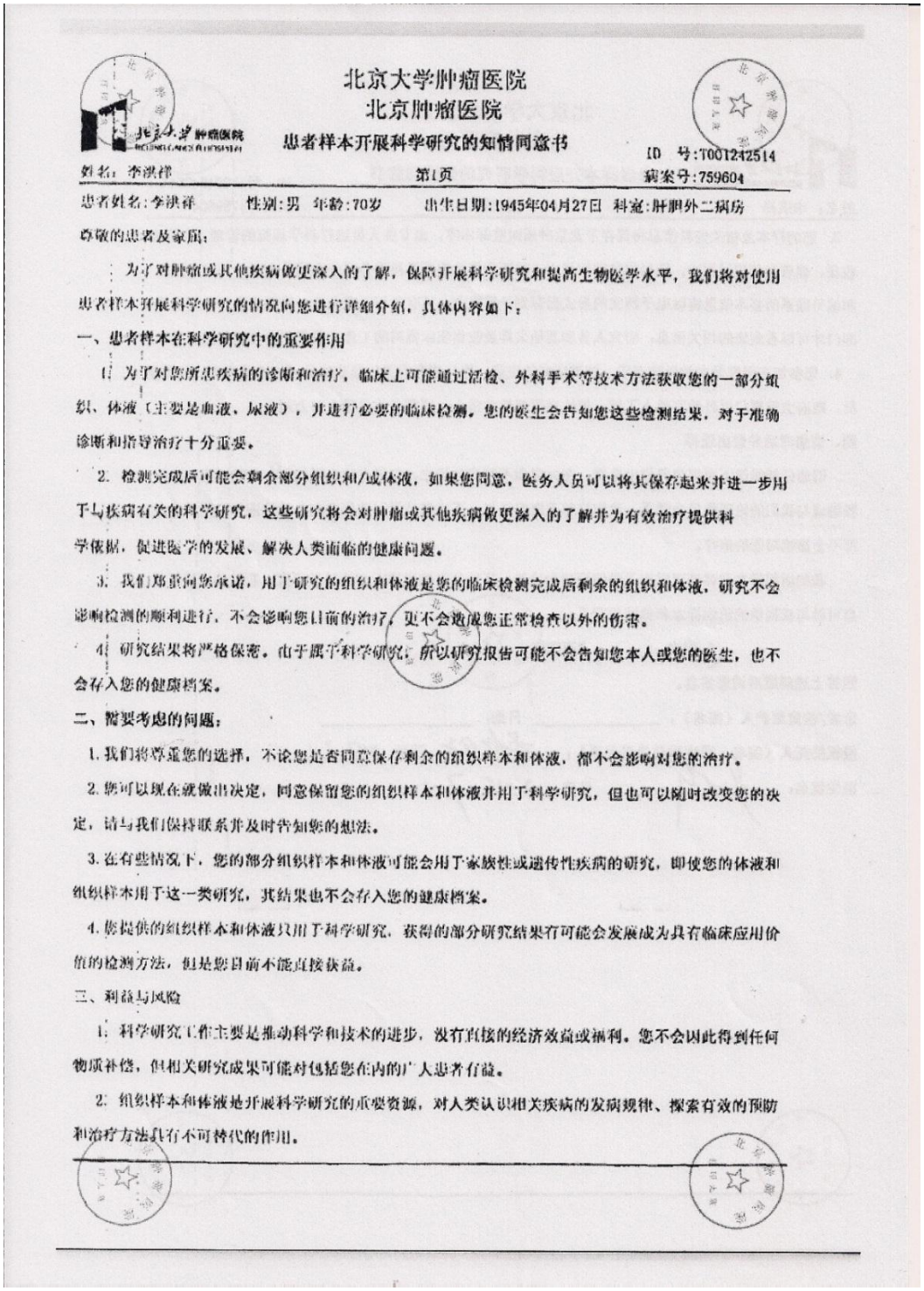

北京大学肿瘤医院
北京肿瘤医院
患者样本开展科学研究的知情同意书

ID 号:T0012425514
姓名：李洪祥　　第1页　　病案号:759604

患者姓名:李洪祥　　性别:男　年龄:70岁　　出生日期:1945年04月27日　科室:肝胆外二病房

尊敬的患者及家属：

为了对肿瘤或其他疾病做更深入的了解，保障开展科学研究和提高生物医学水平，我们将对使用患者样本开展科学研究的情况向您进行详细介绍，具体内容如下：

一、患者样本在科学研究中的重要作用

1. 为了对您所患疾病的诊断和治疗，临床上可能通过活检、外科手术等技术方法获取您的一部分组织、体液（主要是血液、尿液），并进行必要的临床检测。您的医生会告知您这些检测结果，对于准确诊断和指导治疗十分重要。

2. 检测完成后可能会剩余部分组织和/或体液，如果您同意，医务人员可以将其保存起来并进一步用于与疾病有关的科学研究，这些研究将会对肿瘤或其他疾病做更深入的了解并为有效治疗提供科学依据，促进医学的发展、解决人类面临的健康问题。

3. 我们郑重向您承诺，用于研究的组织和体液是您的临床检测完成后剩余的组织和体液，研究不会影响检测的顺利进行，不会影响您目前的治疗，更不会造成您正常检查以外的伤害。

4. 研究结果将严格保密。由于属于科学研究，所以研究报告可能不会告知您本人或您的医生，也不会存入您的健康档案。

二、需要考虑的问题：

1. 我们将尊重您的选择，不论您是否同意保存剩余的组织样本和体液，都不会影响对您的治疗。

2. 您可以现在就做出决定，同意保留您的组织样本和体液并用于科学研究，但也可以随时改变您的决定，请与我们保持联系并及时告知您的想法。

3. 在有些情况下，您的部分组织样本和体液可能会用于家族性或遗传性疾病的研究，即使您的体液和组织样本用于这一类研究，其结果也不会存入您的健康档案。

4. 您提供的组织样本和体液只用于科学研究，获得的部分研究结果有可能会发展成为具有临床应用价值的检测方法，但是您目前不能直接获益。

三、利益与风险

1. 科学研究工作主要是推动科学和技术的进步，没有直接的经济效益或福利。您不会因此得到任何物质补偿，但相关研究成果可能对包括您在内的广大患者有益。

2. 组织样本和体液是开展科学研究的重要资源，对人类认识相关疾病的发病规律、探索有效的预防和治疗方法具有不可替代的作用。

北京大学肿瘤医院
北京肿瘤医院

患者样本开展科学研究的知情同意书

ID 号：T001242514

姓名：李洪祥　　第2页　　病案号：759604

3. 您的样本及相关资料信息将保存于北京肿瘤医院标本库，由专业人员进行科学规范的管理，在标本收集、保管和使用过程中，您提供的组织样本、体液和您的临床资料将会用一个编号表示。与您的姓名和编号联系的基本信息将以电子档案的形式保存到计算机中，只有参与研究人员、伦理委员、政府主管部门才可以看到您的相关信息，研究人员和其他采样及收集临床资料的工作人员都不会知道您的身份。

4. 您参加本研究最大的风险在于，随着研究的进展，您与研究有关的健康信息可能被研究者、伦理委员、政府主管部门以外的其他人了解，但这种可能性非常小，研究者将尽最大努力避免。

四、请您考虑并做出选择

请您仔细阅读下面项目并做出选择，在同意和不同意处标注。如果有什么疑问请与您的医生和护士咨询或与我们的伦理委员会联系。我们将尊重您的选择，不论您是否同意保存剩余的体液和组织样本，都不会影响对您的治疗。

我的组织样本和体液可以用于肿瘤预防和诊治、其他危害健康等方面的科学研究，我的临床资料信息可以与我提供的组织样本和体液相联系。

A √同意　　B不同意

回答上述问题后请您签名。

患者/法定监护人（签名）：_____ 日期：_____

授权委托人（签名，须注明与患者关系）：李欣好 日期：2015.7.1

医生签名：[illegible] 日期：2015-7-1

北京大学肿瘤医院
北京肿瘤医院

患者样本开展科学研究的知情同意书

ID 号:T001195749

姓名：陈萌　　第1页　　病案号:755859

患者姓名:陈萌　　性别:男　年龄:38岁　　出生日期:1976年10月21日　科室:肝胆外二病房

尊敬的患者及家属：

为了对肿瘤或其他疾病做更深入的了解，保障开展科学研究和提高生物医学水平，我们将对使用患者样本开展科学研究的情况向您进行详细介绍，具体内容如下：

一、患者样本在科学研究中的重要作用

1. 为了对您所患疾病的诊断和治疗，临床上可能通过活检、外科手术等技术方法获取您的一部分组织、体液（主要是血液、尿液），并进行必要的临床检测。您的医生会告知您这些检测结果，对于准确诊断和指导治疗十分重要。

2. 检测完成后可能会剩余部分组织和/或体液，如果您同意，医务人员可以将其保存起来并进一步用于与疾病有关的科学研究，这些研究将会对肿瘤或其他疾病做更深入的了解并为有效治疗提供科学依据，促进医学的发展、解决人类面临的健康问题。

3. 我们郑重向您承诺，用于研究的组织和体液是您的临床检测完成后剩余的组织和体液，研究不会影响检测的顺利进行，不会影响您目前的治疗，更不会造成您正常检查以外的伤害。

4. 研究结果将严格保密。由于属于科学研究，所以研究报告可能不会告知您本人或您的医生，也不会存入您的健康档案。

二、需要考虑的问题：

1. 我们将尊重您的选择，不论您是否同意保存剩余的组织样本和体液，都不会影响对您的治疗。

2. 您可以现在就做出决定，同意保留您的组织样本和体液并用于科学研究，但也可以随时改变您的决定，请与我们保持联系并及时告知您的想法。

3. 在有些情况下，您的部分组织样本和体液可能会用于家族性或遗传性疾病的研究，即使您的体液和组织样本用于这一类研究，其结果也不会存入您的健康档案。

4. 您提供的组织样本和体液只用于科学研究，获得的部分研究结果有可能会发展成为具有临床应用价值的检测方法，但是您目前不能直接获益。

三、利益与风险

1. 科学研究工作主要是推动科学和技术的进步，没有直接的经济效益或福利。您不会因此得到任何物质补偿，但相关研究成果可能对包括您在内的广大患者有益。

2. 组织样本和体液是开展科学研究的重要资源，对人类认识相关疾病的发病规律、探索有效的预防和治疗方法具有不可替代的作用。

北京大学肿瘤医院
北京肿瘤医院

患者样本开展科学研究的知情同意书

ID 号:T001195749

姓名：陈萌　　第2页　　病案号:755859

3. 您的样本及相关资料信息将保存于北京肿瘤医院标本库，由专业人员进行科学规范的管理，在标本收集、保管和使用过程中，您提供的组织样本、体液和您的临床资料将会用一个编号表示。与您的姓名和编号联系的基本信息将以电子档案的形式保存到计算机中，只有参与研究人员、伦理委员、政府主管部门才可以看到您的相关信息，研究人员和其他采样及收集临床资料的工作人员都不会知道您的身份。

4. 您参加本研究最大的风险在于，随着研究的进展，您与研究有关的健康信息可能被研究者、伦理委员、政府主管部门以外的其他人了解，但这种可能性非常小，研究者将尽最大努力避免。

四、请您考虑并做出选择

请您仔细阅读下面项目并做出选择，在同意和不同意处标注。如果有什么疑问请与您的医生和护士咨询或与我们的伦理委员会联系。我们将尊重您的选择，不论您是否同意保存剩余的体液和组织样本，都不会影响对您的治疗。

我的组织样本和体液可以用于肿瘤预防和诊治、其他危害健康等方面的科学研究，我的临床资料信息可以与我提供的组织样本和体液相联系。

A同意　　B不同意

回答上述问题后请您签名。

患者/法定监护人（签名）：_____ 日期：_____

授权委托人（签名，须注明与患者关系）：妻 张苹 日期：2015.1.19

医生签名：[illegible] 日期：2015.1.19

Peking University Cancer Hospital
Patients in Consent Information

Name: Gender: Date of Birth: Department:

Dear patients,

In order to make your disease further understood, guarantee scientific research quality and improve the level of medical research, we would like to introduce how we use the Patient Sample to do medical research.

1. The importance of your specimens in medical research

1.1 For the benefit of your diagnosis and treatment, we would like to collect your specimens and blood in order to do necessary clinical examine through bioscopy or surgery.

1.2 If you permit, we would like to reserve the rest of your specimens and blood to do further medical research in order to make a full understanding of cancer and other diseases, and provide more evidence to medicine and treatment.

1.3 We hereby guarantee that we use the rest of your specimens and blood for medical research. This will not affect your examine, treatment and health.

1.4 The medical research is fully confidential. The research reports will not inform you and your doctor, and at the same time, it will not be saved in your personal healthy file.

2. Problems to be considered

2.1 We respect your decision, whether you agree or disagree to preserve your specimens, which will not affect your treatment.

2.2 You can make a decision now, and change your mind at any time. Please keep in touch with us and let us know your decision.

2.3 Your specimens will be used in the study of hereditary diseases; however, results will not be saved in your personal healthy file.

2.4 Your specimens may greatly contribute to research. However, you may not get benefit from them.

3. Benefits and Risks

3.1 The purpose of medical research is to make a contribution to all patients, and you will not get any financial benefit and welfare from them.

3.2 Your specimens and blood are important resources for the understanding of the development of diseases and exploration of effective methods of treatment.

3.3 Your specimens and information will be preserved in the tissue bank of Peking University Cancer Hospital. All of your information will be coded with uniform numbers, and the basic information will be stored in electronic files in the computer. Only involvement of researchers, ethics committees and government officer of departments in charge can get access to your information, researchers and other staff collecting the clinical data will not know your information.

3.4 The risk of your participation in this study is that, within the progress of research, you and your health-related information may be accessible by other people besides researchers, ethics committees and government departments, but researchers will try to avoid it.

4. Please read the above information carefully and make your owe choice. If you have any questions, please feel free to contact our doctors and nurses or ethics committees.

My specimens are used for cancer prevention, diagnostics and scientific research, and at the same time, my clinical data can be associated with my specimens.

A. Agree **B. Disagree**

Patient's name: Date:

Doctor's name: Date:

Appendix 2: H&E staining of PA2081a, Biomax.

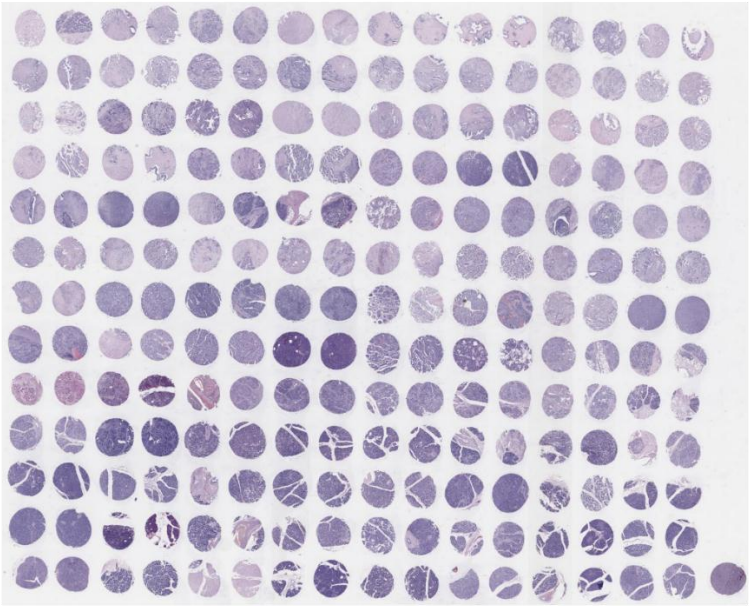

This image was downloaded from https://www.biomax.us/index.php?route=product/zoomify&park=29872. High resolution image is available from this website.

Appendix 3: Original images used in RT-PCR and western blot.

Figure4.1

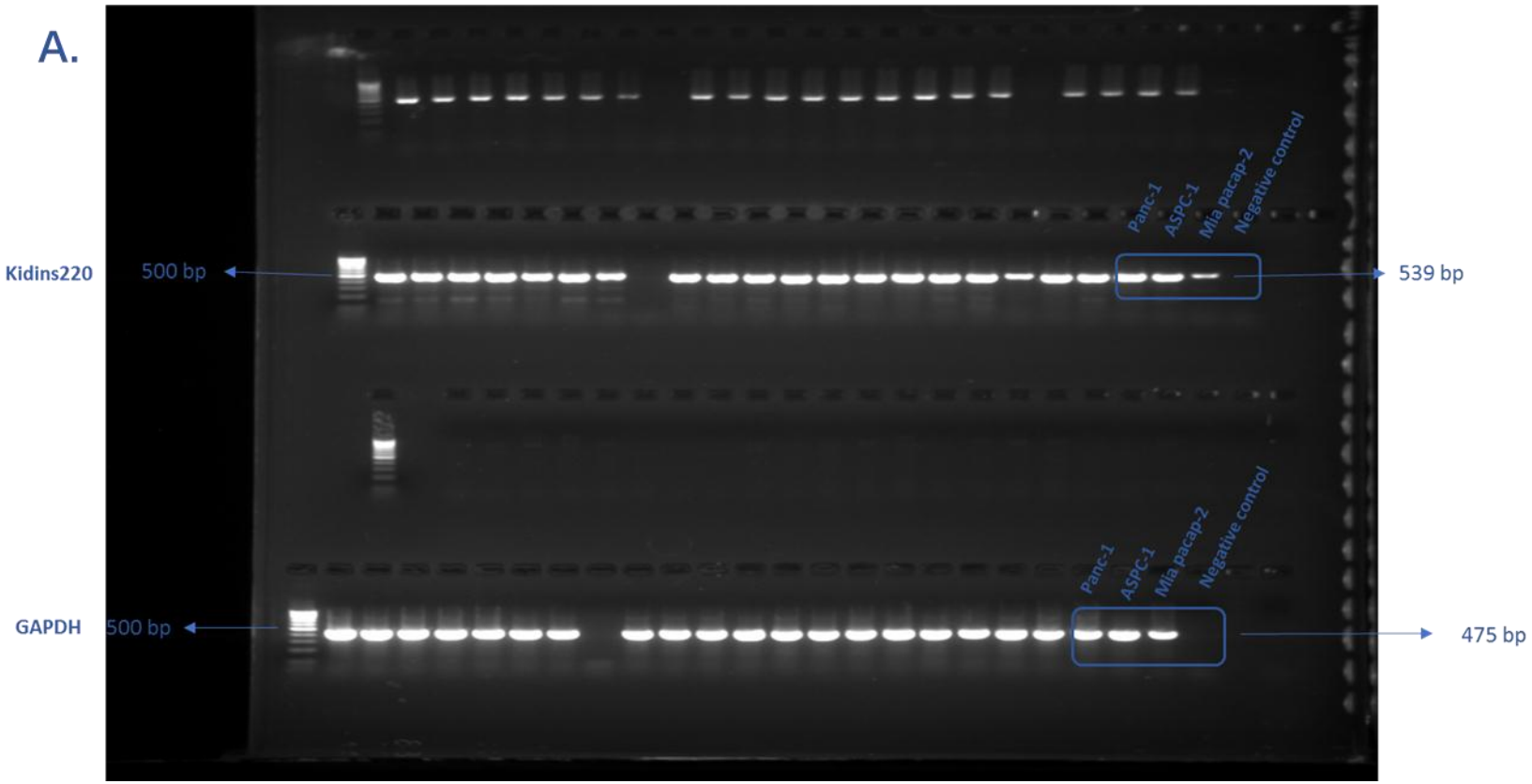

Figure4.1

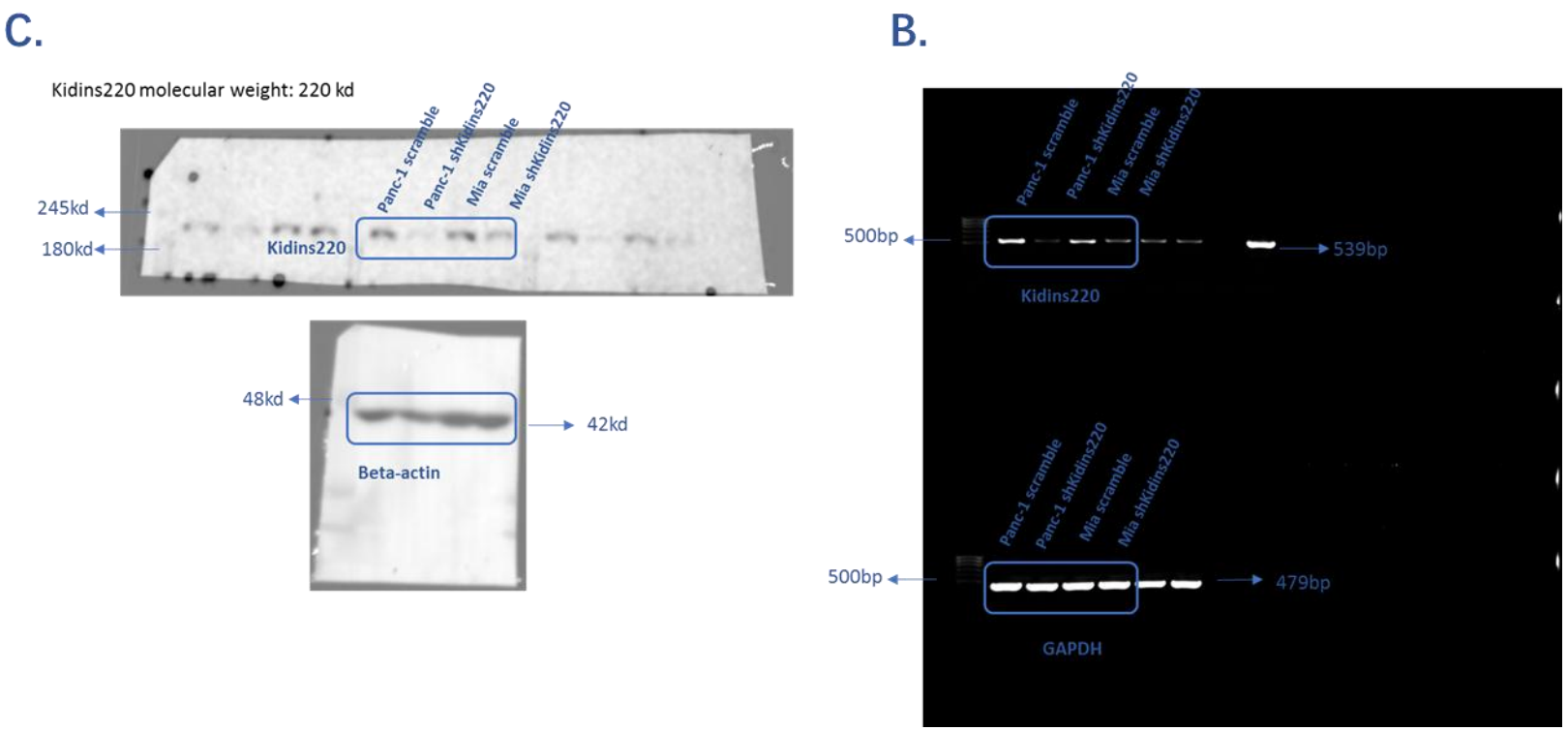

Original images of gel (RT-PCR) and blot (western blot) of Figure 4.1. The highlighted bands in the boxes are the cropped bands presented in Figure4.1

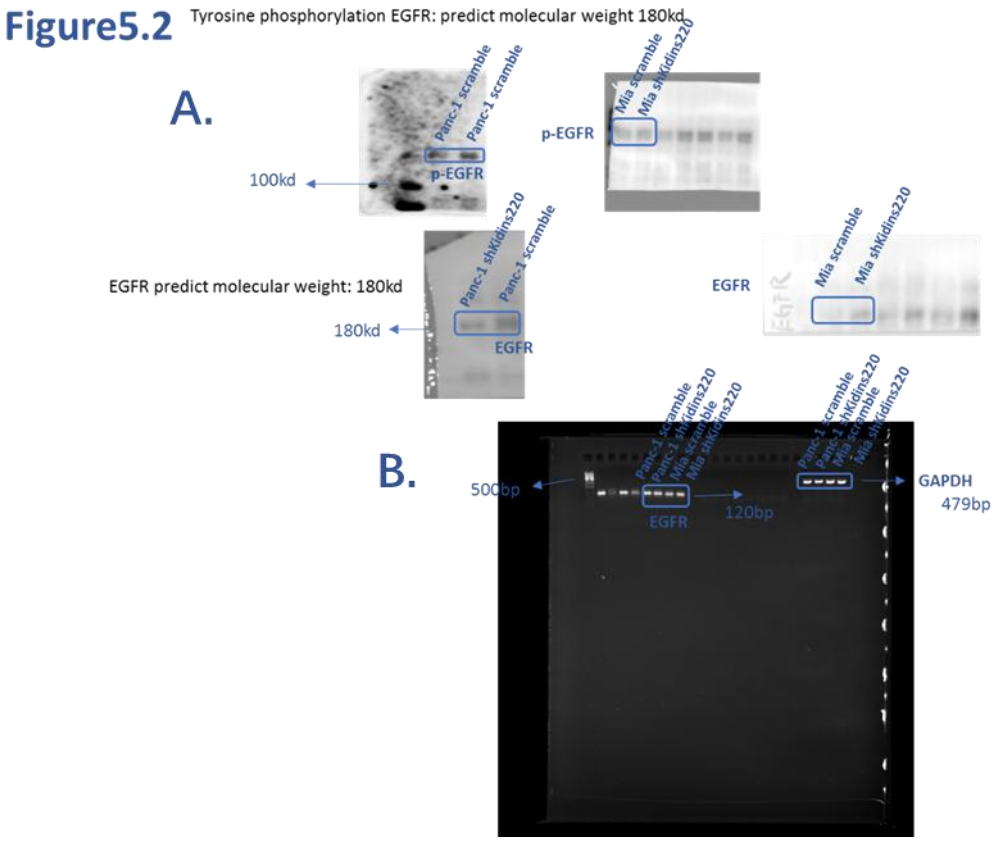

Original images of gel (RT-PCR) and blot (western blot) of Figure 5.2. The highlighted bands in the boxes are the cropped bands presented in Figure5.2.

Figure5.3

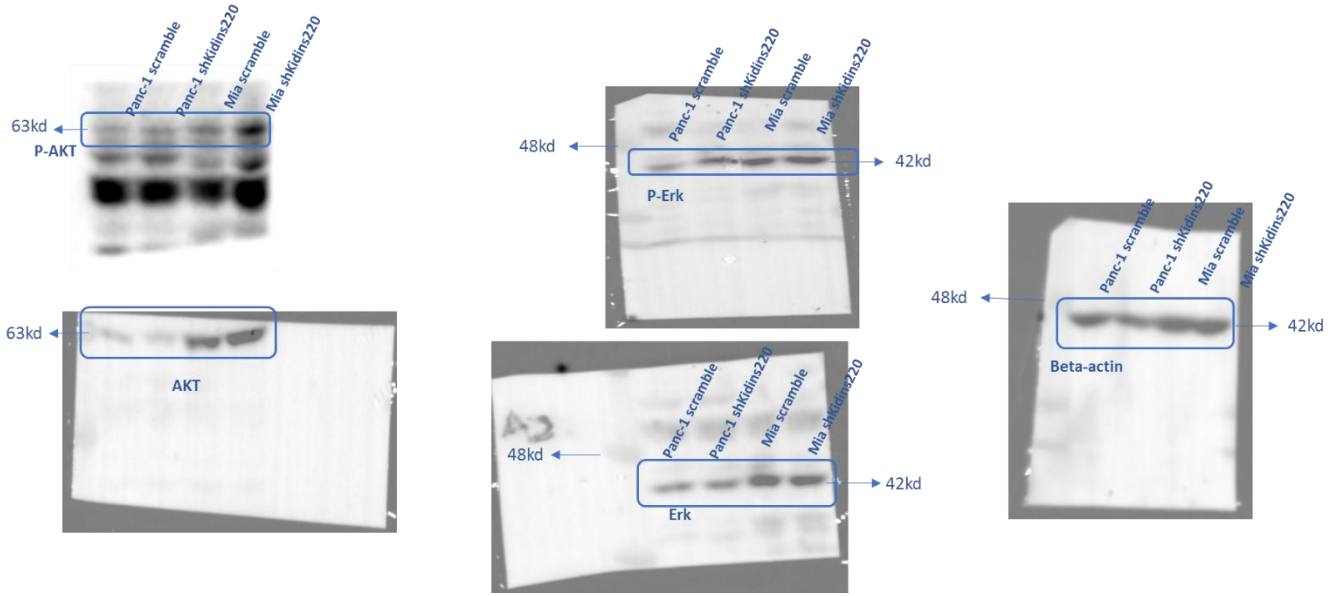

Original images of blot of Figure 5.3 The highlighted bands in the boxes are the cropped bands presented in Figure5.3

Figure5.4

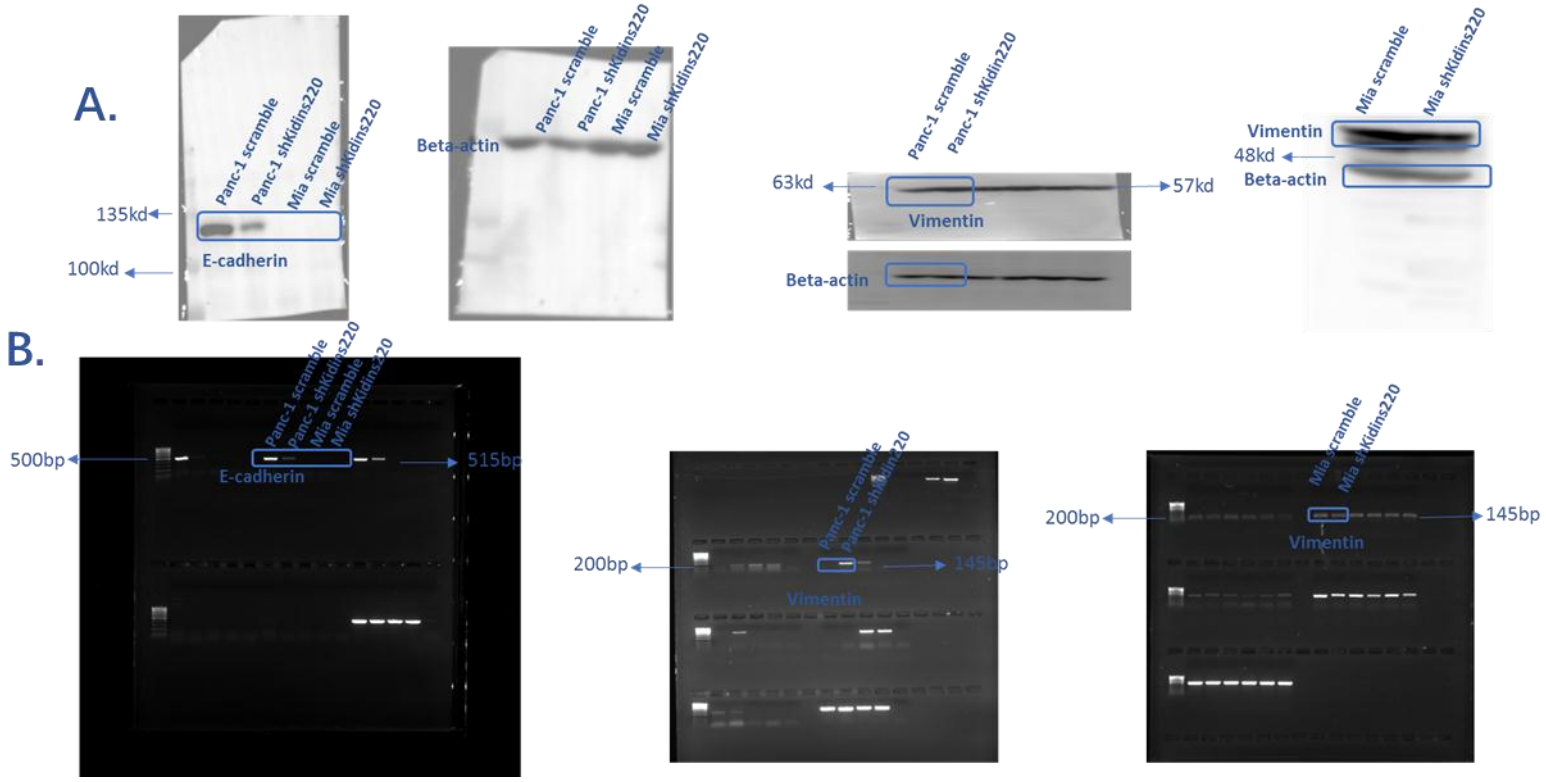

Original images of blot of Figure 5.4. The highlighted bands in the boxes are the cropped bands presented in Figure5.4.

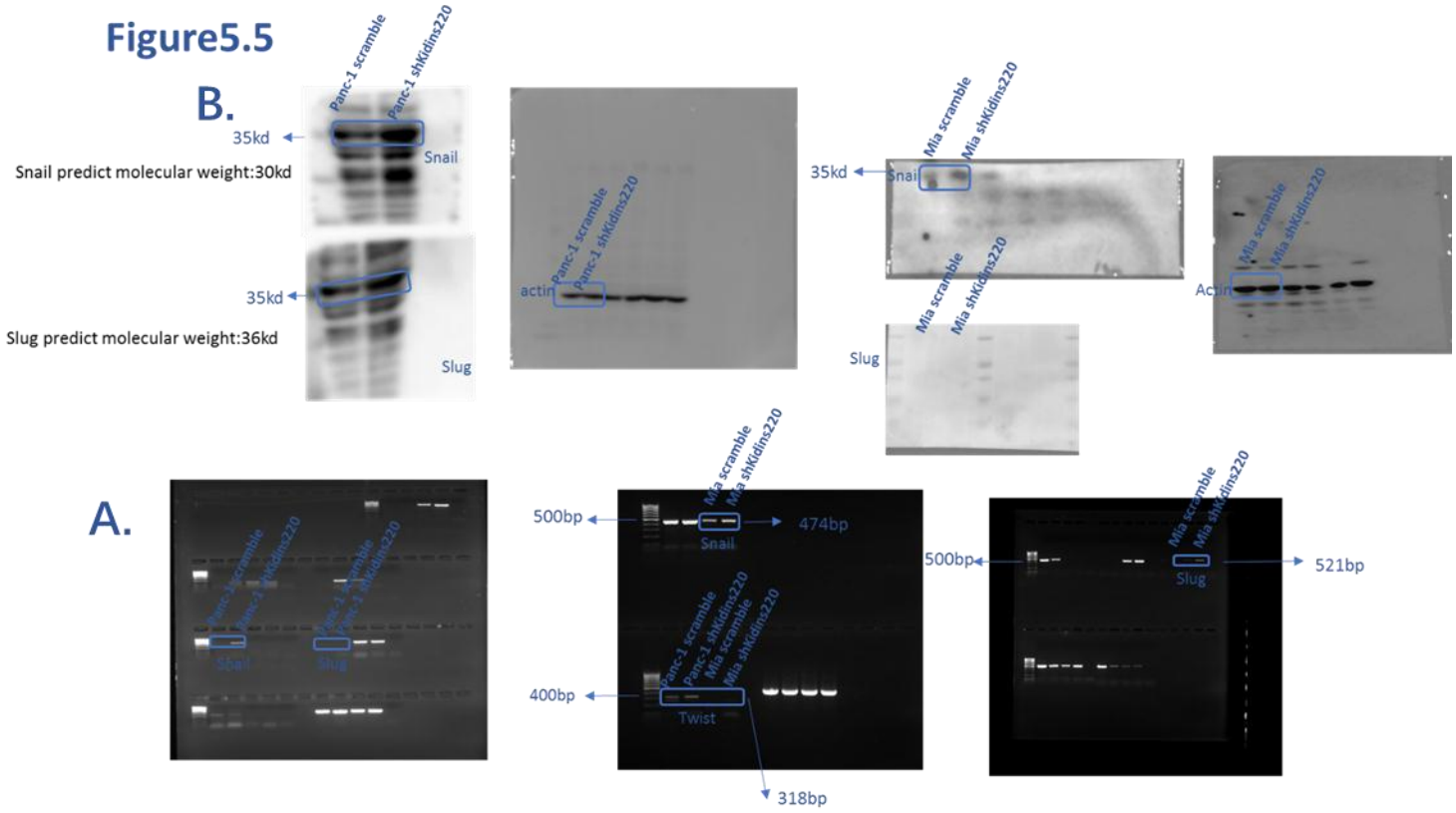

Original images of blot of Figure 5.5. The highlighted bands in the boxes are the cropped bands presented in Figure5.5.

Figure 5.6

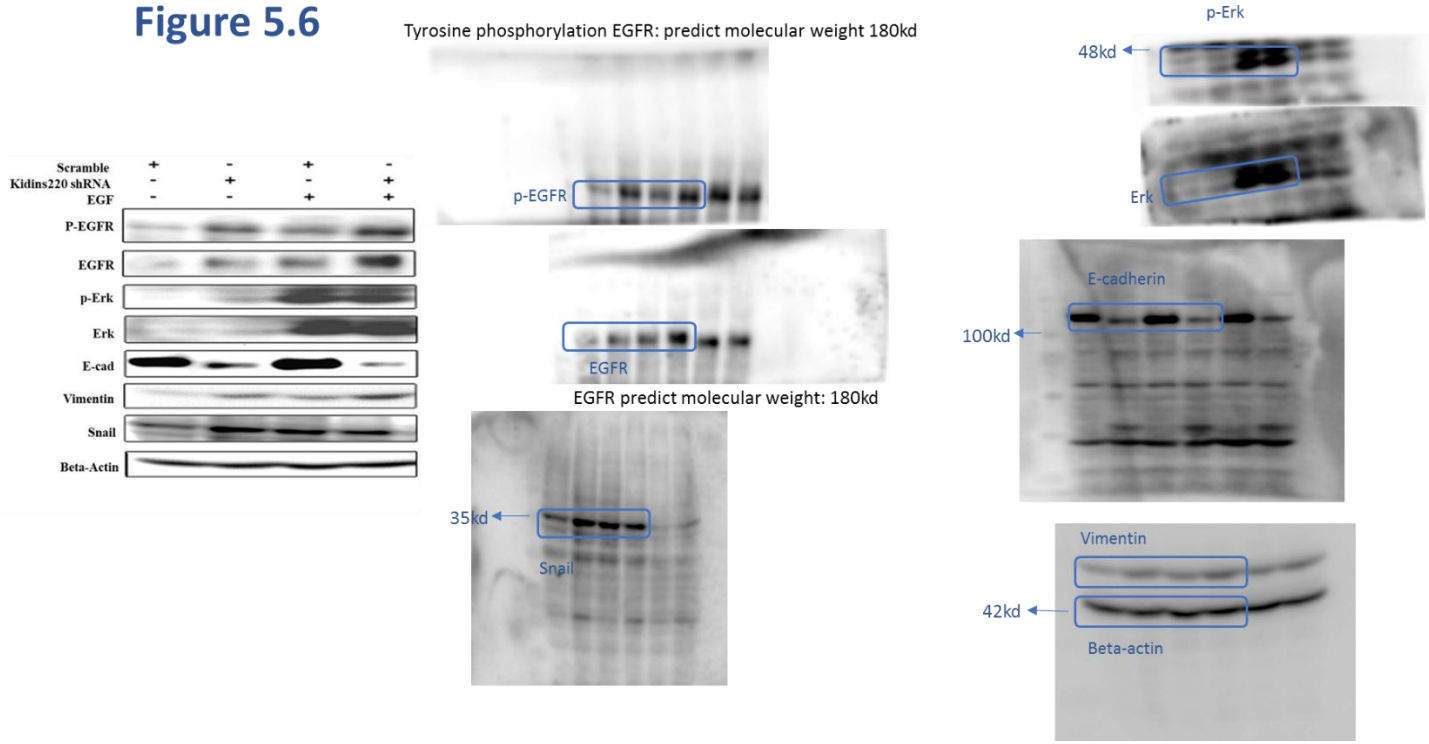

Original images of blot of Figure 5.6. The highlighted bands in the boxes are the cropped bands presented in Figure5.6.